

Polarized Macrophages in Hypertrophic Scar Formation

by

Zhensen Zhu

A thesis submitted in partial fulfillment of the requirements for the degree of

Doctor of Philosophy

in

Experimental Surgery

Department of Surgery
University of Alberta

© Zhensen Zhu, 2016

Abstract

Hypertrophic scars (HTS) are caused by trauma or burn injuries to the deep dermis and can cause cosmetic disfigurement and psychological issues. Our lab has established a human HTS-like nude mouse model, in which the grafted human skin develops red, raised, and firm scarring, resembling hypertrophic scars seen in humans. Macrophages play a key role in the wound healing process and can be divided into classically activated macrophages (M1) and alternatively activated macrophages (M2). Monocytes, M1 and M2 macrophages belong to the mononuclear phagocyte system (MPS). Studies suggest that M2 macrophages are pro-fibrotic and might contribute to HTS formation. In order to test that M2 macrophages contribute to HTS formation, three consecutive experiments were conducted.

The first experiment was to test the effect of M2 macrophages on the fibrogenic activities of the cultured human dermal fibroblasts (HDF). In this study, resting state (M0), M1 and M2 macrophages differentiated from the human monocytic THP-1 cell line were used to co-culture with HDF for 48, 96 and 144 hours. The differentiation and polarization from THP-1 cells to M0, M1 and M2 macrophages were characterized by flow cytometry and cell cycle analysis. Cell sorting was performed to purify M0 and M2 macrophages. Cell proliferation, collagen synthesis, myofibroblast formation, gene expression of anti-fibrotic and pro-fibrotic factors, MMP-1 activity, and cytokine concentration were investigated. Results showed differentiation of M0 and polarization of M1 and M2 macrophages. M2 macrophages promoted the fibrogenic activities of co-cultured HDF by facilitating cell proliferation, increasing the collagen content, alpha-

SMA expressing cells, expression of the pro-fibrotic genes and concentration of M2 macrophage related factors, as well as decreasing the expression of the anti-fibrotic genes and MMP-1 activity. These findings reinforce the pro-fibrotic role of M2 macrophages, suggesting therapeutic strategies in fibrotic diseases should target M2 macrophages in the future.

The second experiment was to explore the natural behavior of MPS in the human HTS-like nude mouse model. Thirty athymic nude mice received human skin grafts (xenograft) and another thirty mice received mouse skin grafts (allograft) as controls. The grafted skin and blood were harvested at 1, 2, 3, 4 and 8 weeks. Wound area, thickness, collagen morphology and level, the cell number of myofibroblasts, M1 and M2 macrophages in the grafted skin were investigated. Xenografted mice developed contracted and thickened scars while the xenografted skin resembled human hypertrophic scar tissue based on enhanced thickness, fibrotic orientation of collagen bundles, increased collagen level and infiltration of myofibroblasts. In the xenografted skin, M1 macrophages were found predominantly at 1 to 2 weeks while M2 macrophages were abundant at 3 to 4 weeks post-grafting. This understanding of the natural behavior of mononuclear phagocytes in our mouse model provides evidence for the role of macrophages in human dermal fibrosis and suggests that macrophage depletion in the subacute phases of wound healing might reduce or prevent HTS formation.

The third experiment was to study the effect of systemic macrophage depletion on scar formation at the subacute phase of wound healing. Thirty-six athymic nude mice that received human skin transplants were randomly divided into macrophage depletion group and control group. The former received intraperitoneal injections of clodronate liposomes

while the controls received sterile saline injections on day 7, 10, 13 post-grafting. Wound area, scar thickness, collagen abundance and collagen bundle structure, mast cell infiltration, myofibroblast formation, M1 and M2 macrophages together with gene expression of M1 and M2 related factors in the grafted skin were investigated at 2, 4 and 8 weeks post-grafting. The skin grafts from the control group developed contracted, elevated and thickened scars while the grafted skin from the depletion group healed with significantly less contraction and elevation. Significant reductions in myofibroblast number, collagen synthesis and hypertrophic fiber morphology as well as mast cell infiltration were observed in the depletion group compared to the control group. Macrophage depletion significantly reduced M1 and M2 macrophage number in the depletion group 2 weeks post-grafting as compared to the control group. Systemic macrophage depletion at subacute phase of wound healing showed reduced scar formation. These findings provide evidence for the pro-fibrotic role of M2 macrophages in human dermal fibrosis as well as insight into the potential benefits of specifically depleting M2 macrophages *in vivo*.

Preface

This thesis is an original work by Zhensen Zhu. The research project, of which this thesis is a part, received research ethics approval from the University of Alberta Research Ethics Board, Project Name “Development and characterization of dermal fibrosis following burn injury”, No. AUP00000344, 5 June 2014. The animal protocol was approved by the University of Alberta Animal Care and Use Committee in accordance with the Canadian Council of Animal Care standards.

All the content in the thesis is my original work. A large portion of Chapter 1 has been published as two invited reviews: (1) Zhu Z, Ding J, Shankowsky HA, Tredget EE. The molecular mechanism of hypertrophic scar. *J Cell Commun Signal*. 2013 Dec;7(4):239-52. doi: 10.1007/s12079-013-0195-5. Epub 2013 Mar 18. I was responsible for the manuscript composition. Ding J and Shankowsky HA contributed to manuscript edits. Tredget EE was the supervisory author and was involved with concept formation and manuscript edits; (2) Zhu ZZ, Ding J, Tredget EE. The molecular basis of hypertrophic scars. *Burns & Trauma*. 2016;4. I was responsible for the manuscript composition. Ding J contributed to manuscript edits. Tredget EE was the supervisory author and was involved with concept formation and manuscript edits.

Chapter 3 of this thesis has been published as Zhu Z, Ding J, Ma Z, Iwashina T, Tredget EE. The natural behavior of mononuclear phagocytes in HTS formation. *Wound Repair Regen*. 2016 Jan;24(1):14-25. doi: 10.1111/wrr.12378. Epub 2015 Nov 20. I was responsible for the design of the research program, the performance of experiments, collection and analysis of the research data as well as the manuscript composition. Ma Z

and Iwashina T assisted with the data collection. Ding J was involved with concept formation and contributed to manuscript edits. Tredget EE was the supervisory author and was involved with concept formation and manuscript edits.

Chapter 4 of this thesis has been published as Zhu Z, Ding J, Ma Z, Iwashina T, Tredget EE. Systemic Depletion of Macrophages in the Subacute Phase of Wound Healing Reduces Hypertrophic Scar Formation. *Wound Repair Regen.* 2016 May 12. doi: 10.1111/wrr.12442. [Epub ahead of print]. I was responsible for the design of the research program, the performance of experiments, collection and analysis of the research data as well as the manuscript composition. Ma Z and Iwashina T assisted with the data collection. Ding J was involved with concept formation and contributed to manuscript edits. Tredget EE was the supervisory author and was involved with concept formation and manuscript edits.

Dedication

For my beloved wife Xiaoli. I couldn't have finished the program without her love and sacrifice for the family.

For my dear daughters Yueqi and Yuexin, who make my life complete and colourful.

Acknowledgements

First and foremost, I'd like to express my sincerest appreciation to my supervisor Dr. Edward E. Tredget for taking me as his student and guiding me through my studies over the last 4 years. I would not be able to have come this far without his help. I'm really grateful to have the privilege to learn from him.

My deep and sincere gratitude to my co-supervisor Dr. Jie Ding, who has always been there whenever I need help. I really appreciate her guidance and valuable advice that helped me get through the program. I'd also like to thank the guidance and help from the rest of my supervisory committee members: Dr. Colin Anderson, Dr. Babita Agrawal. They provided me with new ideas and perspectives that helped me come up with better experimental design. They are professional, knowledgeable and kind.

My appreciation extends to Dr. Tom Churchill who provided me with useful suggestions and support in every important step of my program.

My sincere thanks to Dr. Paige Lacy, Dr. Gina Rayat and Dr. Melancon for their continuous guidance and suggestions during my PhD program.

I'd like to thank my lab members Zengshuan Ma, Takashi Iwashina, Dr. Peter Kwan, Saahil Sanon, Dr. Abelardo Medina, Leah Campeau and Jiajie Wu for their help and support.

Lastly, I'd like to express my gratitude to the Li Ka Shing Sino-Canadian Exchange Program for providing the stipends for my doctoral program.

Table of Contents

Chapter 1 The Molecular and Cellular Mechanisms of Hypertrophic Scars	1
1.1 Hypertrophic scars	2
1.1.1 The physiology of wound healing in the skin.....	3
1.1.2 The pathological features of HTS	5
1.1.3 Depth of dermal injury is an important factor leading to HTS formation ...	6
1.1.4 Differences between HTS and keloids.....	9
1.1.5 Complications of HTS	10
1.1.6 Treatments of HTS.....	11
1.1.6.1 Surgical therapy for HTS	13
1.1.6.2 Non-surgical therapy for HTS	13
1.2 Molecular basis of HTS	15
1.2.1 Cytokines in HTS formation.....	15
1.2.1.1 Interleukin-1 alpha (IL-1 α) and TNF- α inhibit HTS	15
1.2.1.2 Inappropriate release of IL-6 leads to HTS.....	16
1.2.1.3 Interleukin-10 (IL-10) plays an important role in scarless wound healing by regulating pro-inflammatory cytokines.....	16
1.2.1.4 Anti-fibrotic molecules, decorin (DCN) and interferon-alpha2b (IFN- α 2b) inhibit HTS formation by inhibiting transforming growth factor-beta (TGF- β) and regulating fibroblasts	17
1.2.1.5 Chemokines contribute to HTS formation by recruiting monocytes into wound sites	19
1.2.2 Growth factors in HTS formation.....	21
1.2.2.1 TGF- β plays a pivotal role in HTS formation.....	21
1.2.2.2 Connective tissue growth factor (CTGF) acts as a downstream mediator of TGF- β 1 signaling pathway and involves in HTS formation.....	25
1.2.2.3 Platelet-derived growth factor (PDGF) is essential to wound healing and the over-expression of PDGF is important in the formation of HTS.....	27
1.2.2.4 Inhibitory effect of basic fibroblast growth factor (bFGF) on HTS via the regulation of collagen production, myofibroblast differentiation and TGF- β receptor expression.....	28

1.2.3	Matrix metalloproteinase-1, 2, 9 (MMP-1, 2, 9) are involved in the formation of HTS regulated by tissue inhibitors of metalloproteinases (TIMPs).....	29
1.3	The cellular mechanism of HTS	31
1.3.1	Keratinocytes and mast cells participate in scar pathogenesis.....	31
1.3.2	Differences in cellular characteristics of normal dermal and HTS fibroblasts.....	33
1.3.3	Systemic response of Th1, Th2 and Th3 to HTS formation	34
1.3.4	Macrophages involve in HTS formation.....	36
1.3.4.1	Polarized macrophages maintain tissue homeostasis under non-inflammatory conditions	39
1.3.4.2	The role of polarized macrophages in fibrosis.....	40
1.3.4.3	Macrophages involve in HTS formation via SDF-1/CXCR4 chemokine pathway	41
1.4	Conclusions and experimental design.....	44
1.5	References	46

Chapter 2 Alternatively Activated Macrophages Derived from THP-1 Cells Promote the Fibrogenic Activities of Human Dermal Fibroblasts69

2.0	Abstract	70
2.1	Introduction	71
2.2	Materials and methods	72
2.2.1	Cell culture.....	72
2.2.2	Cell cycle analysis.....	71
2.2.3	Confirmation of differentiation of M0, M1 and M2 macrophages.....	74
2.2.4	Purification of m0 and M2 macrophages using cell sorting	75
2.2.5	Co-culture of HDF with M0, M1 and M2 macrophages	75
2.2.6	Cell proliferation by MTT assay.....	76
2.2.7	Collagen synthesis using liquid chromatography/mass spectrometry (LC/MS).....	76
2.2.8	Quantification of alpha-smooth muscle actin (α -SMA) positive cells in the co-cultured HDF by flow cytometry	77

2.2.9	Quantitative polymerase chain reaction (qPCR) analysis of human pro-fibrotic and anti-fibrotic Factors	78
2.2.10	Human MMP-1 activity assay	79
2.2.11	Multiplex analysis of cytokines at 144 hours of co-culture	79
2.2.12	Statistical analysis	80
2.3	Results	80
2.3.1	Differentiation of THP-1 cells to M0 macrophages	80
2.3.2	Characterization of M1 and M2 macrophages as well as the purification of M0 and M2 macrophages.....	82
2.3.3	M2 macrophages significantly increased proliferation of HDF in co-culture	83
2.3.4	M2 macrophages increased the collagen synthesis of HDF in co-culture	85
2.3.5	M2 macrophages increase myofibroblast differentiation of HDF in co-culture	87
2.3.6	The effect of M2 macrophages on anti-fibrotic and pro-fibrotic factor expression	89
2.3.7	M2 macrophages decreased and M1 macrophages increased MMP-1 activity in co-cultured HDF	92
2.3.8	Significant differences in concentration of the M1 and M2 macrophage related factors at 144 hours of co-culture	94
2.4	Discussion	96
2.5	Conclusion	101
2.6	References	102

Chapter 3 The Natural Behavior of Mononuclear Phagocytes in Hypertrophic Scar Formation **106**

3.0	Abstract	107
3.1	Introduction	108
3.2	Materials and methods	109
3.2.1	Harvesting of human split thickness skin grafts	109
3.2.2	Animals	109
3.2.3	Establishment of human HTS-like nude mouse model.....	110

3.2.4	Morphology of wounds by digital photography	110
3.2.5	Processing of graft specimens.....	111
3.2.6	Histology analysis of graft specimens	111
3.2.7	Collagen morphology analysis.....	111
3.2.8	Quantification of 4-Hyp in graft specimens.....	112
3.2.9	IHC staining of myofibroblasts.....	113
3.2.10	Quantification of circulating monocytes using flow cytometry	113
3.2.11	Quantification of M1 & M2 macrophage by immunofluorescence staining	114
3.2.12	qPCR for cytokines from M1 and M2 macrophages	115
3.2.13	Statistical analysis.....	116
3.3	Results.....	116
3.3.1	Grafted human skin developed scar in the mouse model	116
3.3.2	Morphology of collagen fibers resembled human HTS in xenografts not allografts	120
3.3.3	Increased number of myofibroblasts in xenografts and allografts.....	123
3.3.4	Significant increases of collagen in xenografts	123
3.3.5	Monocyte fractions behaved similarly between the allografted and xenografted mice at each time point	125
3.3.6	M1 and M2 macrophages change over time in xenografts and allografts	126
3.3.7	Relative gene expression of M1 and M2 macrophage related cytokines changed over time in xenografts and allografts	130
3.4	Discussion.....	132
3.5	Conclusion	136
3.6	References.....	137

Chapter 4 Systemic Depletion of Macrophages in the Subacute Phase of Wound Healing Reduces Hypertrophic Scar Formation.....141

4.0	Abstract.....	142
4.1	Introduction.....	143

4.2	Materials and methods	144
4.2.1	Preparation of human split thickness skin grafts	144
4.2.2	Animals.....	144
4.2.3	Establishment of human HTS-like nude mouse model.....	145
4.2.4	Morphology of wounds monitored by digital photography	146
4.2.5	Processing of graft specimens.....	146
4.2.6	Histology analysis of graft specimens	146
4.2.7	Collagen morphology analysis.....	147
4.2.8	Measurement of collagen abundance using LC/MS	147
4.2.9	Toluidine blue staining for mast cell infiltration	148
4.2.10	Immunohistochemistry staining of myofibroblasts and macrophages.....	149
4.2.11	Quantification of polarized macrophages (M1 and M2) by immunofluorescence staining	150
4.2.12	qPCR analysis of human pro-fibrotic and anti-fibrotic factors and mouse cytokines from skin grafts.....	151
4.2.13	Statistical analysis	154
4.3	Results.....	154
4.3.1	Confirmation of macrophage depletion in spleen tissue	154
4.3.2	Clodronate liposomes reduced M1 and M2 macrophage number in the grafts	156
4.3.3	Macrophage depletion improved scar formation	160
4.3.4	Macrophage depletion improved collagen remodeling	163
4.3.5	Macrophage depletion reduced mast cell infiltration and myfibroblast differentiation	166
4.3.6	Macrophage depletion decreased pro-fibrotic factor expression	169
4.3.7	Macrophage depletion reduced expression of M1 and M2 related cytokines	171
4.4	Discussion	173
4.5	Conclusion	177
4.6	References.....	179

Chapter 5 Conclusion and Future Directions	183
5.1 Conclusion and future directions	184
5.2 References.....	190
 Bibliography	 192

List of Tables

4.1 Sequences of human primers for qPCR	152
4.2 Sequences of mouse primers for qPCR	153

List of Figures

Figure 1.1 Patients with HTS.....	2
Figure 1.2 Regeneration occurs in superficial wounds while scarring occurs in deeper wounds	7
Figure 1.3 Creation of deep and superficial scratch wounds and histological analysis of resulted scars	8
Figure 1.4 The TGF- β 1 Smad signaling pathway contributes to HTS	24
Figure 1.5 Hypothetical diagram of the role of Th1/Th2/Th3 cells in stimulating bone marrow stem cells to healing wounds.....	36
Figure 1.6 The roles of monocytes and polarized macrophages in HTS formation	43
Figure 2.1 Differentiation of THP-1 cells to M0 macrophages	81
Figure 2.2 Characterization of M1 and M2 macrophages as well as the purification of M0 and M2 macrophages	83
Figure 2.3 M2 macrophages up-regulated the cell viability of co-cultured HDF.....	85
Figure 2.4 M2 macrophages promoted collagen synthesis of co-cultured HDF	87
Figure 2.5 M2 macrophages increase myofibroblast differentiation of HDF in co-culture	89
Figure 2.6 Decreased expression of anti-fibrotic factors and increased expression of pro-fibrotic factors in different group of co-cultured HDF	92

Figure 2.7 M2 macrophages decreased and M1 macrophages increased MMP-1 activity in co-cultured HDF	94
Figure 2.8 Significant differences in concentration of the M1 and M2 macrophage related factors at 144 hours of co-culture	96
Figure 3.1 Xenografted group developed scar at 8 weeks post-grafting	118-119
Figure 3.2 Morphology of collagen fibers resembled human HTS in xenografts not allografts	121-122
Figure 3.3 Increased number of myofibroblasts and collagen level in xenografted group	124
Figure 3.4 Monocyte fractions behaved similarly between the allografted and xenografted mice at each time point	126
Figure 3.5 M1 and M2 macrophages in xenografts were found abundant in different time points	127-129
Figure 3.6 Relative gene expression of M1 and M2 macrophage related cytokines changed over time in xenografts and allografts	131
Figure 4.1 Confirmed macrophage depletion in spleen	155
Figure 4.2 Clodronate liposomes reduced M1 and M2 macrophage number in the grafted tissue at 2 weeks post-grafting	157-159
Figure 4.3 Macrophage depletion improved scar formation	161-162
Figure 4.4 Macrophage depletion improved collagen remodeling	164-165

Figure 4.5 Macrophage depletion reduced mast cell and myofibroblast infiltration 167-168

Figure 4.6 Macrophage depletion increased anti-fibrotic and decreased pro-fibrotic factor expression in the grafted tissue at various time points post-grafting.....170

Figure 4.7 Macrophage depletion reduced the expression of M1 and M2 related cytokines172

Supplementary Figure 1. Few human macrophages were carried in the transplanted human STSG.....174

List of abbreviations

1. ALK1	activin-receptor-like kinase 1
2. ALK5	activin-receptor-like kinase 5
3. ANOVA	analysis of variance
4. Arg-1	Arginase-1
5. α -SMA	alpha-smooth muscle actin
6. ATP	adenosine triphosphate
7. bFGF	basic fibroblast growth factor
8. BSA	bovine serum albumin
9. CBPI	collagen bundle packing index
10. COI	collagen orientation index
11. COL3	type III collagen
12. Co-SMADs	common mediator Smads
13. CTGF	connective tissue growth factor
14. CXCR4	C-X-C chemokine receptor type 4
15. DCN	decorin
16. DMEM	Dulbecco's modified Eagle's medium
17. DTR	diphtheria toxin receptor

18. DW	deep wound
19. ECM	extracellular matrix
20. FBS	fetal bovine serum
21. FFT	fast Fourier transform
22. FGFs	fibroblast growth factors
23. FOXO1	forkhead box protein O1
24. FTSG	full thickness skin graft
25. GAPDH	glyceraldehyde 3-phosphate dehydrogenase
26. GJIC	gap junction intracellular communication
27. HDF	human dermal fibroblast
28. H&E	hematoxylin & eosin
29. HCl	hydrogen chloride
30. HGF	hepatocyte growth factor
31. HPFs	high power fields
32. HPRT	hypoxanthine-guanine phosphoribosyltransferase
33. HTS	hypertrophic scars
34. IHC	immunohistochemistry
35. IFN- α 2b	interferon-alpha2b

36. IL-1 β	interleukin-1 beta
37. I-Smads	inhibitory SMADs
38. LC/MS	liquid chromatography/mass spectrometry
39. LF	liver fibrosis
40. LPS	lipopolysaccharide
41. LysMCre/iDTR	lysozyme M promoter Cre/inducible diphtheria toxin receptor
42. MAPK	mitogen-activated protein kinase
43. MCP-1	monocyte chemotactic protein-1
44. MMPs	matrix metalloproteinases
45. MPS	mononuclear phagocyte system
46. MTT	3-(4,5-dimethylthiazol-2-yl)-2,5- diphenyltetrazolium bromide
47. M1	classically activated macrophages
48. M2	alternatively activated macrophages
49. NF- κ B	nuclear factor-kappa B
50. NO	nitric oxide
51. NOS2	nitric oxide synthase 2
52. PBS	phosphate buffered saline

53. PDGF	platelet-derived growth factor
54. PF	pulmonary fibrosis
55. PFA	paraformaldehyde
56. PMA	phorbol 12-myristate 13-acetate
57. PMNs	polymorphonuclear neutrophils
58. qPCR	quantitative polymerase chain reaction
59. RBC	red blood cells
60. RF	renal fibrosis
61. RFU	relative fluorescence units
62. RPMI	Roswell Park Memorial Institute
63. R-SMADs	receptor-regulated Smads
64. SDF-1	stromal cell-derived factor-1
65. SE	standard error
66. SIP1	Smad interacting protein 1
67. siRNA	small interfering RNA
68. SLRPs	small leucine-rich proteoglycans
69. STAT	signal transducer and activator of transcription
70. STSG	split thickness skin graft

71. SW	superficial wound
72. TGF- β 1	transforming growth factor-beta 1
73. TGF- β RI	TGF- β receptor I
74. Th1	T helper type 1
75. TIMP-1	tissue inhibitors of metalloproteinases-1
76. TNF- α	tumor necrosis factor-alpha
77. VEGF	vascular endothelial growth factor
78. 4-Hyp	4-hydroxyproline
79. 4-Hyp-d3	4-hydroxyproline-d3

Chapter 1

The Molecular and Cellular Mechanisms of Hypertrophic Scars

A Portion of this work came from the papers published in:

1. Zhu Z, Ding J, Shankowsky HA, Tredget EE. The molecular mechanism of hypertrophic scar. *J Cell Commun Signal*. 2013 Dec;7(4):239-52. doi: 10.1007/s12079-013-0195-5. Epub 2013 Mar 18.
2. Zhu ZZ, Ding J, Tredget EE. The molecular basis of hypertrophic scars. *Burns & Trauma*. 2016;4. doi: 10.1186/s41038-015-0026-4

1.1 Hypertrophic scars (HTS)

HTS are considered to be a dermal form of fibroproliferative disorders that are caused by aberrant wound healing due to injuries to the deep dermis, including burn injury, laceration, abrasions, surgery and trauma. HTS are red, raised, rigid and can cause pruritus, pain and joint contracture. HTS formed in the facial area can cause cosmetic disfigurement, which result in psychological and social issues (1, 2) (Figure 1.1).



Figure 1.1. Patients with HTS. A 24-year-old Caucasian male, 11 months after a 21% TBSA burn. This patient developed HTS, resulting in cosmetic and functional problems

that included restricted opening of mouth and tight web spaces of fingers that limited range of motion on hands (From Tredget EE, Levi B, Donelan MB. Biology and principles of scar management and burn reconstruction. Surg Clin North Am. 2014 Aug;94(4):793-815. With permission).

1.1.1 The physiology of wound healing in the skin

Wound healing can be divided into four stages: hemostasis, inflammation, proliferation and tissue remodeling (3). In these four stages, there are complicated interactions within a complex network of pro-fibrotic and anti-fibrotic molecules, such as growth factors, proteolytic enzymes and extracellular matrix (ECM) proteins (4, 5).

The first stage is hemostasis, which relates to the clotting cascade and the formation of a provisional wound matrix. These changes occur immediately after injury and are completed within hours (6). Clotting factors from the injured skin (extrinsic system) and aggregation of thrombocytes or platelets after exposure to collagen fibers (intrinsic system) are activated. The exposed collagen also triggers platelets to begin secreting cytokines and growth factors (7). The provisional wound matrix serves as a scaffold structure for the migration of leukocytes, keratinocytes, fibroblasts and endothelial cells. Platelets induce the vasoconstriction in order to reduce blood loss followed by secretion of a number of inflammatory factors including serotonin, bradykinin, prostaglandins and most importantly histamine, which activate the inflammatory phase.

In the inflammatory phase, polymorphonuclear neutrophils (PMNs) are the first inflammatory cells that are recruited to the inflamed site and are present there for 2-5 days. Several mediators such as tumor necrosis factor-alpha (TNF- α), interleukin-1 beta (IL-1 β) and IL-6 are released by the neutrophils in order to amplify the inflammatory response (8). Monocytes are attracted by the inflammatory mediators and differentiate into macrophages soon after they migrate into the wound site. The main functions of macrophages are phagocytosis of pathogens and cell debris as well as the release of growth factors, chemokines and cytokines which will push the wound healing process into the next stage.

The proliferation stage consists of angiogenesis, re-epithelialization, and granulation tissue formation. The process of angiogenesis is commenced by growth factors such as vascular endothelial growth factor (VEGF) released by activated endothelial cells from uninjured blood vessels. The new blood vessels differentiate into arteries and venules by recruitment of pericytes and smooth muscle cells (9). Re-epithelialization is essential for the re-establishment of tissue integrity, which is ensured by local keratinocytes at the wound edges and epithelial stem cells from skin appendages such as hair follicles or sweat glands (10). Granulation tissue formation is the last step in the proliferation phase, characterized by accumulation of a high density of fibroblasts, granulocytes, macrophages, capillaries and collagen bundles, which replace the provisional wound matrix formed during the inflammation stage. The predominant cells in this tissue are fibroblasts, which produce types I and III collagen and ECM substances, providing a structural framework for cell adhesion and differentiation (11). Later, myofibroblasts

induce wound contraction by virtue of their multiple attachment points to collagen and help to reduce the surface area of the scar (12).

The remodeling stage is already initiated while the granulation tissue is formed. During the maturation of the wound, COL3, which was produced in the proliferation stage, is replaced by the stronger COL1 which is oriented as small parallel bundles and contributes to the basket-weave collagen formation in normal dermis (13).

1.1.2 The pathological features of HTS

The physiological process of normal wound healing will not result in HTS formation. However, if abnormalities occur during the wound healing process, the delicate balance of ECM degradation and deposition will be disrupted. Either insufficient degradation and remodeling of ECM due to an imbalance in expression of matrix metalloproteinases (MMPs) (14) or excessive ECM deposition caused by increased activity of fibroblasts and myofibroblasts (15) might lead to HTS formation. One common mechanism that burn patients often end up with HTS formation is the chronic inflammation or infection due to the severity of the injury, which prolongs the wound healing process and leads to excessive scarring (16). This prolonged inflammatory phase will lead to HTS formation such as increased vessel and cell number as well as excessive collagen deposition (17).

1.1.3 Depth of dermal injury is an important factor leading to HTS formation

The depth of injury is critical to HTS formation and of great clinical importance. The difference between superficial and deep injuries determines how these wounds heal and the severity of the scarring (18). Superficial wounds generally heal within 2 weeks without HTS formation and surgical treatment while deep wounds are prone to HTS and often require surgical interventions such as skin grafting and/or anti-scar procedures. In an experimental dermal scratch model done by the author's laboratory (19, 20), a specially designed and constructed jig was used to create progressively deeper wounds on a burn patient after informed consent. The wounds were along the lines of relaxed skin tension and were 6 cm long, 0 to 0.75mm deep at one end (superficial wound [SW]) and 0.76 to 3 mm deep (deep wound [DW]) at the other end. The SW of the wound scratch model healed with minimal scarring while the DW resulted in HTS that were red, raised, itchy scar confined to the site of injury. This result suggests there is a critical value of depth of the injury beyond which scar formation rather than tissue regeneration occurs (Fig. 1.2 and 1.3).

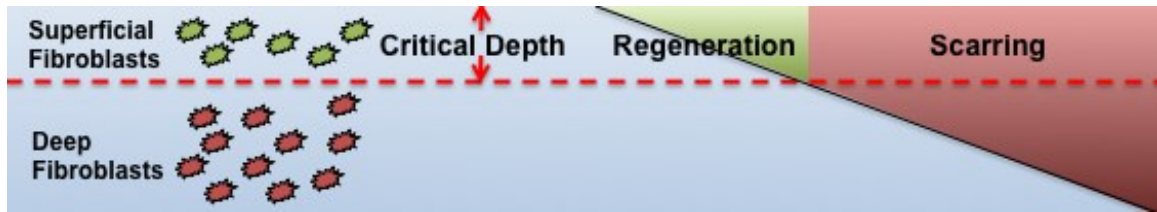


Fig. 1.2. Regeneration occurs in superficial wounds while scarring occurs in deeper wounds. (From Kwan P, Hori K, Ding J, Tredget EE (2009) Scar and contracture: biological principles. *Hand Clin* 25(4):511-28; with permission)

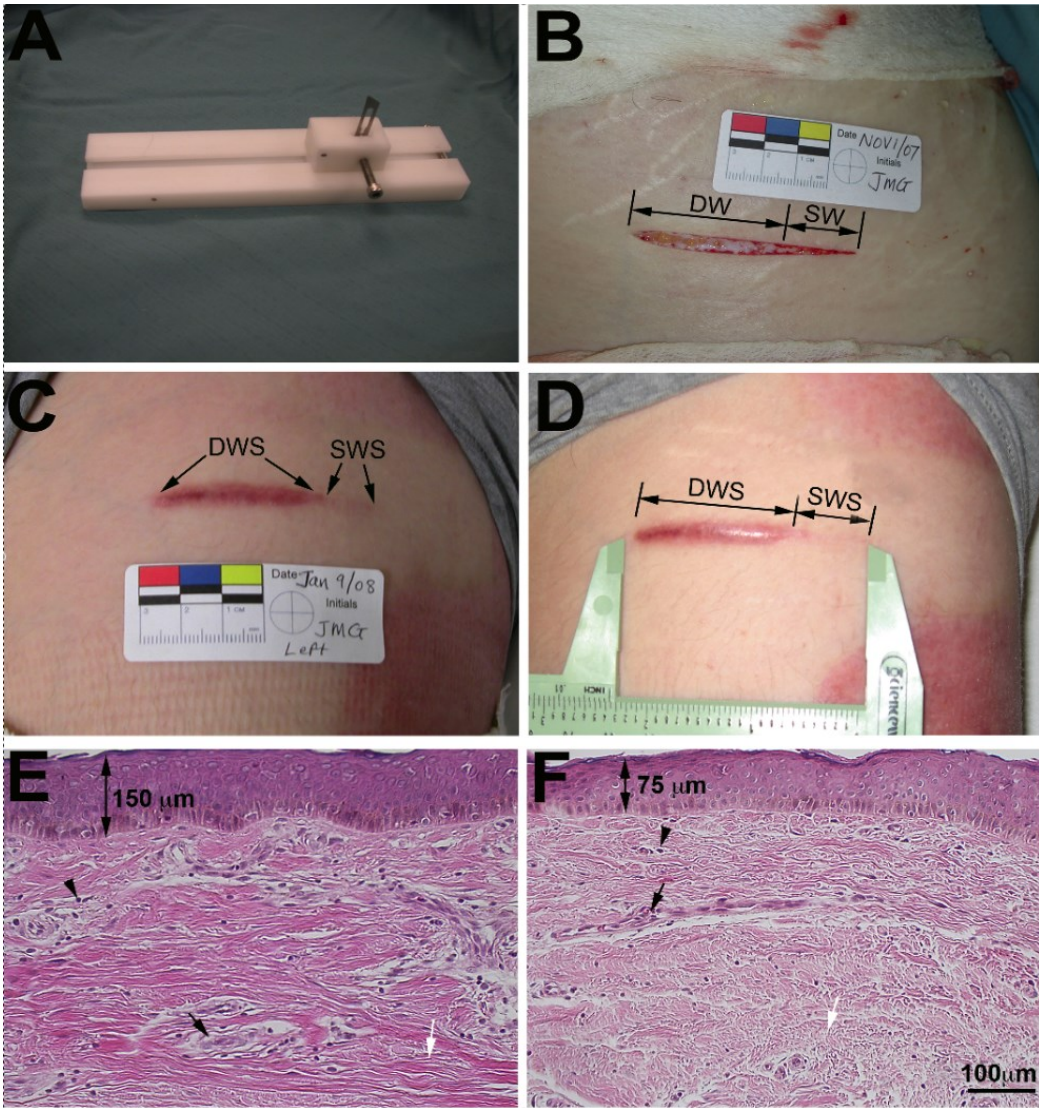


Fig. 1.3 Creation of deep and superficial scratch wounds and histological analysis of resulted scars. A, Jig used to create the scratch wound model. B, Wound created on the anterior thigh. C, Scratch wound 70 days post-wounding. D, Deep and superficial wound scar. E, Deep wound scar tissue stained with hematoxylin and eosin staining (H&E). F, Superficial wound scar tissue stained with H&E. Double-headed arrows in e and f indicate average thickness of epithelium. Arrowheads point to cells. Black arrows point to blood vessels. White arrows point to collagen. DW, deep wound; SW, superficial wound; DWS, deep wound scar; SWS, superficial wound scar (From Honardoust D,

Varkey M, Marcoux Y, Shankowsky HA, Tredget EE (2012) Reduced decorin, fibromodulin, and transforming growth factor- β 3 in deep dermis leads to hypertrophic scarring. *J Burn Care Res* 33(2):218-27; with permission)

1.1.4 Differences between HTS and keloids

HTS and keloids are both caused by abnormal wound healing and are characterized by pathologically excessive fibrosis in the skin (21). Sometimes the differentiation between HTS and keloids can be difficult and lead to incorrect identification, which may result in inappropriate treatment (22).

HTS are mostly caused by trauma or burn injury to the deep dermis and do not extend beyond the boundary of the original injury. Keloids can develop after minor injuries and may even spontaneously form on the sternal region without obvious injury, which will project beyond the original wound borders (23, 24). HTS are red, raised and mostly linear in any regions of the body while keloids appear as pink to purple, shiny, rounded protuberances and are commonly seen in sternal skin, shoulder, upper arms and earlobe. HTS usually appears within a few months of injury, regresses in one or more years and can cause contractures when joint regions are affected, whereas, keloids might take years to develop, grow for years and do not cause contracture. Keloids are commonly seen in darker skin population and have never been reported in albino populations (25).

HTS are characterized by abundant alpha-smooth muscle actin (α -SMA) producing myofibroblasts together with more type III collagen (COL3) than COL1. On the contrary,

there are no α -SMA producing myofibroblasts and a mixture of COL1 and COL3 are found in keloid tissue (21). The collagen bundles in keloids are thick, large and closely packed adjacent to epidermis, whereas fine, well-organized parallel-to-epidermis collagen bundles are found in HTS (26). Adenosine triphosphate (ATP) in keloids remained at higher level for a long time while ATP levels decreased over time in HTS (27). An investigation of the expression of three proteins of the p53 family in keloids and HTS showed that the level of p53 protein was higher in keloids compared to HTS. Protein p73 was elevated only in HTS and no difference was found between keloids and HTS of the level of p63 (28). An *in vitro* analysis of ECM contraction by fibroblasts isolated from different scars showed that HTS fibroblasts had a consistently higher basal level of fibrin matrix gel contraction than keloid fibroblasts (29). Despite all of these differences, HTS and keloids possess similar features including excessive ECM deposition such as high collagen content and rich proteoglycan levels within the dermis and subcutaneous tissue (30). The treatment for HTS and keloids are similar but HTS has a better prognosis for surgical excision because keloids have a much higher recurrence rates (16).

1.1.5 Complications of HTS

Complications of HTS include pain, pruritus, immobility of joint region, disfigurement and psychological issues. Pain and pruritus might not be as devastating as other complications, but they are significant complaints for many patients with HTS and they have been shown to persist for decades. The pain patients with HTS experience is often neuropathic pain, which is caused by dysfunction in the peripheral or central

nervous system due to the primary injury. The neuropathic pain symptoms complained of patients with HTS are pins and needles, burning, stabbing, shooting or electric sensations (31). The mechanism of pruritus is not well understood, but it is associated with histamine, which is released by mast cells and implicated as a primary mediator of itchiness (32). Patients who developed HTS also suffer from reduced functional range of motion due to joint contractures, and disfigurement due to HTS tissue formed in the visible area of the body, which can lead to psychological problems or even social issues. A cross-sectional descriptive study showed that patients with HTS suffered from pain, joint stiffness, limitation in walking or running for an average of 17 years since their burn injury (33). With all these complications, patients with HTS have complicated psychiatric disorders, including concern of body image, anxiety, depression, low self-esteem and posttraumatic stress. They have a need for psychological counseling and rehabilitation, especially for those who are economically disadvantaged or with preexisting mental illness (34). However, a study focused on adolescents with disfiguring burn scars showed that instead of viewing themselves as less personally competent than unburned adolescents, they exhibited a similar or higher degree of self-worth as compared to their peers (35).

1.1.6 Treatments of HTS

The outcome of HTS is quite different because of the varied injured sites, severity of the injuries, and treatments the patients receive which leads to a variety of therapeutic strategies between surgeons and hospitals (36). Current treatment of HTS remains time-

consuming, expensive and with few consistently successful approaches. One of the difficulties is that the outcome of HTS formation varies between patients, locations and conservative interventions. So it is extremely difficult for surgeons to predict whose scar would need surgical excision or whose scar might resolve on its own by the time the patient heals with flat and soft scar (17). In 2002, Mustoe et al. reported a qualitative overview of the available clinical literature by an international advisory panel of experts and provided evidence-based recommendations on prevention and treatment of HTS, which was considered as an outline for scar management (37). Surgical excision combined with adjuvant therapies such as steroids, pressure garments and silicone gel is still the most common current management (38). There are similar studies published in 2014 by Gold et al. (39, 40), which tried to standardize scar management by establishing safe and effective treatment options in order to apply in routine clinical practice. They conducted a comprehensive search of the MEDLINE database over the past 10 years and suggested that the most significant advances were laser therapy (41) and 5-fluorouracil (42). Emerging therapies for HTS were also reported such as bleomycin (43), onion extract gel (44, 45), and Botulinum toxin A (46).

At present, a variety of therapeutic options that are available to treat HTS can be divided into surgical and non-surgical treatment.

1.1.6.1 Surgical therapy for HTS

Surgical excision is common management when used in combination with steroids and/or silicone gel sheeting. However, surgical excision of HTS without adjuvant therapy is associated with a high rate of recurrence, ranging from 50% to 80% (47). HTS resulting from excessive tension or wound complications can be treated effectively with surgery options including intramarginal excision, skin grafts, local flaps and free flaps combined with surgical taping and silicone gel sheeting. However, these technique are not suitable for immature scar.

There are two major kind of lasers, ablative nonselective lasers such as CO₂ laser and nonablative selective lasers such as pulse-dye laser. Ablative lasers might carry a higher risk while nonablative lasers have the advantage of improving scars without incision or wounding. The flash lamp-pumped pulsed dye laser is most extensively used to refine scars by causing direct destruction of the blood vessels and an indirect effect on the surrounding collagen, which result in collagen modeling and wound contraction (48).

1.1.6.2 Non-surgical therapy for HTS

Non-surgical management of HTS includes the use of pressure garments, intralesional corticosteroid administration, silicone gel sheets and so on. Pressure garment are commonly used and are supplied by several companies based on individual patient

measurements (49). Pressure therapy should be applied 24 hours a day until the scar is mature. The optimum pressure for effective treatment is still unknown, but the pressures applied should exceed capillary pressure and recommend that pressure be maintained between 24 and 30 mm Hg (37). The possible mechanism of pressure garment may relate to reduced fibroblast proliferation, decreased collagen synthesis and increased myofibroblast apoptosis (50, 51).

Intralesional corticosteroid administration is also widely used to alleviate HTS. Triamcinolone acetonide is the most commonly used corticosteroid. The administration should be confined to the dermal region of the scar with 10 to 40mg/ml at 2- to 6-weeks interval (52). Silicone gel is a cross-linked polymer of dimethylsiloxane, which has been used for treatment of immature scar. Applying silicone gel sheet topically is a noninvasive and relatively safe treatment since it may decrease the volume of HTS (53). It has been shown that silicone gel sheets may accelerate scar maturation and improve pigmentation, vascularity, pliability, pain and itchiness associated with HTS (54). Thus, prophylactic use of topical silicone gel following scar revision surgery may prevent the development of recurrent HTS (55).

1.2 Molecular basis of HTS

1.2.1 Cytokines in HTS formation

1.2.1.1 IL-1 α and TNF- α inhibit HTS

IL-1 has two subtypes, IL-1 α and IL-1 β . IL-1 α was found to promote the release of MMPs, activate MMP-1 and stimulate the degradation of ECM (56, 57). Thus, decreased levels of IL-1 α may lead to ECM accumulation and HTS. The expression of IL-1 α was found significantly lower in HTS than in normal skin from patients following breast reduction surgery (58). Quite different from IL-1 α , IL-1 β is found to be over-expressed in HTS compared to normal skin (59).

TNF- α participates in the early inflammation stage and the ECM remodeling phase. TNF- α expression was shown to be decreased in HTS compared to normal skin, which indicated that TNF- α may be important for wound healing and HTS might be partially a consequence of a decreased amount of TNF- α (60). Another experiment demonstrated that TNF- α could suppress transforming growth factor beta-1 (TGF- β 1)-induced myofibroblasts phenotypic genes such as α -SMA at the mRNA level as well as at the Smad signaling pathway of TGF- β 1 (61).

1.1.1.2 Inappropriate release of IL-6 leads to HTS

IL-6 is also involved in the wound healing process. It is one of the major regulators of macrophages for stimulation, angiogenesis and ECM synthesis (62). IL-6 could also cause fibrotic diseases such as pulmonary fibrosis and scleroderma (63, 64). In addition, IL-6 was reported to be highly expressed in fibroblasts from HTS tissue compared to normal fibroblasts, influencing scar formation by modulating fibroblasts (65). In order to further investigate the function of IL-6, fibroblasts from HTS were treated with IL-6. Results showed an absence of any up-regulation of MMP-1 and MMP-3, indicating that suppression of MMPs may play a role in the excessive accumulation of collagen formed in HTS (66). In fetal fibroblasts, there was less IL-6 produced compared to adult fibroblasts and the addition of exogenous IL-6 caused scar formation instead of scarless wound healing (67). However, IL-6 knock-out mice showed delayed wound healing (68).

1.2.1.3 IL-10 plays an important role in scarless wound healing by regulating pro-inflammatory cytokines

IL-10 is produced by T helper cells and it could mediate the growth or functions of various immune cells including T cells and macrophages. It has been established that IL-10 acts as a key anti-inflammatory cytokine, which could limit or terminate the inflammatory processes (69). Neutralizing antibodies of IL-10 were administered into incisional wounds in mice and the results demonstrated an inhibited infiltration of

neutrophils and macrophages and an over-expression of monocyte chemoattractant protein-1 (MCP-1), IL-1 β , TNF- α (70) and IL-6 (71). This is supported by another study that IL-10 significantly inhibited lipopolysaccharide (LPS)-induced IL-6 production at a transcriptional level (72). A study tried to evaluate whether IL-10 could change the innervated conditions of full thickness excisional wounds created on the dorsal surface of CD1 mice. The results showed only temporary changes during the wound healing process but no significant changes at 84 days after treatment. However, wounds treated with IL-10 recovered similarly to normal skin compared to the wounds treated with PBS (73). Another experiment reported that scar appeared in IL-10 knockout fetal mice compared to scarless wound healing in the control group (74). A more recent study showed that IL-10 could provide an optimal environment for fetal and postnatal scarless wound healing (75). A similar study also over-expressed IL-10 but in adult murine wounds. The results showed that increased IL-10 reduced inflammation, collagen deposition and created improved wound healing conditions (76).

1.2.1.4 Anti-fibrotic molecules, decorin (DCN) and interferon-alpha2b (IFN- α 2b) inhibit HTS formation by inhibiting TGF- β and regulating fibroblasts

Recently, more research focused on small leucine-rich proteoglycans (SLRPs), a small component of ECM molecules, which contain several repeated leucine-rich regions and cysteine residues. The major SLRPs are DCN, biglycan, lumican, and fibromodulin (77). The most common SLRPs studied is DCN, which is abundantly expressed in the

dermis and connective tissue (78). As well, it appears to promote collagen fibrillogenesis, cell differentiation and inhibits the bioactivity of growth factors such as TGF- β (79). We have reported different levels of DCN in burn wounds with suppressed expression for the first 12 months, then significantly higher expression after one to two years, decreasing to resemble the expression seen in normal skin after three years (80). DCN is considered to be an inhibitor of TGF- β . Animal studies using bleomycin-injected mice treated with adenovirus vector-derived DCN showed that DCN significantly reduced the fibrosis caused by bleomycin by blocking the fibrotic effect of TGF- β (81). Wang et al. previously reported that deep dermal fibroblasts might contribute to HTS formation because of a decrease in DCN production (82). What's more, DCN was used to treat superficial and deep dermal fibroblasts where increased cell apoptosis was seen in superficial dermal fibroblasts compared to deep dermal fibroblasts, suggesting DCN-induced apoptosis might play an anti-fibrotic role (19). Further study was performed to clarify the interaction between SLRPs and TGF- β 1 in superficial and deep wounds to demonstrate how the decreased expression of DCN and increased presence of TGF- β 1 in deep dermal fibroblasts contributes to the formation of HTS (83).

IFN could be divided into three subtypes, type 1 IFN (including IFN- α and IFN- β), type 2 IFN [IFN- γ , known as a T helper type 1 (Th1) cytokine] and type 3 IFN (IFN- λ) (84). IFN- α is produced by leukocytes and fibroblasts, while IFN- γ is produced by T lymphocytes such as activated T cells (85). IFN- α and IFN- γ could decrease cell proliferation and collagen synthesis in normal and HTS fibroblasts *in vitro* (86). IFN- α 2b is an antiviral drug originally used for viral infections and some forms of cancer and has recently been shown to increase collagenase mRNA levels and activity and reduce the

activity of tissue inhibitors of metalloproteinases-1 (TIMP-1) (87), thereby decreasing HTS formation. Further studies were carried out focusing on IFN- α 2b because of the anti-fibrotic effects it exhibited. IFN- α 2b exposure to matched pairs of human HTS and normal fibroblasts could inhibit wound contraction by decreasing fibroblast-populated collagen lattices (88). Patients with severe HTS treated with IFN- α 2b showed a significant improvement in scar quality and volume during the therapy with a significant decrease in serum TGF- β levels (89). Treating HTS and normal fibroblasts with IFN- α 2b or IFN- γ demonstrated that TGF- β protein production was antagonized in part by the down-regulation of TGF- β 1 mRNA levels (90). Additionally, IFN- α 2b treatment decreased angiogenesis in HTS tissue (82). In a double blind placebo controlled trial in 21 burn patients, the administration of IFN- α 2b to burn patients down-regulated stromal cell-derived factor-1 (SDF-1)/ C-X-C chemokine receptor type 4 (CXCR4) signaling in HTS tissues limiting the formation of HTS (91), supporting the contention that IFN- α 2b is an anti-fibrotic protein inhibiting HTS formation.

1.2.1.5 Chemokines contribute to HTS formation by recruiting monocytes into wound sites

Chemokines are small 8-10 kilodalton proteins that induce chemotaxis in responsive cells surrounding the site of injury. They can be divided into four types depending on the spacing and location two cysteine residues in the molecules and include CC, CXC, C and CX3C subfamilies (92).

SDF-1, also known as CXCL12, belongs to CXC group. SDF-1 is similarly expressed in humans, swine and rat skin and is produced by pericytes, endothelial cells and fibroblasts (93). CXCR4 is a CXC chemokine receptor and it exclusively binds to SDF-1, which is unique among receptors because most chemokines have more than one receptor and most receptors have more than one ligand (94). SDF-1/CXCR4 signaling pathway mediates the migration of hemotopoietic cells from fetal liver to bone marrow (95), and could also stimulate angiogenesis by recruiting progenitor cells (96). Studies focused on the functions of SDF-1/CXCR4 signaling have suggested that it involves not only in the tumor metastasis and vascularization but also in the pathogenesis of fibroproliferative diseases (97, 98). Recent studies found up-regulated SDF-1 expression in the HTS tissue and serum of the burn patients as well as increased number of CD14⁺ CXCR4⁺ cells in the peripheral blood mononuclear cells, which suggested that SDF-1/CXCR4 signaling could recruit these CXCR4⁺ cells such as monocytes to the prolonged inflamed injured site and contribute to HTS formation (99). In order to further verify the role of SDF-1/CXCR4 signaling in HTS formation, the CXCR4 antagonist CTCE-9908 was used to inhibit the SDF-1/CXCR4 effect on the human HTS-like nude mouse model. The study showed that CTCE-9908 significantly attenuated scar formation and contraction, reduced the number of macrophages in the tissue, which was differentiated and replenished by CXCR4 expressing monocytes in the circulation (100). These findings support the role of SDF-1/CXCR4 in HTS formation and suggest an important role of macrophages in HTS formation.

Another chemokine involved in the formation of HTS is MCP-1. It belongs to the CC chemokine subfamily and has two receptors, CCR2 and CCR4 (101). Being a major

chemoattractant, it is secreted by macrophages, endothelial cells and fibroblasts. MCP-1 recruits monocytes and dendritic cells to the inflammatory sites (102, 103). A previous study showed that MCP-1 could stimulate fibroblast collagen production in the lung through an up-regulation of endogenous TGF- β (104). A later experiment investigated the role of MCP-1 in fibrosis using MCP-1 knockout mice. Results showed that fibrosis was diminished in MCP-1 knockout mice compared to the bleomycin-induced fibrosis control group (105). Enhanced release of MCP-1 by keloid CD14⁺ cells stimulated fibroblast proliferation through the protein kinase B signaling pathway and might trigger keloid development (106). A study from our research group demonstrated a significant increase of MCP-1 expression in fibroblasts from HTS compared to normal fibroblasts further suggesting a dominant role for MCP-1 in fibrotic diseases (107).

1.2.2 Growth factors in HTS formation

1.2.2.1 TGF- β plays a pivotal role in HTS formation

TGF- β is one of the most important growth factors that regulate tissue regeneration, cell differentiation, embryonic development and regulation of the immune system (108-110). Recent studies showed that TGF- β not only involves in normal wound healing processes but also contributes to fibroproliferative disorders such as pulmonary fibrosis (111) and HTS (112). TGF- β has three isoforms, TGF- β 1, TGF- β 2 and TGF- β 3 (113). Shah et al. used the neutralizing antibody to TGF- β 1 and TGF- β 2 in cutaneous wounds of

adult rodents and found reduced cutaneous scarring formation (114). A subsequent study from Shah and colleagues reported that exogenous addition of TGF- β 3 to cutaneous rat wounds reduced scarring, indicating that TGF- β 1 and TGF- β 2 were related to cutaneous scarring while TGF- β 3 should be considered as a therapeutic agent against scarring (115). A more recent study treated the rabbit ear wounds with anti-TGF- β 1, 2, 3 monoclonal antibodies at different time points of wound healing and early injection of antibodies showed delayed wound healing while the injections of middle or later time points remarkably reduced HTS formation, which implicated the indispensable roles of TGF- β 1, 2, 3 in early stage of wound healing (116). The transcriptional factor forkhead box protein O1 (FOXO1) has recently been found to be important as a regulator in wound healing. It exerts its effect through regulation of TGF- β 1 expression from oxidative stress. The absence of FOXO1 reduced TGF- β 1 expression and led to impaired re-epithelialization of wounds (117). TGF- β has multiple surface receptors, but TGF- β receptor I (TGF- β RI) and TGF- β RII appear to be the predominant forms. TGF- β RI was found to be increased while TGF- β RII was decreased in HTS (118). Another experiment verified that truncated TGF- β RII could inhibit scar formation in rat wounds (119).

There are various types of signaling pathways for TGF- β 1. The most important one is the Smad pathway (Fig. 1.4). Smads are intracellular regulatory signal transduction proteins that respond to activation of the TGF- β receptor complex. Smad proteins can be classified into three categories, the receptor-regulated Smads (R-SMADs), the common mediator Smads (Co-SMADs) and the inhibitory Smads (I-SMADs) (120). Classically, intracellular signaling of TGF- β 1 is initiated after latent TGF- β binding proteins are dissociated from the complex. The activated TGF- β 1 is released and binds to TGF- β RII,

which then activates the TGF- β RI. These two receptors are a ligand-dependent complex of heterodimeric transmembrane serine/threonine kinases. There are two isoforms of TGF- β RI that are involved in the signaling pathway known as activin-receptor-like kinase 1 and 5 (ALK 1 and ALK 5) (121). The signaling pathway progresses when R-SMADs are phosphorylated by ALK 1 and ALK 5 respectively (ALK1 phosphorylates Smad 1, 5, 8 and ALK5 phosphorylates Smad 2, 3). The activated R-SMADs combine with the common mediator Smad 4 and then translocate into the nucleus where they function as transcription factors or participate in transcriptional control of other specific genes involved. I-SMADs (Smad 6 and Smad 7) antagonize the effects of the other two types of Smads, the R-SMADs and Co-SMADs by binding to TGF- β RI. In this way, phosphorylation of the R-SMADs and Smad 4 are inhibited. Thus, I-SMADs are considered to be the negative feedback regulators in the signaling pathway (122). Decreased expression of Smad 7 in primary fibroblasts appears to decrease expression of COL1 and COL3 in a number of inflammatory disorders leading to fibrosis (123, 124). Non-Smad signaling pathways such as mitogen-activated protein kinase (MAPK), extracellular signal-regulated kinases and the c-Jun N-terminal kinases pathway have also been implicated with TGF- β signaling, but the exact mechanisms are not yet clear (125, 126).

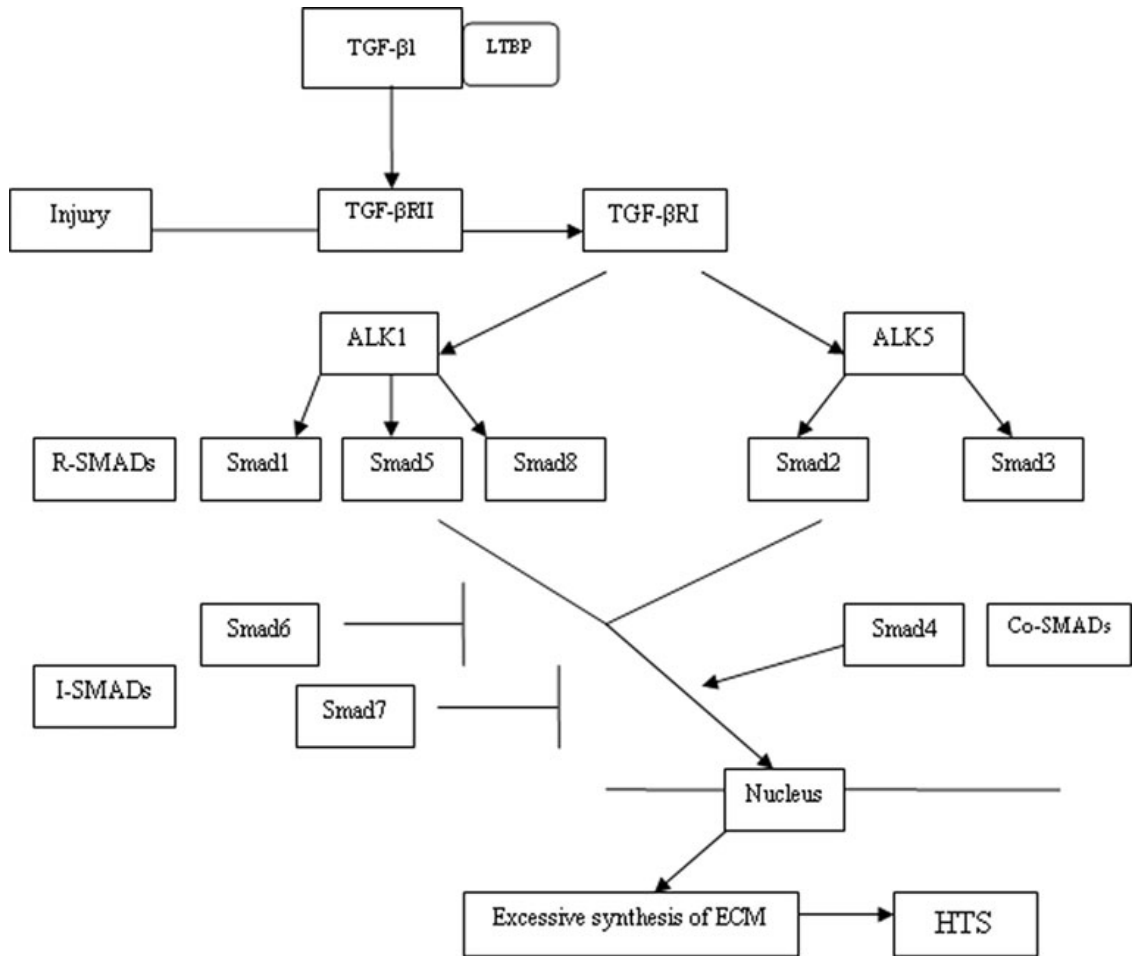


Fig 1.4. The TGF-β1 Smad signaling pathway contributes to HTS. TGF-βRI is activated after TGF-β1 binds to TGF-βRII. R-SMADs are then phosphorylated by ALK1 and ALK 5, two isoforms of TGF-βRI. The activated R-SMADs bind with Smad 4 and then translocate into nucleus and act as transcription factors. I-SMADs antagonize the effects of the R-SMADs and Co-SMADs.

Many studies indicate that aberrant TGF-β expression plays a pivotal role in HTS formation. For example, a previous study showed that the serum level of TGF-β1 was up-

regulated locally and systemically in burn patients and a significant clinical improvement in scar quality and volume was obtained after IFN- α 2b therapy, which was associated with normalization of serum TGF- β 1 (89). Treatment of site-matched HTS and normal fibroblasts with IFN- α 2b and IFN- γ showed antagonized TGF- β 1 protein production, down-regulation of TGF- β 1 mRNA levels (90). Tredget et al. made superficial partial-thickness ear wound and full-thickness back wounds on a transgenic mouse over-expressing TGF- β 1 in order to investigate the endogenous derived TGF- β 1 on wound re-epithelialization. The findings suggested that over-expression of TGF- β 1 speeded the rate of wound closure in partial-thickness wounds; whereas, over-expression of TGF- β 1 slowed the rate of wound re-epithelialization in full-thickness wounds (127). Another study created superficial and deep horizontal dermal scratch experimental wounds on the anterior thigh of adult male patients in order to characterize the related expression of TGF- β 1 and TGF- β 3. HTS formed after injuries to the deep dermis while superficial wounds healed with minimal or no scarring. Higher TGF- β 1 and lower TGF- β 3 expression was found in deep wounds compared to superficial wounds, suggesting the pivotal role of TGF- β 1 in HTS formation (83).

1.2.2.2 Connective tissue growth factor (CTGF) acts as a downstream mediator of TGF- β 1 signaling pathway and is involved in HTS formation

CTGF, also known as CCN2, is a pleiotropic cytokine that is induced by TGF- β 1 in dermal fibroblasts and is considered to be a downstream mediator of TGF- β 1 (128). The

main role of CTGF is to interact with signaling proteins such as TGF- β 1 for the regulation of cell proliferation, differentiation, adhesion, ECM production and granulation tissue formation (129, 130). This collaboration between CTGF and TGF- β 1 has contributed to the pro-fibrotic properties of TGF- β 1 confirming the role of CTGF for TGF- β 1 induction as a co-factor of gene expression.

The expression of CTGF was found to be increased in cultured fibroblasts from HTS, keloids and chronic fibrotic disorders (131). In addition, cultured fibroblasts from HTS showed an increased expression of CTGF after stimulation by TGF- β (132). In order to evaluate the role of CTGF in HTS formation, a rabbit animal model was established by Sisco et al. Antisense therapy was used to inhibit the expression of CTGF. Real-time reverse transcription polymerase chain reaction demonstrated an increased expression of CTGF in scar tissue and decreased CTGF expression after the intradermal injection of antisense oligonucleotides. The study showed that inhibition of CTGF at different times in wound healing has a substantial effect on reducing HTS (133). Another experiment used CTGF small interfering RNA (siRNA) to successfully block the increase in CTGF mRNA levels and the result demonstrated that CTGF could regulate the gene expression of ECM, tissue inhibitor metalloproteinases and partial function of TGF- β 1 (134). In order to elucidate the pathophysiological function of CTGF, CTGF knock-out mice were used in the experiment and those mice died immediately after birth due to malformation of the rib cages. As well, the embryonic fibroblasts from this animal model showed an inability of adhesion and α -SMA formation. All these results suggest that CTGF functions in ECM adhesion and production (135, 136).

Taken together, CTGF acts as a downstream mediator of the TGF- β 1 signaling pathway, directly involved in ECM synthesis and assists with TGF- β 1 in the pathogenesis of HTS.

1.2.2.3 Platelet-derived growth factor (PDGF) is essential to wound healing and the over-expression of PDGF is important in the formation of HTS

PDGF has five isoforms, including PDGF-AA, PDGF-AB, PDGF-BB, PDGF-CC and PDGF-DD which function via the activation of three transmembrane receptor tyrosine kinases (137). PDGF is produced by degranulated platelets in the early phase of the wound healing process and it is also secreted by macrophages during the proliferative phase of wound healing (138). In wound healing-impaired mice, the expression of PDGF and their receptors decreased (139). Moreover, PDGF showed reduced expression in chronic human non-healing ulcers compared to the fresh surgically created acute wounds (140). All these studies support the important role of PDGF in wound healing. However, PDGF also has an important role in several fibrotic diseases including scleroderma, lung and liver fibrosis by promoting the growth and survival of myofibroblasts (141). PDGF was found to mediate the deposition of collagen in fibroblasts and it was highly over-expressed in both the epidermis and the dermis of HTS. Over-production of collagen was not only related to high levels of TGF- β 1, but also with increased expression of PDGF (142). Another experiment showed that PDGF stimulated myofibroblast formation and increased TGF- β RI and TGF- β RII expression (143).

Although there are a lot of studies showing that PDGF plays a role in the pathogenesis of HTS, the exact molecular mechanism is still unknown.

1.2.2.4 Inhibitory effect of basic fibroblast growth factor (bFGF) on HTS via the regulation of collagen production, myofibroblast differentiation and TGF- β receptor expression

Fibroblast growth factors (FGFs) are a large family of growth factors that consist of 22 members with similar structural polypeptides. They have four receptors, which are transmembrane protein tyrosine kinases (144, 145). Among the growth factors that play roles in wound healing, bFGF is particularly important (146). bFGF is produced by keratinocytes and is found in the early stages of wound healing. It stimulates growth and differentiation of several types of cells, such as fibroblasts (147). In a rat model, bFGF was detected in granulation tissue including regenerated epidermis and newborn capillaries (148). As well, bFGF was found to promote wound healing by stimulating angiogenesis and granulation tissue proliferation (149). However, bFGF might inhibit the granulation tissue formation by promoting apoptosis (150) and affect tumor growth (151).

Evidence for the importance of bFGF in the pathogenesis of HTS was provided by Tiede et al. that bFGF reduced α -SMA expression by inhibiting myofibroblast differentiation and it also decreased TGF- β RI and TGF- β RII expression (143). In a rabbit HTS ear model, bFGF was applied every day for three months and the wounds showed decreased collagen expression and increased MMP-1 expression such that bFGF

appeared to have a negative effect on scar formation (152). In humans bFGF was administered to acute incisional wounds after suturing and the patients remained free from HTS (153). Hepatocyte growth factor (HGF) and MMP-1 have been demonstrated to have an anti-scarring effect (154). In a more recent study the expressions of HGF and MMP-1 were highly regulated in bFGF treated HTS and normal fibroblasts. The highly regulated MMP-1 expression might contribute to the increase of type I and type III collagen degradation, which leads to reduced scar formation. *In vitro*, bFGF treatment significantly decreased scar weight and the amount of collagen in nude mice that underwent human scar tissue transplantation (155). Therefore, bFGF can inhibit HTS formation and the mechanism might be related to the regulation of collagen production, myofibroblast differentiation and inhibition of TGF- β receptor expression.

1.2.3 MMP-1, 2, 9 are involved in the formation of HTS regulated by TIMPs

The MMPs are a number of zinc-dependent proteinases, which are known for their critical role in the tissue remodeling process (156, 157). The most particular characteristic of MMPs is the function of the proteolytic cleavage of collagen and degradation of other elements of the ECM (158). There are at least 23 types of MMPs. TIMPs are the specific proteins that regulate the function of MMPs and four specific types of TIMPs exist which block the activity of MMPs by binding to them in a 1:1 ratio (159).

The over-expression of MMPs could result in an imbalance between ECM production and degradation, which could lead to chronic ulcers (160). Alternately, the

alterations of MMPs and TIMPs expression could cause liver cirrhosis the result of a reduction of collagen degradation and excessive accumulation of ECM (161). As mentioned, TGF- β 1 acts as a potent inducer of the differentiation of myofibroblasts by stimulating the expression of α -SMA and it reduces the activity of MMPs by stimulating TIMPs synthesis in fibroblasts. In this way, the degradation process of ECM by MMP is abrogated. Meanwhile, the ECM deposition by fibroblasts is promoted by TGF- β 1. All of these features contribute to the formation of HTS (162).

Many types of MMPs and TIMPs are considered to be related to HTS formation. Several studies showed that MMP-1 expression is decreased in HTS which is an important transcriptional change in HTS and its reversal could be a new therapeutic approach for the treatment of HTS (155, 163). Ghahary et al. showed that differentiated keratinocyte-releasable stratifin (14-3-3 sigma) could stimulate MMP-1 expression in dermal fibroblasts through c-fos and p38 MAPK pathway (164), which may control degradation of the major dermal ECM components and provide useful targets for clinical intervention of HTS formation (165). However, this stimulatory effect could be suppressed by insulin treatment (166). A subsequent study showed that the levels of MMP-2 and MMP-9 were up-regulated by the interaction between fibroblasts and keratinocytes, which may favor resolution of accumulated ECM components (167).

An early study showed that decreased expression of TIMP-1 with the subsequent increased secretion of MMPs caused delayed healing of chronic ulcers (168). A study using athymic nude mice as an animal model showed that MMP-9 was up-regulated in scarless wound healing (169). Similar experiments demonstrated that the expressions of MMP-1 and MMP-9 were highly regulated in scarless fetal rat wounds (170). A human

study of HTS, keloids, atrophic scars from different patients and different regions of the body suggested that MMP-9 played a leading role in scar-free healing (171). A more recent study showed that by transfection of Smad interacting protein 1 (SIP1) to the HTS fibroblasts, MMP-1 expression was up-regulated while COL1A2 was decreased. As well, the knockdown of SIP1 in normal fibroblasts up-regulated COL1A2 levels induced by TGF- β 1. All these findings suggest that SIP1 could be a regulator of skin fibrosis and SIP1 depletion in HTS could result in the up-regulation of COL1A2 and the down-regulation of MMP-1, leading to excessive accumulation of ECM along with formation of HTS (172). Decreased levels of MMP-2, MMP-9 and increased levels of TIMP-1 were found in patients with HTS suggesting that the elevated systemic TIMP-1 concentration might contribute to tissue fibrosis, leading to HTS formation (173). A recent experiment compared TIMP-1 expression in normal skin and HTS, and the result exhibited relatively strong expression of TIMP-1 in HTS biopsies in contrast with very low levels of TIMP-1 in normal skin (174).

1.3 The cellular mechanism of HTS

1.3.1 Keratinocytes and mast cells participate in scar pathogenesis

It is well accepted that fibroblasts and myofibroblasts play essential roles in fibrotic diseases due to their abilities to generate excessive collagen in abnormal wound healing conditions (175, 176). However, growing evidence suggests that other cells actively

participate in scar pathogenesis, for example, keratinocytes and mast cells (177, 178). When co-cultured with keratinocytes, fibroblasts exhibited significant proliferation activity (179). The proliferation of dermal fibroblasts can also be stimulated by intercommunication of epidermal keratinocytes while decreasing the collagen production (180). The activated keratinocytes in HTS tissue showed abnormal epidermal-mesenchymal interactions due to delayed re-epithelialization and prolonged epidermal inflammation, indicating that abnormal wound healing such as severe burn injuries may end up with HTS formation because the regulation of keratinocytes to fibroblasts is impaired (181). However, independently co-culturing layered fibroblasts and keratinocytes on collagen-glycosaminoglycan scaffolds, aiming to assess the influence of keratinocytes and layered fibroblasts on the characteristics of tissue-engineered skin, showed that keratinocytes reduced fibrotic remodeling of the scaffolds by deep dermal fibroblasts, demonstrating an anti-fibrotic role of keratinocytes on layered fibroblasts in a 3D microenvironment (182). In addition mast cells appear to activate fibroblasts through gap junction intercellular communication (GJIC), indicating that mast cell-fibroblast GJIC may also play a role in fibrosis (183). Eliminating the mast cell or its GJIC with fibroblasts may prevent HTS formation or reduce the severity of fibrosis (184). Mast cells are able to stimulate the proliferation of fibroblasts by releasing biological mediators such as histamine, chymase and tryptase via degranulation, which leads to the promotion of fibrogenesis (185, 186). Additionally, histamine is able to enhance the effect on fibroblast migration and proliferation *in vitro* (187). More histamine was found in HTS mast cells compared to normal skin mast cells after stimulation by a neuropeptide, substance P (188). In an *in vivo* experiment, histamine was found significantly elevated in the plasma

of patients with HTS compared to age-matched normal volunteers (189). The elevated histamine can cause vasodilation and itchiness, resulting in the typical pruritic behavior that severely affects patients with HTS (190).

1.3.2 Differences in cellular characteristics of normal dermal and HTS fibroblasts

Fibroblasts are the most common cell in connective tissue and are one of the key elements in wound healing. The main function of fibroblasts is to maintain the physical integrity of connective tissue, participate in wound closure as well as produce and remodel ECM (38, 191). However, fibroblasts from HTS behave quite differently than normal fibroblasts. HTS tissue has greater amounts of fibroblasts that exhibit an altered phenotype than normal skin (176). HTS fibroblasts show higher expression of TGF- β 1 than normal fibroblasts (192). The increase or prolonged activity of TGF- β 1 leads to an overproduction and excess deposition of collagen by fibroblasts that often result in HTS formation (115). HTS fibroblasts have demonstrated reduced mRNA for collagenase as well as net reductions in the ability to digest soluble collagen as compared to their normal paired fibroblasts (193). HTS fibroblasts are also found to have a reduced ability to synthesize nitric oxide (NO), an important mediator of growth factor signaling, which regulates wound healing and collagenase through its anti-proliferative and anti-microbial effects (194). HTS fibroblasts differentiate into myofibroblasts and can account for increased ECM synthesis and contraction of tissue. They are a particular phenotype which differ from fibroblasts by their expression of α -SMA (195). HTS myofibroblasts

are less sensitive to apoptotic signals, coupled with their ability to produce more collagen and less collagenase than fibroblasts, may play an important role in HTS formation (196, 197).

1.3.3 Systemic response of Th1, Th2 and Th3 to HTS formation

The development of HTS involves a complicated interaction between inflammation and the immune response. Recent research suggests that it is not only the severity of inflammation, but the type of immune response links to the fibrotic conditions (198). Wounds of thymectomized rats depleted of CD4⁺ lymphocytes showed a significant decrease in ultimate strength, resilience and toughness while wounds of animals depleted of CD8⁺ lymphocytes showed a significant increase in ultimate strength, resilience and toughness, suggesting that CD4⁺ lymphocytes play a very important role in wound healing (199). As well, it is known that CD4⁺ T lymphocytes predominate in HTS tissue with less CD8⁺ T lymphocytes (200). Once activated by antigen presenting cells such as macrophages and dendritic cells, CD4⁺ T lymphocytes could differentiate into five subtypes of cells known as Th1, Th2, Th3, Th17 and T regulatory cells. Th1 and Th2 cells are the main subtypes defined in the murine model and each has a distinct cytokine profile (201). Th1 cells express IL-2, IFN- γ and IL-12 while Th2 cells express IL-4, IL-5 and IL-10. Th1 cytokines contribute to increased collagenase activity and matrix remodeling, which is anti-fibrotic and in contrast, Th2 cytokines are known to be pro-fibrotic (202). According to the different effects caused by Th1 and Th2 cytokines, HTS

fibroblasts are subject to a Th2 influence by presenting reduced collagenase activity and reduced nitric oxide synthase activity (194).

A burn mouse model showed diminished production of IL-2 and a shift in the Th2 phenotype with increased production of IL-4 and IL-10, indicating an inhibitory effect on Th1 function (203). Our group examined the Th1/Th2 cytokine ratio of 12 burn patients with HTS 4 weeks post-burn which showed a significant decrease in the Th1/Th2 ratio compared with 13 controls. The IL-4 levels in the patient group were significantly higher than controls and IFN- γ levels were significantly lower at 1 month post-burn, suggesting a role of the Th2 cytokine following burn injury (204). Another study detected serum cytokine levels from 22 burn patients showed elevated Th2 levels of IL-4 and IL-10, and reduced Th1 levels of IFN- γ and IL-12. IL-4 mRNA levels in HTS tissue was increased, while IFN- γ mRNA levels were decreased compared to normal skin (205).

Another study reported an increase in the frequency of CD4⁺/ TGF- β -producing T cells in the peripheral blood and HTS of burn patients (206). Medium derived from CD4⁺ T lymphocytes of burn patients was used to treat cultured dermal fibroblasts and results showed increased cell proliferation, collagen synthesis and α -SMA as well as a significant up-regulation of TGF- β compared to fibroblasts treated with medium derived from the CD4⁺ T lymphocytes of normal subjects. We suspect that these CD4⁺/TGF- β producing T cells are identical to Th3 cells which are enhanced by TGF- β , IL-4 and IL-10. Thus, a polarized Th2 systemic immune response enhances the subsequent development of Th3 cells that are capable of producing TGF- β inhibits Th1 cytokine expression and finally contributes to HTS formation (Fig. 1.5).

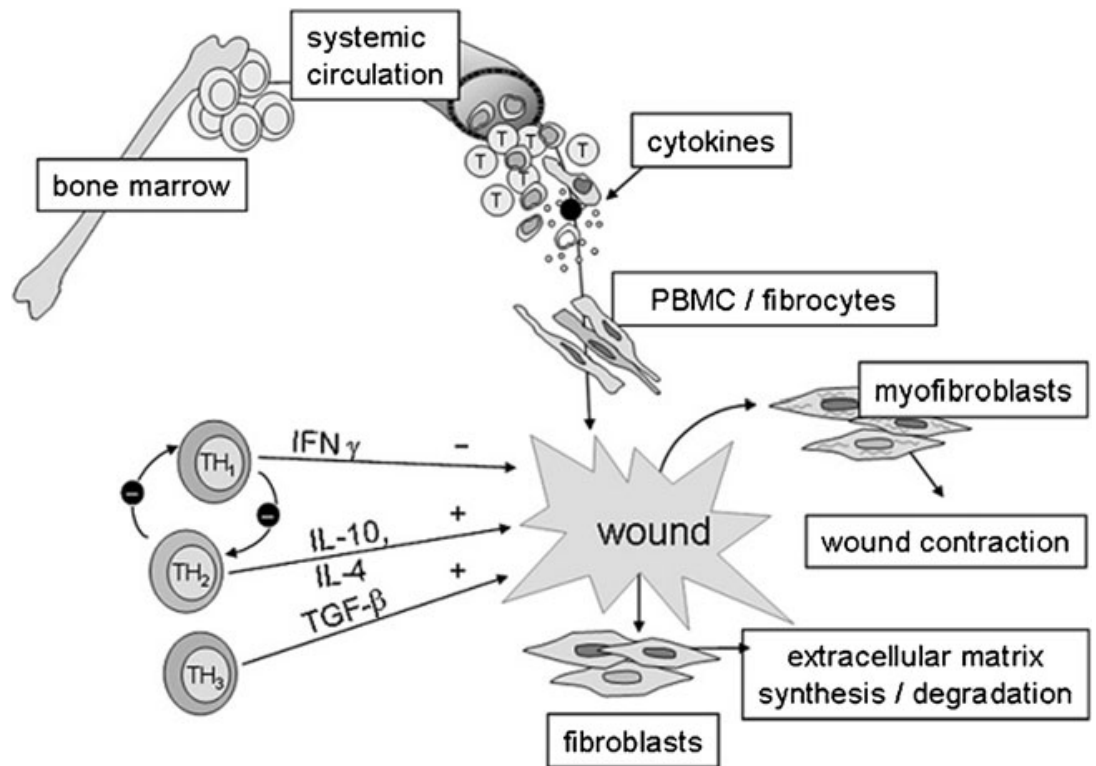


Fig 1.5. Hypothetical diagram of the role of Th1/Th2/Th3 cells in stimulating bone marrow stem cells to healing wounds. (From Armour A, Scott PG, Tredget EE (2007) Cellular and molecular pathology of HTS: basis for treatment. *Wound Repair Regen* 15:S6-17; with permission).

1.3.4 Macrophages are involved in HTS formation

Macrophages were first discovered by a Russian scientist, Élie Metchnikoff, in 1884 (207), which are an essential component of innate immunity and play a central role in the inflammation and host defense (208). They are differentiated from newly recruited

monocytes from the circulation and are considered to play a vital role in the whole wound healing process as recent studies showed that impaired wound healing was associated with decreased numbers of macrophage infiltrating at the injured site (209, 210). In addition, macrophages produce pro-inflammatory cytokines such as TNF- α , IL-1 β , IL-6, IFN- γ , which promote inflammation but also stimulate fibroblast proliferation. Macrophages can also produce TGF- β , which will stimulate myofibroblast proliferation (5). However, pathological functioning of macrophages in the abnormal wound healing process can lead to disordered wound healing, including the formation of HTS (211).

Macrophages have two phenotypes, classically activated macrophages or the so called M1 macrophages and alternatively activated macrophages or the so called M2 macrophages (198). The classification of M1 and M2 can be chased back to the early 1990s that IL-4 was found to induce inflammatory macrophages to adopt an alternative activation phenotype, distinct from that induced by IFN- γ (212). In the 2000s, this classification gained popularity and lots of reviews adopted the statement that M1 macrophages can be activated by LPS and IFN- γ , alone or in combination while M2 macrophages are activated by Th2 cytokines IL-4 or IL-13 *in vitro* (198, 213-215). This statement is also supported by many *in vitro* studies that M1 and M2 macrophages can be differentiated from human blood monocyte-derived macrophages or human monocytic cell line using LPS and IFN- γ or IL-4 and IL-13 respectively (216-218). Additionally, granulocyte macrophage colony-stimulating factor and macrophage colony-stimulating factor are considered to be the stimuli of M1 and M2 macrophages respectively, according to Fernando et al. in 2006 (219). After reassessment of the recent research, Fernando et al. proposed eight years later that the macrophage activation should be

governed by complex combinations of stimuli such as growth factors, cytokines, interaction with pathogens and mechanism of resolution (220). However, a study conducted by Mills CD et al. in 2000 proved otherwise that M1 and M2 macrophage activities do not need the presence of T or B lymphocytes. In that study, macrophages from T and B lymphocyte-deprived mice still produced distinct metabolic products of M1 and M2 macrophages (221). This finding has been recognized recently and more researchers realize the fact that T-lymphocyte-derived cytokines such as IFN- γ or IL-4 may facilitate macrophage polarization, but it doesn't mean that the macrophage polarization could not occur without T lymphocytes (222).

Mahdavian et al. reported that M1 and M2 macrophages have distinct opposite functions in the wound healing process (211). M1 macrophages can induce MMP-1 secretion and promote ECM degradation while M2 macrophages can secrete large amount of TGF- β 1, which can stimulate myofibroblast transformation and lead to ECM deposition. It is also hypothesized that a prolonged inflammatory phase will attract more macrophages, and those macrophages will initially be more of a pro-inflammatory M1 phenotype and then switch to a more pro-fibrotic M2 phenotype due to more intense stimuli from the microenvironment (223). The most distinct difference between M1 and M2 macrophages is based on the catabolism of L-arginine. M1 macrophages express nitric oxide synthase 2 (NOS2), which converts L-arginine to citrulline and NO while M2 macrophages express arginase-1 (Arg-1), which catabolizes L-arginine to ornithine, a precursor of polyamines and proline (221). The difference in catabolism between the two macrophage subsets might explain their distinct opposite functions in homeostasis and immunoregulation (211). Growing evidence suggests that M2 macrophages are not

constituted by a uniform population but can be further subdivided into M2a, M2b, M2c (215, 224). M2a macrophages are induced by IL-4 and IL-13, which are involved in the anti-parasitic immune response and are considered to be pro-fibrotic. M2b macrophages are induced by IL-1 β , LPS and immune complexes while M2c macrophages are induced by IL-10, TGF- β and glucocorticoids (215). The fourth type, M2d macrophages, are characterized by switching from a M1 phenotype into an angiogenic M2-like phenotype, which termed M2d by Leibovich et al. (225).

1.3.4.1 Polarized macrophages maintain tissue homeostasis under non-inflammatory conditions

Under injury, M1 macrophages are found to be predominant in the inflammatory phase while M2 macrophages are found to dominate the proliferation and tissue remodeling phase (226). In the inflammatory phase, M1 macrophages exhibit pro-inflammatory function by secreting pro-inflammatory cytokines such as IL-1 β , IL-6, TNF- α , NO, resulting in antimicrobial processes that contribute to the killing of invading organisms (227). They phagocytize tissue debris as well as dead cells and present the fragments of the pathogens to T helper cells. However, in the proliferation and tissue remodeling phase, the balance of macrophage activation toward an M2 phenotype occurs in order to promote clearance of debris, inhibit the production of inflammatory mediators and restore tissue homeostasis. M2 macrophages produce immunoregulatory cytokines such as IL-10 (228, 229) and promote angiogenesis and tissue repair by secreting VEGF,

PDGF and TGF- β 1 (110, 230). VEGF promotes angiogenesis while PDGF and TGF- β 1 stimulate fibroblast differentiation into myofibroblasts contributing to tissue regeneration. Additionally, M2 macrophages control the quantity of ECM by regulating the production of MMPs and TIMPs (231). M2 macrophages also express immunoregulatory proteins such as IL-10 that can decrease inflammatory response and promote wound healing (228, 229).

1.3.4.2 The role of polarized macrophages in fibrosis

Fibrosis is the excessive deposition of fibrous tissue in an organ or tissue after a reparative or reactive process. It can be benign but can also be used to describe the pathological state in response to disease-related injury that triggers a complex cascade of cellular and molecular reactions. This fibrogenic response may ultimately result in cellular dysfunction and organ failure if it progresses over a prolonged period of time (232). It is proposed that fibrosis has four major phases (233). The first phase is initiation of the reaction to primary injury to the organ, for example, epithelial damage. The second phase is the infiltration of inflammatory cells (neutrophils, monocytes, macrophages, mast cells, lymphocytes and eosinophils) and elevated pro-fibrotic cytokine expression, which leads to the third phase of the elaboration of ECM. The fourth phase is about the dynamic deposition and insufficient degradation of ECM, which promotes progression of fibrosis and ultimately organ failure (234). The common types of fibrosis in organs are pulmonary fibrosis (PF), renal fibrosis (RF), liver fibrosis (LF), cardiac fibrosis and so on.

The key role of macrophages in promoting fibrosis has been demonstrated. For example, selective depletion of macrophages during ongoing injury in CD11b-diphtheria toxin receptor mice caused a reduction in LF (235). As for polarized macrophages, M1 macrophages are mainly correlated to metabolic disorders (236), autoimmune diseases (237) and so on, but not fibrosis. On the contrary, numerous studies have implicated the role of M2 macrophages in the pathogenesis of fibrosis. In a RF model, depletion of M2 macrophages but not M1 macrophages inhibited RF while adoptive transplantation of M2 macrophages deteriorated RF (238, 239). As CCL18 stimulates collagen production in lung fibroblasts, an interaction between M2 macrophages and lung fibroblasts, involving a CCL18-driven positive feedback loop, may perpetuate fibrosis in PF (240).

1.3.4.3 Macrophages involve in HTS formation via SDF-1/CXCR4 chemokine pathway

Although studies suggest a close relationship between SDF-1/CXCR4 signaling and macrophage infiltration in the formation of HTS, more studies on the interaction between the two are still needed. Meanwhile, the roles of macrophage phenotypes in different phases of abnormal wound healing, like HTS-like nude mouse model, are to be investigated. Here we hypothesize that the monocytes, CXCR4 expressing cells in the circulation, will be attracted to the injured site via the SDF-1/CXCR4 signaling pathway due to concentration differences between the circulation and local tissue as well as the chemotactic effect of SDF-1. The monocytes then differentiate into M1 macrophages

(nuclear factor-kappa B [NF- κ B] and signal transducer and activator of transcription [STAT] 1 signaling pathways) and M2 macrophages (STAT3 and STAT6 signaling pathways) (241). M1 macrophages secrete pro-inflammatory cytokines such as IFN- γ , IL-1 β , TNF- α , IL-6, IL-8 and generate reactive oxygen and NO through the activation of NOS2. On the other hand, M2 macrophages inhibit the NOS2 activity via the activation of arginase-1. The distinct opposite and complementary functions of M1 and M2 macrophages will eventually lead to normal wound healing. However, in prolonged inflammatory environment such as wounds from severe thermal injury, large amounts of TGF- β 1 can be produced together with increased myofibroblast proliferation, which will result in ECM deposition and finally HTS formation (Figure 1.6).

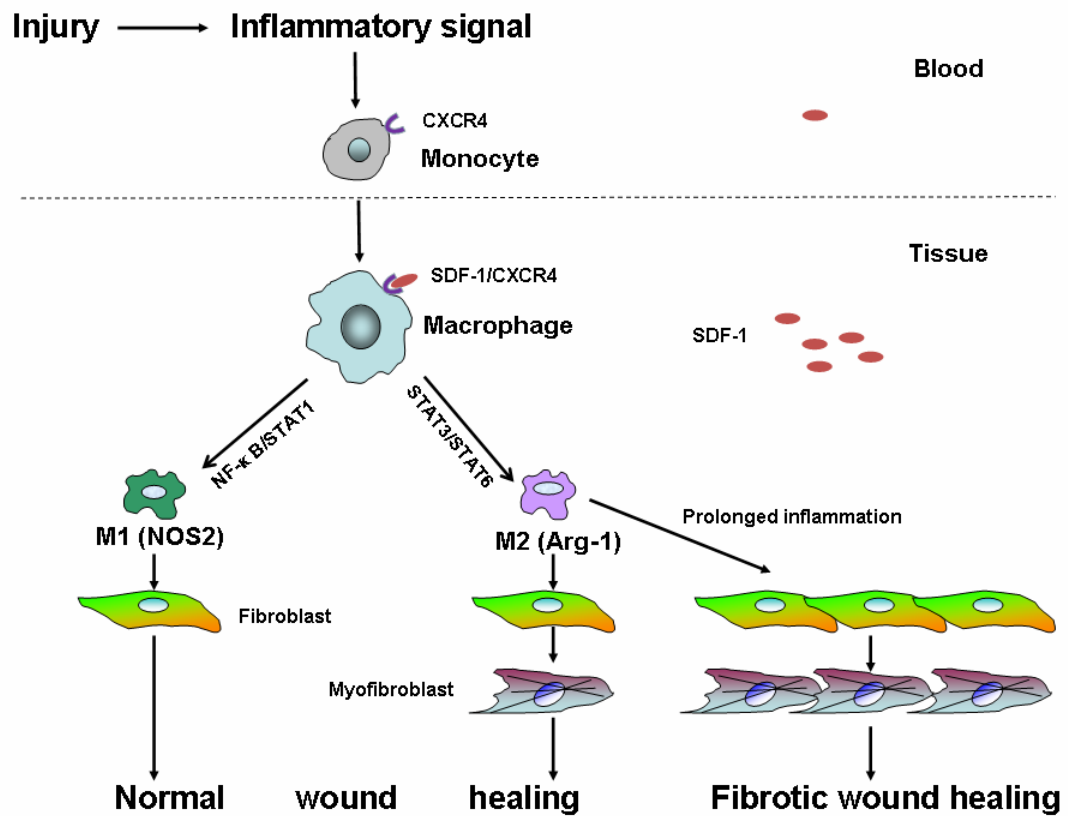


Fig 1.6. The roles of monocytes and polarized macrophages in HTS formation. We hypothesize that monocytes in the blood are recruited to the injured site via the SDF-1/CXCR4 signaling pathway and differentiate into polarized macrophages. The polarized M1 and M2 macrophages then exert their functions via various signaling pathways and involve in wound healing and HTS formation.

1.4 Conclusions and experimental design

Despite the complexity of HTS, more attention has been drawn to the molecular and cellular mechanism of HTS for technological and scientific advances such as the establishment of new animal models and *in vitro* techniques. In this chapter, four phases of normal wound healing are discussed before outlining the pathogenesis of HTS, illustrating the delicate balance of ECM deposition and degradation which influences the outcome of the wound healing process. Differentiating HTS from keloids is also important because the clinical and molecular mechanisms are different leading to distinct therapeutic outcomes. HTS formation is a dynamic, complex process that involves interactions between multiple factors such as cytokines, growth factors, MMPs as well as inflammatory cells. The role of cytokines such as IL-1, TNF- α , IL-6 and IL-10; growth factors such as TGF- β , CTGF, PDGF and bFGF as well as MMPs in HTS formation were discussed. Inflammatory cells such as keratinocytes, mast cells and macrophages are considered to be involved in HTS formation. As growing studies are focusing on the roles of polarized macrophages in fibrotic diseases, we focus on the role of polarized macrophages in HTS formation. The following chapters introduce experiments that are designed and conducted *in vitro* and *in vivo* in order to investigate the role of polarized macrophages in HTS formation, hoping to provide novel findings and potential new treatment and prevention of HTS.

Macrophages can be divided into classically activated macrophages (M1) and alternatively activated macrophages (M2) (198). Studies have reported that M1 macrophages are pro-inflammatory while M2 macrophages are pro-fibrotic (211, 223).

Thus, we hypothesized that M2 macrophages could promote the fibrogenic activities of human dermal fibroblasts by co-culture. An in vitro experiment was designed and conducted.

We also hypothesized that phase-dependent systemic depletion of macrophages would reduce HTS formation. Two in vivo experiments were designed. The first experiment was to investigate the natural behavior of M1 and M2 macrophages in the grafted skin as well as monocytes in the blood during the formation of HTS using the human HTS-like nude mouse model. The second experiment was to explore whether the phase dependent systemic depletion of macrophages based on the first in vivo experiment would reduce HTS formation.

The experiments would be able to provide evidence for the pro-fibrotic role of M2 macrophages in HTS formation and potential clinical strategy to the treatment and prevention of HTS.

1.5 References

1. Engrav LH, Garner WL, Tredget EE. Hypertrophic scar, wound contraction and hyper-hypopigmentation. *J Burn Care Res.* 2007;28:593-7.
2. Bombaro KM, Engrav LH, Carrougher GJ, Wiechman SA, Faucher L, Costa BA, et al. What is the prevalence of hypertrophic scarring following burns? *Burns.* 2003;29:299-302.
3. Reinke JM, Sorg H. Wound repair and regeneration. *Eur Surg Res.* 2012;49:35-43.
4. Miller MC, Nanchahal J. Advances in the modulation of cutaneous wound healing and scarring. *BioDrugs.* 2005;19:363-81.
5. Werner S, Grose R. Regulation of wound healing by growth factors and cytokines. *Physiol Rev.* 2003;83:835-70.
6. Robson MC, Steed DL, Franz MG. Wound healing: biologic features and approaches to maximize healing trajectories. *Curr Probl Surg.* 2001;38:72-140.
7. Midwood KS, Williams LV, Schwarzbauer JE. Tissue repair and the dynamics of the extracellular matrix. *Int J Biochem Cell Biol.* 2004;36:1031-7.
8. Eming SA, Krieg T, Davidson JM. Inflammation in wound repair: molecular and cellular mechanisms. *J Invest Dermatol.* 2007;127:514-25.
9. Bauer SM, Bauer RJ, Velazquez OC. Angiogenesis, vasculogenesis, and induction of healing in chronic wounds. *Vasc Endovascular Surg.* 2005;39:293-306.
10. Lau K, Paus R, Tiede S, Day P, Bayat A. Exploring the role of stem cells in cutaneous wound healing. *Exp Dermatol.* 2009;18:921-33.
11. Barker TH. The role of ECM proteins and protein fragments in guiding cell behavior in regenerative medicine. *Biomaterials.* 2011;32:4211-4.

12. Profyris C, Tziotzios C, Do Vale I. Cutaneous scarring: Pathophysiology, molecular mechanisms, and scar reduction therapeutics Part I. The molecular basis of scar formation. *J Am Acad Dermatol.* 2012;66:1-10; quiz 1-2.
13. Greenhalgh DG. The role of apoptosis in wound healing. *Int J Biochem Cell Biol.* 1998;30:1019-30.
14. Ghahary A, Shen YJ, Nedelec B, Wang R, Scott PG, Tredget EE. Collagenase production is lower in post-burn hypertrophic scar fibroblasts than in normal fibroblasts and is reduced by insulin-like growth factor-1. *J Invest Dermatol.* 1996;106:476-81.
15. Brown JJ, Bayat A. Genetic susceptibility to raised dermal scarring. *Br J Dermatol.* 2009;161:8-18.
16. Gauglitz GG, Korting HC, Pavicic T, Ruzicka T, Jeschke MG. Hypertrophic scarring and keloids: pathomechanisms and current and emerging treatment strategies. *Mol Med.* 2011;17:113-25.
17. Tredget EE, Nedelec B, Scott PG, Ghahary A. Hypertrophic scars, keloids, and contractures. The cellular and molecular basis for therapy. *Surg Clin North Am.* 1997;77:701-30.
18. Monstrey S, Hoeksema H, Verbelen J, Pirayesh A, Blondeel P. Assessment of burn depth and burn wound healing potential. *Burns.* 2008;34:761-9.
19. Honardoust D, Ding J, Varkey M, Shankowsky HA, Tredget EE. Deep dermal fibroblasts refractory to migration and decorin-induced apoptosis contribute to hypertrophic scarring. *J Burn Care Res.* 2012;33:668-77.
20. Dunkin CS, Pleat JM, Gillespie PH, Tyler MP, Roberts AH, McGrouther DA. Scarring occurs at a critical depth of skin injury: precise measurement in a graduated dermal scratch in human volunteers. *Plast Reconstr Surg.* 2007;119:1722-32; discussion 33-4.
21. Arno AI, Gauglitz GG, Barret JP, Jeschke MG. Up-to-date approach to manage keloids and hypertrophic scars: a useful guide. *Burns.* 2014;40:1255-66.
22. Tritto M, Kanat IO. Management of keloids and hypertrophic scars. *J Am Podiatr Med Assoc.* 1991;81:601-5.

23. Slemp AE, Kirschner RE. Keloids and scars: a review of keloids and scars, their pathogenesis, risk factors, and management. *Curr Opin Pediatr.* 2006;18:396-402.
24. Murray JC. Keloids and hypertrophic scars. *Clin Dermatol.* 1994;12:27-37.
25. Halim AS, Emami A, Salahshourifar I, Kannan TP. Keloid scarring: understanding the genetic basis, advances, and prospects. *Arch Plast Surg.* 2012;39:184-9. doi: 10.5999/aps.2012.39.3.184. Epub May 10.
26. Ehrlich HP, Desmouliere A, Diegelmann RF, Cohen IK, Compton CC, Garner WL, et al. Morphological and immunochemical differences between keloid and hypertrophic scar. *Am J Pathol.* 1994;145:105-13.
27. Ueda K, Furuya E, Yasuda Y, Oba S, Tajima S. Keloids have continuous high metabolic activity. *Plast Reconstr Surg.* 1999;104:694-8.
28. Tanaka A, Hatoko M, Tada H, Iioka H, Niitsuma K, Miyagawa S. Expression of p53 family in scars. *J Dermatol Sci.* 2004;34:17-24.
29. Younai S, Venters G, Vu S, Nichter L, Nimni ME, Tuan TL. Role of growth factors in scar contraction: an in vitro analysis. *Ann Plast Surg.* 1996;36:495-501.
30. Ledon JA, Savas J, Franca K, Chacon A, Nouri K. Intralesional treatment for keloids and hypertrophic scars: a review. *Dermatol Surg.* 2013;39:1745-57.
31. Schneider JC, Harris NL, El Shami A, Sheridan RL, Schulz JT, 3rd, Bilodeau ML, et al. A descriptive review of neuropathic-like pain after burn injury. *J Burn Care Res.* 2006;27:524-8.
32. Wilgus TA, Wulff BC. The Importance of Mast Cells in Dermal Scarring. *Adv Wound Care (New Rochelle).* 2014;3:356-65.
33. Holavanahalli RK, Helm PA, Kowalske KJ. Long-Term Outcomes in Patients Surviving Large Burns: The Musculoskeletal System. *J Burn Care Res.* 2015.
34. Stoddard FJ, Jr., Ryan CM, Schneider JC. Physical and psychiatric recovery from burns. *Surg Clin North Am.* 2014;94:863-78.

35. Robert R, Meyer W, Bishop S, Rosenberg L, Murphy L, Blakeney P. Disfiguring burn scars and adolescent self-esteem. *Burns*. 1999;25:581-5.
36. Zhu Z, Ding J, Shankowsky HA, Tredget EE. The molecular mechanism of hypertrophic scar. *J Cell Commun Signal*. 2013;7:239-52.
37. Mustoe TA, Cooter RD, Gold MH, Hobbs FD, Ramelet AA, Shakespeare PG, et al. International clinical recommendations on scar management. *Plast Reconstr Surg*. 2002;110:560-71.
38. Kwan P, Hori K, Ding J, Tredget EE. Scar and contracture: biological principles. *Hand Clin*. 2009;25:511-28.
39. Gold MH, Berman B, Clementoni MT, Gauglitz GG, Nahai F, Murcia C. Updated international clinical recommendations on scar management: part 1--evaluating the evidence. *Dermatol Surg*. 2014;40:817-24.
40. Gold MH, McGuire M, Mustoe TA, Pusic A, Sachdev M, Waibel J, et al. Updated international clinical recommendations on scar management: part 2--algorithms for scar prevention and treatment. *Dermatol Surg*. 2014;40:825-31.
41. Lee KK, Mehrany K, Swanson NA. Surgical revision. *Dermatol Clin*. 2005;23:141-50, vii.
42. Manuskiatti W, Fitzpatrick RE. Treatment response of keloidal and hypertrophic sternotomy scars: comparison among intralesional corticosteroid, 5-fluorouracil, and 585-nm flashlamp-pumped pulsed-dye laser treatments. *Arch Dermatol*. 2002;138:1149-55.
43. Aggarwal H, Saxena A, Lubana PS, Mathur RK, Jain DK. Treatment of keloids and hypertrophic scars using bleom. *J Cosmet Dermatol*. 2008;7:43-9. doi: 10.1111/j.473-2165.008.00360.x.
44. Draelos ZD. The ability of onion extract gel to improve the cosmetic appearance of postsurgical scars. *J Cosmet Dermatol*. 2008;7:101-4.
45. Chanprapaph K, Tanrattanakorn S, Wattanakrai P, Wongkitisophon P, Vachiramon V. Effectiveness of onion extract gel on surgical scars in asians. *Dermatol Res Pract*. 2012;2012:212945.:10.1155/2012/212945. Epub 2012 Aug 8.

46. Gassner HG, Brissett AE, Otley CC, Boahene DK, Boggust AJ, Weaver AL, et al. Botulinum toxin to improve facial wound healing: A prospective, blinded, placebo-controlled study. *Mayo Clin Proc.* 2006;81:1023-8.
47. Darzi MA, Chowdri NA, Kaul SK, Khan M. Evaluation of Various Methods of Treating Keloids and Hypertrophic Scars - a 10-Year Follow-up-Study. *British Journal of Plastic Surgery.* 1992;45:374-9.
48. Lee KK, Mehrany K, Swanson NA. Surgical revision. *Dermatologic Clinics.* 2005;23:141-+.
49. Macintyre L, Baird M. Pressure garments for use in the treatment of hypertrophic scars - a review of the problems associated with their use. *Burns.* 2006;32:10-5.
50. Armour A, Scott PG, Tredget EE. Cellular and molecular pathology of HTS: basis for treatment. *Wound Repair Regen.* 2007;15 Suppl 1:S6-17.
51. Anzarut A, Olson J, Singh P, Rowe BH, Tredget EE. The effectiveness of pressure garment therapy for the prevention of abnormal scarring after burn injury: a meta-analysis. *J Plast Reconstr Aesthet Surg.* 2009;62:77-84.
52. Atiyeh BS. Nonsurgical management of hypertrophic scars: evidence-based therapies, standard practices, and emerging methods. *Aesthetic Plast Surg.* 2007;31:468-92; discussion 93-4.
53. Ahn ST, Monafo WW, Mustoe TA. Topical silicone gel: a new treatment for hypertrophic scars. *Surgery.* 1989;106:781-6; discussion 6-7.
54. Momeni M, Hafezi F, Rahbar H, Karimi H. Effects of silicone gel on burn scars. *Burns.* 2009;35:70-4.
55. Gold MH, Foster TD, Adair MA, Burlison K, Lewis T. Prevention of hypertrophic scars and keloids by the prophylactic use of topical silicone gel sheets following a surgical procedure in an office setting. *Dermatologic Surgery.* 2001;27:641-4.
56. Heckmann M, Adelman-Grill BC, Hein R, Krieg T. Biphasic effects of interleukin-1 alpha on dermal fibroblasts: enhancement of chemotactic responsiveness at low concentrations and of mRNA expression for collagenase at high concentrations. *J Invest Dermatol.* 1993;100:780-4.

57. Elias JA, Gustilo K, Baeder W, Freundlich B. Synergistic stimulation of fibroblast prostaglandin production by recombinant interleukin 1 and tumor necrosis factor. *J Immunol.* 1987;138:3812-6.
58. Niessen FB, Andriessen MP, Schalkwijk J, Visser L, Timens W. Keratinocyte-derived growth factors play a role in the formation of hypertrophic scars. *J Pathol.* 2001;194:207-16.
59. Salgado RM, Alcantara L, Mendoza-Rodriguez CA, Cerbon M, Hidalgo-Gonzalez C, Mercadillo P, et al. Post-burn hypertrophic scars are characterized by high levels of IL-1beta mRNA and protein and TNF-alpha type I receptors. *Burns.* 2012;38:668-76.
60. Castagnoli C, Stella M, Berthod C, Magliacani G, Richiardi PM. TNF production and hypertrophic scarring. *Cell Immunol.* 1993;147:51-63.
61. Goldberg MT, Han YP, Yan C, Shaw MC, Garner WL. TNF-alpha suppresses alpha-smooth muscle actin expression in human dermal fibroblasts: an implication for abnormal wound healing. *J Invest Dermatol.* 2007;127:2645-55.
62. Witte MB, Barbul A. General principles of wound healing. *Surg Clin North Am.* 1997;77:509-28.
63. O'Donoghue RJ, Knight DA, Richards CD, Prele CM, Lau HL, Jarnicki AG, et al. Genetic partitioning of interleukin-6 signalling in mice dissociates Stat3 from Smad3-mediated lung fibrosis. *EMBO Mol Med.* 2012;4:939-51.
64. O'Reilly S, Ciechomska M, Cant R, Hugle T, van Laar JM. Interleukin-6, its role in fibrosing conditions. *Cytokine Growth Factor Rev.* 2012;23:99-107.
65. Xue H, McCauley RL, Zhang W, Martini DK. Altered interleukin-6 expression in fibroblasts from hypertrophic burn scars. *J Burn Care Rehabil.* 2000;21:142-6.
66. Dasu MR, Hawkins HK, Barrow RE, Xue H, Herndon DN. Gene expression profiles from hypertrophic scar fibroblasts before and after IL-6 stimulation. *J Pathol.* 2004;202:476-85.
67. Liechty KW, Adzick NS, Crombleholme TM. Diminished interleukin 6 (IL-6) production during scarless human fetal wound repair. *Cytokine.* 2000;12:671-6.

68. McFarland-Mancini MM, Funk HM, Paluch AM, Zhou M, Giridhar PV, Mercer CA, et al. Differences in wound healing in mice with deficiency of IL-6 versus IL-6 receptor. *J Immunol.* 2010;184:7219-28.
69. Moore KW, de Waal Malefyt R, Coffman RL, O'Garra A. Interleukin-10 and the interleukin-10 receptor. *Annu Rev Immunol.* 2001;19:683-765.
70. Sato Y, Ohshima T, Kondo T. Regulatory role of endogenous interleukin-10 in cutaneous inflammatory response of murine wound healing. *Biochem Biophys Res Commun.* 1999;265:194-9.
71. Fortunato SJ, Menon R, Swan KF, Lombardi SJ. Interleukin-10 inhibition of interleukin-6 in human amniochorionic membrane: transcriptional regulation. *Am J Obstet Gynecol.* 1996;175:1057-65.
72. Dagvadorj J, Naiki Y, Tumurkhuu G, Noman AS, Iftekar EKI, Koide N, et al. Interleukin (IL)-10 attenuates lipopolysaccharide-induced IL-6 production via inhibition of IkappaB-zeta activity by Bcl-3. *Innate Immun.* 2009;15:217-24.
73. Henderson J, Ferguson MW, Terenghi G. The reinnervation and revascularization of wounds is temporarily altered after treatment with interleukin 10. *Wound Repair Regen.* 2011;19:268-73. doi: 10.1111/j.524-475X.2011.00667.x.
74. Liechty KW, Kim HB, Adzick NS, Crombleholme TM. Fetal wound repair results in scar formation in interleukin-10-deficient mice in a syngeneic murine model of scarless fetal wound repair. *J Pediatr Surg.* 2000;35:866-72; discussion 72-3.
75. Gordon A, Kozin ED, Keswani SG, Vaikunth SS, Katz AB, Zoltick PW, et al. Permissive environment in postnatal wounds induced by adenoviral-mediated overexpression of the anti-inflammatory cytokine interleukin-10 prevents scar formation. *Wound Repair Regen.* 2008;16:70-9.
76. Peranteau WH, Zhang L, Muvarak N, Badillo AT, Radu A, Zoltick PW, et al. IL-10 overexpression decreases inflammatory mediators and promotes regenerative healing in an adult model of scar formation. *J Invest Dermatol.* 2008;128:1852-60.
77. Sidgwick GP, Bayat A. Extracellular matrix molecules implicated in hypertrophic and keloid scarring. *Journal of the European Academy of Dermatology and Venereology.* 2012;26:141-52.

78. Honardoust D, Varkey M, Hori K, Ding J, Shankowsky HA, Tredget EE. Small leucine-rich proteoglycans, decorin and fibromodulin, are reduced in postburn hypertrophic scar. *Wound Repair Regen.* 2011;19:368-78.
79. Schonherr E, Hausser HJ. Extracellular matrix and cytokines: a functional unit. *Dev Immunol.* 2000;7:89-101.
80. Sayani K, Dodd CM, Nedelec B, Shen YJ, Ghahary A, Tredget EE, et al. Delayed appearance of decorin in healing burn scars. *Histopathology.* 2000;36:262-72.
81. Kolb M, Margetts PJ, Galt T, Sime PJ, Xing Z, Schmidt M, et al. Transient transgene expression of decorin in the lung reduces the fibrotic response to bleomycin. *Am J Respir Crit Care Med.* 2001;163:770-7.
82. Wang J, Chen H, Shankowsky HA, Scott PG, Tredget EE. Improved scar in postburn patients following interferon-alpha2b treatment is associated with decreased angiogenesis mediated by vascular endothelial cell growth factor. *J Interferon Cytokine Res.* 2008;28:423-34.
83. Honardoust D, Varkey M, Marcoux Y, Shankowsky HA, Tredget EE. Reduced decorin, fibromodulin, and transforming growth factor-beta3 in deep dermis leads to hypertrophic scarring. *J Burn Care Res.* 2012;33:218-27.
84. Ladak A, Tredget EE. Pathophysiology and management of the burn scar. *Clin Plast Surg.* 2009;36:661-74.
85. Sarkhosh K, Tredget EE, Karami A, Uludag H, Iwashina T, Kilani RT, et al. Immune cell proliferation is suppressed by the interferon-gamma-induced indoleamine 2,3-dioxygenase expression of fibroblasts populated in collagen gel (FPCG). *Journal of Cellular Biochemistry.* 2003;90:206-17.
86. Tredget EE, Nedelec B, Scott PG, Ghahary A. Hypertrophic scars, keloids, and contractures - The cellular and molecular basis for therapy. *Surgical Clinics of North America.* 1997;77:701-&.
87. Ghahary A, Shen YJ, Nedelec B, Scott PG, Tredget EE. Interferons gamma and alpha-2b differentially regulate the expression of collagenase and tissue inhibitor of metalloproteinase-1 messenger RNA in human hypertrophic and normal dermal fibroblasts. *Wound Repair Regen.* 1995;3:176-84.

88. Nedelec B, Shen YJ, Ghahary A, Scott PG, Tredget EE. The effect of interferon alpha 2b on the expression of cytoskeletal proteins in an in vitro model of wound contraction. *J Lab Clin Med.* 1995;126:474-84.
89. Tredget EE, Shankowsky HA, Pannu R, Nedelec B, Iwashina T, Ghahary A, et al. Transforming growth factor-beta in thermally injured patients with hypertrophic scars: effects of interferon alpha-2b. *Plast Reconstr Surg.* 1998;102:1317-28; discussion 29-30.
90. Tredget EE, Wang R, Shen Q, Scott PG, Ghahary A. Transforming growth factor-beta mRNA and protein in hypertrophic scar tissues and fibroblasts: antagonism by IFN-alpha and IFN-gamma in vitro and in vivo. *J Interferon Cytokine Res.* 2000;20:143-51.
91. Ding J, Hori K, Zhang R, Marcoux Y, Honardoust D, Shankowsky HA, et al. Stromal cell-derived factor 1 (SDF-1) and its receptor CXCR4 in the formation of postburn hypertrophic scar (HTS). *Wound Repair and Regeneration.* 2011;19:568-78.
92. Fernandez EJ, Lolis E. Structure, function, and inhibition of chemokines. *Annu Rev Pharmacol Toxicol.* 2002;42:469-99.
93. Mirshahi F, Pourtau J, Li H, Muraine M, Trochon V, Legrand E, et al. SDF-1 activity on microvascular endothelial cells: consequences on angiogenesis in in vitro and in vivo models. *Thromb Res.* 2000;99:587-94.
94. Choi WT, An J. Biology and clinical relevance of chemokines and chemokine receptors CXCR4 and CCR5 in human diseases. *Exp Biol Med (Maywood).* 2011;236:637-47.
95. Zou YR, Kottmann AH, Kuroda M, Taniuchi I, Littman DR. Function of the chemokine receptor CXCR4 in haematopoiesis and in cerebellar development. *Nature.* 1998;393:595-9.
96. Nagasawa T. Role of chemokine SDF-1/PBSF and its receptor CXCR4 in blood vessel development. *Ann N Y Acad Sci.* 2001;947:112-5; discussion 5-6.
97. Balkwill F. Cancer and the chemokine network. *Nat Rev Cancer.* 2004;4:540-50.
98. Xu J, Mora A, Shim H, Stecenko A, Brigham KL, Rojas M. Role of the SDF-1/CXCR4 axis in the pathogenesis of lung injury and fibrosis. *Am J Respir Cell Mol Biol.* 2007;37:291-9. Epub 2007 Apr 26.

99. Ding J, Hori K, Zhang R, Marcoux Y, Honardoust D, Shankowsky HA, et al. Stromal cell-derived factor 1 (SDF-1) and its receptor CXCR4 in the formation of postburn hypertrophic scar (HTS). *Wound Repair Regen.* 2011;19:568-78. doi: 10.1111/j.524-475X.2011.00724.x.
100. Ding J, Ma Z, Liu H, Kwan P, Iwashina T, Shankowsky HA, et al. The therapeutic potential of a C-X-C chemokine receptor type 4 (CXCR-4) antagonist on hypertrophic scarring in vivo. *Wound Repair Regen.* 2014;22:622-30.
101. Craig MJ, Loberg RD. CCL2 (Monocyte Chemoattractant Protein-1) in cancer bone metastases. *Cancer and Metastasis Reviews.* 2006;25:611-9.
102. Hasegawa M, Sato S. The roles of chemokines in leukocyte recruitment and fibrosis in systemic sclerosis. *Frontiers in Bioscience.* 2008;13:3637-47.
103. Xu LL, Warren MK, Rose WL, Gong W, Wang JM. Human recombinant monocyte chemotactic protein and other C-C chemokines bind and induce directional migration of dendritic cells in vitro. *J Leukoc Biol.* 1996;60:365-71.
104. Gharaee-Kermani M, Denholm EM, Phan SH. Costimulation of fibroblast collagen and transforming growth factor beta1 gene expression by monocyte chemoattractant protein-1 via specific receptors. *J Biol Chem.* 1996;271:17779-84.
105. Ferreira AM, Takagawa S, Fresco R, Zhu X, Varga J, DiPietro LA. Diminished induction of skin fibrosis in mice with MCP-1 deficiency. *J Invest Dermatol.* 2006;126:1900-8.
106. Liao WT, Yu HS, Arbiser JL, Hong CH, Govindarajan B, Chai CY, et al. Enhanced MCP-1 release by keloid CD14+ cells augments fibroblast proliferation: role of MCP-1 and Akt pathway in keloids. *Exp Dermatol.* 2010;19:e142-50.
107. Wang J, Hori K, Ding J, Huang Y, Kwan P, Ladak A, et al. Toll-like receptors expressed by dermal fibroblasts contribute to hypertrophic scarring. *J Cell Physiol.* 2011;226:1265-73.
108. Alexandrow MG, Moses HL. Transforming growth factor beta and cell cycle regulation. *Cancer Res.* 1995;55:1452-7.

109. McGee GS, Broadley KN, Buckley A, Aquino A, Woodward SC, Demetriou AA, et al. Recombinant transforming growth factor beta accelerates incisional wound healing. *Curr Surg*. 1989;46:103-6.
110. Roberts AB, Sporn MB, Assoian RK, Smith JM, Roche NS, Wakefield LM, et al. Transforming growth factor type beta: rapid induction of fibrosis and angiogenesis in vivo and stimulation of collagen formation in vitro. *Proc Natl Acad Sci U S A*. 1986;83:4167-71.
111. Broekelmann TJ, Limper AH, Colby TV, McDonald JA. Transforming growth factor beta 1 is present at sites of extracellular matrix gene expression in human pulmonary fibrosis. *Proc Natl Acad Sci U S A*. 1991;88:6642-6.
112. Ghahary A, Shen YJ, Scott PG, Tredget EE. Immunolocalization of TGF-beta 1 in human hypertrophic scar and normal dermal tissues. *Cytokine*. 1995;7:184-90.
113. Bock O, Yu H, Zitron S, Bayat A, Ferguson MW, Mrowietz U. Studies of transforming growth factors beta 1-3 and their receptors I and II in fibroblast of keloids and hypertrophic scars. *Acta Derm Venereol*. 2005;85:216-20.
114. Shah M, Foreman DM, Ferguson MW. Neutralising antibody to TGF-beta 1,2 reduces cutaneous scarring in adult rodents. *J Cell Sci*. 1994;107 (Pt 5):1137-57.
115. Shah M, Foreman DM, Ferguson MW. Neutralisation of TGF-beta 1 and TGF-beta 2 or exogenous addition of TGF-beta 3 to cutaneous rat wounds reduces scarring. *J Cell Sci*. 1995;108 (Pt 3):985-1002.
116. Lu L, Saulis AS, Liu WR, Roy NK, Chao JD, Ledbetter S, et al. The temporal effects of anti-TGF-beta1, 2, and 3 monoclonal antibody on wound healing and hypertrophic scar formation. *J Am Coll Surg*. 2005;201:391-7.
117. Hameedaldeen A, Liu J, Batres A, Graves GS, Graves DT. FOXO1, TGF-beta regulation and wound healing. *Int J Mol Sci*. 2014;15:16257-69.
118. Bock O, Yu HY, Zitron S, Bayat A, Ferguson MWJ, Mrowietz U. Studies of transforming growth factors beta 1-3 and their receptors I and II in fibroblast of keloids and hypertrophic scars. *Acta Dermato-Venereologica*. 2005;85:216-20.

119. Liu W, Chua C, Wu YL, Wang DR, Ying DM, Cui L, et al. Inhibiting scar formation in rat wounds by adenovirus-mediated overexpression of truncated TGF-beta receptor II. *Plastic and Reconstructive Surgery*. 2005;115:860-70.
120. Kopp J, Preis E, Said H, Hafemann B, Wickert L, Gressner AM, et al. Abrogation of transforming growth factor-beta signaling by SMAD7 inhibits collagen gel contraction of human dermal fibroblasts. *J Biol Chem*. 2005;280:21570-6.
121. Pannu J, Nakerakanti S, Smith E, ten Dijke P, Trojanowska M. Transforming growth factor-beta receptor type I-dependent fibrogenic gene program is mediated via activation of Smad1 and ERK1/2 pathways. *Journal of Biological Chemistry*. 2007;282:10405-13.
122. Stopa M, Anhuf D, Terstegen L, Gatsios P, Gressner AM, Dooley S. Participation of Smad2, Smad3, and Smad4 in transforming growth factor beta (TGF-beta)-induced activation of Smad7. THE TGF-beta response element of the promoter requires functional Smad binding element and E-box sequences for transcriptional regulation. *J Biol Chem*. 2000;275:29308-17.
123. Monteleone G, Pallone F, MacDonald TT. Smad7 in TGF-beta-mediated negative regulation of gut inflammation. *Trends Immunol*. 2004;25:513-7.
124. Wang B, Hao J, Jones SC, Yee MS, Roth JC, Dixon IM. Decreased Smad 7 expression contributes to cardiac fibrosis in the infarcted rat heart. *Am J Physiol Heart Circ Physiol*. 2002;282:H1685-96.
125. Moustakas A, Heldin CH. Non-Smad TGF-beta signals. *J Cell Sci*. 2005;118:3573-84.
126. Klass BR, Grobbelaar AO, Rolfe KJ. Transforming growth factor beta1 signalling, wound healing and repair: a multifunctional cytokine with clinical implications for wound repair, a delicate balance. *Postgrad Med J*. 2009;85:9-14.
127. Tredget EB, Demare J, Chandran G, Tredget EE, Yang L, Ghahary A. Transforming growth factor-beta and its effect on reepithelialization of partial-thickness ear wounds in transgenic mice. *Wound Repair Regen*. 2005;13:61-7.
128. Mori T, Kawara S, Shinozaki M, Hayashi N, Kakinuma T, Igarashi A, et al. Role and interaction of connective tissue growth factor with transforming growth factor-beta in persistent fibrosis: A mouse fibrosis model. *J Cell Physiol*. 1999;181:153-9.

129. Frazier K, Williams S, Kothapalli D, Klapper H, Grotendorst GR. Stimulation of fibroblast cell growth, matrix production, and granulation tissue formation by connective tissue growth factor. *J Invest Dermatol.* 1996;107:404-11.
130. Shi-wen X, Stanton LA, Kennedy L, Pala D, Chen Y, Howat SL, et al. CCN2 is necessary for adhesive responses to transforming growth factor-beta1 in embryonic fibroblasts. *J Biol Chem.* 2006;281:10715-26. Epub 2006 Feb 16.
131. Igarashi A, Nashiro K, Kikuchi K, Sato S, Ihn H, Fujimoto M, et al. Connective tissue growth factor gene expression in tissue sections from localized scleroderma, keloid, and other fibrotic skin disorders. *J Invest Dermatol.* 1996;106:729-33.
132. Colwell AS, Phan TT, Kong W, Longaker MT, Lorenz PH. Hypertrophic scar fibroblasts have increased connective tissue growth factor expression after transforming growth factor-beta stimulation. *Plast Reconstr Surg.* 2005;116:1387-90; discussion 91-2.
133. Sisco M, Kryger ZB, O'Shaughnessy KD, Kim PS, Schultz GS, Ding XZ, et al. Antisense inhibition of connective tissue growth factor (CTGF/CCN2) mRNA limits hypertrophic scarring without affecting wound healing in vivo. *Wound Repair Regen.* 2008;16:661-73. doi: 10.1111/j.524-475X.2008.00416.x.
134. Wang JF, Olson ME, Ma L, Brigstock DR, Hart DA. Connective tissue growth factor siRNA modulates mRNA levels for a subset of molecules in normal and TGF-beta 1-stimulated porcine skin fibroblasts. *Wound Repair Regen.* 2004;12:205-16.
135. Ivkovic S, Yoon BS, Popoff SN, Safadi FF, Libuda DE, Stephenson RC, et al. Connective tissue growth factor coordinates chondrogenesis and angiogenesis during skeletal development. *Development.* 2003;130:2779-91.
136. Chen Y, Abraham DJ, Shi-Wen X, Pearson JD, Black CM, Lyons KM, et al. CCN2 (connective tissue growth factor) promotes fibroblast adhesion to fibronectin. *Mol Biol Cell.* 2004;15:5635-46.
137. Heldin CH, Eriksson U, Ostman A. New members of the platelet-derived growth factor family of mitogens. *Arch Biochem Biophys.* 2002;398:284-90.
138. Mori R, Shaw TJ, Martin P. Molecular mechanisms linking wound inflammation and fibrosis: knockdown of osteopontin leads to rapid repair and reduced scarring. *J Exp Med.* 2008;205:43-51.

139. Beer HD, Longaker MT, Werner S. Reduced expression of PDGF and PDGF receptors during impaired wound healing. *J Invest Dermatol.* 1997;109:132-8.
140. Pierce GF, Tarpley JE, Tseng J, Bready J, Chang D, Kenney WC, et al. Detection of platelet-derived growth factor (PDGF)-AA in actively healing human wounds treated with recombinant PDGF-BB and absence of PDGF in chronic nonhealing wounds. *J Clin Invest.* 1995;96:1336-50.
141. Bonner JC. Regulation of PDGF and its receptors in fibrotic diseases. *Cytokine Growth Factor Rev.* 2004;15:255-73.
142. Tan EM, Qin H, Kennedy SH, Rouda S, Fox JWt, Moore JH, Jr. Platelet-derived growth factors-AA and -BB regulate collagen and collagenase gene expression differentially in human fibroblasts. *Biochem J.* 1995;310 (Pt 2):585-8.
143. Tiede S, Ernst N, Bayat A, Paus R, Tronnier V, Zechel C. Basic fibroblast growth factor: a potential new therapeutic tool for the treatment of hypertrophic and keloid scars. *Ann Anat.* 2009;191:33-44.
144. Ornitz DM, Itoh N. Fibroblast growth factors. *Genome Biol.* 2001;2:REVIEWS3005.
145. Johnson DE, Williams LT. Structural and functional diversity in the FGF receptor multigene family. *Adv Cancer Res.* 1993;60:1-41.
146. Nissen NN, Polverini PJ, Gamelli RL, DiPietro LA. Basic fibroblast growth factor mediates angiogenic activity in early surgical wounds. *Surgery.* 1996;119:457-65.
147. Chen GJ, Forough R. Fibroblast growth factors, fibroblast growth factor receptors, diseases, and drugs. *Recent Pat Cardiovasc Drug Discov.* 2006;1:211-24.
148. Kibe Y, Takenaka H, Kishimoto S. Spatial and temporal expression of basic fibroblast growth factor protein during wound healing of rat skin. *Br J Dermatol.* 2000;143:720-7.
149. Klingbeil CK, Cesar LB, Fiddes JC. Basic fibroblast growth factor accelerates tissue repair in models of impaired wound healing. *Prog Clin Biol Res.* 1991;365:443-58.

150. Akasaka Y, Ono I, Yamashita T, Jimbow K, Ishii T. Basic fibroblast growth factor promotes apoptosis and suppresses granulation tissue formation in acute incisional wounds. *J Pathol.* 2004;203:710-20.
151. Agasse F, Nicoleau C, Petit J, Jaber M, Roger M, Benzakour O, et al. Evidence for a major role of endogenous fibroblast growth factor-2 in apoptotic cortex-induced subventricular zone cell proliferation. *Eur J Neurosci.* 2007;26:3036-42.
152. Xie JL, Bian HN, Qi SH, Chen HD, Li HD, Xu YB, et al. Basic fibroblast growth factor (bFGF) alleviates the scar of the rabbit ear model in wound healing. *Wound Repair Regen.* 2008;16:576-81.
153. Ono I, Akasaka Y, Kikuchi R, Sakemoto A, Kamiya T, Yamashita T, et al. Basic fibroblast growth factor reduces scar formation in acute incisional wounds. *Wound Repair Regen.* 2007;15:617-23.
154. Jinnin M, Ihn H, Mimura Y, Asano Y, Yamane K, Tamaki K. Effects of hepatocyte growth factor on the expression of type I collagen and matrix metalloproteinase-1 in normal and scleroderma dermal fibroblasts. *J Invest Dermatol.* 2005;124:324-30.
155. Eto H, Suga H, Aoi N, Kato H, Doi K, Kuno S, et al. Therapeutic potential of fibroblast growth factor-2 for hypertrophic scars: upregulation of MMP-1 and HGF expression. *Lab Invest.* 2012;92:214-23.
156. Das S, Mandal M, Chakraborti T, Mandal A, Chakraborti S. Structure and evolutionary aspects of matrix metalloproteinases: a brief overview. *Mol Cell Biochem.* 2003;253:31-40.
157. Yuan W, Varga J. Transforming growth factor-beta repression of matrix metalloproteinase-1 in dermal fibroblasts involves Smad3. *J Biol Chem.* 2001;276:38502-10.
158. Chakraborti S, Mandal M, Das S, Mandal A, Chakraborti T. Regulation of matrix metalloproteinases: an overview. *Mol Cell Biochem.* 2003;253:269-85.
159. Stamenkovic I. Extracellular matrix remodelling: the role of matrix metalloproteinases. *J Pathol.* 2003;200:448-64.

160. Saito S, Trovato MJ, You R, Lal BK, Fasehun F, Padberg FT, Jr., et al. Role of matrix metalloproteinases 1, 2, and 9 and tissue inhibitor of matrix metalloproteinase-1 in chronic venous insufficiency. *J Vasc Surg.* 2001;34:930-8.
161. Lichtinghagen R, Michels D, Haberkorn CI, Arndt B, Bahr M, Flemming P, et al. Matrix metalloproteinase (MMP)-2, MMP-7, and tissue inhibitor of metalloproteinase-1 are closely related to the fibroproliferative process in the liver during chronic hepatitis C. *J Hepatol.* 2001;34:239-47.
162. Desmouliere A, Geinoz A, Gabbiani F, Gabbiani G. Transforming growth factor-beta 1 induces alpha-smooth muscle actin expression in granulation tissue myofibroblasts and in quiescent and growing cultured fibroblasts. *J Cell Biol.* 1993;122:103-11.
163. Reynolds JJ. Collagenases and tissue inhibitors of metalloproteinases: a functional balance in tissue degradation. *Oral Dis.* 1996;2:70-6.
164. Lam E, Kilani RT, Li YY, Tredget EE, Ghahary A. Stratifin-induced matrix metalloproteinase-1 in fibroblast is mediated by c-fos and p38 mitogen-activated protein kinase activation. *Journal of Investigative Dermatology.* 2005;125:230-8.
165. Ghahary A, Marcoux Y, Karimi-Busheri F, Li YY, Tredget EE, Kilani RT, et al. Differentiated keratinocyte-releasable stratifin (14-3-3 sigma) stimulates MMP-1 expression in dermal fibroblasts. *Journal of Investigative Dermatology.* 2005;124:170-7.
166. Lam E, Tredget EE, Marcoux Y, Li YY, Ghahary A. Insulin suppresses collagenase stimulatory effect of stratifin in dermal fibroblasts. *Molecular and Cellular Biochemistry.* 2004;266:167-74.
167. Sawicki G, Marcoux Y, Sarkhosh K, Tredget E, Ghahary A. Interaction of keratinocytes and fibroblasts modulates the expression of matrix metalloproteinases-2 and-9 and their inhibitors. *Molecular and Cellular Biochemistry.* 2005;269:209-16.
168. Vaalamo M, Leivo T, Saarialho-Kere U. Differential expression of tissue inhibitors of metalloproteinases (TIMP-1,-2,-3, and-4) in normal and aberrant wound healing. *Human Pathology.* 1999;30:795-802.
169. Manuel JA, Gawronska-Kozak B. Matrix metalloproteinase 9 (MMP-9) is upregulated during scarless wound healing in athymic nude mice. *Matrix Biology.* 2006;25:505-14.

170. Dang CM, Beanes SR, Lee H, Zhang XL, Soo C, Ting K. Scarless fetal wounds are associated with an increased matrix metalloproteinase-to-tissue-derived inhibitor of metalloproteinase ratio. *Plastic and Reconstructive Surgery*. 2003;111:2273-85.
171. Tanriverdi-Akhisaroglu S, Menderes A, Oktay G. Matrix metalloproteinase-2 and-9 activities in human keloids, hypertrophic and atrophic scars: a pilot study. *Cell Biochemistry and Function*. 2009;27:81-7.
172. Zhang ZF, Zhang YG, Hu DH, Shi JH, Liu JQ, Zhao ZT, et al. Smad interacting protein 1 as a regulator of skin fibrosis in pathological scars. *Burns*. 2011;37:665-72.
173. Ulrich D, Noah EM, von Heimburg D, Pallua N. TIMP-1, MMP-2, MMP-9, and PIINP as serum markers for skin fibrosis in patients following severe burn trauma. *Plastic and Reconstructive Surgery*. 2003;111:1423-31.
174. Simon F, Bergeron D, Larochelle S, Lopez-Valle CA, Genest H, Armour A, et al. Enhanced secretion of TIMP-1 by human hypertrophic scar keratinocytes could contribute to fibrosis. *Burns*. 2012;38:421-7.
175. Scott PG, Ghahary A, Tredget EE. Molecular and cellular aspects of fibrosis following thermal injury. *Hand Clin*. 2000;16:271-87.
176. Nedelec B, Shankowsky H, Scott PG, Ghahary A, Tredget EE. Myofibroblasts and apoptosis in human hypertrophic scars: the effect of interferon-alpha2b. *Surgery*. 2001;130:798-808.
177. Smith CJ, Smith JC, Finn MC. The possible role of mast cells (allergy) in the production of keloid and hypertrophic scarring. *J Burn Care Rehabil*. 1987;8:126-31.
178. Huang C, Murphy GF, Akaishi S, Ogawa R. Keloids and hypertrophic scars: update and future directions. *Plast Reconstr Surg Glob Open*. 2013;1:e25. doi: 10.1097/GOX.0b013e31829c4597. eCollection 2013 Jul.
179. Funayama E, Chodon T, Oyama A, Sugihara T. Keratinocytes promote proliferation and inhibit apoptosis of the underlying fibroblasts: an important role in the pathogenesis of keloid. *J Invest Dermatol*. 2003;121:1326-31.
180. Garner WL. Epidermal regulation of dermal fibroblast activity. *Plast Reconstr Surg*. 1998;102:135-9.

181. Machesney M, Tidman N, Waseem A, Kirby L, Leigh I. Activated keratinocytes in the epidermis of hypertrophic scars. *Am J Pathol.* 1998;152:1133-41.
182. Varkey M, Ding J, Tredget EE. Fibrotic remodeling of tissue-engineered skin with deep dermal fibroblasts is reduced by keratinocytes. *Tissue Eng Part A.* 2014;20:716-27. doi: 10.1089/ten.TEA.2013.0434. Epub 2013 Nov 9.
183. Moyer KE, Siggers GC, Ehrlich HP. Mast cells promote fibroblast populated collagen lattice contraction through gap junction intercellular communication. *Wound Repair Regen.* 2004;12:269-75.
184. Foley TT, Ehrlich HP. Through gap junction communications, co-cultured mast cells and fibroblasts generate fibroblast activities allied with hypertrophic scarring. *Plast Reconstr Surg.* 2013;131:1036-44. doi: 10.97/PRS.0b013e3182865c3f.
185. Gruber BL, Kew RR, Jelaska A, Marchese MJ, Garlick J, Ren S, et al. Human mast cells activate fibroblasts: tryptase is a fibrogenic factor stimulating collagen messenger ribonucleic acid synthesis and fibroblast chemotaxis. *J Immunol.* 1997;158:2310-7.
186. Kofford MW, Schwartz LB, Schechter NM, Yager DR, Diegelmann RF, Graham MF. Cleavage of type I procollagen by human mast cell chymase initiates collagen fibril formation and generates a unique carboxyl-terminal propeptide. *J Biol Chem.* 1997;272:7127-31.
187. Kupietzky A, Levi-Schaffer F. The role of mast cell-derived histamine in the closure of an in vitro wound. *Inflamm Res.* 1996;45:176-80.
188. Chen L, Liu S, Li SR, Cong L, Wu JL, Wang ZX. [Influence of substance P on the release of histamine in the human hypertrophic scar tissue]. *Zhonghua Shao Shang Za Zhi.* 2006;22:192-4.
189. Tredget EE, Iwashina T, Scott PG, Ghahary A. Determination of plasma Ntau-methylhistamine in vivo by isotope dilution using benchtop gas chromatography-mass spectrometry. *J Chromatogr B Biomed Sci Appl.* 1997;694:1-9.
190. Eishi K, Bae SJ, Ogawa F, Hamasaki Y, Shimizu K, Katayama I. Silicone gel sheets relieve pain and pruritus with clinical improvement of keloid: possible target of mast cells. *J Dermatolog Treat.* 2003;14:248-52.

191. McDougall S, Dallon J, Sherratt J, Maini P. Fibroblast migration and collagen deposition during dermal wound healing: mathematical modelling and clinical implications. *Philos Trans A Math Phys Eng Sci.* 2006;364:1385-405.
192. Scott PG, Dodd CM, Tredget EE, Ghahary A, Rahemtulla F. Immunohistochemical localization of the proteoglycans decorin, biglycan and versican and transforming growth factor-beta in human post-burn hypertrophic and mature scars. *Histopathology.* 1995;26:423-31.
193. Ghahary A, Shen YJ, Nedelec B, Wang R, Scott PG, Tredget EE. Collagenase production is lower in post-burn hypertrophic scar fibroblasts than in normal fibroblasts and is reduced by insulin-like growth factor-1. *J Invest Dermatol.* 1996;106:476-81.
194. Wang R, Ghahary A, Shen YJ, Scott PG, Tredget EE. Human dermal fibroblasts produce nitric oxide and express both constitutive and inducible nitric oxide synthase isoforms. *J Invest Dermatol.* 1996;106:419-27.
195. Junker JP, Kratz C, Tollback A, Kratz G. Mechanical tension stimulates the transdifferentiation of fibroblasts into myofibroblasts in human burn scars. *Burns.* 2008;34:942-6.
196. Nedelec B, Ghahary A, Scott PG, Tredget EE. Control of wound contraction. Basic and clinical features. *Hand Clin.* 2000;16:289-302.
197. Moulin V, Larochele S, Langlois C, Thibault I, Lopez-Valle CA, Roy M. Normal skin wound and hypertrophic scar myofibroblasts have differential responses to apoptotic inductors. *J Cell Physiol.* 2004;198:350-8.
198. Wynn TA. Fibrotic disease and the T(H)1/T(H)2 paradigm. *Nat Rev Immunol.* 2004;4:583-94.
199. Davis PA, Corless DJ, Aspinall R, Wastell C. Effect of CD4(+) and CD8(+) cell depletion on wound healing. *Br J Surg.* 2001;88:298-304.
200. Castagnoli C, Stella M, Magliacani G. Role of T-lymphocytes and cytokines in post-burn hypertrophic scars. *Wound Repair Regen.* 2002;10:107-8.
201. Mosmann TR, Coffman RL. TH1 and TH2 cells: different patterns of lymphokine secretion lead to different functional properties. *Annu Rev Immunol.* 1989;7:145-73.

202. Doucet C, Brouty-Boye D, Pottin-Clemenceau C, Canonica GW, Jasmin C, Azzarone B. Interleukin (IL) 4 and IL-13 act on human lung fibroblasts. Implication in asthma. *J Clin Invest.* 1998;101:2129-39.
203. O'Sullivan ST, Lederer JA, Horgan AF, Chin DH, Mannick JA, Rodrick ML. Major injury leads to predominance of the T helper-2 lymphocyte phenotype and diminished interleukin-12 production associated with decreased resistance to infection. *Ann Surg.* 1995;222:482-90; discussion 90-2.
204. Kilani RT, Delehanty M, Shankowsky HA, Ghahary A, Scott P, Tredget EE. Fluorescent-activated cell-sorting analysis of intracellular interferon-gamma and interleukin-4 in fresh and frozen human peripheral blood T-helper cells. *Wound Repair Regen.* 2005;13:441-9.
205. Tredget EE, Yang L, Delehanty M, Shankowsky H, Scott PG. Polarized Th2 cytokine production in patients with hypertrophic scar following thermal injury. *J Interferon Cytokine Res.* 2006;26:179-89.
206. Wang J, Jiao H, Stewart TL, Shankowsky HA, Scott PG, Tredget EE. Increased TGF-beta-producing CD4+ T lymphocytes in postburn patients and their potential interaction with dermal fibroblasts in hypertrophic scarring. *Wound Repair Regen.* 2007;15:530-9.
207. Zalkind SIA. Ilya Mechnikov, his life and work. Moscow: Foreign Languages Pub. House, 1959.
208. Gordon S, Martinez FO. Alternative activation of macrophages: mechanism and functions. *Immunity.* 2010;32:593-604.
209. Nagaoka T, Kaburagi Y, Hamaguchi Y, Hasegawa M, Takehara K, Steeber DA, et al. Delayed wound healing in the absence of intercellular adhesion molecule-1 or L-selectin expression. *Am J Pathol.* 2000;157:237-47.
210. Eming SA, Werner S, Bugnon P, Wickenhauser C, Siewe L, Utermohlen O, et al. Accelerated wound closure in mice deficient for interleukin-10. *Am J Pathol.* 2007;170:188-202.
211. Mahdavian Delavary B, van der Veer WM, van Egmond M, Niessen FB, Beelen RH. Macrophages in skin injury and repair. *Immunobiology.* 2011;216:753-62.

212. Stein M, Keshav S, Harris N, Gordon S. Interleukin 4 potently enhances murine macrophage mannose receptor activity: a marker of alternative immunologic macrophage activation. *J Exp Med.* 1992;176:287-92.
213. Mosser DM, Edwards JP. Exploring the full spectrum of macrophage activation. *Nat Rev Immunol.* 2008;8:958-69.
214. Gordon S, Taylor PR. Monocyte and macrophage heterogeneity. *Nat Rev Immunol.* 2005;5:953-64.
215. Martinez FO, Sica A, Mantovani A, Locati M. Macrophage activation and polarization. *Front Biosci.* 2008;13:453-61.
216. Ploeger DTA, Hosper NA, Schipper M, Koerts JA, de Rond S, Bank RA. Cell plasticity in wound healing: paracrine factors of M1/M2 polarized macrophages influence the phenotypical state of dermal fibroblasts. *Cell Communication and Signaling.* 2013;11.
217. Stewart DA, Yang YM, Makowski L, Troester MA. Basal-like Breast Cancer Cells Induce Phenotypic and Genomic Changes in Macrophages. *Molecular Cancer Research.* 2012;10:727-38.
218. Solinas G, Germano G, Mantovani A, Allavena P. Tumor-associated macrophages (TAM) as major players of the cancer-related inflammation. *Journal of Leukocyte Biology.* 2009;86:1065-73.
219. Martinez FO, Gordon S, Locati M, Mantovani A. Transcriptional profiling of the human monocyte-to-macrophage differentiation and polarization: New molecules and patterns of gene expression. *Journal of Immunology.* 2006;177:7303-11.
220. Martinez FO, Gordon S. The M1 and M2 paradigm of macrophage activation: time for reassessment. *F1000Prime Rep.* 2014;6:13.
221. Mills CD, Kincaid K, Alt JM, Heilman MJ, Hill AM. M-1/M-2 macrophages and the Th1/Th2 paradigm. *J Immunol.* 2000;164:6166-73.
222. Italiani P, Boraschi D. From Monocytes to M1/M2 Macrophages: Phenotypical vs. Functional Differentiation. *Front Immunol.* 2014;5:514.

223. Song E, Ouyang N, Horbelt M, Antus B, Wang M, Exton MS. Influence of alternatively and classically activated macrophages on fibrogenic activities of human fibroblasts. *Cell Immunol.* 2000;204:19-28.
224. Mantovani A, Sica A, Sozzani S, Allavena P, Vecchi A, Locati M. The chemokine system in diverse forms of macrophage activation and polarization. *Trends Immunol.* 2004;25:677-86.
225. Grinberg S, Hasko G, Wu D, Leibovich SJ. Suppression of PLCbeta2 by endotoxin plays a role in the adenosine A(2A) receptor-mediated switch of macrophages from an inflammatory to an angiogenic phenotype. *Am J Pathol.* 2009;175:2439-53.
226. Murray PJ, Wynn TA. Protective and pathogenic functions of macrophage subsets. *Nat Rev Immunol.* 2011;11:723-37.
227. Sindrilaru A, Peters T, Wieschalka S, Baican C, Baican A, Peter H, et al. An unrestrained proinflammatory M1 macrophage population induced by iron impairs wound healing in humans and mice. *J Clin Invest.* 2011;121:985-97.
228. London A, Itskovich E, Benhar I, Kalchenko V, Mack M, Jung S, et al. Neuroprotection and progenitor cell renewal in the injured adult murine retina requires healing monocyte-derived macrophages. *J Exp Med.* 2011;208:23-39.
229. Wilson MS, Elnekave E, Mentink-Kane MM, Hodges MG, Pesce JT, Ramalingam TR, et al. IL-13Ralpha2 and IL-10 coordinately suppress airway inflammation, airway-hyperreactivity, and fibrosis in mice. *J Clin Invest.* 2007;117:2941-51.
230. Ferrara N, Heinsohn H, Walder CE, Bunting S, Thomas GR. The regulation of blood vessel growth by vascular endothelial growth factor. *Ann N Y Acad Sci.* 1995;752:246-56.
231. Wynn TA. Cellular and molecular mechanisms of fibrosis. *J Pathol.* 2008;214:199-210.
232. Tsou PS, Haak AJ, Khanna D, Neubig RR. Cellular mechanisms of tissue fibrosis. 8. Current and future drug targets in fibrosis: focus on Rho GTPase-regulated gene transcription. *Am J Physiol Cell Physiol.* 2014;307:C2-13.

233. Rockey DC, Bell PD, Hill JA. Fibrosis--a common pathway to organ injury and failure. *N Engl J Med*. 2015;372:1138-49.
234. Wynn TA. Integrating mechanisms of pulmonary fibrosis. *J Exp Med*. 2011;208:1339-50.
235. Duffield JS, Forbes SJ, Constandinou CM, Clay S, Partolina M, Vuthoori S, et al. Selective depletion of macrophages reveals distinct, opposing roles during liver injury and repair. *J Clin Invest*. 2005;115:56-65.
236. Chawla A, Nguyen KD, Goh YP. Macrophage-mediated inflammation in metabolic disease. *Nat Rev Immunol*. 2011;11:738-49.
237. Kawane K, Ohtani M, Miwa K, Kizawa T, Kanbara Y, Yoshioka Y, et al. Chronic polyarthritis caused by mammalian DNA that escapes from degradation in macrophages. *Nature*. 2006;443:998-1002.
238. Pan B, Liu G, Jiang Z, Zheng D. Regulation of renal fibrosis by macrophage polarization. *Cell Physiol Biochem*. 2015;35:1062-9.
239. Shen B, Liu XH, Fan Y, Qiu JX. Macrophages Regulate Renal Fibrosis Through Modulating TGF beta Superfamily Signaling. *Inflammation*. 2014;37:2076-84.
240. Prasse A, Pechkovsky DV, Toews GB, Jungraithmayr W, Kollert F, Goldmann T, et al. A vicious circle of alveolar macrophages and fibroblasts perpetuates pulmonary fibrosis via CCL18. *American Journal of Respiratory and Critical Care Medicine*. 2006;173:781-92.
241. Sica A, Mantovani A. Macrophage plasticity and polarization: in vivo veritas. *J Clin Invest*. 2012;122:787-95.

Chapter 2

Alternatively Activated Macrophages Derived from THP-1 Cells Promote the Fibrogenic Activities of Human Dermal Fibroblasts

This chapter has been submitted to *Wound Repair and Regeneration* on April 15, 2016, and is currently under review.

2.0 Abstract

Macrophages play a key role in the wound healing process and can be divided into M1 macrophages and M2 macrophages. Fibroblasts maintain the physical integrity of connective tissue, participate in wound closure as well as produce and remodel extracellular matrix. Macrophages have a close relationship with fibroblast by affecting the production of MMP-1 for faster wound closure and myofibroblast differentiation from fibroblasts. In this study, resting state (M0), M1 and M2 macrophages differentiated from the human monocytic THP-1 cell line were used to co-culture with human dermal fibroblasts (HDF) for 48, 96 and 144 hours to investigate the effect of macrophage subsets on the fibrogenic activity of fibroblasts. The differentiation and polarization from THP-1 cells to M0, M1 and M2 macrophages were characterized by flow cytometry and cell cycle analysis. Cell sorting was performed to purify M0 and M2 macrophages. Cell proliferation, collagen synthesis, myofibroblast formation, gene expression of anti-fibrotic and pro-fibrotic factors, MMP-1 activity, and cytokine concentration were investigated. Results showed differentiation of M0 and polarization of M1 and M2 macrophages. M2 macrophages promoted the fibrogenic activities of co-cultured HDF by facilitating cell proliferation, increasing the collagen content, α -SMA expressed cells, expression of the pro-fibrotic genes and concentration of M2 macrophage related factors, as well as decreasing the expression of the anti-fibrotic genes and MMP-1 activity. These findings reinforce the pro-fibrotic role of M2 macrophages, suggesting therapeutic strategies in fibrotic diseases should target M2 macrophages in the future.

2.1 Introduction

Macrophages exist as resident tissue-specific cells and act as key innate immune cells by phagocytizing tissue debris, dead and apoptotic cells. They also act as antigen presenting cells in response to various pathogens, which bridge the innate and adaptive immunity in order to reestablish homeostasis. In the processes of inflammation and infection, macrophages are activated and replenished by circulating blood monocytes that are recruited to the tissue (1, 2).

The wound microenvironment influences the phenotypic polarization of macrophages, which can be classified into two activation states based on their reactions to different stimuli, the M1 macrophages and the M2 macrophages (3). M1 macrophage polarization can be induced by lipopolysaccharide (LPS) and IFN- γ ; whereas, M2 macrophage polarization can be induced by IL-4 and IL-13 (4). M1 macrophages are found in the inflammatory phase of wound healing and are characterized by the production of pro-inflammatory cytokines including TNF- α , IL-1 β , IL-6 and IL-12; whereas, M2 macrophages are more found in the proliferation phase and are related to tissue repair and fibrosis with the production of TGF-1 β , IL-10 and IL-1 α (5, 6).

Fibroblasts are the most abundant cells in connective tissue and are one of the key elements in the healing wound where they function to restore the physical integrity of connective tissue via wound closure through the production and remodeling of the ECM via the differentiation into myofibroblasts (7). Macrophages have a close relationship with fibroblasts in the wound healing process. During the inflammatory phase, M1 macrophages produce pro-inflammatory cytokines and facilitate the wound healing process by inducing fibroblasts to produce MMP-1, which enhances ECM degradation.

During the proliferation phase in the abnormal wound healing, M2 macrophages produce large amount of TGF- β 1, which promotes myofibroblast formation from fibroblasts and subsequent production of collagen, and excessive ECM deposition, leading to fibrosis (8, 9).

In order to determine how macrophages polarization modulates the fibrogenic activities of human dermal fibroblasts, the human monocytic cell line THP-1, were differentiated to the M0 macrophages and then polarized into either the M1 or M2 macrophage phenotype in cell culture by Th1 or Th2 cytokines (10). In this study, M1 and M2 macrophages differentiated from human THP-1 cell line were then co-cultured with HDF. The effect of M1 and M2 macrophages on fibroblast regulation of collagen synthesis, myofibroblast differentiation, and MMP-1 activity was investigated in addition to the concentration of M1 and M2 macrophage related factors released into the co-cultured media.

2.2 Materials and methods

2.2.1 Cell culture

Human monocytic THP-1 cells (ATCC, ATCC® TIB-202™) were purchased from ATCC (were maintained in culture in Roswell Park Memorial Institute medium (RPMI) 1640 (GE Healthcare Life Sciences, Logan, UT) culture medium containing 10% of heat inactivated fetal bovine serum (FBS) (PAA Laboratories. Inc, Etobicoke, ON) and supplemented with 10 mM Hepes (Life Technologies Inc., #15630-080), 1 mM pyruvate (Life Technologies Inc., #11360-039) and 1% Gibco® Antibiotic-Antimycotic (Life

Technologies Inc., #15240-096). Treatment of THP-1 cells with phorbol 12-myristate 13-acetate (PMA) was used as a method for M0 macrophage differentiation by incubation of THP-1 cells with 320 nM PMA (Sigma-Aldrich, #P8195) for 24 hours as previously reported (11, 12). Thereafter M0 macrophages were polarized into M1 macrophages by incubation with 20 ng/ml of IFN- γ (PeproTech, #AF-300-02) and 100 ng/ml of lipopolysaccharide (LPS, Sigma-Aldrich, # L-2880) for a further 24 hours. M2 macrophages were obtained by incubation of M0 macrophages with 20 ng/ml of IL-4 (PeproTech, #200-04) and 20 ng/ml of IL-13 (PeproTech, #200-13) for 24 hours.

HDF were harvested and isolated from abdominal skin obtained from female patients underwent abdominoplasty with documented informed consent in their personal health record. HDF were cultured in Dulbecco's Modified Eagle's Medium (DMEM, Life Technologies Inc., Burlington, ON) containing 4.5 g/l D-glucose, L-glutamine, 110 mg/l sodium pyruvate, 1% Gibco® Antibiotic-Antimycotic (Life Technologies Inc., #15240-096) and 10% of heat inactivated FBS (PAA Laboratories. Inc, Etobicoke, ON) in a 5% CO₂ humidified incubator for 24 hours after seeding.

2.2.2 Cell cycle analysis

Cell cycle analysis was performed after propidium iodide staining and flow cytometry as described earlier (13). Briefly, 1×10^6 THP-1 cells and M0 macrophages were washed in phosphate-buffered saline (PBS), centrifuged and fixed in 4 ml ice cold 70% ethanol by incubation at 4 °C for 1 hour. The cells were then centrifuged and re-suspended in PBS before they were treated with 100 μ g/ml RNase A (Life Technologies Inc., Burlington, ON) for 30 minutes at 37 °C. After washing, 50 μ g/ml propidium iodide

was added and the samples were analyzed in a BD FACSCanto II flow cytometer (BD Biosciences, San Jose, CA). The distribution of cells in different phases of cell cycle was estimated using FCS Express 4 Plus software (De Novo Software, LA, CA), which reported the percentages of cells in synthesis (S) phase of the cell cycle using a DNA histogram.

2.2.3 Confirmation of differentiation of M0, M1 and M2 macrophages

1×10^6 THP-1 cells and M0 macrophages were washed in PBS and incubated with human specific FcR blocking reagent (Miltenyi Biotec Inc., #130-059-901). The FcR blocked cells were then incubated with FITC Mouse Anti-Human CD14 IgG antibody (BD Biosciences, Cat. #555397). After washing and fixation, the two cell populations were then detected by flow cytometry using a BD FACSCanto II (BD Biosciences, San Jose, CA).

For the confirmation of M1 macrophage polarization, 1×10^6 cells were washed in PBS, fixed with 4% paraformaldehyde (PFA) (Sigma-Aldrich, #P6148) followed by the incubation with human specific FcR blocking reagent (Miltenyi Biotec Inc., #130-059-901). FcR blocked cells were then incubated with 0.5% saponin (Sigma-Aldrich, #S2149) to permeabilize the cell membrane for intracellular staining and then incubated with rabbit polyclonal nitric oxide synthase 2 (NOS2) IgG antibody (Santa Cruz, Cat. #sc-651 FITC). For the confirmation of M2 macrophage polarization, 1×10^6 cells were washed in PBS and incubated with human specific FcR blocking reagent (Miltenyi Biotec Inc., #130-059-901). The three populations of M0, M1 and M2 FcR blocked cells were then incubated with the mouse anti-human CD163 APC IgG antibody (eBioscience, #17-1639-

42). The cells were analyzed in a flow cytometer, BD FACSCanto II (BD Biosciences, San Jose, CA) and the percentages of the positive stained cells was determined using the BD FACSDiva software (BD Biosciences, San Jose, CA).

2.2.4 Purification of M0 and M2 macrophages using cell sorting

In order to purify the M0 and M2 macrophages for the co-culture with HDF, the M0 and M2 macrophages were mechanically detached from six well plates using a cell lifter. The cells were washed with PBS and then incubated with human specific FcR blocking reagent (Miltenyi Biotec Inc., #130-059-901). The M0 macrophages then incubated with FITC mouse anti-human CD14 IgG antibody (BD Biosciences, Cat. #555397) while the M2 macrophages were incubated with the mouse anti-human CD163 FITC IgG antibody (Biolegend, #333617). The M0 and M2 macrophages then underwent cell sorting using FACS Aria IIIU (BD Biosciences, San Jose, CA) in low speed mode using 100 u nozzle. Fluorescence was detected with 530/30 nm band pass filter for CD14⁺ FITC and CD163⁺ FITC antibodies. CD14⁺ singlet cells were collected, centrifuged and then seeded into the cell inserts respectively for co-culture with HDF. All procedures were performed using aseptic technique.

2.2.5 Co-culture of HDF with M0, M1 and M2 macrophages

M1 macrophages and purified M0 and M2 cells grown in cell inserts (1×10^6 cells per insert) were co-cultured with HDF cells in six-well plates (BD Biosciences, #353046) (2×10^5 cells per well) in RPMI 1640 medium. After 48, 96, 144 hours of co-culture, the

upper inserts were discarded and the medium in the six-well plates was collected and stored at -20 °C for further analysis, and the HDF cells were harvested and used for subsequent experiments.

2.2.6 Cell proliferation by MTT assay

Briefly, HDF were suspended and dispensed in 96-well plate after 48, 96 and 144 hours of co-culture. The cells were incubated with 300 μ L of 5 mg/ml (3-(4,5-dimethylthiazol-2-yl)-2,5-diphenyltetrazolium bromide (MTT) reagent (Sigma-Aldrich, #M2128) for 4 hours at 37 °C as previously described (14). The medium was removed and then the purple crystals were dissolved with 1mL of acidified isopropanol (0.1 N hydrochloric acid [HCl] in isopropanol). The plate was covered with aluminum foil and gently shaken for 15 minutes before the absorbance was measured by ThermoMax microplate reader (Molecular Devices, LLC. Sunnyvale, CA) at 550 nm with a reference filter of 620 nm.

2.2.7 Collagen synthesis using liquid chromatography/mass spectrometry (LC/MS)

The amount of 4-hydroxyproline (4-Hyp) as a unique amino acid in collagen, was measured by LC/MS as previously described (15). Briefly, the cell culture medium samples collected after the co-culture of 48, 96 and 144 hours were treated with acetonitrile to precipitate the collagen. The precipitates were dried with the speed vacuum concentrator before they were hydrolyzed by 6N hydrochloric acid at 110°C overnight. A known amount of 4-hydroxyproline-d₃ (4-Hyp-d₃) as internal standard was added to the

hydrolysate and then dried with the speed vacuum concentrator. The n-butyl ester reagent was added to the mixture and heated at 110 °C for 30 minutes in order to produce the n-butyl ester derivatives of 4-Hyp and 4-Hyp-d₃. After drying, the residue was dissolved in 20% methanol and water before analyzing by LC/MS (Agilent Technologies, Santa Clara, CA). 4-Hyp and 4-Hyp-d₃ were separated from the other compounds by LC, and then the two pseudo molecular ions of 188⁺ 4-Hyp n-butyl ester and 191⁺ 4-Hyp-d₃ n-butyl ester were detected as the two ion peaks using the mass selective detection method on MS. The calibration curve was constructed through a range of 4-Hyp over 6 concentrations using the peak area ratio. The ratio was obtained by dividing 4-Hyp peak area by the internal standard (4-Hyp-d₃) and the amount of 4-Hyp in each sample was analyzed using the calibration curve. The data was expressed in 4-Hyp (ng) / cell culture medium (ml).

2.2.8 Quantification of alpha-smooth muscle actin (α -SMA) positive cells in the co-cultured HDF by flow cytometry

The α -SMA positive cells in the co-culture HDFs were quantified using flow cytometry as previously described (16). Briefly, the HDF co-cultured with M0, M1 and M2 macrophages for 48, 96 and 144 hours were collected, washed in PBS and fixed with 4% PFA (Sigma-Aldrich, #P6148) followed by the incubation with human specific FcR blocking reagent (Miltenyi Biotec Inc., #130-059-901). The FcR blocked cells were then incubated with 0.5% saponin (Sigma-Aldrich, #S2149) to permeabilize the cell membranes and then incubated with PE mouse anti human α -SMA IgG2a antibody (R&D Systems, Inc., #IC1420P). The cells were analyzed in a flow cytometer, BD FACSCanto

II (BD Biosciences, San Jose, CA). The percentages of the positive cells was determined using the FCS Express 4 Plus software (De Novo Software, LA, CA).

2.2.9 Quantitative polymerase chain reaction (qPCR) analysis of human pro-fibrotic and anti-fibrotic Factors

HDF that were co-cultured with M0, M1 and M2 macrophages for 48, 96 and 144 hours were lysed using TRIzol reagent (Thermo Fisher Scientific., Waltham, MA). Total RNA was extracted using RNeasy® mini kit (Qiagen, Hilden, Germany). Contamination from genomic DNA was removed by DNase digestion for 60 minutes. First strand cDNA was synthesized using random primers in a first strand synthesis kit (Sigma, Oakville, ON). qPCR was conducted using Power SYBR® Green PCR Master Mix in a 25µl tube for a total reaction volume of 25µl, containing 1µl first strand product, and 0.2µM gene specific upstream and downstream primers for human pro-fibrotic and anti-fibrotic factors. Human hypoxanthine-guanine phosphoribosyltransferase (HPRT) primers were used as controls. Amplification and analysis were performed using an ABI 7300 real-time system (Applied Biosystems, Foster City, CA). Cycling conditions were an initial denaturation at 95°C for 3 minutes, followed by 40 cycles consisting of a 15-second denaturation interval at 95° C, and a 30-second interval for annealing and primer extension at 60°C. mRNA expression levels were normalized to the levels of human HPRT for human pro-fibrotic and anti-fibrotic factors. Relative quantitation was expressed as fold-induction compared with control conditions. Primers sequences were as follows: HPRT, forward CGTCTTGCTCGAGATGTGATG and reverse GCACACAGAGGGCTACAATGTG; MMP-1, forward TCGCTGGGAGCAAACACA

and reverse TTGGCAAATCTGGCGTGAA; DCN, forward TGAAGAAGCTCTCCTACATCC and reverse AA ACTCAATCCCAACTTAGCC; TGF- β 1, forward ACCCACAACGAAATCTATGAC and reverse GCTCCACTTTTAACTTGAGCC; COL1A1, forward CGAAGACATCCCACCAATCAC and reverse TCATCGCACAAACACCTTGC; TIMP-1, forward CGCTGACATCCGGTTCGT and reverse GTGGAAGTATCCGCAGACACTCT.

2.2.10 Human MMP-1 activity assay

The cell culture supernatant in the six-well plates was collected after the co-culture of HDF with M0, M1 and M2 macrophages for 48, 96 and 144 hours. MMP-1 activity in the cell culture supernatant was quantified by fluorescent assay using the Fluorokine E Human Active MMP-1 Fluorescent Assay Kit (R&D Systems, Inc., Minneapolis, MN) according to the manufacturer's protocol (17). The relative fluorescence units (RFU) was determined using the Tecan Infinite® 200 fluorescence plate reader (Tecan Group Ltd., Männedorf, Switzerland). The active MMP-1 concentration of each sample was determined by the standard curve according to the manufacturer's protocol.

2.2.11 Multiplex analysis of cytokines at 144 hours of co-culture

The cell culture supernatants in six-well plates was collected after co-culture of HDF with M0, M1 and M2 macrophages for 144 hours. Simultaneous analysis of IFN- γ , IL-1 β ,

TNF- α , IL-4, IL-10 and TGF- β 1 were performed by Eve Technologies (Calgary, Alberta, Canada) (18). The multiplex assay was performed using the Bio-Plex™ 200 system (Bio-Rad Laboratories, Inc., Hercules, CA) and a Milliplex human cytokines kit (Millipore, St. Charles, MO) according to their protocol. The concentration of cytokines and TGF- β 1 was calculated using the fluorescent intensity and the standard curve acquired in each sample according to the manufacturer's protocol.

2.2.12 Statistical analysis

All data were displayed as mean \pm standard error (SE) of the mean of at least three independent experiments and were analyzed by STATA 12 for Windows (StataCorp LP, College Station, TX). Statistical analysis was performed using a two-tailed unpaired Student's t-test or one-way analysis of variance (ANOVA) with the Bonferroni method. A p-value of less than 0.05 ($p < 0.05$) was considered statistically significant.

2.3 Results

2.3.1 Differentiation of THP-1 cells to M0 macrophages

To determine the induction of M0 macrophages from THP-1, the M0 macrophages and THP-1 cells were stained with CD14 fluorochrome, a general marker for macrophages but not THP-1 cells (19). Few THP-1 cells stained positive for CD14; whereas a significantly higher population of M0 macrophages were CD14 positive as compared to THP-1 cells ($p < 0.001$) (Figure 2.1A). Cell cycle analysis on THP-1 cells and

M0 macrophages after differentiation revealed a significant reduction of M0 macrophages entering the S phase, as compared to THP-1 cells ($p < 0.001$) (Figure 2.1B).

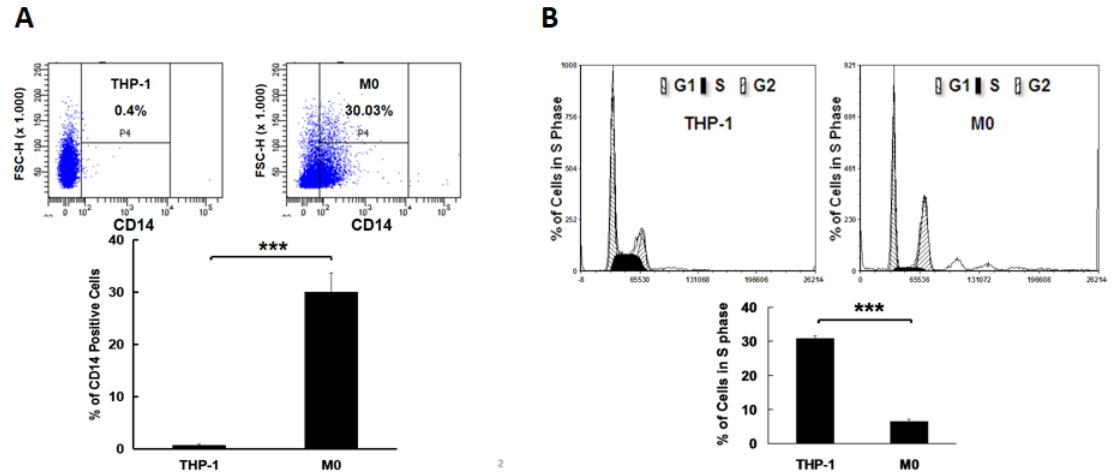


Figure 2.1 Differentiation of THP-1 cells to M0 macrophages. CD14⁺ positive cells between THP-1 cells and M0 macrophages were analyzed by flow cytometry (A). Percentages of cells entering the S phase from THP-1 cells and M0 macrophages were measured and analyzed using cell cycle analysis (B). Triplicate, *** $p < 0.001$.

2.3.2 Characterization of M1 and M2 macrophages as well as the purification of M0 and M2 macrophages

M0 macrophages differentiated from THP-1 cells were treated with LPS/ IFN- γ to induce M1 macrophages and IL-4/IL-13 to induce M2 macrophage polarization. Figure 2.2A illustrates the morphological differences between the THP-1 cells, M0, M1 and M2 macrophages. THP-1 cells were small, oval cells while M0 macrophages were larger with more granules in the cytoplasm. M1 macrophages displayed a spindle-like morphology with pseudopods while the majority of M2 macrophages adopted a rounded-shape with dense granules and fewer pseudopods as compared to the M1 macrophages.

In order to further characterize the polarization of M1 and M2 macrophages, flow cytometry using specific markers of M1 (NOS2) and M2 (CD163) macrophages were performed on M0, M1 and M2 macrophages as previously reported (20). NOS2, a specific marker for M1 macrophages, were solely expressed in M1 macrophages (77.2%), as compared to those of M0 and M2 macrophage (0.2%). Significant differences between M1 and M0 ($p < 0.001$) as well as M1 and M2 ($p < 0.001$) were observed (Figure 2.2B). A significantly higher expression of CD163 was found in M2 macrophages, as compared to M0 ($p < 0.001$) and M1 ($p < 0.001$) macrophages (Figure 2.2C). Purification of M0 and M2 macrophages using cell sorting increased the proportion of M0 macrophages positively staining for CD14 from 25.4% to 81.6% after the cell sorting; whereas, the percentages of CD163 positive M2 macrophages increased from 19.8% to 83.6% as a result of cell sorting (Figure 2.2D).

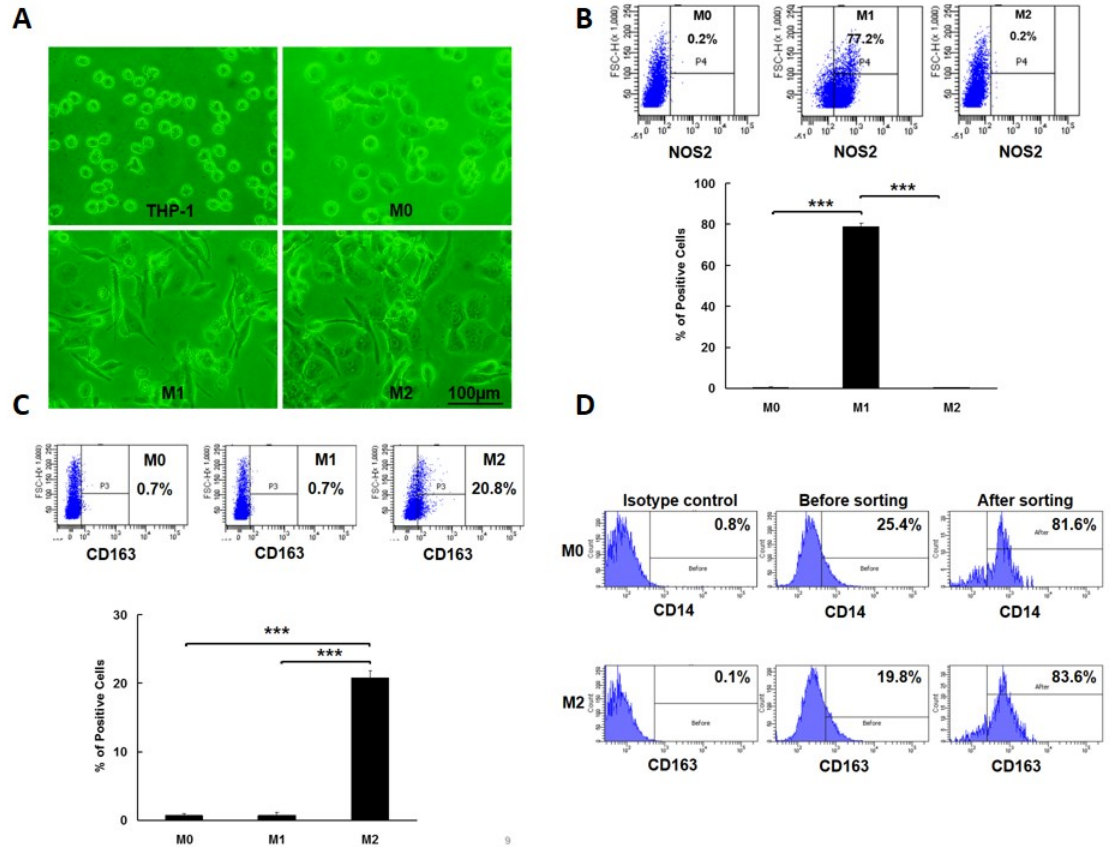


Figure 2.2 Characterization of M1 and M2 macrophages as well as the purification of M0 and M2 macrophages. Figure A shows different morphologic appearances of THP-1 cells, M0, M1 and M2 macrophages. Percentages of positive stained M1 or M2 macrophages were analyzed using specific markers of M1 (NOS2) and M2 (CD163) by flow cytometry (B, C). M0 and M2 macrophages were purified using cell sorting (D). , *** $p < 0.001$.

2.3.3 M2 macrophages significantly increased proliferation of HDF in co-culture

As shown in Figure 2.3, the cell proliferation increased gradually in groups of the

HDF, HDF+M0, HDF+M1 and HDF+M2 over time; however, significantly higher of cell proliferation were observed in the HDF co-cultured with M2 macrophages. There were significant differences between HDF and HDF+M2 ($p<0.05$) as well as HDF+M0 and HDF+M2 ($p<0.05$) at 96 hours after co-culture. Significant differences were also found between groups of HDF and HDF+M2 ($p<0.01$), HDF+M0 and HDF+M2 ($p<0.01$) and HDF+M1 and HDF+M2 ($p<0.05$) at 144 hours after co-culture. Within groups, there were significant differences in the HDF group between 48 and 144h ($p<0.01$), 96 and 144h ($p<0.01$); HDF+M0 group between 48 and 144h ($p<0.001$), 96 and 144h ($p<0.01$); HDF+M1 group between 48 and 96h ($p<0.05$), 48 and 144h ($p<0.001$), 96 and 144h ($p<0.01$); HDF+M2 group between 48 and 144h ($p<0.01$) after co-culture.

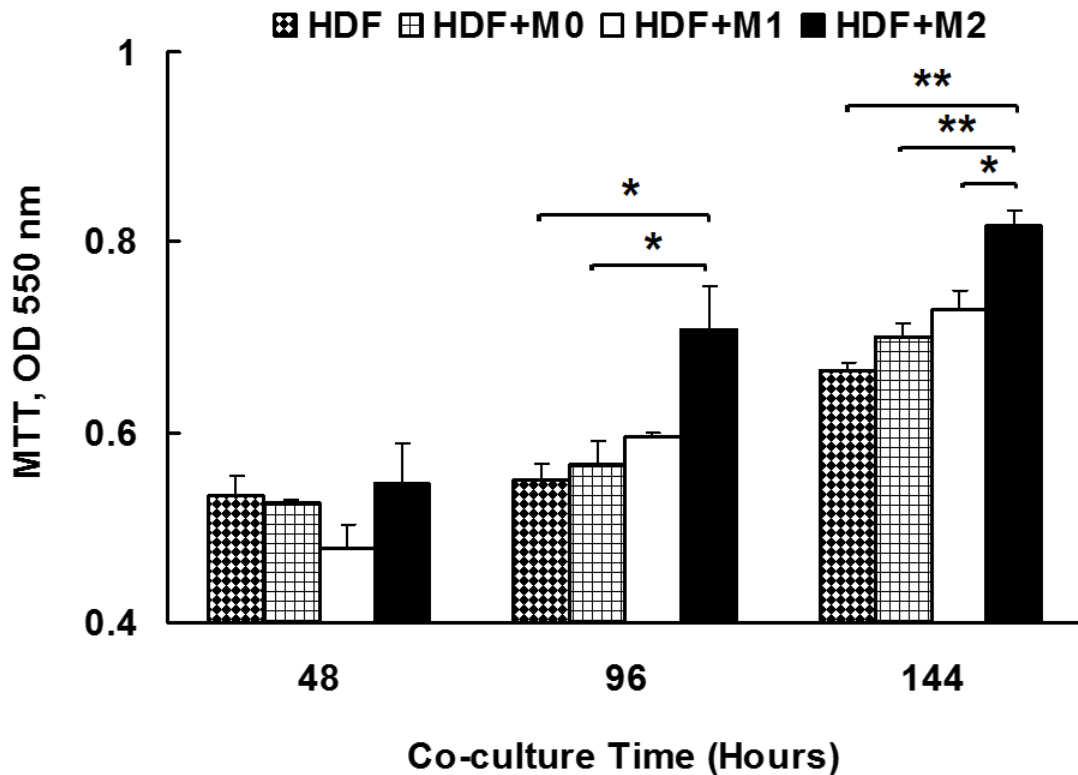


Figure 2.3 M2 macrophages up-regulated the cell viability of co-cultured HDF.

Figure 2.3 shows cell proliferation of the four groups after 48, 96 and 144 hours of co-culture. Triplicate, * $p < 0.05$, ** $p < 0.01$.

2.3.4 M2 macrophages increased the collagen synthesis of HDF in co-culture

Collagen synthesis was quantified by the measurement of 4-Hyp using LC/MS. At 96 and 144 hours, a similar trend was observed that collagen synthesis was significantly lower in HDF co-cultured with M1 macrophages whereas collagen synthesis was significantly higher in HDF co-cultured with M2 macrophages compared to the level of

HDF co-cultured alone. No significant difference in collagen synthesis was found between the media collected from the four groups after co-culture at 48 hours. There were significant differences between HDF and HDF+M1 ($p<0.01$), HDF+M0 and HDF+M1 ($p<0.05$), HDF+M1 and HDF+M2 ($p<0.05$) at 96 hours after co-culture. Significant differences were also found between HDF and HDF+M1 ($p<0.05$), HDF and HDF+M2 ($P<0.01$), HDF+M1 and HDF+M2 ($p<0.001$) at 144 hours after co-culture. In the HDF+M2 group, there was significant difference between 48 and 144h ($p<0.01$) after co-culture (Figure 2.4).

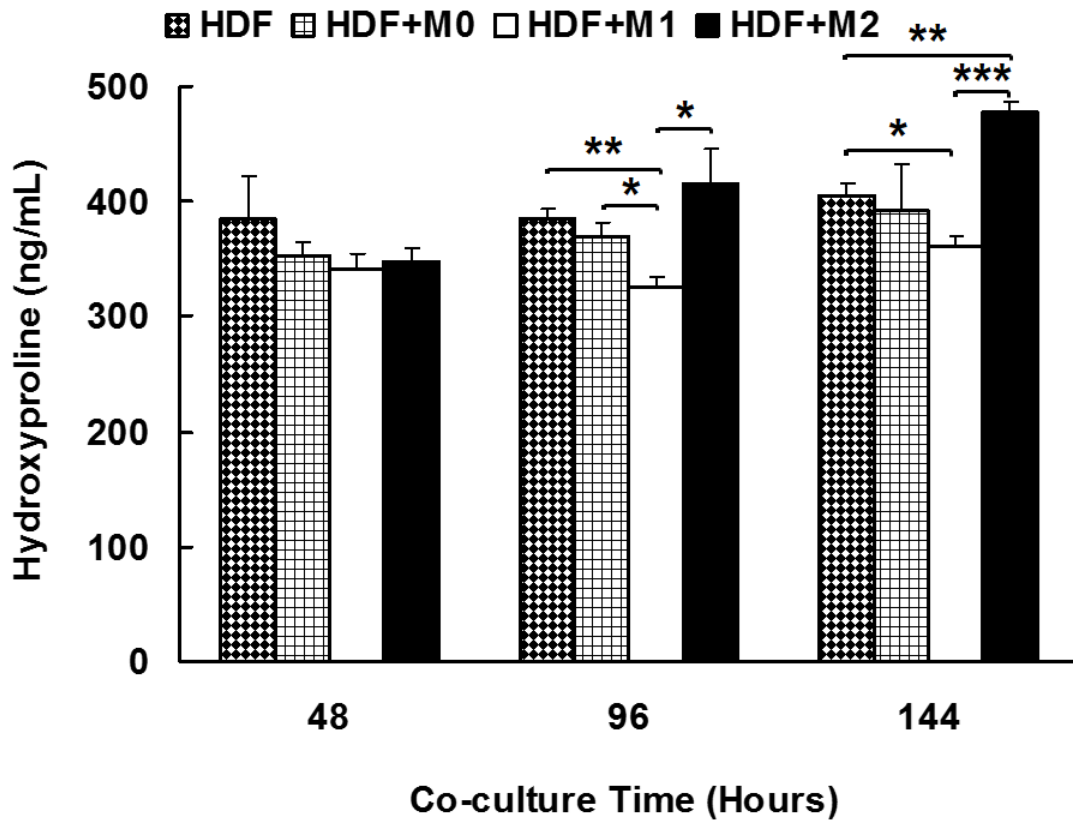


Figure 2.4 M2 macrophages promoted collagen synthesis of co-cultured HDF. The collagen synthesis were measured by LC/MS. The results are shown in Figure 2.4. Triplicate, * $p < 0.05$, ** $p < 0.01$, *** $p < 0.001$.

2.3.5 M2 macrophages increase myofibroblast differentiation of HDF in co-culture

Myofibroblasts are characterized by the expression of α -SMA, which are differentiated from the fibroblast population after pro-fibrotic stimulation (21). To determine the effect of M0, M1 and M2 macrophages on the co-cultured HDF, HDF from the four groups were stained with α -SMA and analyzed by flow cytometry as illustrated

in Figure 2.5A. Significant increases in α -SMA positive myofibroblasts were apparent by 144 hours when HDF were co-cultured with M2 macrophages (31.5%, $p < 0.05$) compared to the other three groups. In contrast, co-culture of HDF with M1 macrophages inhibited myofibroblast differentiation to levels significantly below HDF co-cultured alone and HDF in co-culture with M0 macrophages.

As was shown in Figure 2.5B, there was no significant difference of α -SMA positive cells between the four groups at 48 and 96 hours of co-culture. Significant differences were found between groups of HDF and HDF+M1 ($p < 0.05$), HDF and HDF+M2 ($p < 0.05$), HDF+M0 and HDF+M1 ($p < 0.05$), HDF+M1 and HDF+M2 ($p < 0.01$) at 144 hours of co-culture.

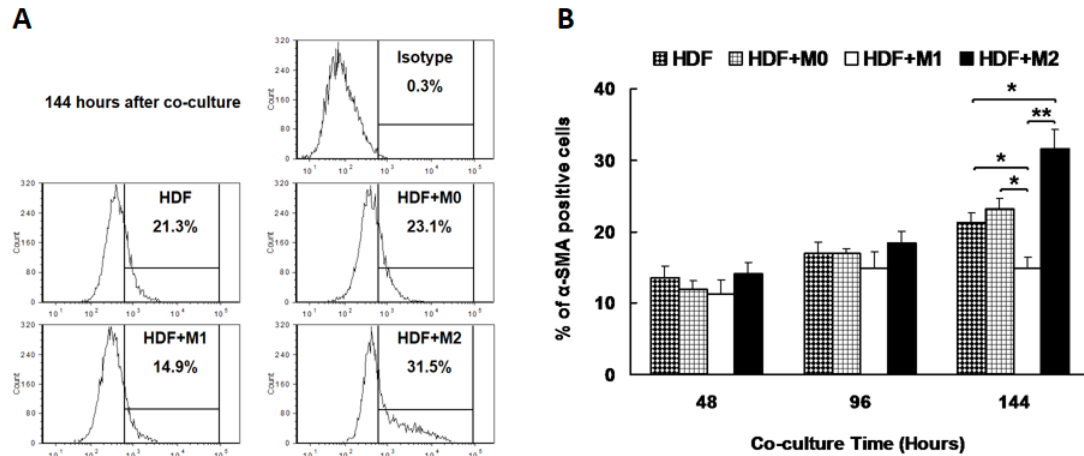


Figure 2.5 M2 macrophages increase myofibroblast differentiation of HDF in co-culture. Figure A shows the percentages of α -SMA positive cells after 144 hours of co-culture (A). Figure B shows the differences in percentages of α -SMA positive cells between the four groups after 48, 96 and 144 hours of co-culture. Triplicate, * $p < 0.05$, ** $p < 0.01$.

2.3.6 The effect of M2 macrophages on anti-fibrotic and pro-fibrotic factor expression

qPCR revealed the relative gene expression of anti-fibrotic factors and pro-fibrotic factors in the co-cultured HDF over time during the experimental time course (Figure

2.6). Anti-fibrotic factors, MMP-1 and DCN in the HDF+M1 group had a higher expression compared to the HDF group while HDF+M2 group had a lower expression compared to the HDF group at 96 and 144 hours in co-culture. Significant differences were observed in the expression of MMP-1 between HDF and HDF+M1 ($p<0.05$), HDF+M1 and HDF+M2 ($p<0.05$) at 96 hours; HDF and HDF+M1 ($p<0.01$), HDF+M0 and HDF+M2 ($p<0.01$), HDF+M1 and HDF+M2 ($p<0.05$) at 144 hours. There were significant differences in the expression of DCN between HDF+M0 and HDF+M1 ($p<0.05$), HDF+M1 and HDF+M2 ($p<0.05$) at 96 hours; HDF and HDF+M1 ($p<0.05$), HDF+M0 and HDF+M1 ($p<0.01$), HDF+M1 and HDF+M2 ($p<0.05$) at 144 hours of co-culture.

The expression of pro-fibrotic factor, TGF- β 1, was significantly higher in HDF co-cultured with M2 macrophages at 96 hours compared to the HDF co-cultured with M1 macrophages and HDF co-cultured alone. Co-culture of HDF with M2 macrophages increased the expression of COL1A1 at all the time points to levels significantly above HDF co-cultured alone, whereas, HDF co-cultured with M1 macrophages decreased the expression of COL1A1 at all the time points to levels significantly below HDF co-cultured alone. The expression of TIMP-1 was significantly higher in the HDF+M2 group while the TIMP-1 expression was significantly lower in the HDF+M1 group at 96 and 144 hours compared to HDF group. Significant differences were observed in the expression of TGF- β 1 between HDF and HDF+M0 ($p<0.05$), HDF and HDF+M2 ($p<0.05$), HDF+M0 and HDF+M1 ($p<0.05$), HDF+M1 and HDF+M2 ($p<0.05$) at 96 hours of co-culture. There were significant differences in the expression of COL1A1 between HDF and HDF+M2 ($p<0.01$), HDF+M1 and HDF+M2 ($p<0.001$) at 48 hours;

HDF and HDF+M0 ($p<0.05$), HDF and HDF+M1 ($p<0.05$), HDF and HDF+M2 ($p<0.05$), HDF+M0 and HDF+M2 ($p<0.01$), HDF+M1 and HDF+M2 ($p<0.05$) at 96 hours; HDF+M0 and HDF+M1 ($p<0.01$), HDF+M1 and HDF+M2 ($p<0.01$) at 144 hours of co-culture. Significant differences were found in the expression of TIMP-1 between HDF and HDF+M1 ($p<0.01$), HDF+M0 and HDF+M2 ($p<0.05$), HDF+M1 and HDF+M2 ($p<0.01$) at 96 hours; HDF+M0 and HDF+M2 ($p<0.01$), HDF+M1 and HDF+M2 ($p<0.05$) at 144 hours of co-culture.

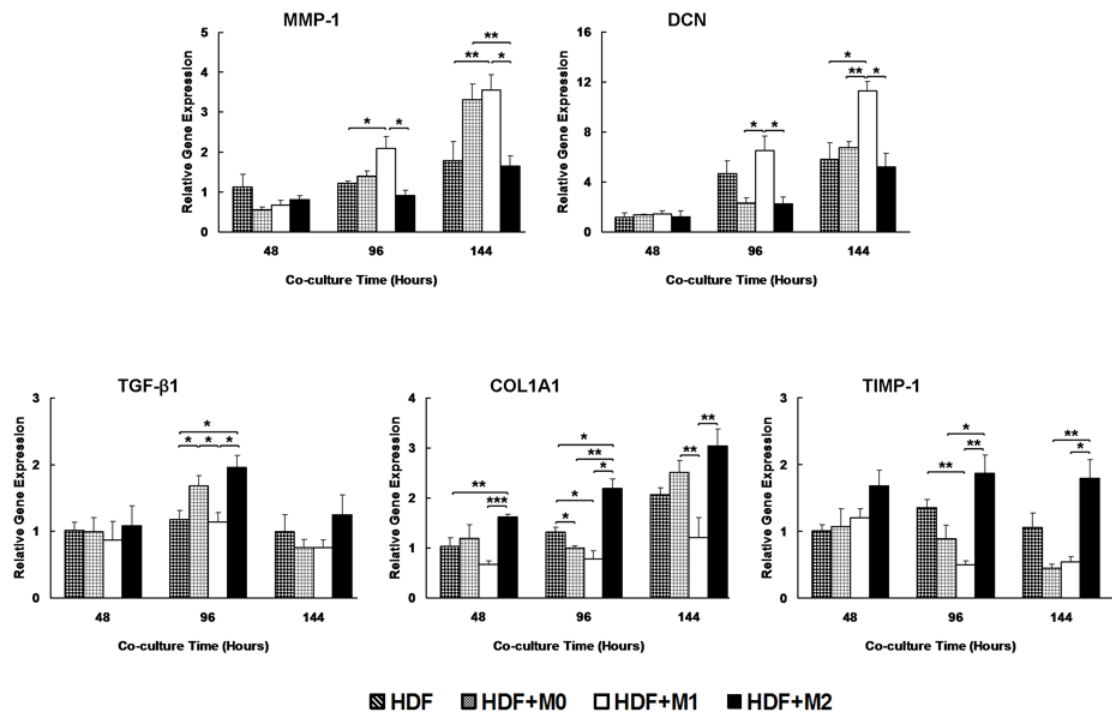


Figure 2.6 Decreased expression of anti-fibrotic factors and increased expression of pro-fibrotic factors in different group of co-cultured HDF. This figure reveals the relative gene expression of anti-fibrotic factors (MMP-1, DCN) and pro-fibrotic factors (TGF-β1, COL1A1, TIMP-1) in the four groups after the co-culture for 48, 96 and 144 hours. Triplicate, *p<0.05, **p<0.01, ***p<0.001.

2.3.7 M2 macrophages decreased and M1 macrophages increased MMP-1 activity in co-cultured HDF

The effect of macrophages co-culture on HDF MMP-1/collagenase activity between

the four groups was analyzed. As shown in Figure 2.7, M2 macrophages significantly decreased MMP-1 activity in co-cultured HDF at all the time points. In contrast M1 macrophages increased the MMP-1 activity in the co-cultured HDF. There were significant differences between groups of HDF+M0 and HDF+M2 ($p < 0.01$), HDF+M1 and HDF+M2 ($p < 0.05$) at 48 hours; HDF+M1 and HDF+M2 ($p < 0.05$) at 96 hours; HDF and HDF+M0 ($p < 0.05$), HDF and HDF+M2 ($p < 0.01$), HDF+M0 and HDF+M2 ($p < 0.01$), HDF+M1 and HDF+M2 ($p < 0.05$) at 144 hours of co-culture.

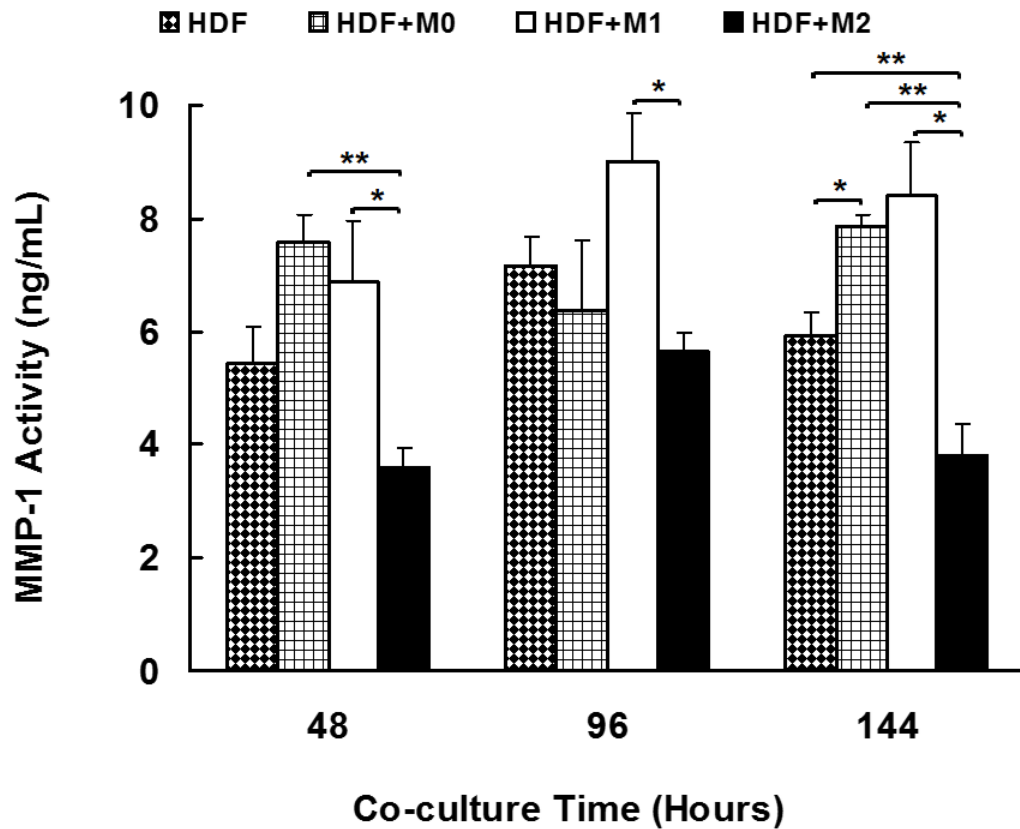


Figure 2.7 M2 macrophages decreased and M1 macrophages increased MMP-1 activity in co-cultured HDF. MMP-1 activity assay was performed to investigate the effect of M1, M2 macrophages on the co-cultured HDF after 48, 96 and 144 hours of co-culture. Triplicate, *p<0.05, **p<0.01.

2.3.8 Significant differences in concentration of the M1 and M2 macrophage related factors at 144 hours of co-culture

In order to explore the M0, M1 and M2 macrophage related factors in the co-cultured media, the cell culture supernatant was collected after 144 hours of co-culture and subjected to multiplex cytokine discovery assay. In Figure 2.8, IFN- γ , IL-1 β and TNF- α ,

M1 macrophage related factors with anti-fibrotic properties, were significantly higher in the group of HDF co-cultured with M1 macrophages as compared to the other three groups after 144 hours of co-culture. In contrast, the concentration of IFN- γ , IL-1 β and TNF- α were significantly lower in HDF co-cultured with M2 macrophages compared to the HDF co-cultured with M1 macrophages. There were significant differences in IFN- γ between groups of HDF and HDF+M0 ($p<0.05$), HDF and HDF+M1 ($p<0.001$), HDF and HDF+M2 ($p<0.05$), HDF+M0 and HDF+M1 ($p<0.01$), HDF+M1 and HDF+M2 ($p<0.001$); in IL-1 β between groups of HDF and HDF+M0 ($p<0.001$), HDF and HDF+M1 ($p<0.001$), HDF and HDF+M2 ($p<0.001$), HDF+M1 and HDF+M2 ($p<0.05$); in TNF- α between groups of HDF and HDF+M0 ($p<0.01$), HDF and HDF+M1 ($p<0.001$), HDF and HDF+M2 ($p<0.01$), HDF+M0 and HDF+M2 ($p<0.05$), HDF+M1 and HDF+M2 ($p<0.01$).

Similarly, the concentration of M2 macrophage related pro-fibrotic factors such as IL-4, IL-10 and TGF- β 1 was significantly higher in the group of HDF co-cultured with M2 macrophages compared to the other three groups after 144 hours of co-culture, whereas, HDF co-cultured with M1 macrophages significantly reduced the production of IL-4, IL-10, and most importantly TGF- β 1 at all the time points to levels significantly below HDF co-cultured with M2 macrophages. Significant differences were found in IL-4 between the groups of HDF and HDF+M2 ($p<0.01$), HDF+M0 and HDF+M2 ($p<0.01$), HDF+M1 and HDF+M2 ($p<0.01$); in IL-10 between the groups of HDF and HDF+M0 ($p<0.01$), HDF and HDF+M1 ($p<0.001$), HDF and HDF+M2 ($p<0.01$), HDF+M0 and HDF+M2 ($p<0.01$), HDF+M1 and HDF+M2 ($p<0.01$); in TGF- β 1 between the groups of HDF and HDF+M1 ($p<0.01$), HDF and HDF+M2 ($p<0.05$), HDF+M0 and HDF+M1

($p < 0.01$), HDF+M1 and HDF+M2 ($p < 0.01$).

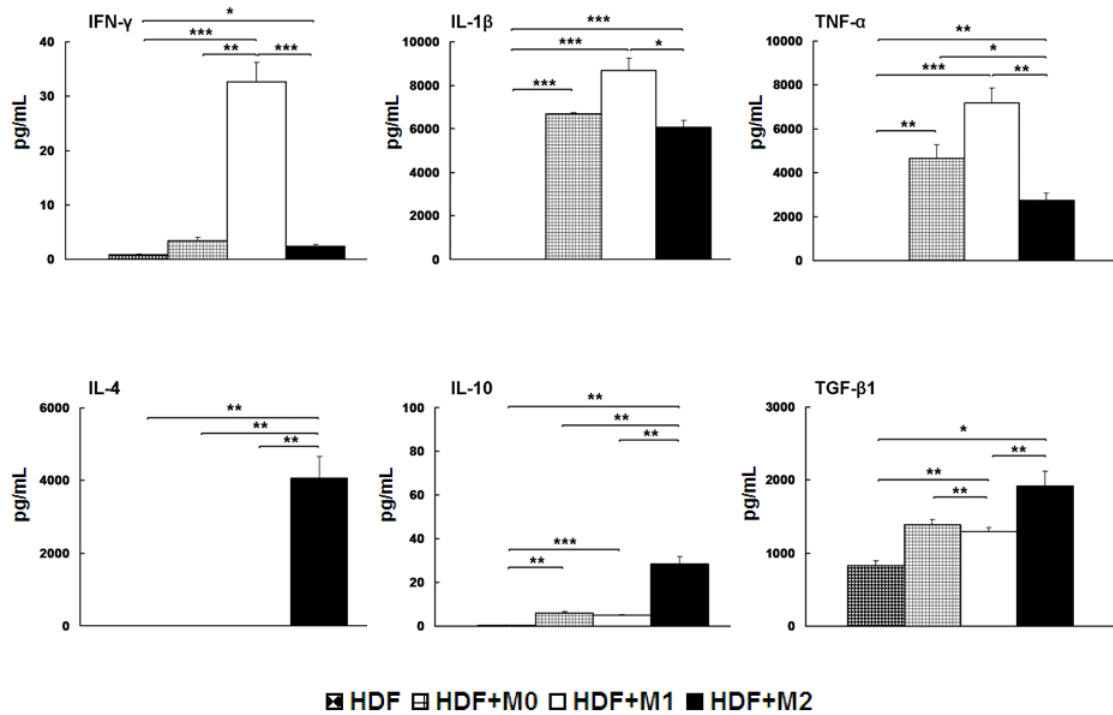


Figure 2.8 Multiplex analysis of cytokines at 144 hours of co-culture. The concentration of IFN- γ , IL-1 β , TNF- α , IL-4, IL-10 and TGF- β 1 was determined by multiplex discovery assay after 144 hours of co-culture. Triplicate, * $p < 0.05$, ** $p < 0.01$, *** $p < 0.001$.

2.4 Discussion

Significant differences were found between the groups of HDF+M1 and HDF+M2

after the co-culture especially after 96 and 144 hours, for example, HDF co-cultured with M2 macrophages had higher proliferation ability, collagen synthesis, myofibroblast differentiation, pro-fibrotic factor gene expression as well as lower anti-fibrotic factor gene expression and MMP-1 activity compared to those in HDF co-cultured with M1 macrophages. These findings are similar to Song et al., who used human polarized macrophage to co-culture with a human fibroblast cell line and suggested that M2 macrophages enhance while M1 macrophages inhibit the fibrogenesis of fibroblasts (22). In the current study, M0 macrophages were used together with M1 and M2 macrophages. HDF co-cultured with M0 macrophages did behave quite differently compared to the HDF co-cultured with M1 or M2 macrophages, indicating that M0, M1 and M2 macrophages were three different cell populations and the polarization of M1 and M2 macrophages was successful.

In cell culture, THP-1 is a cell line in suspension that has potentially unlimited proliferation ability while M0 macrophages differentiated from THP-1 cells will stop proliferating and become adherent. Therefore, cell cycle analysis was used to confirm the correct differentiation from THP-1 cells to M0 macrophages by quantifying the percentages of cells entering the S phase. Our data showed that there was significantly more THP-1 cells in S phase compared to those of M0 macrophages, indicating a successful differentiation from THP-1 cells to M0 macrophages in our experiments.

Previous studies have adopted PCR to determine the polarization of M1 and M2 macrophages differentiated from THP-1 cells by analyzing the M1 and M2 mRNA gene expression (23, 24). However, the mRNA expression is not always related to the protein synthesis. Thus, flow cytometry was used to detect the percentages of positive stained

M0, M1 and M2 macrophages using the relative expression of specific markers as mentioned above. Furthermore, our study is a first to use cell sorting technique to enrich the polarized macrophage cells before the co-culture. After cell sorting, the percentages of M0 and M2 positive macrophages reached more than 80%, which was much higher compared to those before the cell sorting. Cell sorting was not performed on M1 macrophages because NOS2 is an intracellular marker, and the cell membrane required permeabilization in order to get the fluorochrome antibody to NOS2 inside the cells, which would have reduced M1 macrophage viability before the co-culture. In contrast, the average percentage of NOS2 positive cells was 77%, which was considerably higher than 24% of M2 positive macrophages using arginase-1 (Arg-1), a canonical marker for murine M2 macrophages by flow cytometry reported by Jablonski et al. (25). This suggests that the canonical markers of human (CD163) or murine (Arg-1) M2 macrophages only label low percentages of positively stained cells, suggesting the need to explore additional novel markers for human M2 macrophages and additional methods for polarization in future studies.

Macrophages can be divided into two subtypes, which have opposite activation states and functions. However, macrophage phenotypes *in vivo* exhibit more complex phenotypes in different phases of wound healing. For example, there is a predominance of M1 macrophages in the inflammatory phase while a predominance of M2 macrophages exists in the proliferation phase (26). Nonetheless, mixed phenotypes of macrophages may exist during transition between phases of wound healing (27). Furthermore, there is growing recognition of the M2 macrophage subtypes, such as M2a, M2b, M2c (28). A fourth subtype, termed M2d by Leibovich et al., switches from a M1

phenotype into an anigogenic M2-like phenotype (29). Each subtype of M2 macrophages has a different activation state and its own products, which would add more complexity to the understanding of the role of M2 macrophages in vivo. Under such circumstances, it is advantageous to examine THP-1 cells in vitro to define numbers of quantitated polarized macrophages, which could be investigated similarly to the other studies where THP-1 cells have been used for co-culture studies with well-established protocols (30, 31).

MMP-1, also known as interstitial or fibroblast collagenase, is an enzyme that plays a profound role in the breakdown of ECM in normal wound healing processes like tissue remodeling. It is also involved in the disease processes such as arthritis and cancer cell metastasis (17, 32). In this study, HDF co-cultured with M1 macrophages increased the MMP-1 activity while HDF co-cultured with M2 macrophages decreased the MMP-1 activity compared to the HDF. However, since both fibroblasts and macrophages produce MMP-1, it may be that the co-cultured HDF or M1 macrophages or both are the source of the increase of MMP-1 activity. In contrast, M2 macrophages appear to inhibit HDF from secretion of MMP-1, decreasing its activity. On the whole, our findings suggest that M1 macrophages are anti-fibrotic whereas M2 macrophages play a pro-fibrotic role.

There was no direct contact between the polarized macrophages in the cell insert and the HDF in the bottom of the wells during the co-culture. This suggests that factors produced and secreted by the polarized macrophages on the cell insert were secreted into the media of the co-culture with HDF, led to the different behavioral changes. Some of these factors could include the fact that M1 macrophages metabolize L-arginine to nitric oxide, which inhibits cell proliferation; whereas M2 macrophages metabolize L-arginine

to ornithine, which promotes cell proliferation (33). The distinct opposite functions of the two products made by M1 and M2 macrophages correlate with the result of MTT proliferation assay in this study, where M2 macrophage had higher proliferation ability compared to the M1 macrophage co-cultured HDF.

Very likely other factors including cytokines released into the co-culture media also contributed to the dramatic differences in behavior of HDF. The multiplex cytokine discovery assay demonstrated significant differences in patterns of multiple growth factors released into the media over 144 hours of co-culture in our study. Our result indicated that that the inflammatory cytokines secreted by M1 macrophages and fibrotic factors secreted by M2 macrophages contributed to the behavioral changes between the HDF co-cultured with M1 or M2 macrophages.

M1 macrophages showed an anti-fibrotic role in our study by inhibiting proliferation of HDF, collagen synthesis, myofibroblast differentiation as well as increasing the MMP-1 activity of HDF, which can be explained by the significantly higher concentration of IFN- γ , an inflammatory cytokine secreted by M1 macrophages. The behavioral changes in HDF co-cultured with M1 macrophages were consistent with the findings from previous published studies. For instance, inhibition of IFN- γ resulted in accelerated healing after burn injury by dampening collagen deposition and myofibroblast differentiation (34). What's more, Higashi et al. reported that IFN- γ inhibits collagen synthesis by interfering with TGF- β signaling pathway (35). However, our study only exhibited an indirect effect of M1 macrophages on co-cultured HDF, the direct role of IFN- γ on HDF needs to be investigated in the future.

2.5 Conclusion

In conclusion, our study showed that M2 macrophages promotes the fibrogenic activities of HDF by facilitating the cell proliferation, increasing the collagen synthesis and myofibroblast differentiation, in part by enhancing the expression of the pro-fibrotic factors and productions of M2 macrophage related factor while antagonizing the expression of the anti-fibrotic genes and MMP-1 activity. Our study is a first to use cell sort to purify macrophage subsets prior to co-culture. Moreover, our data reinforce the pro-fibrotic role of M2 macrophages, which may be a strategic target for the treatment of fibrotic diseases in the future.

2.6 References

1. Ginhoux F, Jung S. Monocytes and macrophages: developmental pathways and tissue homeostasis. *Nat Rev Immunol.* 2014;14:392-404.
2. Gordon S. The macrophage: past, present and future. *Eur J Immunol.* 2007;37 Suppl 1:S9-17.
3. Mosser DM, Edwards JP. Exploring the full spectrum of macrophage activation. *Nat Rev Immunol.* 2008;8:958-69.
4. Wynn TA. Fibrotic disease and the T(H)1/T(H)2 paradigm. *Nat Rev Immunol.* 2004;4:583-94.
5. Martinez FO, Helming L, Gordon S. Alternative Activation of Macrophages: An Immunologic Functional Perspective. *Annual Review of Immunology.* 2009;27:451-83.
6. Jaguin M, Houlbert N, Fardel O, Lecreur V. Polarization profiles of human M-CSF-generated macrophages and comparison of M1-markers in classically activated macrophages from GM-CSF and M-CSF origin. *Cell Immunol.* 2013;281:51-61.
7. McDougall S, Dallon J, Sherratt J, Maini P. Fibroblast migration and collagen deposition during dermal wound healing: mathematical modelling and clinical implications. *Philos Trans A Math Phys Eng Sci.* 2006;364:1385-405.
8. Mahdavian Delavary B, van der Veer WM, van Egmond M, Niessen FB, Beelen RH. Macrophages in skin injury and repair. *Immunobiology.* 2011;216:753-62.
9. Nishida M, Hamaoka K. Macrophage phenotype and renal fibrosis in obstructive nephropathy. *Nephron Experimental Nephrology.* 2008;110:E31-E6.
10. Chanput W, Mes JJ, Savelkoul HF, Wichers HJ. Characterization of polarized THP-1 macrophages and polarizing ability of LPS and food compounds. *Food Funct.* 2013;4:266-76.
11. Ferret PJ, Soum E, Negre O, Wollman EE, Fradelizi D. Protective effect of thioredoxin upon NO-mediated cell injury in THP1 monocytic human cells. *Biochemical*

Journal. 2000;346:759-65.

12. Traore K, Trush MA, George M, Spannhake EW, Anderson W, Asseffa A. Signal transduction of phorbol 12-myristate 13-acetate (PMA)-induced growth inhibition of human monocytic leukemia THP-1 cells is reactive oxygen dependent. *Leukemia Research*. 2005;29:863-79.
13. Aggarwal S, Das SN. Garcinol inhibits tumour cell proliferation, angiogenesis, cell cycle progression and induces apoptosis via NF-kappaB inhibition in oral cancer. *Tumour Biol*. 2015.
14. Ding J, Ma Z, Shankowsky HA, Medina A, Tredget EE. Deep dermal fibroblast profibrotic characteristics are enhanced by bone marrow-derived mesenchymal stem cells. *Wound Repair Regen*. 2013;21:448-55.
15. Tredget EE, Iwashina T, Scott PG, Ghahary A. Determination of plasma Ntau-methylhistamine in vivo by isotope dilution using benchtop gas chromatography-mass spectrometry. *J Chromatogr B Biomed Sci Appl*. 1997;694:1-9.
16. Wang J, Dodd C, Shankowsky HA, Scott PG, Tredget EE, Wound Healing Research G. Deep dermal fibroblasts contribute to hypertrophic scarring. *Lab Invest*. 2008;88:1278-90.
17. Lee YR, Kweon SH, Kwon KB, Park JW, Yoon TR, Park BH. Inhibition of IL-1beta-mediated inflammatory responses by the IkappaB alpha super-repressor in human fibroblast-like synoviocytes. *Biochem Biophys Res Commun*. 2009;378:90-4.
18. Egli A, Kumar D, Broscheit C, O'Shea D, Humar A. Comparison of the Effect of Standard and Novel Immunosuppressive Drugs on CMV-Specific T-Cell Cytokine Profiling. *Transplantation*. 2013;95:448-55.
19. Park EK, Jung HS, Yang HI, Yoo MC, Kim C, Kim KS. Optimized THP-1 differentiation is required for the detection of responses to weak stimuli. *Inflammation Research*. 2007;56:45-50.
20. Stewart DA, Yang YM, Makowski L, Troester MA. Basal-like Breast Cancer Cells Induce Phenotypic and Genomic Changes in Macrophages. *Molecular Cancer Research*. 2012;10:727-38.

21. Darby IA, Hewitson TD. Fibroblast differentiation in wound healing and fibrosis. *International Review of Cytology - a Survey of Cell Biology*, Vol 257. 2007;257:143-+.
22. Song E, Ouyang N, Horbelt M, Antus B, Wang M, Exton MS. Influence of alternatively and classically activated macrophages on fibrogenic activities of human fibroblasts. *Cell Immunol*. 2000;204:19-28.
23. Fujisaka S, Usui I, Bukhari A, Ikutani M, Oya T, Kanatani Y, et al. Regulatory mechanisms for adipose tissue M1 and M2 macrophages in diet-induced obese mice. *Diabetes*. 2009;58:2574-82.
24. Chanput W, Mes J, Vreeburg RA, Savelkoul HF, Wichers HJ. Transcription profiles of LPS-stimulated THP-1 monocytes and macrophages: a tool to study inflammation modulating effects of food-derived compounds. *Food Funct*. 2010;1:254-61.
25. Jablonski KA, Amici SA, Webb LM, Ruiz-Rosado Jde D, Popovich PG, Partida-Sanchez S, et al. Novel Markers to Delineate Murine M1 and M2 Macrophages. *PLoS One*. 2015;10:e0145342.
26. Zhu Z, Ding J, Ma Z, Iwashina T, Tredget EE. The natural behavior of mononuclear phagocytes in HTS formation. *Wound Repair Regen*. 2015.
27. Stables MJ, Shah S, Camon EB, Lovering RC, Newson J, Bystrom J, et al. Transcriptomic analyses of murine resolution-phase macrophages. *Blood*. 2011;118:e192-208.
28. Mantovani A, Sica A, Sozzani S, Allavena P, Vecchi A, Locati M. The chemokine system in diverse forms of macrophage activation and polarization. *Trends Immunol*. 2004;25:677-86.
29. Ferrante CJ, Leibovich SJ. Regulation of Macrophage Polarization and Wound Healing. *Adv Wound Care (New Rochelle)*. 2012;1:10-6.
30. Tjiu JW, Chen JS, Shun CT, Lin SJ, Liao YH, Chu CY, et al. Tumor-associated macrophage-induced invasion and angiogenesis of human basal cell carcinoma cells by cyclooxygenase-2 induction. *J Invest Dermatol*. 2009;129:1016-25.
31. Stewart DA, Yang Y, Makowski L, Troester MA. Basal-like breast cancer cells

induce phenotypic and genomic changes in macrophages. *Mol Cancer Res.* 2012;10:727-38.

32. Tolboom TC, Pieterman E, van der Laan WH, Toes RE, Huidekoper AL, Nelissen RG, et al. Invasive properties of fibroblast-like synoviocytes: correlation with growth characteristics and expression of MMP-1, MMP-3, and MMP-10. *Ann Rheum Dis.* 2002;61:975-80.

33. Mills CD. Anatomy of a discovery: m1 and m2 macrophages. *Front Immunol.* 2015;6:212.

34. Shen H, Yao P, Lee E, Greenhalgh D, Soulika AM. Interferon-gamma inhibits healing post scald burn injury. *Wound Repair Regen.* 2012;20:580-91.

35. Higashi K, Inagaki Y, Fujimori K, Nakao A, Kaneko H, Nakatsuka I. Interferon-gamma interferes with transforming growth factor-beta signaling through direct interaction of YB-1 with Smad3. *Journal of Biological Chemistry.* 2003;278:43470-9.

Chapter 3

The Natural Behavior of Mononuclear Phagocytes in Hypertrophic Scar Formation

This chapter has been published as: Zhu Z, Ding J, Ma Z, Iwashina T, Tredget EE. The natural behavior of mononuclear phagocytes in HTS formation. *Wound Repair Regen.* 2016 Jan;24(1):14-25. doi: 10.1111/wrr.12378. Epub 2015 Nov 20.

3.0 Abstract

HTS are caused by trauma or burn injuries to the deep dermis and are considered fibrosis in the skin. Monocytes, M1 and M2 macrophages are mononuclear phagocytes. Studies suggest that M2 macrophages are pro-fibrotic and might contribute to hypertrophic scar formation. Our lab has established a human HTS-like nude mouse model, in which the grafted human skin develops red, raised, and firm scarring, resembling hypertrophic scars seen in humans. In this study, we observed the natural behavior of mononuclear phagocytes in this nude mouse model of dermal fibrosis at multiple time points. Thirty athymic nude mice received human skin grafts and an equal number of mice received mouse skin grafts as controls. The grafted skin and blood were harvested at 1, 2, 3, 4 and 8 weeks. Wound area, thickness, collagen morphology and level, the cell number of myofibroblasts, M1 and M2 macrophages in the grafted skin, as well as monocyte fraction in the blood were investigated at each time point. Xenografted mice developed contracted and thickened scars grossly. The xenografted skin resembled human hypertrophic scar tissue based on enhanced thickness, fibrotic orientation of collagen bundles, increased collagen level and infiltration of myofibroblasts. In the blood, monocytes dramatically decreased at 1 week post-grafting and gradually returned to normal in the following 8 weeks. In the xenografted skin, M1 macrophages were found predominantly at 1 to 2 weeks post-grafting; whereas, M2 macrophages were abundant at later time points, 3 to 4 weeks post-grafting coincident with the development of fibrosis in the human skin tissues. This understanding of the natural behavior of mononuclear phagocytes in vivo in our mouse model provides evidence for the role of M2 macrophages in fibrosis of human skin and suggests that macrophage depletion in the subacute phases of wound healing might reduce or prevent HTS formation.

3.1 Introduction

Monocytes are derived from the bone marrow and circulate through the blood stream before they are attracted into the local tissue after injury, where they replenish the local population of tissue macrophages during the wound healing process (1). In addition to retaining the phagocytic capacity of monocytes which functions to digest tissue debris and dead cells, macrophages play a critical role in the innate and adaptive immunity (2). Thus monocytes in the blood and macrophages in the tissue constitute the major cellular components of mononuclear phagocyte system (MPS) (3).

Macrophages have an intimate relationship with wound healing by exerting diverse functions in inflammation, proliferation and tissue remodeling phases. In response to various signals from the local microenvironment, macrophages may polarize into two distinct phenotypes, M1 or M2 macrophages (4). However, it has been shown that the phenotypic change of macrophages is reversible, switching from one phenotype to another depending on the microenvironment (5, 6), which underlines their plasticity. In normal wound healing, M1 macrophages are observed in the early phases of tissue repair where they exhibit a pro-inflammatory phenotype and produce cytokines such as TNF- α , IL-6, IL-1 β ; whereas, M2 macrophages are more typically seen in later phases of wound healing and produce cytokines such as TGF- β 1, IL-10 and IL-1 α . They are also associated with allergic and anti-parasite responses (7). M1 macrophages are considered to be anti-fibrotic because they can inhibit fibroblast proliferation and collagen production. In contrast, M2 macrophages can enhance the pro-fibrotic activities of fibroblasts through stimulation of proliferation and increased ECM production (8).

To investigate the natural appearance of mononuclear phagocytes, monocytes in the blood and macrophage phenotypes in scar tissues were analyzed during the development of skin fibrosis at multiple time points after engraftment of human skin in the nude mouse model.

3.2 Materials and methods

3.2.1 Harvesting of human split thickness skin grafts

Abdominal skin tissue were obtained from female patients who underwent abdominoplasty with documented informed consent in their personal health record. Under sterile condition, split thickness skin grafts (STSG) were harvested by using a Padgett electric dermatome (Padgett Instruments, Inc., Kansas City, MO) set at 0.4 mm thickness. Skin that was atrophic or had developed striae was avoided. The STSG were trimmed to a consistent size using a $2.0 \times 1.5 \text{ cm}^2$ template. The grafts were stored in DMEM supplemented with 10% FBS until grafting.

3.2.2 Animals

Sixty 4-week-old male athymic nude mice (outbred) weighing 20 grams that lacked T-cells due to absence of thymus were purchased from Charles River Laboratories (Wilmington, MA, USA). They were rested for two weeks in a virus-free biocontainment facility before grafting. The animal protocol was approved by the University of Alberta Animal Care and Use Committee in accordance with the Canadian Council of Animal Care

standards.

3.2.3 Establishment of human HTS-like nude mouse model

As previously described (9, 10), the mice were anesthetized using isoflurane (Halocarbon Laboratories, River Edge, NJ). Surgical sites were disinfected using Prepodyne Solution (West Penetone INC, Anjou, QC) and then wiped clean with 70% ethanol. A $2.0 \times 1.5 \text{ cm}^2$ region of dorsal full thickness skin was outlined using a template and the skin was carefully excised using sharp dissection without damaging underlying panniculus carnosus. Thirty mice were grafted with human STSG (xenografts) while additional thirty mice received the excised full thickness mouse skin (allografts) as controls. The grafts were then sutured using 4-0 braided silk suture (Ethicon, Somerville, NJ) and covered with Xeroform (Covidien, Mansfield, MA) using a tie-over dressing to maximize complete contact between the graft and the wound. The mice received hydromorphone (Sandoz, Boucherville, QC), 0.05mg/ml subcutaneously for postoperative pain management. The dressings and sutures were removed 1 week post-grafting under isoflurane general anesthesia. The mice were euthanized at 1, 2, 3, 4, 8 weeks post-grafting. Blood was obtained by cardiac puncture. Allografts and xenografts were excised at each time point for further analysis.

3.2.4 Morphology of wounds by digital photography

Standardized digital photographs of the wounds were taken weekly after grafting with ruler in order to record the scar formation over time. The area of the wounds was measured

for assessment of wound contraction using ImageJ software (National Institutes of Health, Bethesda, MD). The scale in the software was reset for each image to avoid magnification errors.

3.2.5 Processing of graft specimens

The entire engrafted skin samples were harvested at different time points and prepared for paraffin and cryosection blocks. Paraffin sections were stained for H&E staining, Masson's trichrome staining and immunohistochemistry (IHC) staining. Cryosection were used for IHC staining.

3.2.6 Histology analysis of graft specimens

H&E and Masson's trichrome stained tissues were imaged under bright field microscopy (Nikon OIPHOT-2, Nikon Instruments Inc., Melville, NY). Dermal thickness in the grafts was analyzed by ImageJ software using a micrometer to standardize the reference image. As previously described (11), the dermal thickness was defined as distance (μm) from epidermis to junction of the dermal-adipose layer. Three measurements were obtained from each sample including the thickest, thinnest and midpoint region were recorded and the mean value was calculated.

3.2.7 Collagen morphology analysis

Masson's trichrome staining was used to show the morphology of collagen fibers,

which showed green collagen fibers, red keratin and dark brown or black cell nuclei under the bright field microscope. Collagen orientation index (COI) and collagen bundle packing index (CBPI) were calculated using fast Fourier transformation (FFT) module in ImageJ software to describe collagen bundle features in the grafts. The equation “1-width/height ratio of the zeroth-order maximum” was used to calculate COI. The CBPI was calculated using the distance between the centers of gravity of the first-order maxima through the formula “ $\lambda = 794\mu\text{m} / 0.5 \times d$ ” (12).

3.2.8 Quantification of 4-Hyp in graft specimens

The amount of 4-Hyp, a unique amino acid in collagen, was measured by LC/MS as previously described with modifications (13). Briefly, the skin sample (dry weight: 0.5~3.9mg) in a pyrex screw-capped glass tube was added to 6N HCl solution and then hydrolyzed at 110°C overnight. A known amount of 4-Hyp-d₃ as internal standard was added to the hydrolysate. The n-butyl ester reagent was added to the dried hydrolysate in order to produce the n-butyl ester derivatives of 4-Hyp and 4-Hyp-d₃. The samples were analyzed by LC/MS (Agilent Technologies, Santa Clara, CA) monitored using Mass Selective detection the ions 188 (4-Hyp n-butyl ester) and 191 (4-Hyp-d₃ n-butyl ester). The calibration curve was constructed through a range of 4-Hyp (6 points amount) using the peak area ratio. The ratio was obtained by dividing 4-Hyp peak area by the internal standard (4-Hyp-d₃) peak area. The amount of 4-Hyp in each sample was analyzed using the calibration curve. The data was expressed in 4-Hyp (μg) / dry weight sample (mg).

3.2.9 Immunohistochemistry staining of myofibroblasts

For IHC staining of myofibroblasts, paraffin sections were warmed for 20 minutes at 60°C in a vacuum oven and then underwent deparaffinization by xylene and rehydration through decreasing concentrations of ethanol from 100% to 70%. After antigen retrieval using 0.05% trypsin, the skin sections were incubated with 10% bovine serum albumin (BSA) (Sigma-Aldrich, St. Louis, MO) to block non-specific binding, followed by incubation with rabbit anti-human α -SMA antibodies (Millipore, Cat. # MABT381) (1:1000) at 4°C overnight and biotinylated goat anti-rabbit IgG (H+L) (Vector Laboratories Inc. Cat. # BA-1000) (1:500) at room temperature for one hour.

The tissue sections were then incubated using VECTASTAIN® ABC kit (Vector Laboratories Inc., Cat. # PK-4005) and developed using diaminobenzidine (Sigma-Aldrich, Cat. # D8001). The nuclei were counter-stained using hematoxylin. After dehydration, the sections were mounted and checked under light microscope. Positive stained cells excluding perivascular cells surrounding the blood vessels were counted in five random high power fields (HPFs) for each sample.

3.2.10 Quantification of circulating monocytes using flow cytometry

100 μ l of blood collected by cardiac puncture was transferred to each 5 ml polystyrene round-bottom tube (Falcon, Corning, NY) and incubated with mouse specific FcR blocking reagent (Miltenyi Biotec Inc., San Diego, CA) after the red blood cells (RBC) were lysed using RBC lysis buffer (eBioscience, San Diego, CA). The FcR blocked cells were then

incubated with anti-CD11b-FITC (eBioscience, Cat. # 11-0112-81) and anti-CD115-APC antibodies (eBioscience, Cat. # 17-1152-80). After washing and fixation, the monocyte population was then detected by flow cytometry using a BD FACSCanto II (BD Biosciences, San Jose, CA). The monocyte population was gated around CD115 and CD11b double positive events (14). The data files were analyzed by FCS express 4.0 software (DeNovo Software; Los Angeles, CA).

3.2.11 Quantification of M1 & M2 macrophage by immunofluorescence staining

Cryosections were fixed in ice-cold acetone (Thermo Fisher Scientific Inc., Waltham, MA) after warming and air-dried. After rinsing in PBS, sections were incubated with 10% BSA to avoid non-specific binding, and then incubated with primary antibodies and followed by specific secondary antibodies. For general marker of mouse macrophages, rat anti-mouse F4/80 was detected (eBioscience, Cat. # 14-4801-82). The primary antibody for M1 macrophages was rabbit polyclonal NOS2 IgG (Santa Cruz, Cat. # sc-651 FITC) and goat polyclonal Arg-1 IgG antibody (Santa Cruz, Cat. # sc-18351) for M2 macrophages. The secondary antibody was Alexa Fluor® 594 donkey anti-rat IgG (Life Technologies, Cat. # A-21209) for F4/80 and Alexa Fluor® 488 donkey anti-goat IgG (Life Technologies, Cat. # A-11055) for Arg-1. The slides were mounted with ProLong Gold anti-fade reagent with DAPI (Life Technologies, Carlsbad, CA) after washing. Images were taken at the lower dermis of the skin grafts using a confocal microscope (Leica TCS SP5, Leica Microsystems, Concord, ON) with 63X optical lens. Double positive cells were counted using image analysis software (LAS AF Lite, Leica Microsystems, Concord, ON).

3.2.12 qPCR for cytokines from M1 and M2 macrophages

Skin grafts from allografted and xenografted mice were powdered using Mikro-Dismembrator S (B. Braun Biotech Inc., Allentown, PA) and then lysed using TRIzol reagent (Thermo Fisher Scientific., Waltham, MA). Total RNA was extracted using RNeasy Mini Kit (Qiagen Sciences, Germantown, MD). A 0.5µg of total RNA was used for cDNA synthesis using cDNA Syntheses Kit (Invitrogen). The qPCR was conducted using RT² SYBR® Green qPCR Mastermix (Qiagen Sciences, Germantown, MD) and mouse primers of TNF- α , forward GTAACGCCAGGAATTGTTGCTA and reverse GGGAGTAGACAAGGTACAACCC; IL-6, forward TCTATAACCACTTCACAAGTCGGA and reverse GAATTGCCATTGCACAACCTCTTT; IL-1 β , forward GAAATGCCACCTTTTGACAGTG and reverse TGGATGCTCTCATCAGGACAG; TGF- β 1, forward CTTCAATACGTCAGACATTCGGG and reverse GTAACGCCAGGAATTGTTGCTA; IL-10, forward GCTGGACAACATACTGCTAACC and reverse GCTGGACAACATACTGCTAACC; IL-1 α , forward TCTCAGATTCACAACCTGTTTCGTG and reverse AGAAAATGAGGTCGGTCTCACTA. Mouse glyceraldehyde 3-phosphate dehydrogenase (GAPDH) (forward AGGTCGGTGAGAACGGATTTG and reverse GGGGTCGTTGATGGCAACA) was used as a normalization/internal control (Eurofins MWG Operon, Huntsville, AL). Amplification and analysis of cDNA were performed using the StepOnePlus Real-Time System (Applied Biosystems, Foster City, CA). Relative gene expression was measure as cycle threshold (Ct) and the data was displayed as fold change calculated by the equation of $2^{\Delta\Delta Ct}$, in which the $\Delta\Delta Ct$ was normalized with individual internal control Ct value.

3.2.13 Statistical analysis

Six mice were used in each group of each time point. Data were imported into STATA 12 for windows (StataCorp LP, Collage Station, TX) and displayed as mean \pm SE. Statistical analysis was performed using a two-tailed unpaired student's t-test or one-way ANOVA with the Bonferroni method. A p-value of less than 0.05 ($p < 0.05$) was considered statistically significant.

3.3 Results

3.3.1 Grafted human skin developed scar in the mouse model

The grafted skin remained viable throughout the whole experiment. One week post-grafting, the grafted skin looked erythematous and moist after the dressing and sutures were removed. Two weeks after the transplantation, the grafted skin in the allografted mice healed much better than those in the xenografted mice. The wounds of xenografted mice showed a prolong inflammation with obvious margin up to 2 weeks post-grafting before developing a contracted, pigmented, thickened, raised scar progressively up to 8 weeks post-grafting (Figure 3.1A) while no obvious scar thickening nor contraction were observed in the allografted mice overtime. The figure at 0 week (0W) illustrates the skin tissue thickness before grafting.

The grafted area was monitored and digitally photographed weekly. The wound areas were then quantified by ImageJ software to evaluate wound contraction (11). Compared to

the initial graft, the area of wounds in the allografted mice reduced quickly in the first 2 weeks post-grafting and had no significant changes thereafter, while the wounds in xenografted mice became progressively more contracted over time. There were significant differences of wound area between 0 and 2 ($p<0.01$, $p<0.05$), 0 and 3 ($p<0.01$, $p<0.001$), 0 and 4 ($p<0.01$, $p<0.001$), 0 and 8 ($p<0.01$, $p<0.001$) weeks post-grafting in both allografted and xenografted mice. At 8 weeks after grafting there was a significant decrease ($p<0.05$) in wound size between allografted and xenografted mice (Figure 3.1B).

Compared to mouse skin, the engrafted human skin in the xenografted mice retained the structural characteristics of human skin microscopically (Figure 3.1C). The graft thicknesses at different time points were displayed as percentages of the original thickness of the STSG before grafting. The skin thickness gradually increased from 1 to 4 weeks post-grafting in xenografted mice and then decreased slowly thereafter. In allografted mice, the graft thickness increased to a peak at 2 weeks and remained stable over time. There were significant differences between 0 and 3 ($p<0.05$), 0 and 4 ($p<0.05$) weeks post-grafting in xenografted mice. Significant differences were also found in 3 ($p<0.05$) and 4 ($p<0.05$) weeks between the allografted and xenografted mice (Figure 3.1D).

A

1 week

2 weeks

3 weeks

4 weeks

8 weeks

Allograft



Xenograft



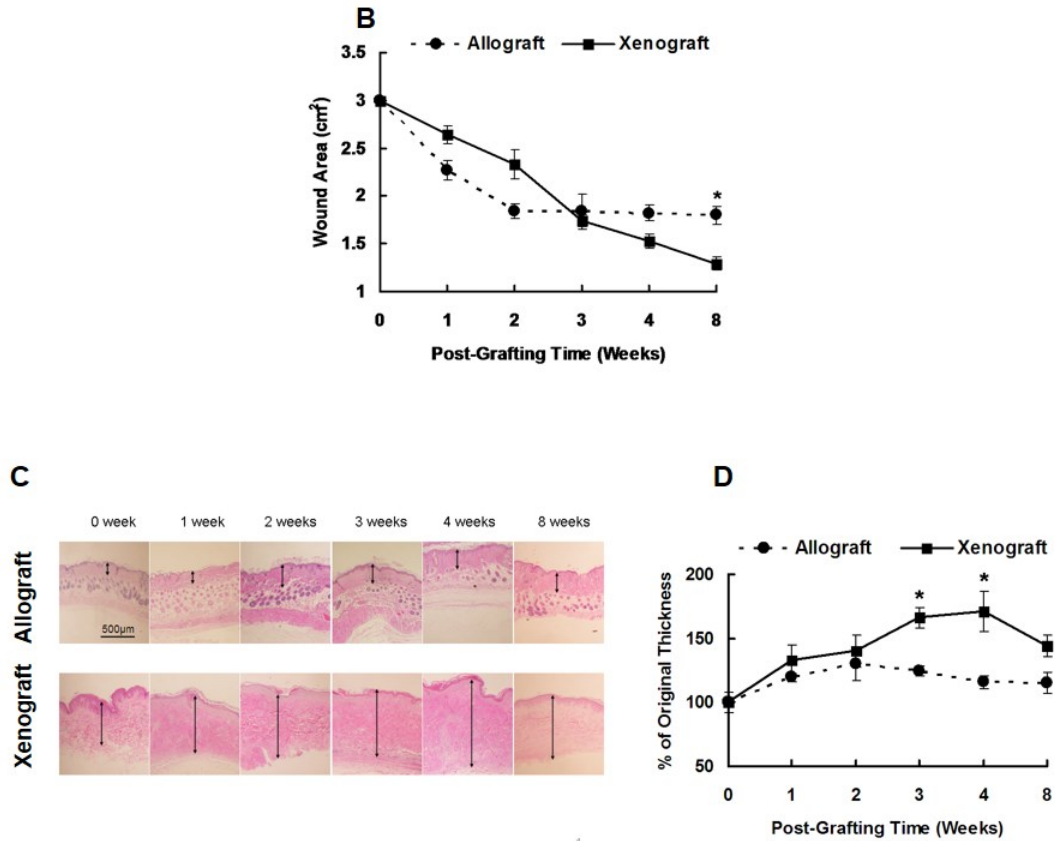


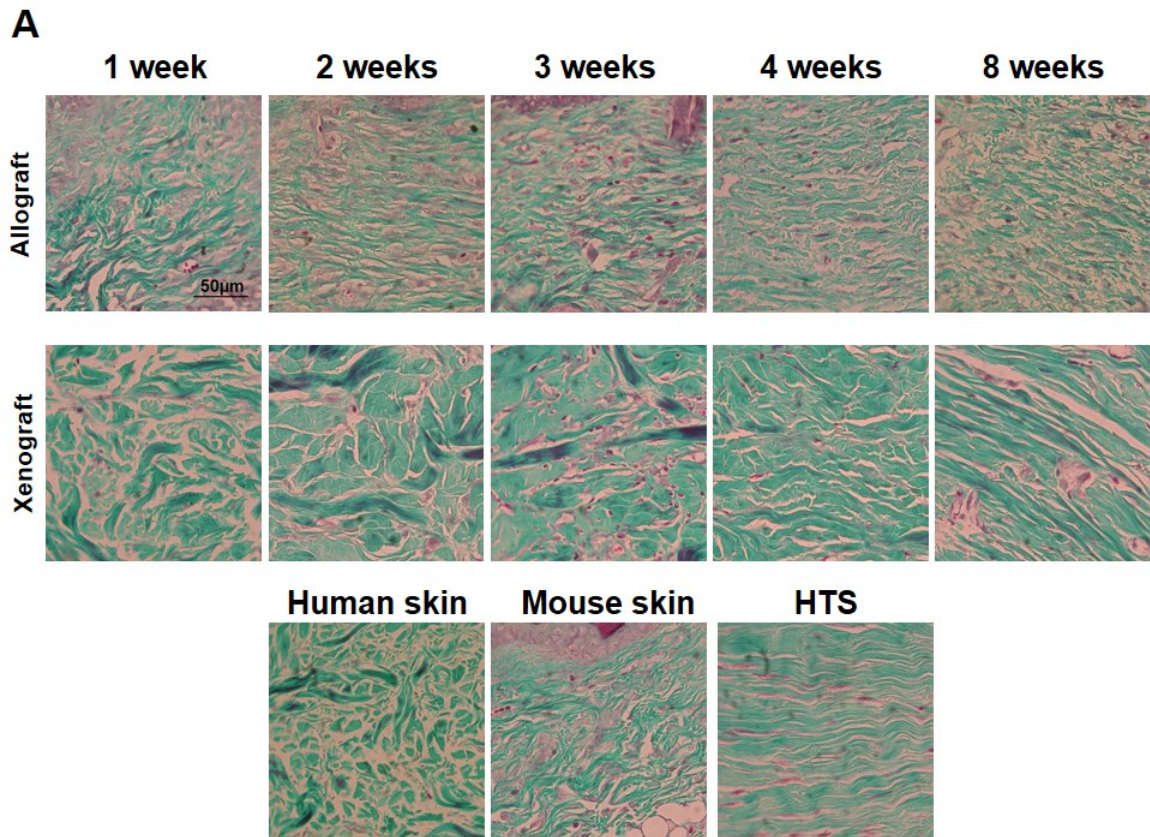
Figure 3.1. Xenografted group developed scar at 8 weeks post-grafting. The xenografted mice showed clear margin of wounds since 2 weeks post-grafting and contracted scar formation 8 weeks post-grafting. In contrast, a favorable healing of wounds was observed without redness, pigmentation or obvious contour in allografted mice since 2 weeks post-grafting (A). Wound area at different time points were measured and analyzed (B). Digital photos of grafted skin were taken using H&E sections of normal STSG before grafting and grafts from allografted and xenografted mice (C) at different time points. The skin thickness was measured and analyzed (D). N=3, experiment was done in duplicate, *p<0.05.

3.3.2 Morphology of collagen fibers resembled human HTS in xenografts not allografts

Masson's trichrome stain was used to assess the morphology of collagen fiber or bundles in the grafts. The collagen bundles in the xenografts were large and irregular up to 1 week post-grafting and then became smaller over time. A parallel pattern of collagen bundles was seen at 8 weeks post-grafting exhibiting a striking similarity to human HTS tissue, which was completely different from the basket-weave-like normal human skin collagen bundles. However, collagen bundles in engrafted skins from allografted mice showed a similar pattern to normal mouse skin at all the time points (Figure 3.2A).

COI value of "0" means collagen bundles are randomly oriented, such as those in normal skin while "1" means collagen bundles are highly ordered, such as those in HTS, which are in a parallel orientation. The CBPI represents the distance between collagen bundles, thus being a measurement of collagen bundle density. A lower value of CBPI represents higher collagen bundle density. Generally, COI is lower in normal skin tissue but higher in HTS tissue, while CBPI is higher in normal skin but lower in HTS tissue. Figure 3.2B showed the measurement of parameters needed for the calculation of COI and CBPI. COI of xenografts increased over time and was significantly higher at 3, 4 and 8 weeks post-grafting compared to 0 week post-grafting ($p < 0.001$). COI of allografted mice reached maximum at 3 weeks post-grafting, decreased over time and COI at 3 weeks was significantly higher than 0 week post-grafting ($p < 0.01$). There were significant differences between the two groups at 4 ($p < 0.01$) and 8 ($p < 0.001$) weeks post-grafting (Figure 3.2C). CBPI of xenografted skin showed a decreased trend over time and significant differences were found between 0 and 2 ($p < 0.01$), 0 and 3 ($p < 0.01$), 0 and 4 ($p < 0.001$), 0 and 8

($p < 0.001$) weeks post-grafting, which was also consistent with the definition of CBPI. There were significant differences between the two groups at 0 ($p < 0.05$), 1 ($p < 0.05$), 2 ($p < 0.05$) and 8 ($p < 0.01$) weeks post-grafting (Figure 3.2D).



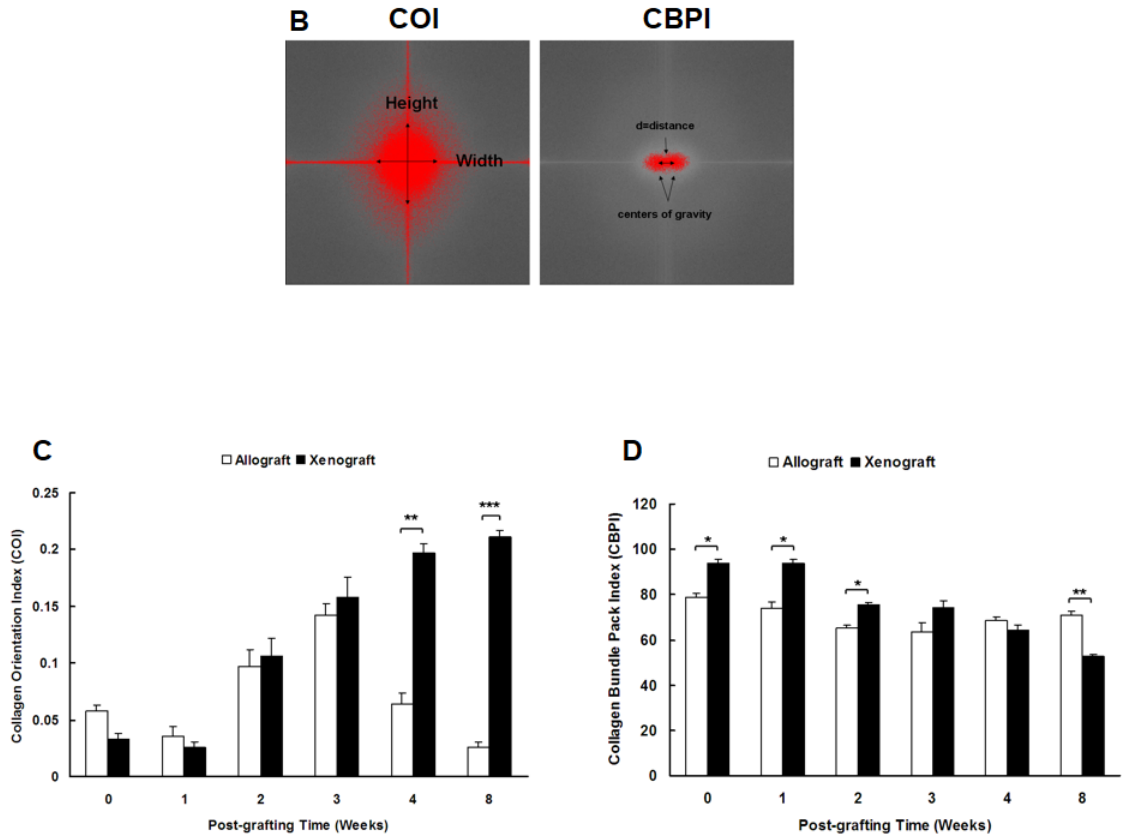


Figure 3.2 Morphology of collagen fibers resembled human HTS in xenografts not allografts. Engrafted skins from xenografted mice consisted of smaller bundles aligned in a parallel fashion to the epidermis, which was close to human HTS tissue, but not normal human skin with collagen bundles showing a basket-weave-like pattern with a more or less random structure. However, collagen bundles from allografted mice showed similar pattern between normal mouse skin and the other time points (A). COI and CBPI at different time points were analyzed using FFT module. Figure B showed the measurement of parameters needed for the calculation of COI and CBPI. The COI and CBPI of both groups were showed in (C) and (D). N=3, experiment was done in duplicate, * $p < 0.05$, ** $p < 0.01$, *** $p < 0.001$.

3.3.3 Increased number of myofibroblasts in xenografts and allografts

α -SMA is commonly considered as a marker of myofibroblasts (15), which is a special type of fibroblasts that is abundant in human HTS (16). Representative images of myofibroblast staining in xenografts and allografts were shown in Figure 3.3A. Figure 3.3B showed changes of myofibroblast number in the two groups. In the allografts, myofibroblast number reached its peak at 2 weeks post-grafting and decreased over time. In the xenografts, the number of myofibroblasts dramatically increased at 2 weeks post-grafting, reached the highest point up to 4 weeks post-grafting and then decreased sharply at 8 weeks post-grafting. There was significant difference between 0 and 2 ($p < 0.001$) weeks post-grafting in the allografted mice while there were significant differences between 0 and 2 ($p < 0.001$), 0 and 3 ($p < 0.001$), 0 and 4 ($p < 0.001$) and 0 and 8 ($p < 0.01$) weeks as well as 4 and 8 ($p < 0.001$) weeks post-grafting in the xenografted mice.

3.3.4 Significant increases of collagen in xenografts

4-Hyp is primarily found in protein collagen, which plays a key role together with proline for collagen stability (17). The collagen composition can be determined by the measurement of 4-Hyp by LC/MS, which was previously reported by our research group (18). In the allografts, the level of 4-Hyp slowly increased over time but there was no significant difference between all the time points. In the xenografts, the level of 4-Hyp increased after the grafting and reached to the peak at 4 weeks and then decreased in 8 weeks post-grafting. Significant differences were found between 0 and 3 ($p < 0.05$), 0 and 4 ($p < 0.05$) weeks post-grafting in xenografted mice. There were significant differences

between the two groups at all the time points ($p < 0.01$) (Figure 3.3C).

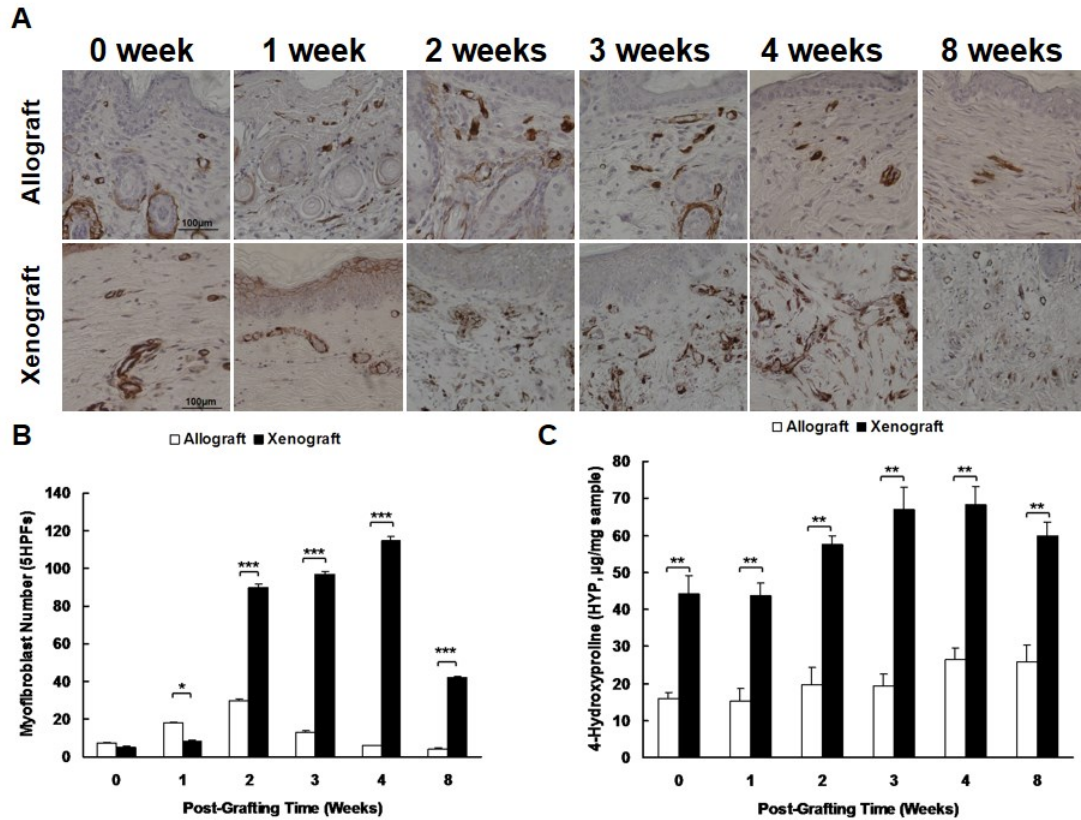


Figure 3.3 Increased number of myofibroblasts and collagen level in xenografted group. Figure A showed representative images of α -SMA (brown) positive myofibroblasts at various time points post-grafting in allografted and xenografted mice. α -SMA positive cells were counted under light microscope in 5 HPFs in the dermis and the total number was calculated and compared using ANOVA (B) Collagen level was determined by measurement of 4-Hyp in the allografted and xenografted skin using LC/MS (C). N=3, experiment was done in duplicate, * $p < 0.05$, ** $p < 0.01$, *** $p < 0.001$.

3.3.5 Monocyte fractions behaved similarly between the allografted and xenografted mice at each time point

Monocyte populations were determined by the expression of CD115 and CD11b markers in the blood harvested at different time points post-grafting using flow cytometry. Only the cells that were positive for both markers were considered to be monocytes. The quadrant gate was set according to the isotype control. The double positive events were gated and analyzed. Representative figures of monocyte fraction in allografted mice, xenografted mice and isotype control 1 week post-grafting were shown (Figure 3.4A-C). The fraction of monocytes at various time points was shown in a line chart (Figure 3.4D). Three mice were used as negative controls and data were shown as 0 week post-grafting. The changes of monocyte population were almost the same in both allografted and xenografted mice. A sharp drop of fraction was observed 1 week post-grafting and then the fraction gradually returned to normal at 8 weeks post-grafting. There were significant differences at 1 week post-grafting ($p < 0.05$) between the allografted and xenografted mice, 0 and 1 ($p < 0.001$), 0 and 2 ($p < 0.001$), 0 and 3 ($p < 0.001$), 0 and 4 ($p < 0.05$) weeks post-grafting in the allografted mice as well as 0 and 1 ($p < 0.001$), 0 and 2 ($p < 0.001$), 0 and 3 ($p < 0.001$) weeks post-grafting in xenografted mice.

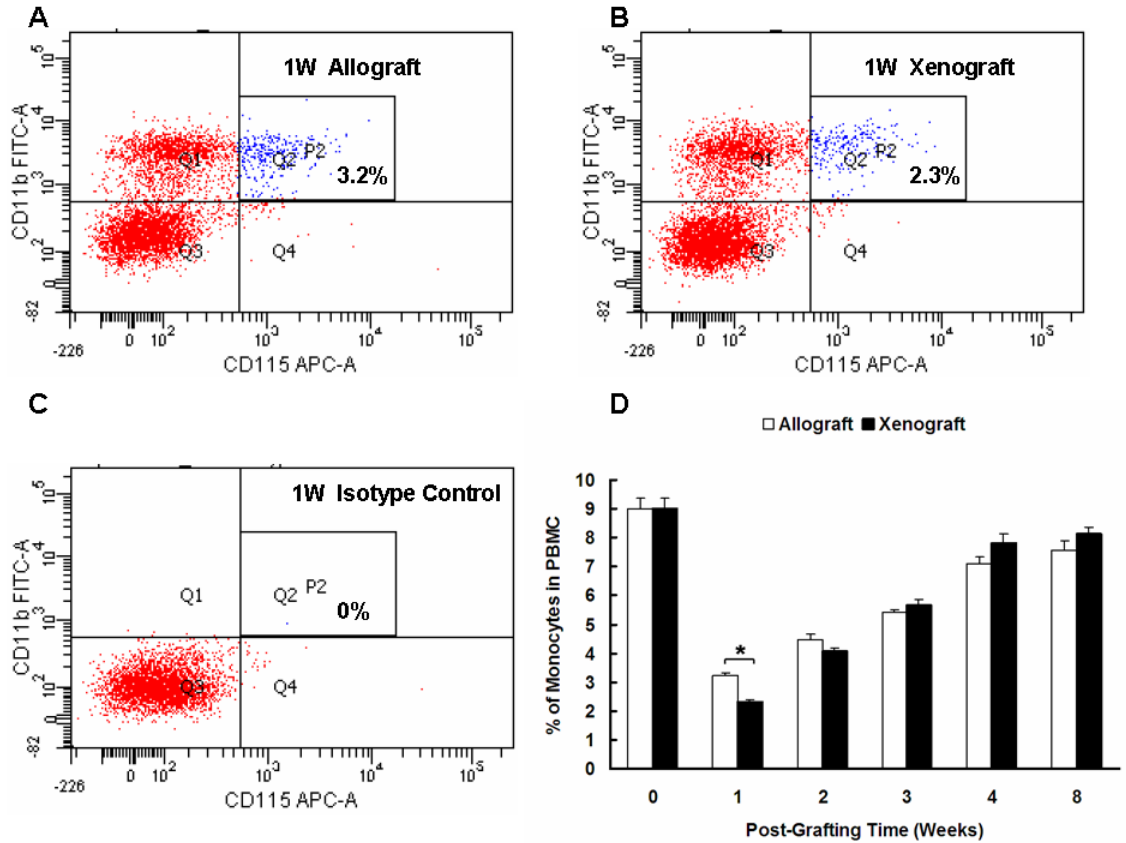
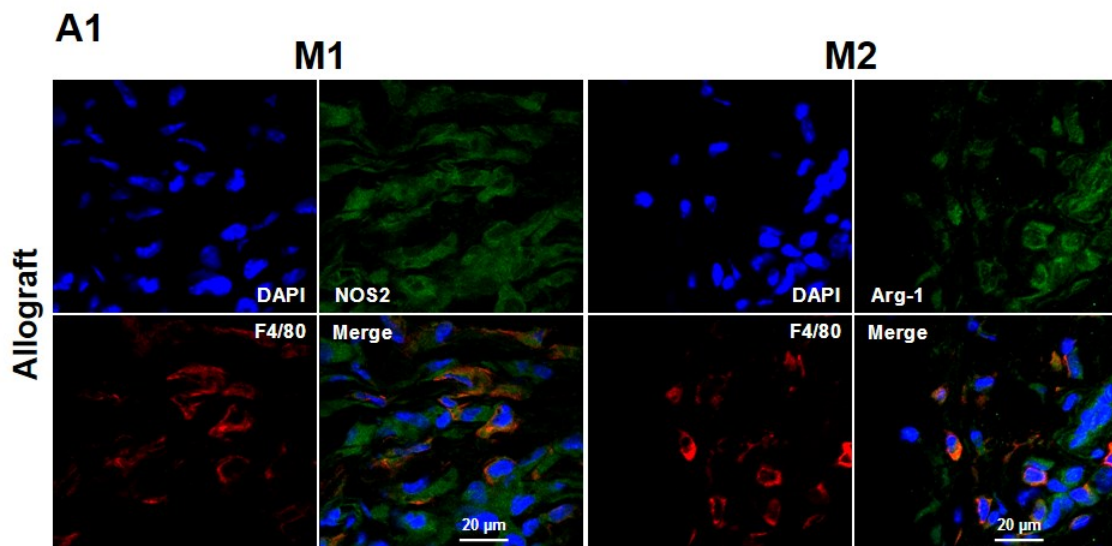


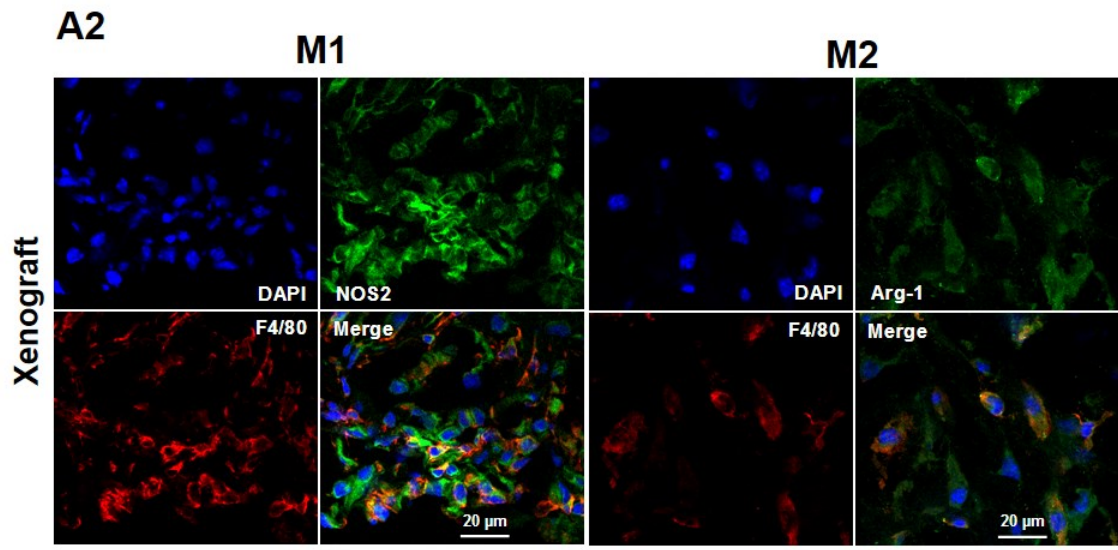
Figure 3.4 Monocyte fractions behaved similarly between the allografted and xenografted mice at each time point. Representative images of monocyte fractions in allografted (A) and xenografted mouse (B) and isotype control (C) 1 week post-grafting were shown. The fractions of the monocytes were analyzed and compared within groups at different time points using ANOVA and between groups at each time point using student's t-tests (D). N=3, experiment was done in duplicate, *p<0.05.

3.3.6 M1 and M2 macrophages change over time in xenografts and allografts

Grafted skin sections from both groups were analyzed for M1 and M2 macrophages using immunofluorescent staining. The cells that co-expressed F4/80 (+)/NOS2 (+) were identified as M1 macrophages while F4/80 (+) /Arg-1 (+) cells were identified as M2

macrophages (orange, figure 3.5A1, A2). As mentioned in the method section, the number of double positive cells was counted in five HPFs. M1 macrophages were found predominantly at 1 to 2 weeks post-grafting in both allografted and xenografted mice then the number decreased over time. In allografted mice, M2 macrophages appeared early at 1 week post-grafting, reached to maximum at 2 weeks post-grafting and then dropped sharply over time, whereas, M2 macrophages in xenografted mice were abundant at later time points, that is, 3 to 4 weeks post-grafting (Figure 3.5B).





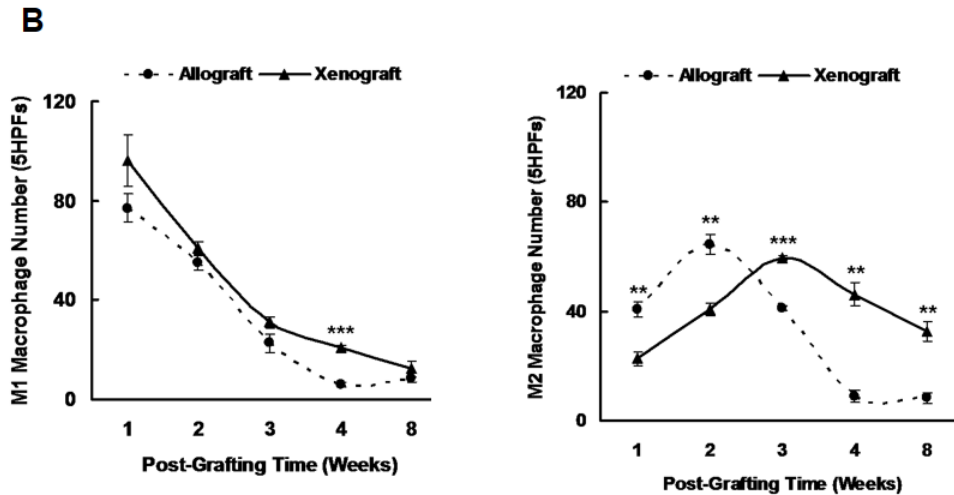


Figure 3.5 M1 and M2 macrophages in xenografts were found abundant in different time points. The M1 macrophages were identified as double positive for F4/80 (red) and NOS2 (green). Similarly M2 macrophages were double positive for F4/80 (red) and Arg-1 (green). Representative image of dual stained of M1 (1 week post-grafting) and M2 macrophages (4 week post-grafting) (orange) were shown (A). The double positive cells were counted under 5HPFs and the total cell number of M1 and M2 macrophages in allografted and xenografted mice was shown (B). N=3, experiment was done in duplicate, **p<0.01, ***p<0.001.

3.3.7 Relative gene expression of M1 and M2 macrophage related cytokines changed over time in xenografts and allografts

qPCR revealed the relative gene expression of M1 and M2 macrophage related cytokines (Figure 3.6) over time during the experimental time course, which were consistent with the cell number changes of M1 and M2 macrophages over time post-grafting. The expressions of TNF- α , IL-6 and IL-1 β were found similarly between the allografted and xenografted mice, which reached peak at 1 week post-grafting and the expression decreased over time. There were significant differences in TNF- α at 1 ($p < 0.05$) and 2 ($p < 0.05$) weeks; in IL-6 and IL-1 β at 2 ($p < 0.05$) and 4 ($p < 0.05$) weeks post-grafting between the allografted and xenografted mice. The highest expressions of TGF- β 1, IL-10 and IL-1 α in xenografted mice were observed at later time points at 2 or 3 weeks post-grafting and the expressions decreased thereafter; whereas the highest expression in allografted mice were at 1 or 2 weeks post-grafting and then decreased over time. There were significant differences between the allografted and xenografted mice in TGF- β 1 at 2 ($p < 0.05$), 3 ($p < 0.01$) and 4 ($p < 0.05$) weeks; in IL-10 at 3 ($p < 0.05$) and 4 ($p < 0.05$) weeks; and in IL-1 α at 3 ($p < 0.05$) weeks post-grafting. In allografted or xenografted mice, there was no significant difference between all the time points in each cytokine.

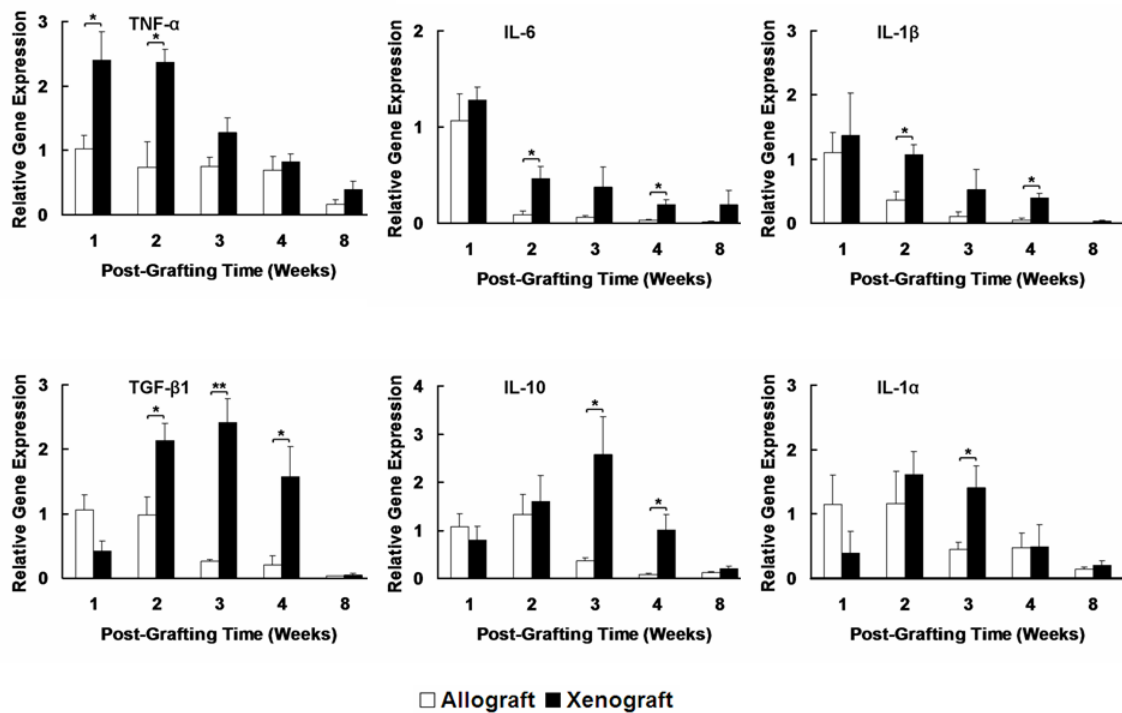


Figure 3.6 Relative gene expression of M1 and M2 macrophage related cytokines changed over time in xenografts and allografts. qPCR revealed the relative gene expression of cytokines from M1 and M2 macrophages over time during the experimental time course. In both allografted and xenografted mice, the expressions of TNF- α , IL-6 and IL-1 β in allografted and xenografted mice reached peak at 1 week post-grafting and then decreased over time. The highest expressions of TGF- β 1, IL-10 and IL-1 α in allografted mice were at 1 or 2 weeks post-grafting while the expressions in xenografted mice were observed at later time points at 2 or 3 weeks post-grafting while. N=3, experiment was done in duplicate, *p<0.05, **p<0.01.

3.4 Discussion

Yang et al. first introduced the concept of establishing human HTS model by transplanting full-thickness human skin on nude mice (19), which was a novel attempt compared to other animal model such as rabbit ear model (20), red Duroc pig model (21) and so on. Later our lab improved the model by transplanting human STSG on nude mice and obtained a more obvious HTS formation compared to full-thickness skin graft (9). In this study, significant differences in wound healing were found between the xenografted mice and allografted mice by gross digital photos and histological analysis after successful engraftment of human skin in the nude mouse model.

COI and CBPI was adopted as a quantitative method to evaluate the morphologic differences between the collagen bundles at different time points post-grafting using the Masson's trichrome images. From our findings, the COI was higher and CBPI was lower at 8 weeks post-grafting, which suggested the grafted skin resembled HTS tissue according to the definition of COI and CBPI. The adoption of COI and CBPI transformed the original qualitative information obtained from Masson's trichrome staining into quantitative comparable data, which substantially enhances the value of Masson's trichrome staining data.

One of the important findings in this study is the changes of monocyte fraction in the blood after the establishment of human HTS-like nude mouse model. The fraction of monocytes dramatically decreased in 1 week and then gradually came back to normal while there was a remarkable increase of M1 and M2 macrophage number 1 week post-grafting. These two observed behaviors suggest that there might be a replenishment of monocytes from the peripheral blood to the wound area, which is similar to the findings of Mosser et

al. (22) and Bain et al. (23). The latter claimed that the tissue-resident macrophages were not derived from embryonic precursors *in situ* but was replenished constantly by blood monocytes. In our animal model, we assumed that the monocytes infiltrated to the wound area by migration shortly after grafting and the replenishment reached the peak level around 1 week post-grafting, which might be associated with the sharp decrease of monocyte fraction as well as the large increase of M1 and M2 macrophage number. Further experiments would be necessary to support this potential relationship between these behaviors. Another explanation for the sharp decrease of monocyte fraction might be a relative increase in other cell populations such as B cell or NK cells. In addition, there is still more to understand regarding the mechanism of monocyte replenishment in this animal model. Wynn et al. claimed that not all the monocytes would replenish tissue resident macrophages in mice and that inflammatory monocytes (Ly6c+) were the predominant cells that replenished tissue macrophages by being recruited to the wound area while the function of resident Ly6c- monocytes were more related to immune responses (24, 25). Another study demonstrated Ly6c- monocytes would differentiate into M1 macrophages and shift to the M2 phenotype later in a murine model of rheumatoid arthritis (26). In this study, the circulating monocytes and their differentiation into Ly6c- or Ly6c+ cells was not examined; however, in the future we plan to investigate the specific subsets or phenotypes of monocytes and their roles in HTS formation in the HTS-like nude mouse model.

As mentioned above, M1 macrophages are predominant in early phases of wound healing while M2 macrophages are abundant in later phases of wound healing. Our study is the first to explicitly unravel the cell number changes for M1 and M2 macrophages at different time points post-grafting in human HTS-like nude mouse model. In the allografted

group, the peak of M2 macrophage number appeared 1 week earlier than the xenografted group, which might be due to shorter inflammation phase and early transition to proliferation phase. In the xenografted mice, M1 macrophages were seen more in the early time points (1 to 2 weeks) post-grafting while M2 macrophages reached the highest number 3 weeks post-grafting. In xenografted mice, the relative gene expressions of M1 macrophage specific cytokines, TNF- α , IL-6 and IL-1 β , were highly expressed at 1 to 2 weeks post-grafting while the gene expression of M2 macrophage specific cytokines, TGF- β 1, IL-10 and IL-1 α , were highly expressed at 2 to 3 weeks post-grafting, which were consistent to the findings of cell number changes of M1 and M2 macrophages during the grafting time course. In addition, the total number of M1 and M2 macrophages was inversely correlated to the fraction changes of monocytes at each time point. At 8 weeks post-grafting, M2 macrophages were the predominant ones in the grafted skin, which supported the finding that M2 macrophages were fibrotic and their roles in HTS formation (27, 28). The investigation of the fraction of monocytes in the blood and the number of M1 and M2 macrophages in the tissue offers a novel perspective to ponder the relationship between natural changes of the MPS and the histological changes of human HTS-like nude mouse model.

In Figure 3.5 of the dual staining of M1 and M2 macrophages, many F4/80 negative but NOS2 or Arg-1 positive cells were shown. Many cells including neutrophils, granulocytes, erythrocytes, dendritic cells, natural killer cells, endothelial cells and smooth muscle cells can also express arginase-1 or NOS2 activity and these single positive cells may also contribute to HTS formation. Thus, it will be very interesting to understand the roles of these other cells in future experiments to determine their roles in HTS formation.

It is suggested by Nishida et al. that the inhibition of M2 macrophages would reduce the fibrotic response and it might be of therapeutic value to switch M2 macrophages to M1 phenotype (29). Furthermore, many studies investigated the role of macrophages in the disease pathogenesis by performing macrophage depletion (30-32). Understanding the natural behavior of MPS in this model will give us insight on future studies about when and what specific phenotype of macrophages to deplete or the timing to perform plasticity switching of macrophages in order to clarify the effect of M2 macrophages on HTS formation.

Our group has reported that the SDF-1/CXCR4 signaling pathway was up-regulated in burn patients (33) and by blocking this signaling pathway a significant reduction of scarring was observed in human skin grafted nude mouse model (11), suggesting an intimate relationship between HTS and this signaling pathway. At the same time, SDF-1 was found to be a potent chemoattractant that mediate the migration of the MPS (34, 35) and is involved in the fibroproliferative disorders (36, 37) and tumor pathogenesis (38). Furthermore, our group has also reported increased numbers of fibrocytes and macrophages in the grafted skin using a similar animal model (10). All the findings suggest that the migration of MPS plays a role in HTS formation.

Based on the previous findings from our lab and other research groups, we hypothesize that SDF-1 is released by fibroblasts or endothelial cells due to the inflammatory signals after skin injury occurs. The CXCR4 expressing cells in the circulation, mostly monocytes, will be attracted to the wound site under the SDF-1/CXCR4 signaling pathway due to concentration gradient as well as the chemotactic effect of SDF-1. The monocytes then differentiate into polarized macrophages in response to stimulations from various

inflammatory mediators. M1 macrophages are more abundant in the early phase of wound healing and a remarkable activation of NF- κ B and STAT1 signaling pathway will promote M1 macrophages polarization whereas a predominance of STAT3 and STAT6 activation promotes M2 macrophages polarization (39). M1 macrophages then exert the pro-inflammatory function by secreting proinflammatory cytokines such as IFN- γ , IL-1 β , TNF- α , IL-6, IL-8, IL-12 and others. M1 macrophages also have the bactericidal ability by generating reactive oxygen and nitrogen species such as nitric oxide through the activation of NOS2. In contrast, the functions of M2 macrophages are more related to angiogenesis and tissue repair. M2 macrophages inhibit the NOS2 activity via the activation of Arg-1. What's more, M2 macrophages can reduce the inflammatory response by secreting anti-inflammatory cytokines such as IL-10, TGF- β 1. The opposite and complementary functions of M1 and M2 macrophages will eventually lead to normal wound healing. If more intensive stimuli are generated in a prolonged inflammatory wound environment, for example, a severely burned patient, where M2 macrophages appear to produce large amounts of TGF- β 1 and induce myofibroblast proliferation, leads to more ECM deposition and finally results in HTS formation.

3.5 Conclusion

Above all, the understanding of the natural behavior of MPS *in vivo* in our mouse model provides evidence for the role of macrophages in fibrosis of human skin and suggests that therapeutic attempts to deplete macrophages or alter their phenotypes is likely best tested in the subacute phases of wound healing.

3.6 References

1. Ginhoux F, Jung S. Monocytes and macrophages: developmental pathways and tissue homeostasis. *Nat Rev Immunol*. 2014;14:392-404.
2. Twigg HL, 3rd. Macrophages in innate and acquired immunity. *Semin Respir Crit Care Med*. 2004;25:21-31.
3. Hume DA. The mononuclear phagocyte system. *Curr Opin Immunol*. 2006;18:49-53.
4. Martinez FO, Sica A, Mantovani A, Locati M. Macrophage activation and polarization. *Front Biosci*. 2008;13:453-61.
5. Stout RD, Jiang C, Matta B, Tietzel I, Watkins SK, Suttles J. Macrophages sequentially change their functional phenotype in response to changes in microenvironmental influences. *J Immunol*. 2005;175:342-9.
6. Ferrante CJ, Leibovich SJ. Regulation of Macrophage Polarization and Wound Healing. *Adv Wound Care (New Rochelle)*. 2012;1:10-6.
7. Martinez FO, Helming L, Gordon S. Alternative activation of macrophages: an immunologic functional perspective. *Annu Rev Immunol*. 2009;27:451-83.:10.1146/annurev.immunol.021908.132532.
8. Song E, Ouyang N, Horbelt M, Antus B, Wang M, Exton MS. Influence of alternatively and classically activated macrophages on fibrogenic activities of human fibroblasts. *Cell Immunol*. 2000;204:19-28.
9. Momtazi M, Kwan P, Ding J, Anderson CC, Honardoust D, Goekjian S, et al. A nude mouse model of hypertrophic scar shows morphologic and histologic characteristics of human hypertrophic scar. *Wound Repair Regen*. 2013;21:77-87. doi: 10.1111/j.524-475X.2012.00856.x. Epub 2012 Nov 5.
10. Wang J, Ding J, Jiao H, Honardoust D, Momtazi M, Shankowsky HA, et al. Human hypertrophic scar-like nude mouse model: characterization of the molecular and cellular biology of the scar process. *Wound Repair Regen*. 2011;19:274-85.

11. Ding J, Ma Z, Liu H, Kwan P, Iwashina T, Shankowsky HA, et al. The therapeutic potential of a C-X-C chemokine receptor type 4 (CXCR-4) antagonist on hypertrophic scarring in vivo. *Wound Repair Regen.* 2014;22:622-30.
12. van Zuijlen PP, Ruurda JJ, van Veen HA, van Marle J, van Trier AJ, Groenevelt F, et al. Collagen morphology in human skin and scar tissue: no adaptations in response to mechanical loading at joints. *Burns.* 2003;29:423-31.
13. Tredget EE, Iwashina T, Scott PG, Ghahary A. Determination of plasma Ntau-methylhistamine in vivo by isotope dilution using benchtop gas chromatography-mass spectrometry. *J Chromatogr B Biomed Sci Appl.* 1997;694:1-9.
14. Breslin WL, Strohacker K, Carpenter KC, Haviland DL, McFarlin BK. Mouse blood monocytes: standardizing their identification and analysis using CD115. *J Immunol Methods.* 2013;390:1-8. doi: 10.1016/j.jim.2011.03.005. Epub Apr 2.
15. Nagamoto T, Eguchi G, Beebe DC. Alpha-smooth muscle actin expression in cultured lens epithelial cells. *Invest Ophthalmol Vis Sci.* 2000;41:1122-9.
16. Nedelec B, Shankowsky H, Scott PG, Ghahary A, Tredget EE. Myofibroblasts and apoptosis in human hypertrophic scars: the effect of interferon-alpha2b. *Surgery.* 2001;130:798-808.
17. Kotch FW, Guzei IA, Raines RT. Stabilization of the collagen triple helix by O-methylation of hydroxyproline residues. *J Am Chem Soc.* 2008;130:2952-3.
18. Wang JF, Jiao H, Stewart TL, Shankowsky HA, Scott PG, Tredget EE. Fibrocytes from burn patients regulate the activities of fibroblasts. *Wound Repair Regen.* 2007;15:113-21.
19. Yang DY, Li SR, Wu JL, Chen YQ, Li G, Bi S, et al. Establishment of a hypertrophic scar model by transplanting full-thickness human skin grafts onto the backs of nude mice. *Plast Reconstr Surg.* 2007;119:104-9; discussion 10-1.
20. Saulis AS, Mogford JH, Mustoe TA. Effect of Mederma on hypertrophic scarring in the rabbit ear model. *Plast Reconstr Surg.* 2002;110:177-83; discussion 84-6.
21. Gallant CL, Olson ME, Hart DA. Molecular, histologic, and gross phenotype of skin wound healing in red Duroc pigs reveals an abnormal healing phenotype of

hypercontracted, hyperpigmented scarring. *Wound Repair Regen.* 2004;12:305-19.

22. Mosser DM, Edwards JP. Exploring the full spectrum of macrophage activation. *Nat Rev Immunol.* 2008;8:958-69.

23. Bain CC, Mowat AM. Macrophages in intestinal homeostasis and inflammation. *Immunol Rev.* 2014;260:102-17. doi: 10.1111/imr.12192.

24. Wynn TA, Chawla A, Pollard JW. Macrophage biology in development, homeostasis and disease. *Nature.* 2013;496:445-55.

25. Hammond MD, Taylor RA, Mullen MT, Ai YX, Aguila HL, Mack M, et al. CCR2(+)Ly6C(hi) Inflammatory Monocyte Recruitment Exacerbates Acute Disability Following Intracerebral Hemorrhage. *Journal of Neuroscience.* 2014;34:3901-9.

26. Misharin AV, Cuda CM, Saber R, Turner JD, Gierut AK, Haines GK, 3rd, et al. Nonclassical Ly6C(-) monocytes drive the development of inflammatory arthritis in mice. *Cell Rep.* 2014;9:591-604. doi: 10.1016/j.celrep.2014.09.032. Epub Oct 16.

27. Gharib SA, Johnston LK, Huizar I, Birkland TP, Hanson J, Wang Y, et al. MMP28 promotes macrophage polarization toward M2 cells and augments pulmonary fibrosis. *J Leukoc Biol.* 2014;95:9-18.

28. Stawski L, Haines P, Fine A, Rudnicka L, Trojanowska M. MMP-12 deficiency attenuates angiotensin II-induced vascular injury, M2 macrophage accumulation, and skin and heart fibrosis. *PLoS One.* 2014;9:e109763.

29. Nishida M, Hamaoka K. Macrophage phenotype and renal fibrosis in obstructive nephropathy. *Nephron Exp Nephrol.* 2008;110:e31-6.

30. Fritz JM, Tennis MA, Orlicky DJ, Lin H, Ju C, Redente EF, et al. Depletion of tumor-associated macrophages slows the growth of chemically induced mouse lung adenocarcinomas. *Front Immunol.* 2014;5:587.

31. Lucas T, Waisman A, Ranjan R, Roes J, Krieg T, Muller W, et al. Differential roles of macrophages in diverse phases of skin repair. *J Immunol.* 2010;184:3964-77.

32. Kim JH, Lee D, Jung MH, Cho H, Jeon D, Chang S, et al. Macrophage Depletion

Ameliorates Glycerol-Induced Acute Kidney Injury in Mice. *Nephron Exp Nephrol.* 2014;128:21-9.

33. Ding J, Hori K, Zhang R, Marcoux Y, Honardoust D, Shankowsky HA, et al. Stromal cell-derived factor 1 (SDF-1) and its receptor CXCR4 in the formation of postburn hypertrophic scar (HTS). *Wound Repair Regen.* 2011;19:568-78. doi: 10.1111/j.524-475X.2011.00724.x.

34. Bleul CC, Fuhlbrigge RC, Casasnovas JM, Aiuti A, Springer TA. A highly efficacious lymphocyte chemoattractant, stromal cell-derived factor 1 (SDF-1). *J Exp Med.* 1996;184:1101-9.

35. Vogel DY, Heijnen PD, Breur M, de Vries HE, Tool AT, Amor S, et al. Macrophages migrate in an activation-dependent manner to chemokines involved in neuroinflammation. *J Neuroinflammation.* 2014;11:23.

36. Lin CH, Shih CH, Tseng CC, Yu CC, Tsai YJ, Bien MY, et al. CXCL12 induces connective tissue growth factor expression in human lung fibroblasts through the Rac1/ERK, JNK, and AP-1 pathways. *PLoS One.* 2014;9:e104746. doi: 10.1371/journal.pone.0104746. eCollection 2014.

37. Xu J, Mora A, Shim H, Stecenko A, Brigham KL, Rojas M. Role of the SDF-1/CXCR4 axis in the pathogenesis of lung injury and fibrosis. *Am J Respir Cell Mol Biol.* 2007;37:291-9. Epub 2007 Apr 26.

38. Nakamura T, Shinriki S, Jono H, Guo J, Ueda M, Hayashi M, et al. Intrinsic TGF-beta2-triggered SDF-1-CXCR4 signaling axis is crucial for drug resistance and a slow-cycling state in bone marrow-disseminated tumor cells. *Oncotarget.* 2014;25:25.

39. Sica A, Mantovani A. Macrophage plasticity and polarization: in vivo veritas. *J Clin Invest.* 2012;122:787-95.

Chapter 4

Systemic Depletion of Macrophages in the Subacute Phase of Wound Healing Reduces Hypertrophic Scar Formation

This chapter has been published as: Zhu Z, Ding J, Ma Z, Iwashina T, Tredget EE.

Systemic Depletion of Macrophages in the Subacute Phase of Wound Healing Reduces Hypertrophic Scar Formation. *Wound Repair Regen.* 2016 May 12. doi:

10.1111/wrr.12442. [Epub ahead of print].

4.0 Abstract

HTS are caused by trauma or burn injuries to the deep dermis and can cause cosmetic disfigurement and psychological issues. Studies suggest that M2-like macrophages are pro-fibrotic and contribute to hypertrophic scar formation. A previous study from our lab showed that M2 macrophages were present in developing hypertrophic scar tissues in vivo at 3 to 4 weeks after wounding. In this study, the effect of systemic macrophage depletion on scar formation was explored at the subacute phase of wound healing. Thirty-six athymic nude mice that received human skin transplants were randomly divided into macrophage depletion group and control group. The former received intraperitoneal injections of clodronate liposomes while the controls received sterile saline injections on day 7, 10, 13 post-grafting. Wound area, scar thickness, collagen abundance and collagen bundle structure, mast cell infiltration, myofibroblast formation, M1 and M2 macrophages together with gene expression of M1 and M2 related factors in the grafted skin were investigated at 2, 4 and 8 weeks post-grafting. The transplanted human skin from the control group developed contracted, elevated and thickened scars while the grafted skin from the depletion group healed with significant less contraction and elevation. Significant reductions in myofibroblast number, collagen synthesis and hypertrophic fiber morphology as well as mast cell infiltration were observed in the

depletion group compared to the control group. Macrophage depletion significantly reduced M1 and M2 macrophage number in the depletion group 2 weeks post-grafting as compared to the control group. These findings suggest that systemic macrophage depletion at the subacute phase of wound healing reduces scar formation, which provides evidence for the pro-fibrotic role of macrophages in fibrosis of human skin as well as insight into the potential benefits of specifically depleting M2 macrophages in vivo.

4.1 Introduction

As previously described, HTS are caused by trauma or burn injury to the deep dermis and can lead to cosmetic disfigurement or cause limitations of joint mobility (1, 2). The human HTS-like nude mouse model established by our lab develops scars resembling human HTS tissue (3).

Macrophages are tissue-resident immune cells differentiated from monocytes, which are blood-borne phagocytes (4). They provide a bridge between the innate and adaptive immune systems and act as effectors and coordinators of inflammation and homeostasis (5). In response to various microenvironment signals, macrophages exert their function by differentiating into two functional subtypes, the M1 macrophages and the M2 macrophages (6). Recent studies have reported that M1 macrophages inhibit fibrogenesis while M2 macrophages promote fibrogenesis (7, 8). In order to investigate the differential role of macrophage subtypes in HTS formation, macrophages were depleted from the systemic circulation 1 to 2 weeks (subacute phase of wound healing after the grafting)

after human skin transplantation in the human HTS-like nude mouse model. Scar formation and macrophage phenotypes in the grafted tissues were analyzed at multiple time points.

4.2 Materials and methods

4.2.1 Preparation of human split thickness skin grafts

Abdominal skin tissue were obtained from female patients undergoing abdominoplasty after documented informed consent recorded in their personal health record. Under sterile conditions, STSG were harvested by using a Padgett electric dermatome (Padgett Instruments, Inc., Kansas City, MO) set at 0.4 mm (0.016 inches) thickness. Skin that was atrophic or had developed striae was avoided. The STSG were trimmed to a consistent size using a 2.0×1.5 cm² template. The grafts were stored in DMEM supplemented with 10% FBS until grafting.

4.2.2 Animals

Thirty-six 4-week-old male athymic nude mice that lacked T-cells due to absence of thymus weighing 20 grams were purchased from Charles River Laboratories (Wilmington, MA, USA). They were rested for two weeks in a virus antigen free

biocontainment facility before grafting. The animal protocol was approved by the University of Alberta Animal Care and Use Committee in accordance with the Canadian Council of Animal Care standards.

4.2.3 Establishment of human HTS-like nude mouse model

As previously described (9), the mice were anesthetized using isoflurane (Halocarbon Laboratories, River Edge, NJ). Surgical sites were disinfected using Prepodyne Solution (West Penetone INC, Anjou, QC) and then wiped clean with 70% ethanol. A $2.0 \times 1.5 \text{ cm}^2$ region of dorsal full thickness skin was outlined using a template and the skin was carefully excised using sharp dissection without damaging the underlying panniculus carnosus. 36 mice were grafted with human STSG which were sutured using 4-0 braided silk suture (Ethicon, Somerville, NJ) and covered with Xeroform (Covidien, Mansfield, MA) using a tie-over dressing to maximize contact between the graft and the wound bed. The mice received hydromorphone (Sandoz, Boucherville, QC), 0.05mg/ml subcutaneously for postoperative pain management. The dressings and sutures were removed 1 week post-grafting under isoflurane general anesthesia. The mice in the depletion group received clodronate liposomes (Clodrosome®, Encapsula NanoSciences LLC, Brentwood, TN) via intraperitoneal injections while the control group received sterile saline at day 7, 10, 13 post-grafting. The mice were euthanized at 2, 4, 8 weeks post-grafting. Spleen and skin graft tissues were excised at each time point for further analysis.

4.2.4 Morphology of wounds monitored by digital photography

Standardized digital photographs of the wounds with a micrometer were taken weekly after grafting to record the thickness of scar tissue formed over time. The wound area was measured using ImageJ software (National Institutes of Health, Bethesda, MD) for assessment of wound contraction. The scale in the software was reset for each image to control for magnification errors.

4.2.5 Processing of graft specimens

The spleen and transplanted human skin tissues were harvested at different time points and embedded in paraffin blocks before sectioning for H&E staining, Masson's trichrome and IHC staining. Cryosections were used for IHC staining.

4.2.6 Histology analysis of graft specimens

H&E and Masson's trichrome stained tissue sections were imaged under bright field microscopy (Nikon OIPHOT-2, Nikon Instruments Inc., Melville, NY). Dermal thickness in the grafts was analyzed by ImageJ software using a micrometer to standardize the reference images as previously described (10). The dermal thickness was defined as distance (μm) from epidermis to junction of the dermal-adipose layer. Three measurements were obtained from the thickest, thinnest and midpoint region from each sample and the mean value was calculated.

4.2.7 Collagen morphology analysis

Masson's trichrome staining was used to illustrate the morphology of collagen fibers, which showed green collagen fibers, red keratin and dark brown or black cell nuclei under bright field microscopy. As previously described (11), COI and CBPI were calculated using FFT module in ImageJ software to describe collagen bundle morphology in the grafts. The value of COI closer to 0 represents "randomly oriented" typical of normal human skin, while value closer to 1 is "highly ordered", which is similar to the parallel pattern of collagen bundles seen in human HTS tissue. The CBPI represents the distance between collagen bundles, where a lower value represents a higher density similar to the high collagen bundle density seen in human HTS tissue.

4.2.8 Measurement of collagen abundance using LC/MS

The amount of 4-Hyp, a unique amino acid in collagen, was measured by LC/MS as previously described with modifications (12). Briefly, the skin sample (dry weight: 0.5~3.9mg) in a pyrex screw-capped glass tube was added to 6N HCl solution and then hydrolyzed at 110°C overnight. A known amount of 4-Hyp-d₃ as internal standard was added to the hydrolysate. The n-butyl ester reagent was added to the dried hydrolysate in order to produce the n-butyl ester derivatives of 4-Hyp and 4-Hyp-d₃. The samples were analyzed by LC/MS (Agilent Technologies, Santa Clara, CA) monitored using Mass Selective detection the ions 188 (4-Hyp n-butyl ester) and 191 (4-Hyp-d₃ n-butyl ester). The calibration curve was constructed through a range of 4-Hyp (6 points amount) using the peak area ratio. The ratio was obtained by dividing 4-Hyp peak area by the internal standard (4-Hyp-d₃) peak area. The amount of 4-Hyp in each sample was analyzed using the calibration curve. The data was expressed in 4-Hyp (μg) / dry weight sample (mg).

4.2.9 Toluidine blue staining for mast cell infiltration

Mast cells were detected using toluidine blue staining as previously described (9). Briefly, paraffin sections were deparaffinized and rehydrated through five changes of a decreasing ethanol gradient from 100% to 70%. Sections were stained in toluidine blue (Fisher Scientific, Pittsburgh, PA) solution for 3 minutes, washed in distilled water and dehydration through five changes of an increasing ethanol gradient from 70% to 100%. Sections were cleared in two changes of xylene and mounted with glass coverslips. Mast

cells were quantified by counting the number of reddish-purple cells in five random HPFs in all sections and from each time point.

4.2.10 IHC staining of myofibroblasts and macrophages

For IHC staining of myofibroblasts in the skin and spleen, paraffin sections were warmed for 20 minutes at 60°C in a vacuum oven and then deparaffinized by xylene and rehydrated through concentrations of ethanol from 100% to 70%. After antigen retrieval using 0.05% trypsin for myofibroblasts and 0.05% Protease Type XIV (Sigma-Aldrich, Cat. # P5147) for macrophages, the skin sections were incubated with 10% BSA (Sigma-Aldrich, St. Louis, MO) to block non-specific binding, followed by incubation with rabbit anti-human α -SMA antibody (Millipore, Cat. # MABT381) (1:1000) or rat anti-mouse F4/80 antibody (eBioscience, Cat. # 14-4801-82) at 4°C overnight and biotinylated goat anti-rabbit IgG (H+L) (Vector Laboratories Inc. Cat. # BA-1000) (1:500) for α -SMA and biotinylated rabbit anti-rat IgG (DAKO, Cat. # E0468) (1:500) for F4/80 at room temperature for one hour.

The tissue sections were then incubated using VECTASTAIN® ABC kit (Vector Laboratories Inc., Cat. # PK-4005) and developed using diaminobenzidine (Sigma-Aldrich, Cat. # D8001). The nuclei were counter-stained using hematoxylin. After dehydration, the sections were mounted and examined by light microscopy.

For myofibroblasts, positive stained cells were counted in five random HPFs for each sample excluding positive stained perivascular cells surrounding blood vessels. Positive stained areas for F4/80 were imaged under bright field microscopy (Nikon OIPHOT-2, Nikon Instruments Inc., Melville, NY) at each time point.

4.2.11 Quantification of polarized macrophages (M1 and M2) by immunofluorescence staining

Cryosections were fixed in ice-cold acetone (Thermo Fisher Scientific Inc., Waltham, MA) after warming and air-dried. After rinsing in PBS, sections were incubated with 10% BSA to avoid non-specific binding, and then incubated with primary antibodies and followed by specific secondary antibodies. Rat anti-mouse F4/80 was used as a general marker of mouse macrophages (eBioscience, Cat. # 14-4801-82). The primary antibody for M1 macrophages was rabbit polyclonal NOS2 IgG (Santa Cruz, Cat. # sc-651 FITC) and goat polyclonal Arg-1 IgG antibody (Santa Cruz, Cat. # sc-18351) for M2 macrophages. The secondary antibody was Alexa Fluor® 594 donkey anti-rat IgG (Life Technologies, Cat. # A-21209) for F4/80 and Alexa Fluor® 488 donkey anti-goat IgG (Life Technologies, Cat. # A-11055) for Arg-1. After washing, the slides were mounted with ProLong Gold anti-fade reagent with DAPI (Life Technologies, Carlsbad, CA). Images of the slides were taken using a confocal microscope (Leica TCS SP5, Leica Microsystems, Concord, ON) and double positive cells were counted using image analysis software (LAS AF Lite, Leica Microsystems, Concord, ON).

4.2.12 qPCR analysis of human pro-fibrotic and anti-fibrotic factors and mouse cytokines from skin grafts

Total RNA was extracted from snap frozen tissue specimens. Tissue was deep frozen in liquid nitrogen, then homogenized using a micro-dismembrator (B. Braun Biotech Inc., Allentown, PA). The powder was reconstituted in TRIzol reagent (Thermo Fisher Scientific., Waltham, MA). Total RNA was extracted using RNeasy[®] mini kit (Qiagen, Hilden, Germany). Contamination from genomic DNA was removed by DNase digestion for 60 minutes. First strand cDNA was synthesized using random primers in a first strand synthesis kit (Sigma, Oakville, ON). qPCR was conducted using Power SYBR[®] Green PCR Master Mix in a 25 μ l tube for a total reaction volume of 25 μ l, containing 1 μ l first strand product, and 0.2 μ M gene specific upstream and downstream primers for human pro-fibrotic and anti-fibrotic factors as well as cytokines released by M1 or M2 macrophages. Human HPRT and mouse GAPDH primers were used as controls. Amplification and analysis were performed using an ABI 7300 real-time system (Applied Biosystems, Foster City, CA). Cycling conditions were an initial denaturation at 95°C for 3 minutes, followed by 40 cycles consisting of a 15-second denaturation interval at 95°C, and a 30-second interval for annealing and primer extension at 60°C. mRNA expression

levels were normalized to the levels of human HPRT for human pro-fibrotic and anti-fibrotic factors as well as mouse GAPDH for mouse cytokines from polarized macrophages. Relative quantitation was expressed as fold-induction compared with control conditions. Primers sequences were listed in Table 5.1, 5.2.

Gene	Direction	Sequences 5'-3'
Homo Sapiens primers		
HPRT	F	CGTCTTGCTCGAGATGTGATG
	R	GCACACAGAGGGCTACAATGTG
MMP-1	F	TCGCTGGGAGCAAACACA
	R	TGGCAAATCTGGCGTGAA
DCN	F	TGAAGAAGCTCTCCTACATCC
	R	AAACTCAATCCCAACTAGCC
TGF- β 1	F	ACCCACAACGAAATCTATGAC
	R	GCTCCACTTTTAACTTGAGCC
CTGF	F	TCCACCCGGGTACCAATG
	R	CAGGCGGCTCTGCTTCTCTA
α -SMA	F	GAGAAGAGTTACGAGTTGCCTGATG
	R	GGCAGCGGAAACGTCA

HPRT, hypoxanthine-guanine phosphonibosyltransferase; MMP-1, matrix metalloproteinase-1; DCN, decorin; TGF- β 1, transforming growth factor-beta 1; CTGF, connective tissue growth factor; α -SMA, alpha-smooth muscle actin.

TABLE 4.1 Sequences of human primers for qPCR

Gene	Direction	Sequences 5'-3'
Mus musculus primers		
GAPDH	F	AGGTCGGTGAGAACGGATTG
	R	GGGGTCGTTGATGGCAACA
TNF-α	F	GTAACGCCAGGAATTGTTGCTA
	R	GGGAGTAGACAAGGTACAACCC
IL-6	F	TCTATACCACTTCACAAGTCGGA
	R	GAATTGCCATTGCACAACCTTTT
IL-1β	F	GAAATGCCACCTTTTGACAGTG
	R	TGGATGCTCTCATCAGGACAG
TGF-β1	F	CTTCAATACGTCAGACATTGGGG
	R	GTAACGCCAGGAATTGTTGCTA
IL-10	F	GCTGGACAACATACTGCTAACC
	R	GCTGGACAACATACTGCTAACC
IL-1	F	TCTCAGATTCAAACTGTTGCTG
	R	AGAAAATGAGGTCGGTCTCACTA

GAPDH, glyceraldehyde 3-phosphate dehydrogenase; TNF- α , tumor necrosis factor-alpha; IL-6, interleukin 6; IL-1 β , interleukin 1 beta; TGF- β 1, transforming growth factor-beta 1; IL-10, interleukin 10; IL-1, interleukin 1.

TABLE 4.2 Sequences of mouse primers for qPCR

4.2.13 Statistical analysis

Six mice were used in each group of each time point. Data were imported into STATA 12 for Windows (StataCorp LP, Collage Station, TX) and displayed as mean \pm SE. Statistical analysis was performed using a two-tailed unpaired student's t-test or one-way ANOVA with the Bonferroni method. A p-value of less than 0.05 ($p < 0.05$) was considered statistically significant.

4.3 Results

4.3.1 Confirmation of macrophage depletion in spleen tissue

The spleen plays an important role as a reservoir for red blood cells and a center of activity of the mononuclear phagocyte system where it contains 50% of the body's monocytes (13). In addition, the red pulp contains large number of macrophages that can phagocytize ageing erythrocytes (14) and are strongly positive for F4/80 expressed by mature macrophages rendering it a good marker for this population of cells (15). As illustrated in Figure 4.1, there were red pulp macrophages in the spleens of the control group; whereas little positive staining was seen in the depletion group at 2 weeks post-grafting, indicating successful depletion of the red pulp macrophages by the clodronate

liposomes. However, there was no significant differences between the two groups at weeks 4 and 8 post-grafting, suggesting that macrophage numbers recovered in the depletion group at those time points.

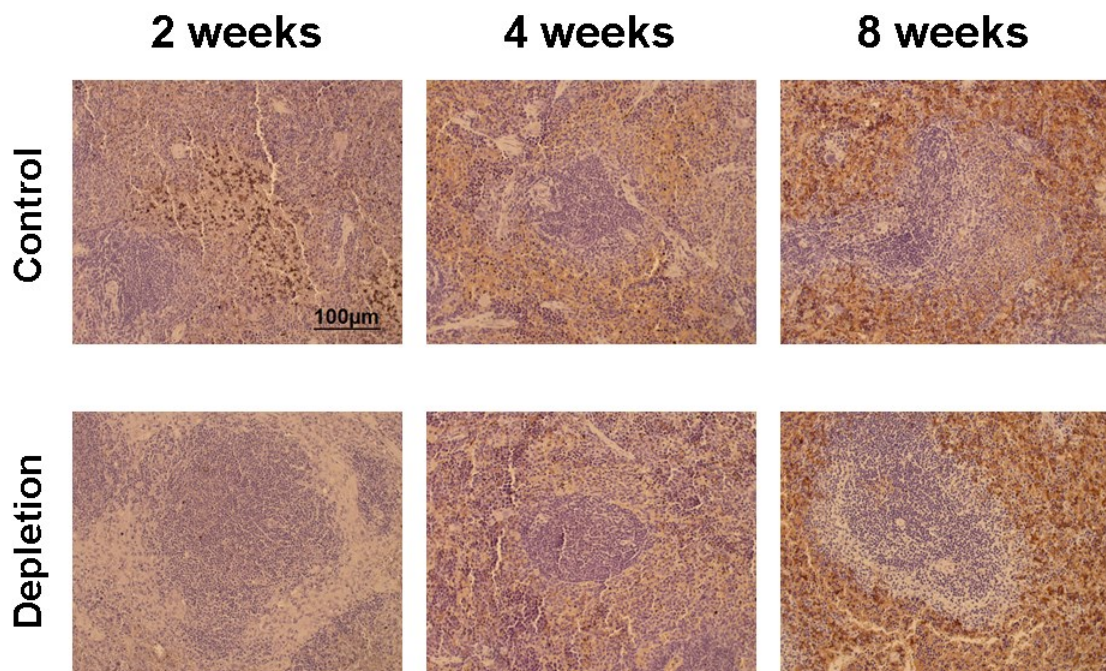
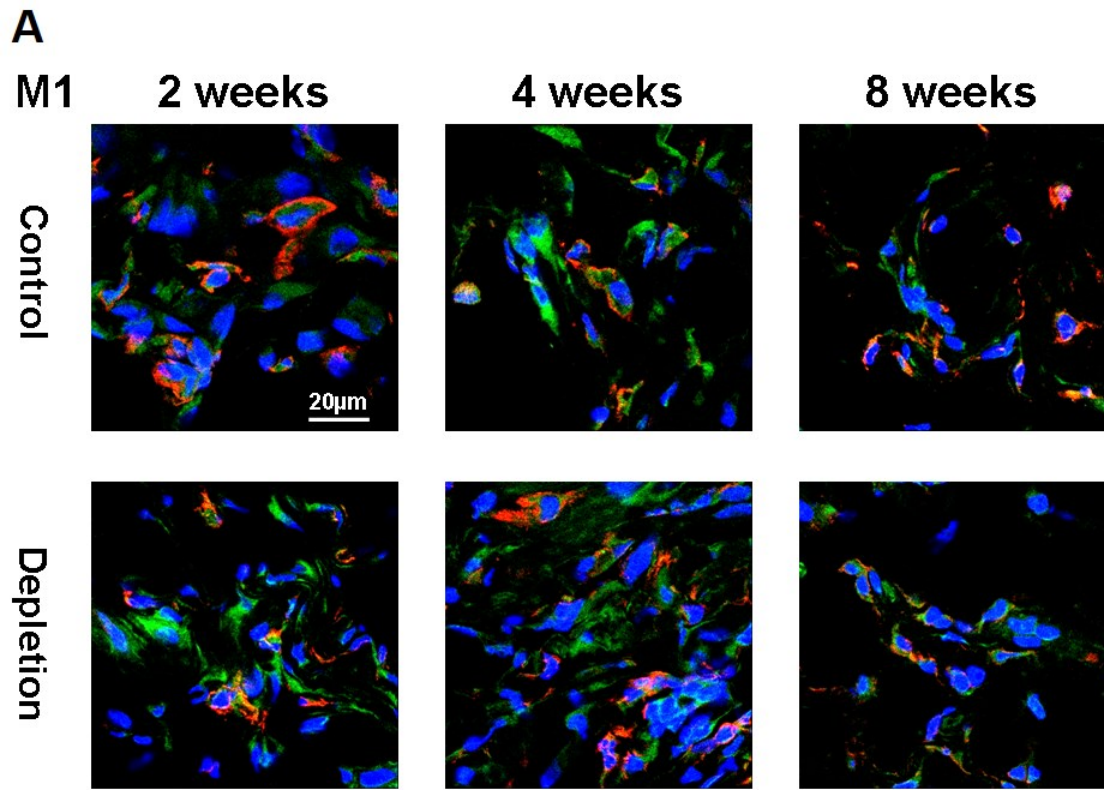


Figure 4.1 Confirmed macrophage depletion in spleen. Representative images of spleen sections using immunohistochemistry staining for macrophages were shown. There was positive stained area (brown) for red pulp macrophages in the control group whereas there was minimal positive staining found in the depletion group at 2 weeks post-grafting. However, there was no significant difference between the two groups at 4 and 8 weeks post-grafting.

4.3.2 Clodronate liposomes reduced M1 and M2 macrophage number in the grafts

Macrophages in the grafted skin from both groups that co-expressed F4/80 (+)/NOS2 (+) were identified as M1 macrophages (Figure 4.2A), whereas F4/80 (+) /Arg-1 (+) cells were identified as M2 macrophages (Figure 4.2B). M1 macrophages were found predominantly at 2 weeks post-grafting in the control group; however, there was a significant decrease in M1 macrophage number at 2 weeks post-grafting in the depletion group ($p < 0.05$) (Figure 4.2C). A similar significant decrease in M2 macrophage number were observed in the depletion group at 2 weeks post-grafting ($p < 0.05$) (Figure 4.2D); however there were no significant differences at week 4 and 8 between the two groups. Significant differences were found in the control group between weeks 2 and 4 ($p < 0.01$), 2 and 8 ($p < 0.001$) as well as weeks 2 and 8 ($p < 0.05$), 4 and 8 ($p < 0.05$) in the depletion group.



B

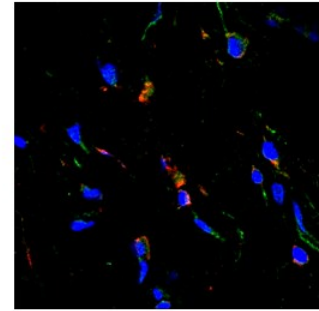
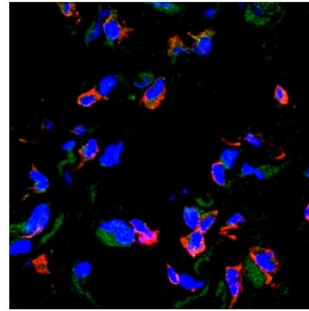
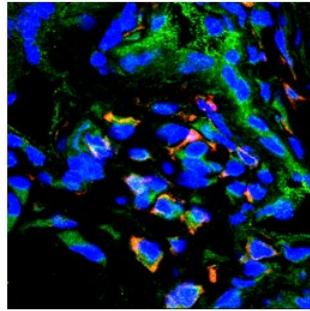
M2

2 weeks

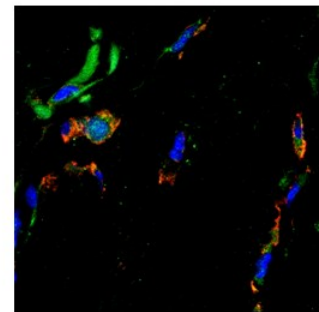
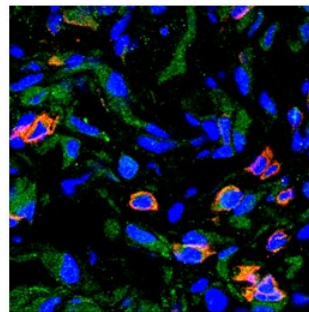
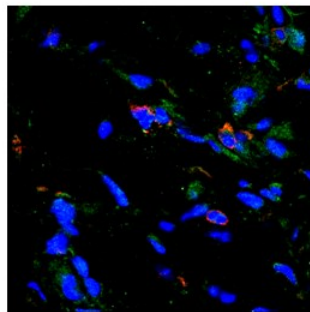
4 weeks

8 weeks

Control



Depletion



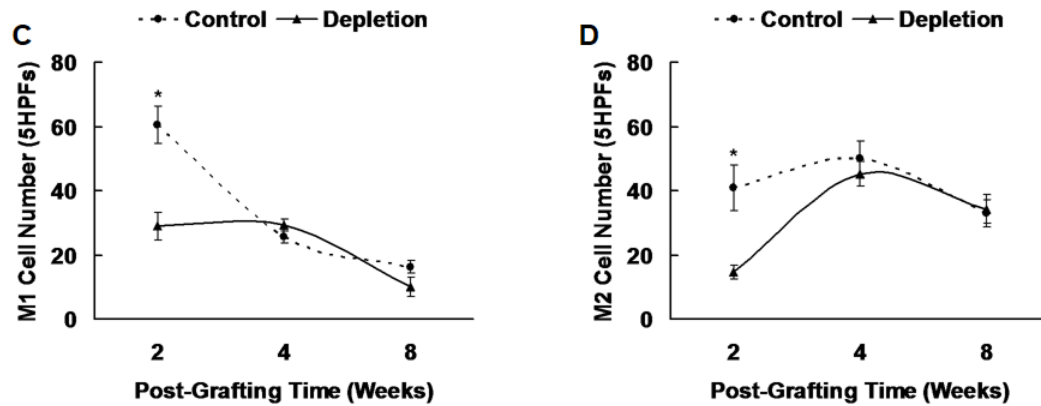


Figure 4.2 Clodronate liposomes reduced M1 and M2 macrophage number in the grafted tissue at 2 weeks post-grafting. The M1 cells were identified as double positive for F4/80 (red) and NOS2 (green). Similarly M2 cells were double positive for F4/80 (red) and Arg-1 (green). Representative images of dual stained of M1 macrophages (orange) (A) and M2 macrophages (orange) (B) at different time points post-grafting were shown. The double positive cells were counted under 5HPFs, the total cell number was analyzed and the number of M1 and M2 macrophages was compared and analyzed (C, D). N=3, experiment was done in duplicate. *p<0.05.

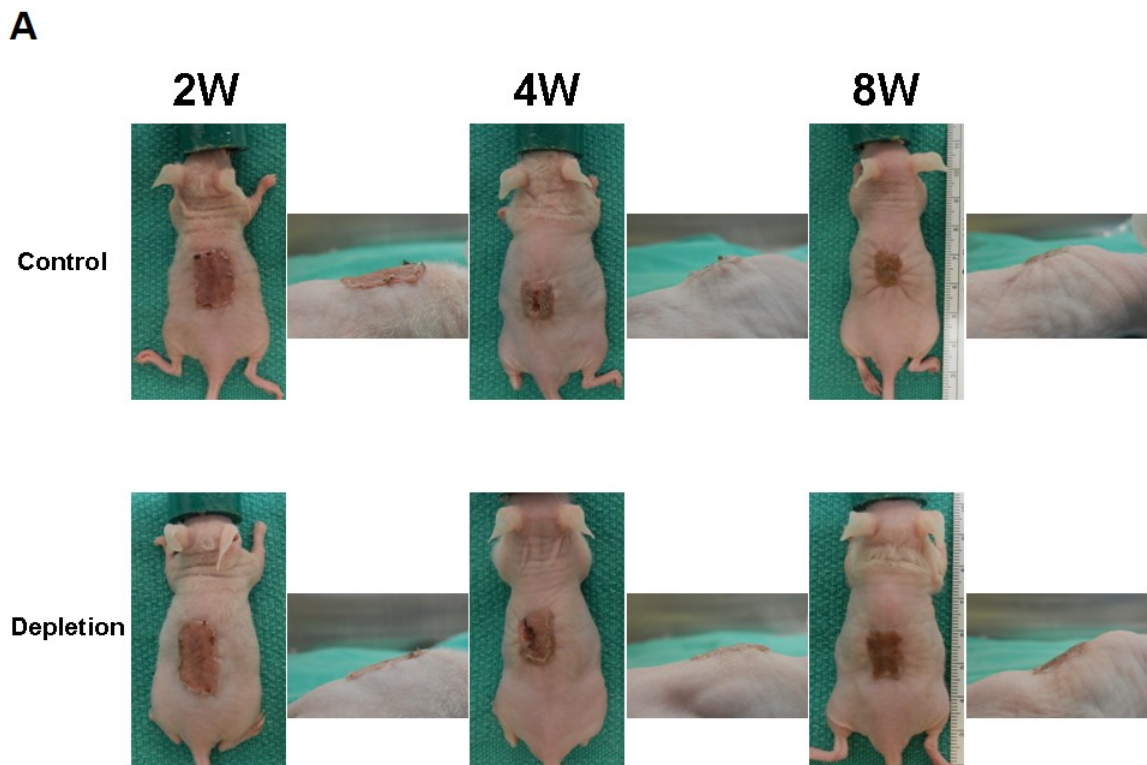
4.3.3 Macrophage depletion improved scar formation

Each of the transplanted human skin grafts remained viable throughout the duration of the experiment. One week post-grafting, the grafted skin looked erythematous and moist after the dressing and sutures were removed. The wounds of control mice developed contracted, pigmented, thickened, raised scars; whereas no obvious scar contraction and thickening was observed in the depletion group at 8 weeks post-grafting (Figure 4.3A). The figures at 0 week (0W) illustrate the skin tissue thickness before grafting.

The wounds were digitally photographed weekly and the wound area was quantified by ImageJ software to evaluate wound contraction (10). As compared to the initial time point after grafting, the transplanted human skin grafts in the depletion group contracted slowly over time while the grafts in the control group became progressively more contracted over time. There were significant differences of wound areas between the two groups at 2 ($p<0.01$), 4 ($p<0.01$) and 8 ($p<0.01$) weeks post-grafting. Also, within each group, there were significant differences between weeks 0 and 2 ($p<0.01$), 0 and 4 ($p<0.001$), 0 and 8 ($p<0.001$), 2 and 4 ($p<0.001$), 2 and 8 ($p<0.001$) in the control group, as well as weeks 0 and 4 ($p<0.01$), 0 and 8 ($p<0.001$), 2 and 8 ($p<0.05$) in the depletion group (Figure 4.3B).

The grafted human skin in both groups retained the structural characteristics of human skin microscopically (Figure 4.3C). The graft thickness at different time points was displayed as a percentage of the original thickness of the STSG before grafting. The

skin thickness gradually increased from 2 to 4 weeks post-grafting in the control group and then decreased slowly thereafter. The graft thickness of the depletion group increased slower than the control group from 2 to 4 weeks and became stable at 8 weeks post-grafting. There were significant differences in 4 ($p<0.05$) and 8 ($p<0.05$) weeks post-grafting between the two groups. Significant differences in graft thickness were also found between weeks 0 and 4 ($p<0.001$), 0 and 8 ($p<0.001$), 2 and 4 ($p<0.001$), 2 and 8 ($p<0.01$) in the control group, as well as weeks 0 and 4 ($p<0.01$), 0 and 8 ($p<0.01$), 2 and 4 ($p<0.01$), 2 and 8 ($p<0.01$) in the depletion group (Figure 4.3D).



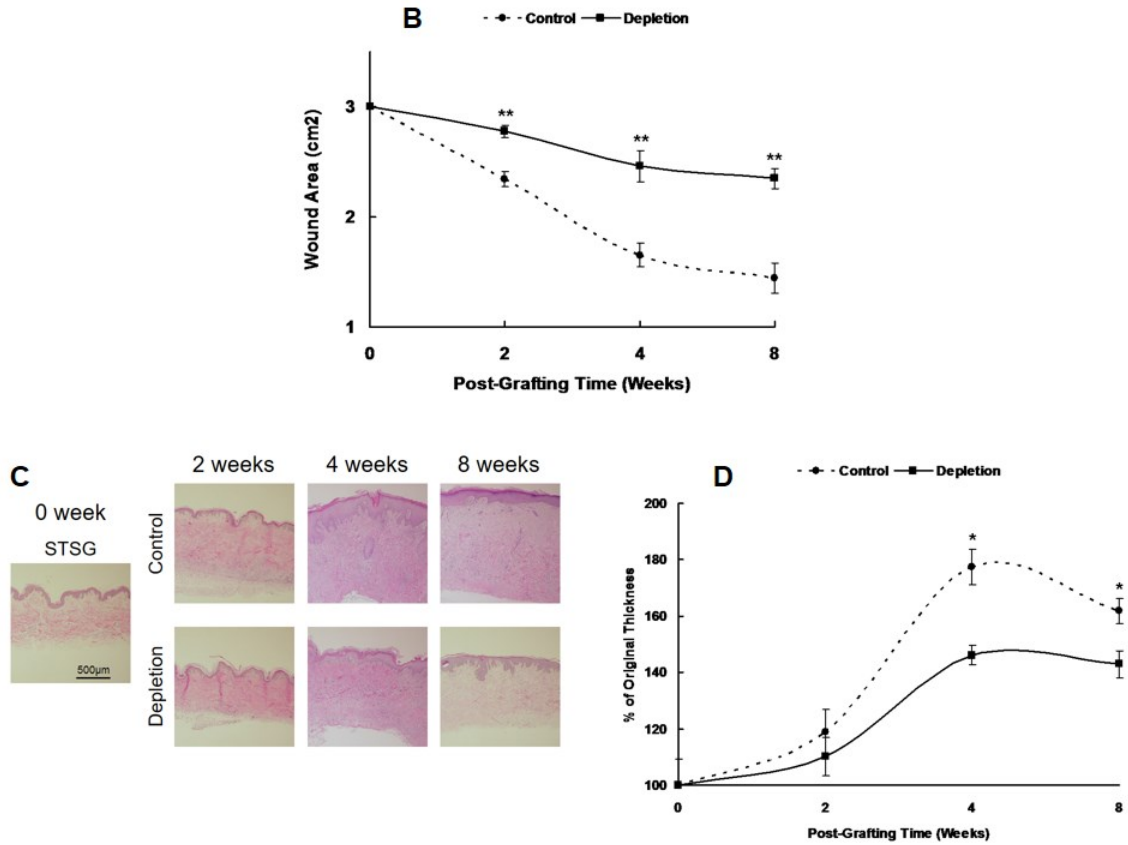


Figure 4.3 Macrophage depletion improved scar formation. The wounds were monitored by digital photography after grafting (A). Wound area at different time points between the two groups were measured and analyzed (B). Images of H&E sections from grafted skin of the two groups were taken together with normal STSG before grafting at different time points (C). The skin thickness was measured and analyzed (D). N=3, experiment was done in duplicate, * $p < 0.05$, ** $p < 0.01$.

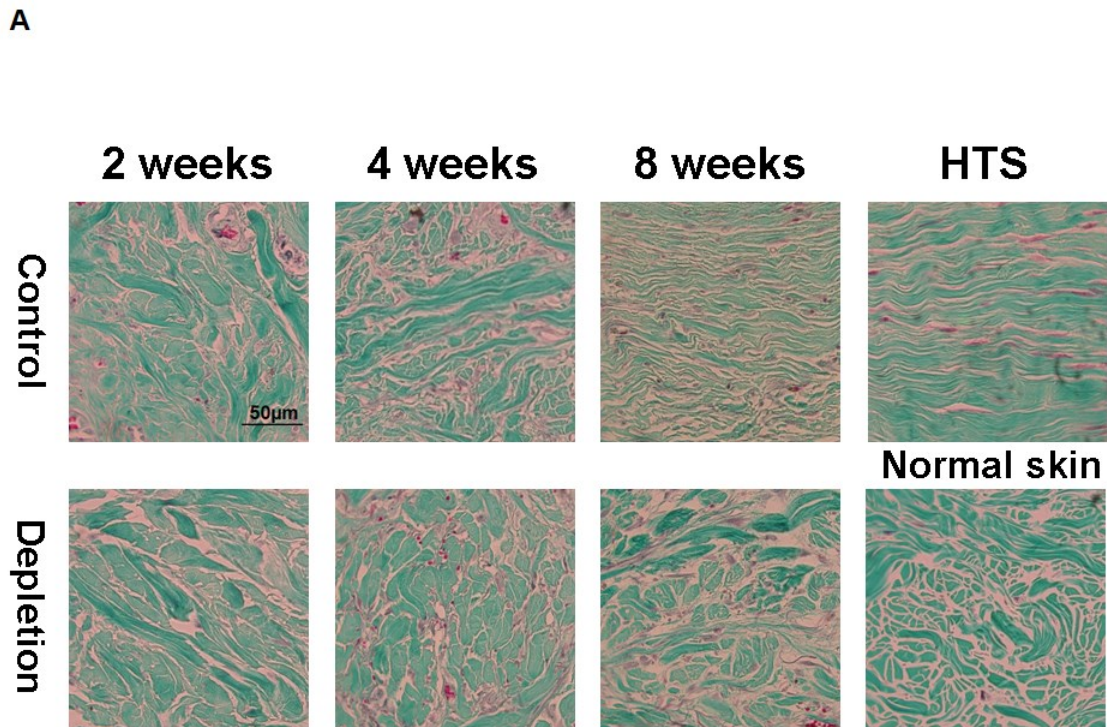
4.3.4 Macrophage depletion improved collagen remodeling

Masson's trichrome staining was used to assess the morphology of collagen fiber or bundles in the grafts. The collagen bundles in the control group were larger and more irregular and then became smaller over time. A parallel pattern of collagen bundles was seen at 8 weeks post-grafting exhibiting a striking similarity to human HTS tissue, which was substantially different from the basket-weave-like normal human skin collagen bundles; whereas, collagen bundles in the depletion group showed similar pattern to normal human skin at all the time points (Figure 4.4A).

FFT enables the simultaneous analysis of collagen bundles in a chosen area where COI is lower in normal skin tissue but higher in HTS tissue. The CBPI represents the distance between collagen bundles where a lower value of CBPI represents a higher density, which resembles HTS tissue. COI of the control group increased sharply over time while COI of the depletion group increased slowly until 4 weeks post-grafting and decreased at 8 weeks post-grafting. There were significant differences between the two groups at weeks 4 ($p < 0.001$) and 8 ($p < 0.001$) post-grafting. Significant differences in COI were also found in the control group between weeks 0 and 2 ($p < 0.05$), 0 and 4 ($p < 0.001$), 0 and 8 ($p < 0.001$), 2 and 4 ($p < 0.001$), 2 and 8 ($p < 0.001$), 4 and 8 ($p < 0.05$) (Figure 4.4B). CBPI of both groups showed a reduction over time but a faster decrease was observed in the control group where more fibrotic collagen morphology was found, which was significantly different between the two groups at 8 ($p < 0.001$) weeks post-grafting. Significant differences were also observed in the control group between weeks 0 and 2 ($p < 0.05$), 0 and 4 ($p < 0.001$), 0 and 8 ($p < 0.001$), 2 and 4 ($p < 0.01$), 2 and 8 ($p < 0.001$)

as well as between weeks 0 and 2 ($p < 0.01$), 0 and 4 ($p < 0.01$), 0 and 8 ($p < 0.001$) in the depletion group (Figure 4.4C).

Collagen protein was quantified by the measurement of 4-Hyp by LC/MS, as previously reported (16). In the control group, the amount of collagen increased after the grafting and reached a peak at week 4 and then decreased at 8 weeks post-grafting. In the depletion group, the amount of collagen was similar, which increased slowly over time until week 4 and decreased at 8 weeks post-grafting where a significant difference existed between the two groups ($p < 0.01$) (Figure 4.4D).



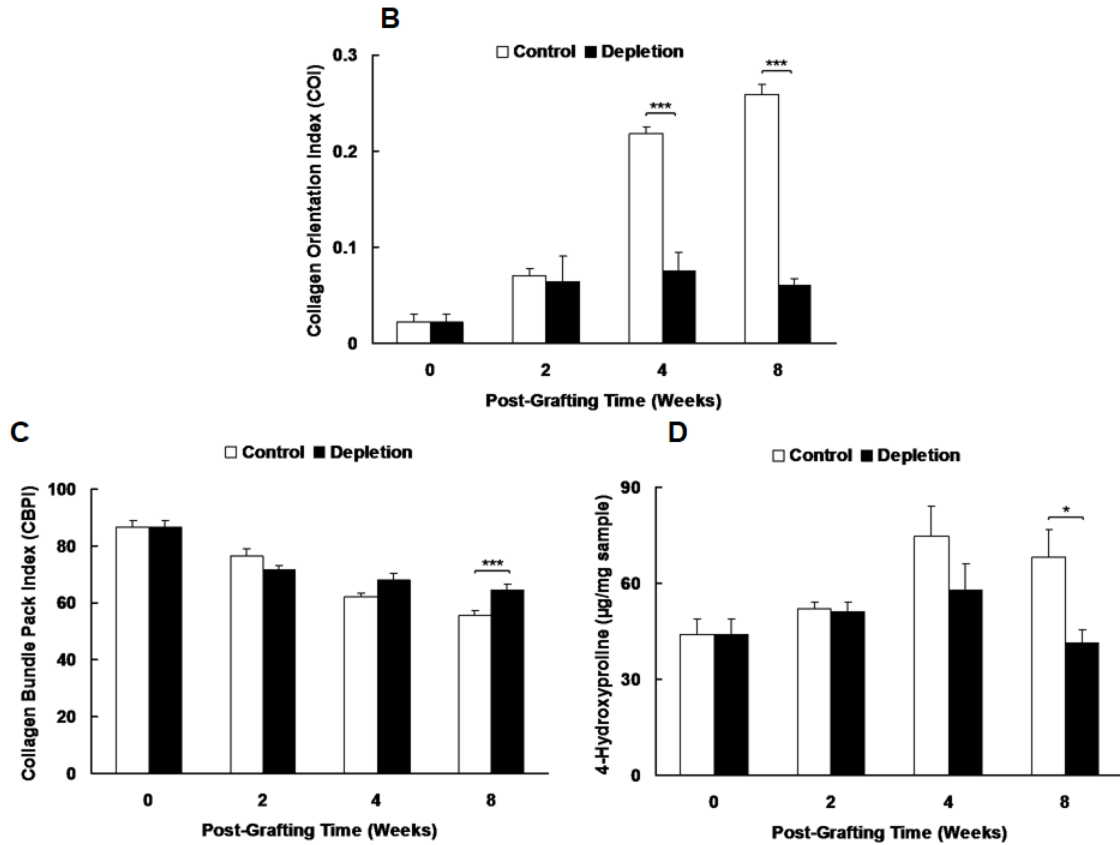


Figure 4.4 Macrophage depletion improved collagen remodeling. Masson’s trichrome staining showed collagen bundle morphology in the two groups after grafting as well as in normal skin and HTS tissue (A). COI and CBPI at different time points were analyzed using FFT module (B, C). Collagen level was determined by measurement of 4-Hyp in the grafted skin of both groups using LC/MS (D). N=3, experiment was done in duplicate, *p<0.05, ***p<0.001.

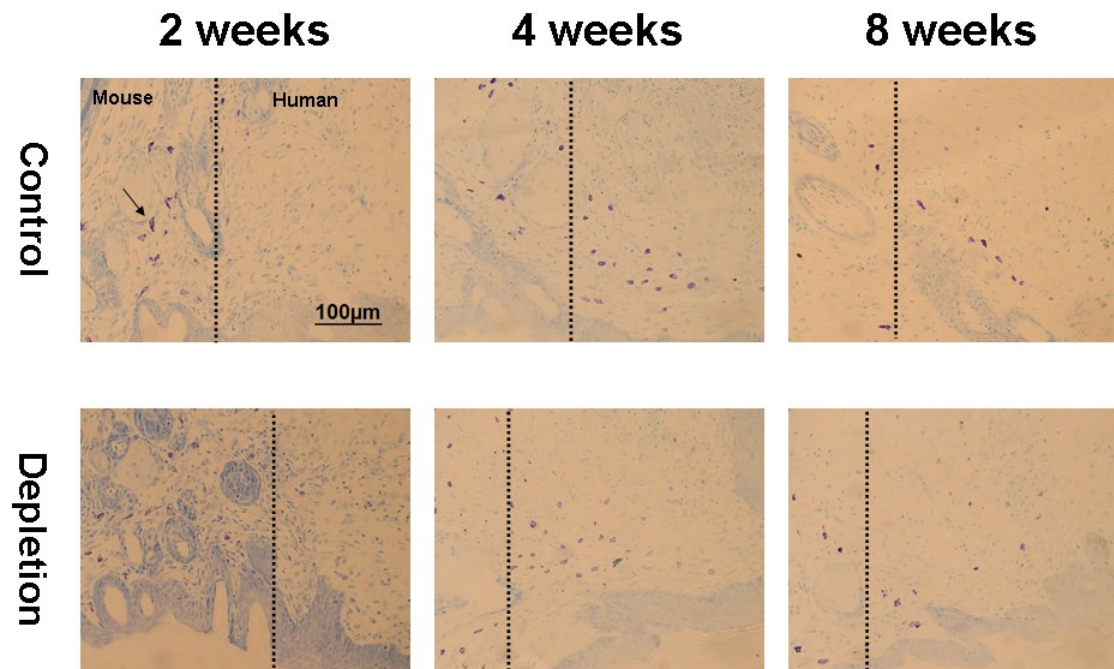
4.3.5 Macrophage depletion reduced mast cell infiltration and myfibroblast differentiation

As shown in Figure 4.5A, positively stained reddish-purple murine mast cells accumulated in the mouse skin close to the junction between the mouse skin on the left and human grafts region (indicated by the dotted line) at 2 weeks post-grafting. Varying degrees of mast cell infiltration from the mouse to human grafted skin was observed at different time points. The peak of mast cell infiltration was observed at week 4 in both groups while significantly fewer mast cells were seen in the human skin grafts in the depletion group at week 8 ($p < 0.05$) as compared to the control group. There were significant differences between weeks 2 and 4 ($p < 0.05$) in the control group as well as weeks 2 and 4 ($p < 0.05$), 4 and 8 ($p < 0.05$) in the depletion group (Figure 4.5B).

As previously described, α -SMA is commonly used as a myofibroblast marker (17), which are abundant in human HTS (18). Representative images of myofibroblast staining in both groups were shown in Figure 4.5C. Figure 4.5D showed myofibroblast number changes in both groups at different time points post-grafting. The number of myofibroblasts in the control group increased dramatically at week 2, peaked at week 4 and then decreased sharply at week 8 post-grafting. Nevertheless, the number of myofibroblasts in the depletion group showed a similar pattern but a slower increase at weeks 2 to 4 post-grafting, which became significantly different between the two groups at week 4 ($p < 0.05$) and 8 ($p < 0.05$) post-grafting. In addition, there were significant differences between weeks 0 and 2 ($p < 0.001$), 0 and 4 ($p < 0.001$), 0 and 8 ($p < 0.001$), 2 and 4 ($p < 0.05$), 2 and 8 ($p < 0.05$), 4 and 8 ($p < 0.001$) in the control group as well as weeks

0 and 2 ($p < 0.001$), 0 and 4 ($p < 0.001$), 0 and 8 ($p < 0.01$), 4 and 8 ($p < 0.001$), 2 and 8 ($p < 0.01$), 4 and 8 ($p < 0.001$) in the depletion group.

A



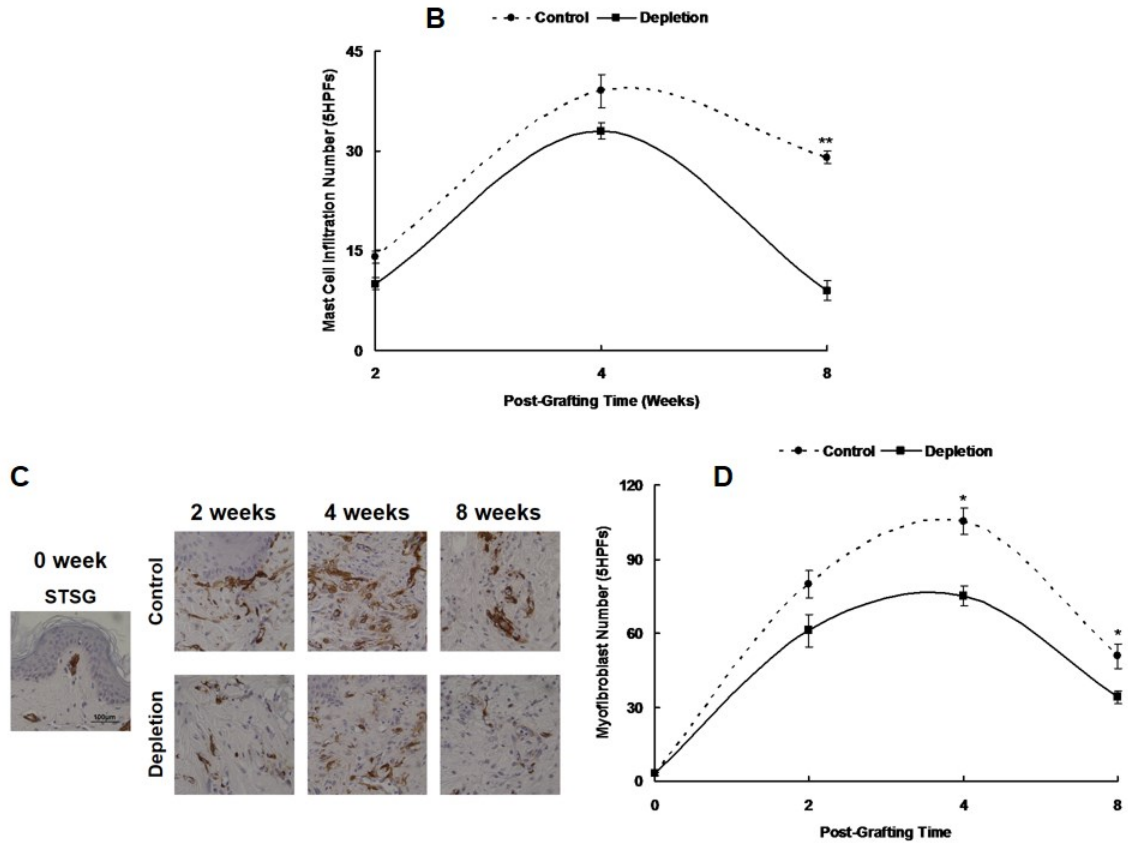


Figure 4.5 Macrophage depletion reduced mast cell and myofibroblast infiltration.

Various degrees of mast cell infiltration from mouse skin to human grafted skin was observed at different time points post-grafting between the two groups (A). Toluidine blue positive stained mast cells were counted and the total number was calculated and analyzed (B). Representative images of α -SMA (brown) positive myofibroblasts in the two groups at various time points post-grafting (C). α -SMA positive cells were counted and the total number was calculated and analyzed (D). N=3, experiment was done in duplicate, * $p < 0.05$, ** $p < 0.01$.

4.3.6 Macrophage depletion decreased pro-fibrotic factor expression

qPCR revealed the relative gene expression of human anti-fibrotic factors and pro-fibrotic factors in the grafted tissues over time during the experimental time course (Figure 4.6). Anti-fibrotic factors such as MMP-1 and DCN had a higher expression in the depletion group at all the time points compared to control group. However, the expression of pro-fibrotic factors such as TGF- β 1, CTGF and α -SMA were found higher in the control group at all the time points compared to the depletion group. Significant differences were observed between the two groups in the expression of MMP-1 at weeks 2 ($p < 0.05$) and 4 ($p < 0.05$), DCN at week 4 ($p < 0.05$), TGF- β 1 at week 8 ($p < 0.01$), CTGF at week 4 ($p < 0.05$), α -SMA at weeks 2 ($p < 0.05$) and 4 ($p < 0.05$) post-grafting. In addition, the expression of F4/80 in the spleen section showed a significant reduction in the depletion group compared to the control group at 2 weeks post-grafting ($p < 0.05$).

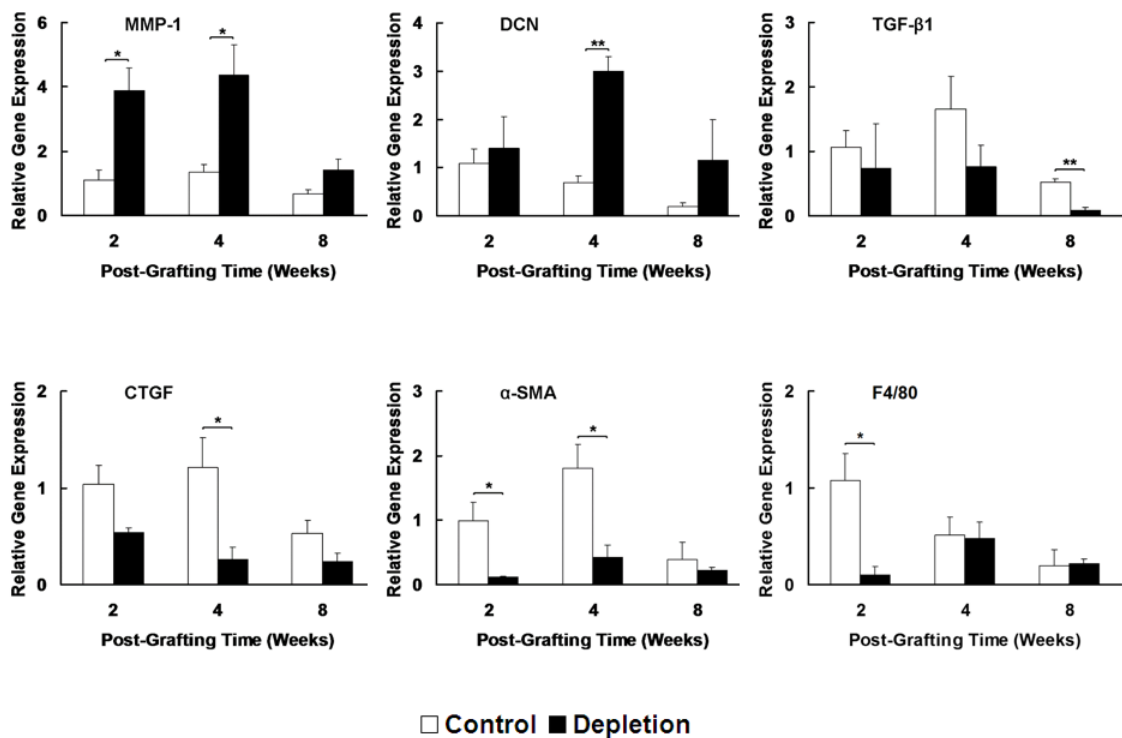


Figure 4.6 Macrophage depletion increased anti-fibrotic and decreased pro-fibrotic factor expression in the grafted tissue at various time points post-grafting. qPCR revealed the relative gene expressions of anti-fibrotic factors (MMP-1, DCN) and pro-fibrotic factors (TGF-β1, CTGF, α-SMA) in the grafted skins. The gene expressions of anti-fibrotic factors had a higher expressions in the depletion group at all the time points compared to control group. However, the gene expressions of pro-fibrotic factors were found higher in the control group at all the time points compared to the depletion group. In addition, the expression of F4/80 in the spleen section showed a significant reduction in the depletion group compared to the control group at 2 weeks post-grafting. N=3, experiment was done in duplicate, *p<0.05, **p<0.01.

4.3.7 Macrophage depletion reduced expression of M1 and M2 related cytokines

Figure 4.7 showed the relative gene expression of mouse M1 macrophage related cytokines (TNF- α , IL-6 and IL-1 β) and mouse M2 macrophage related cytokines (TGF- β 1, IL-10 and IL-1 α) at all the time points post-grafting. The expression of TNF- α , IL-6 and IL-1 β were found much lower in the depletion group compared to the control group at all the time points post-grafting. There were significant differences in TNF- α at week 2 ($p < 0.05$); in IL-6 at weeks 2 ($p < 0.05$), 4 ($p < 0.05$), 8 ($p < 0.05$) and IL-1 β at week 2 ($p < 0.05$) post-grafting. A similar pattern was also observed in the expression of TGF- β 1, IL-10 and IL-1 α , where lower expression was found in the depletion group as compared to the control group at all the time points post-grafting. Significant differences were found between the two groups in TGF- β 1 at weeks 2 ($p < 0.05$) and 4 ($p < 0.05$); in IL-10 at week 2 ($p < 0.05$) and in IL-1 α at weeks 2 ($p < 0.01$) and 4 ($p < 0.05$) post-grafting.

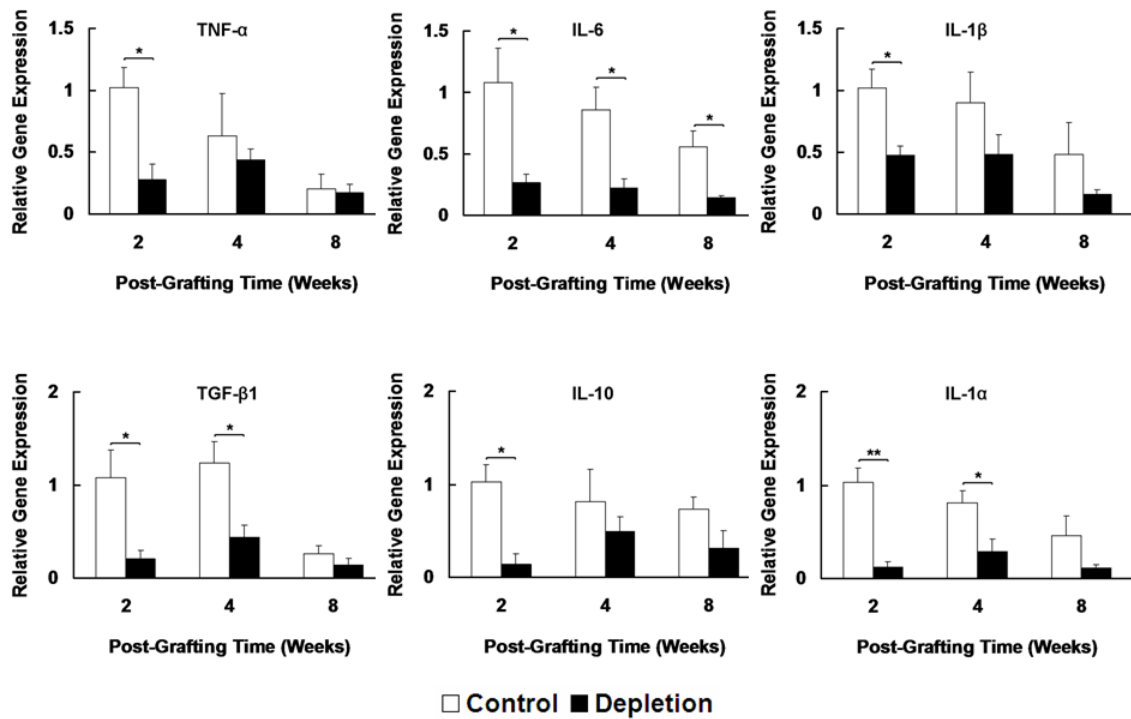
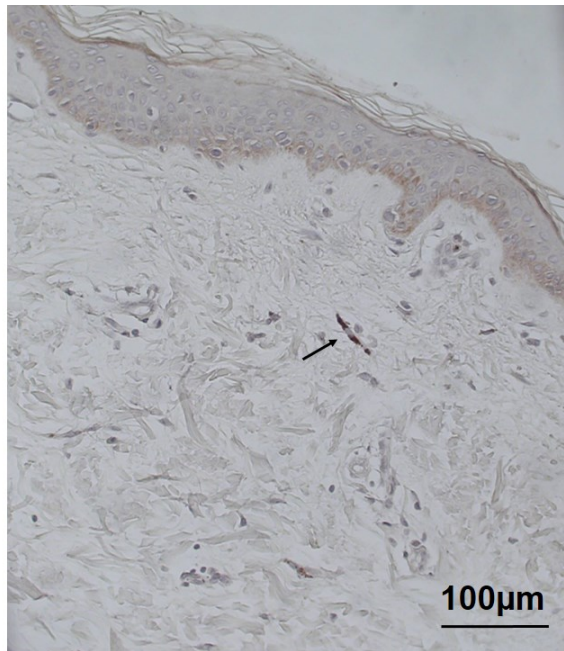


Figure 4.7 Macrophage depletion reduced the expression of M1 and M2 related cytokines. qPCR revealed the relative gene expression of cytokines from M1 and M2 macrophages over time during the experimental time course. The expressions of M1 cytokines such as TNF- α , IL-6 and IL-1 β were found much lower in the depletion group compared to the control group at all the time points post-grafting. A similar pattern was also observed in the expressions of M2 cytokines such as TGF- β 1, IL-10 and IL-1 α , that is, much lower expressions were found in the depletion group compared to the control group at all the time points post-grafting. N=3, experiment was done in duplicate, *p<0.05, **p<0.01.

4.4 Discussion

Previous literature has shown that the number of mast cells have increased in HTS tissue and thus may be of importance in the development of fibrosis (3, 19). In this experiment we found similar findings that there were increased mast cell number in the control group and the decreased mast cell number in the depletion group. The improvements in scarring seen in the depletion group of animals may due to the decrease in mast cell number. In addition, we have found that the infiltration pattern of mast cells in the mouse skin was different than that of the human skin grafts, which we felt is novel and worthy of illustration.

It is possible that these human skin grafts contain a mixture of infiltrating murine derived macrophages and human resident macrophages. However, human macrophages resided in the skin are mainly found at the deeper layer of dermis; whereas, the human skin grafts used in the experiments were split thickness and contained a portion of the upper dermis, where there are normally smaller numbers of human macrophages. In addition, we have looked for human macrophages in the split thickness skin grafts by staining the skin with CD163, which is a specific marker for human macrophage. There are few human macrophages that are carried in the transplanted human split thickness skin grafts (Supplementary Figure 1). For these reasons we focused on murine macrophages in this study and found abundant murine macrophages which had infiltrated into the human skin grafts. Thus we feel it is unlikely that human macrophages, are a substantial contributor to the development of HTS.



Supplementary Figure 1. Few human macrophages were carried in the transplanted human STSG. Human macrophages in the split thickness skin grafts were stained with CD163, which is a specific marker for human macrophages. There were few human macrophages that were carried in the transplanted human STSG.

In 1984, Nico Van Rooijen used liposome-encapsulated clodronate to deplete macrophages systemically (20). Since then, liposomal clodronate has become a standard choice for macrophage depletion studies where it reduced the severity of fibrotic diseases such as renal fibrosis (21, 22), pulmonary fibrosis (23), systemic sclerosis (24), and liver fibrosis (25); however, our study is the first to adopt macrophage depletion in the human HTS-like nude mouse model. The mice in the depletion group that received the clodronate liposome injections showed reduced numbers of M1 and M2 macrophages in the grafted skin; reduced macrophages in splenic tissues, and decreased expression of M1 and M2

related factors at 2 weeks post-grafting. As such, it suggests that systemic depletion of macrophages was achieved and significant differences in scar formation was observed in the depletion group. Macrophage depletion improved scar formation, collagen remodeling; inhibited mast cell infiltration and myofibroblast transformation associated with increased expression of anti-fibrotic factors and decreased pro-fibrotic factors in the depletion group. These changes suggest macrophages have a critical role in many elements of wound healing that lead to the formation of HTS and their depletion in subacute phase of wound healing reduced HTS formation *in vivo*.

Lucas et al have recently demonstrated the essential role of macrophages in the early phases of wound repair (26) where transgenic mice expressing the human diphtheria toxin receptor under the control of the CD11b promoter (CD11b-DTR mice) were used to selectively deplete macrophages from skin wounds at different phases of repair. Wounds depleted of macrophages during the early stages of wound repair demonstrated markedly attenuated wound repair. In addition, loss of macrophages in the early stage of excisional healing impaired induction of granulation tissue formation, myofibroblast differentiation and angiogenesis. To avoid impaired healing in the early phase of wound healing after the grafting in this study, injection of clodronate liposomes began at day 7 when the grafted wound had healed based on our previous study (11) where the natural abundance of mononuclear phagocytes started to increase at 2 weeks and was maximal at 3 to 4 weeks post-grafting in the human HTS-like nude mouse model. In order to prevent the increasing numbers of M2 macrophages which began at 2 weeks post-grafting, the last injection of clodronate liposomes was given on day 13.

A critical consideration in designing macrophage depletion experiments is the route of administration of clodronate liposomes. In the preliminary experiments intravenous injection via tail vein was difficult to perform and the tail vein was thrombosed readily in the relatively small nude mice after injection of the viscous drug. Thus, we chose to perform intraperitoneal injections to deliver clodronate liposomes due to the simplicity of the technique. In addition, other studies have successfully depleted macrophages systemically using intraperitoneal injection (27, 28). Intraperitoneal injected clodronate liposomes are able to pass the parathymic lymph nodes that drain the peritoneal cavity, enter the blood circulation via the larger lymph vessels such as ductus thoracicus. As a consequence, macrophages of parathymic lymph nodes, liver and spleen are depleted. Another advantage of the intraperitoneal route of delivery is the relatively large volume that can be administered and repeated injections can be delivered such that a greater number of macrophages can be depleted than by intravenous injections (29).

One limitation of this study is that the macrophage depletion by injections of clodronate liposomes is not specific to M2 macrophages alone. Thus, it is possible that the diminished scar formation in the depletion group may also be due to the depletion of M1 macrophage population. However, the time of depletions in this study was selected after the peak of M1 macrophages and before the maximum abundance of M2 macrophages based on our earlier experiments. Thus, the number of M1 macrophages had begun to decrease by the time of the first injection of clodronate liposomes compared to the number at 4 weeks post-grafting, suggesting that the majority M1 macrophages were not affected. Conversely, the three injections of clodronate liposomes depleted the M2 macrophages at 2 weeks post-grafting, suggesting that the systemic depletion of

predominately M2 macrophages may be important in the development of HTS. In order to more clearly establish that the diminished fibrosis in the depletion group is M2 macrophage-dependent, future experiments using adoptive transfer of M2 macrophages after the systemic macrophage depletion may more specifically establish their importance. However, M2 macrophages from bone marrow aspirates proven to be feasible (30) would need to be purified, differentiated into M2 macrophages and the phenotype of these targeted cells confirmed prior to the adoptive transfer. Furthermore, transgenic mouse models may be another alternative approach to specific M2 depletion as reported (31, 32).

The dichotomy of macrophages into M1 and M2 macrophages as a classification of the biology of mononuclear phagocytes may be oversimplified due to new evidence suggesting that a wider spectrum of macrophage activation exists. For example, M2 macrophages can be further subdivided into M2a, M2b, M2c, and M2d subsets (33, 34). These diverse functional phenotypes are induced by different stimuli encountered in the dynamic changing microenvironments (35). Thus, it will be challenging to investigate the roles and the mechanisms of these functional subtypes of macrophages.

4.5 Conclusion

The systemic depletion of macrophage in subacute phase of wound healing reduced scarring in transplanted human skin grafts *in vivo*. These findings provide evidence for the pro-fibrotic role of macrophages in fibrosis of human skin. Future experiments are needed in order to confirm that M2 macrophages alone contribute to the development of

HTS, which will provide the basis for macrophage-centered diagnostic and therapeutic strategies in the future.

4.6 References

1. Engrav LH, Garner WL, Tredget EE. Hypertrophic scar, wound contraction and hyper-hypopigmentation. *J Burn Care Res.* 2007;28:593-7.
2. Bombaro KM, Engrav LH, Carrougher GJ, Wiechman SA, Faucher L, Costa BA, et al. What is the prevalence of hypertrophic scarring following burns? *Burns.* 2003;29:299-302.
3. Wang J, Ding J, Jiao H, Honardoust D, Momtazi M, Shankowsky HA, et al. Human hypertrophic scar-like nude mouse model: characterization of the molecular and cellular biology of the scar process. *Wound Repair Regen.* 2011;19:274-85.
4. Yona S, Gordon S. From the Reticuloendothelial to Mononuclear Phagocyte System - The Unaccounted Years. *Front Immunol.* 2015;6:328.
5. Sica A, Erreni M, Allavena P, Porta C. Macrophage polarization in pathology. *Cell Mol Life Sci.* 2015;72:4111-26.
6. Martinez FO, Sica A, Mantovani A, Locati M. Macrophage activation and polarization. *Front Biosci.* 2008;13:453-61.
7. Song E, Ouyang N, Horbelt M, Antus B, Wang M, Exton MS. Influence of alternatively and classically activated macrophages on fibrogenic activities of human fibroblasts. *Cell Immunol.* 2000;204:19-28.
8. Nishida M, Hamaoka K. Macrophage phenotype and renal fibrosis in obstructive nephropathy. *Nephron Exp Nephrol.* 2008;110:e31-6.
9. Momtazi M, Kwan P, Ding J, Anderson CC, Honardoust D, Goekjian S, et al. A nude mouse model of hypertrophic scar shows morphologic and histologic characteristics of human hypertrophic scar. *Wound Repair Regen.* 2013;21:77-87. doi: 10.1111/j.524-475X.2012.00856.x. Epub 2012 Nov 5.
10. Ding J, Ma Z, Liu H, Kwan P, Iwashina T, Shankowsky HA, et al. The therapeutic potential of a C-X-C chemokine receptor type 4 (CXCR-4) antagonist on hypertrophic scarring in vivo. *Wound Repair Regen.* 2014;22:622-30.

11. Zhu Z, Ding J, Ma Z, Iwashina T, Tredget EE. The natural behavior of mononuclear phagocytes in HTS formation. *Wound Repair Regen.* 2015.
12. Tredget EE, Iwashina T, Scott PG, Ghahary A. Determination of plasma Ntau-methylhistamine in vivo by isotope dilution using benchtop gas chromatography-mass spectrometry. *J Chromatogr B Biomed Sci Appl.* 1997;694:1-9.
13. Swirski FK, Nahrendorf M, Etzrodt M, Wildgruber M, Cortez-Retamozo V, Panizzi P, et al. Identification of splenic reservoir monocytes and their deployment to inflammatory sites. *Science.* 2009;325:612-6.
14. Mebius RE, Kraal G. Structure and function of the spleen. *Nat Rev Immunol.* 2005;5:606-16.
15. Gordon S, Hamann J, Lin HH, Stacey M. F4/80 and the related adhesion-GPCRs. *Eur J Immunol.* 2011;41:2472-6.
16. Wang JF, Jiao H, Stewart TL, Shankowsky HA, Scott PG, Tredget EE. Fibrocytes from burn patients regulate the activities of fibroblasts. *Wound Repair Regen.* 2007;15:113-21.
17. Nagamoto T, Eguchi G, Beebe DC. Alpha-smooth muscle actin expression in cultured lens epithelial cells. *Invest Ophthalmol Vis Sci.* 2000;41:1122-9.
18. Nedelec B, Shankowsky H, Scott PG, Ghahary A, Tredget EE. Myofibroblasts and apoptosis in human hypertrophic scars: the effect of interferon-alpha2b. *Surgery.* 2001;130:798-808.
19. Ibrahim MM, Bond J, Bergeron A, Miller KJ, Ehanire T, Quiles C, et al. A novel immune competent murine hypertrophic scar contracture model: a tool to elucidate disease mechanism and develop new therapies. *Wound Repair Regen.* 2014;22:755-64.
20. van Rooijen N, van Nieuwmegen R. Elimination of phagocytic cells in the spleen after intravenous injection of liposome-encapsulated dichloromethylene diphosphonate. An enzyme-histochemical study. *Cell Tissue Res.* 1984;238:355-8.
21. Braga TT, Correa-Costa M, Guise YF, Castoldi A, de Oliveira CD, Hyane MI, et al. MyD88 signaling pathway is involved in renal fibrosis by favoring a TH2 immune response and activating alternative M2 macrophages. *Mol Med.* 2012;18:1231-9.

22. Machida Y, Kitamoto K, Izumi Y, Shiota M, Uchida J, Kira Y, et al. Renal fibrosis in murine obstructive nephropathy is attenuated by depletion of monocyte lineage, not dendritic cells. *J Pharmacol Sci.* 2010;114:464-73.
23. Gibbons MA, MacKinnon AC, Ramachandran P, Dhaliwal K, Duffin R, Phythian-Adams AT, et al. Ly6Chi monocytes direct alternatively activated profibrotic macrophage regulation of lung fibrosis. *Am J Respir Crit Care Med.* 2011;184:569-81.
24. Li H, Nagai T, Hasui K, Matsuyama T. Depletion of folate receptor beta-expressing macrophages alleviates bleomycin-induced experimental skin fibrosis. *Mod Rheumatol.* 2014;24:816-22.
25. Duffield JS, Forbes SJ, Constandinou CM, Clay S, Partolina M, Vuthoori S, et al. Selective depletion of macrophages reveals distinct, opposing roles during liver injury and repair. *Journal of Clinical Investigation.* 2005;115:56-65.
26. Lucas T, Waisman A, Ranjan R, Roes J, Krieg T, Muller W, et al. Differential Roles of Macrophages in Diverse Phases of Skin Repair. *Journal of Immunology.* 2010;184:3964-77.
27. Konig S, Nitzki F, Uhmman A, Dittmann K, Theiss-Suennemann J, Herrmann M, et al. Depletion of cutaneous macrophages and dendritic cells promotes growth of basal cell carcinoma in mice. *PLoS One.* 2014;9:e93555.
28. Kushiyama T, Oda T, Yamada M, Higashi K, Yamamoto K, Oshima N, et al. Effects of liposome-encapsulated clodronate on chlorhexidine gluconate-induced peritoneal fibrosis in rats. *Nephrol Dial Transplant.* 2011;26:3143-54.
29. Weissig V, SpringerLink (Online service). Liposomes Methods and Protocols, Volume 1: Pharmaceutical Nanocarriers. *Methods in Molecular Biology, Methods and Protocols*;XII, 546p. 304 illus., 152 illus. in color.
30. Weisser SB, McLarren KW, Voglmaier N, van Netten-Thomas CJ, Antov A, Flavell RA, et al. Alternative activation of macrophages by IL-4 requires SHIP degradation. *Eur J Immunol.* 2011;41:1742-53.
31. Frieler RA, Nadimpalli S, Boland LK, Xie A, Kooistra LJ, Song J, et al. Depletion of macrophages in CD11b diphtheria toxin receptor mice induces brain inflammation and enhances inflammatory signaling during traumatic brain injury. *Brain Res.* 2015;1624:103-12.

32. Lucas T, Waisman A, Ranjan R, Roes J, Krieg T, Muller W, et al. Differential roles of macrophages in diverse phases of skin repair. *J Immunol.* 2010;184:3964-77.
33. Mantovani A, Sica A, Sozzani S, Allavena P, Vecchi A, Locati M. The chemokine system in diverse forms of macrophage activation and polarization. *Trends Immunol.* 2004;25:677-86.
34. Ferrante CJ, Leibovich SJ. Regulation of Macrophage Polarization and Wound Healing. *Adv Wound Care (New Rochelle).* 2012;1:10-6.
35. Xue J, Schmidt SV, Sander J, Draffehn A, Krebs W, Quester I, et al. Transcriptome-based network analysis reveals a spectrum model of human macrophage activation. *Immunity.* 2014;40:274-88.

Chapter 5

Conclusions and Future Directions

5.1 Conclusions and future directions

Since HTS are characterized by abundant α -SMA producing myofibroblasts accumulation (1), cells that are involved in the activation of fibroblasts and myofibroblasts are considered to directly or indirectly participate in HTS formation, such as macrophages, mast cells, T lymphocytes, Langerhans cells, fibrocytes and keratinocytes (2). Although there is evidence indicating that these cells might contribute to HTS formation (3-7), macrophages among them play a far more important role in the whole wound healing process from inflammation to tissue remodeling phase (8). Macrophages are the majority leukocytes in the sterile wound. They are antigen presenting cells and phagocytes that actively participate in innate and adaptive immune responses. There are two types of macrophages, M1 and M2 macrophages. M1 macrophages produce pro-inflammatory cytokines such as TNF- α , IL-1 β , IL-6, IFN- γ , which promote inflammation but also stimulate fibroblast proliferation (9). M2 macrophages produce TGF- β 1, which stimulate myofibroblast proliferation. Abnormal functioning of M2 macrophages might lead to overproduction of TGF- β 1 resulting in HTS formation.

Here, we focus on the role of polarized macrophages in HTS formation using *in vitro* and *in vivo* experiments in order to confirm whether M2 macrophages have contributed to HTS formation.

The *in vitro* experiment used THP-1 differentiated polarized macrophages to co-culture with HDF. We showed that M2 macrophages promoted the fibrogenic activities

of HDF while M1 macrophages exhibited an anti-fibrotic role in HDF behavior after co-culture. Our results reinforce the findings from previous published studies that M1 macrophages are anti-fibrotic and M2 macrophages are pro-fibrotic (10). However, our study only exhibited an indirect effect of polarized macrophages on co-cultured HDF. It is the factors secreted by polarized macrophages into the conditioned media that cause the behavioral changes of the co-cultured HDF, but we are not clear what exactly are causing the changes. Future studies may focus on the detailed identification of the content in the co-cultured media by proteomic analysis together with further cytokine assay analysis, which will allow us to apply specific molecules directly to the HDF to achieve similar behavioral changes comparing to the HDF that are co-cultured with M1 or M2 macrophages.

The first part of the *in vivo* experiment adopted the human HTS-like nude mouse model to explore the natural behaviors of mononuclear phagocytes including monocytes and polarized macrophages. We found that monocytes dramatically decreased at 1 week post-grafting, correlated with the dramatic increase of M1 macrophages in the grafted skin tissue. M1 macrophages were found predominantly at 1 to 2 weeks post-grafting; whereas, M2 macrophages were abundant at 3 to 4 weeks post-grafting coincident with the development of fibrosis in the human skin tissues after grafting. The findings of this *in vivo* experiment shows indirect evidence for the role of M2 macrophages in human dermal fibrosis and indicates an appropriate timing of macrophage depletion is at the subacute phases of wound healing.

The second part of the *in vivo* experiment, in addition to using the same animal model, depleted macrophages systemically using clodronate liposomes during 1 to 2

week period post-grafting. The mice in the depletion group showed significantly reduced the number of M1 and M2 macrophages at 2 weeks post-grafting together with reduced scar formation. It confirmed that the systemic depletion of macrophages in subacute phase of wound healing reduced scarring. One limitation of this experiment is that the depletion of macrophages is systemic, not specific to M2 macrophages alone, which means that we couldn't rule out the effect of the depletion of M1 macrophages on the diminished scar formation. However, M1 macrophages were shown to be anti-fibrotic in the *in vitro* study, the depletion of M1 macrophages might have no effect on reducing scar formation. The *in vivo* study conducted in the future should confirm the anti-fibrotic role of M1 macrophages. In addition, future experiment should focus on the specific depletion of M2 macrophages. Transgenic mouse models might be an approach to conditionally deplete M2 macrophages. For example, with the integration of M2 macrophage gene sequence such as Arg-1, a myeloid cell-specific lysozyme M promoter Cre/inducible diphtheria toxin receptor (LysMCre/iDTR) mice model (11) can become a M2 macrophage specific depletion model. Once injected with diphtheria toxin, the Arg-1 gene expressing M2 macrophages inside the LysMCre/iDTR mice will be depleted. However, the LysMCre/iDTR mice are not immunodeficient. The human skin would not survive if transplanted on these mice. What type of fibrosis model could be adopted when using this specific knockout model is the question remains to be solved. Another alternative is to use the M2 macrophage neutralizing antibody. Recent studies focused on cancer therapy has used anti-colony stimulating factor-1 receptor to deplete tumor associated macrophages, also recognized as M2 macrophages (12, 13). We can use this

neutralizing antibody to deplete M2 macrophages in our human HTS-like nude mouse model. However, a detailed literature study and preliminary experiments are required.

Up until now, my focus is all about macrophages, which I believe are the key element in the pathogenesis of HTS. However, HTS are multifactorial fibroproliferative disorders, we cannot say for sure that macrophages alone contribute to HTS formation. My future research plans should not only focus on macrophages. Below are some additional ideas that I come up with during my PhD program.

In my previous clinical practice, patients who developed HTS after severe burn injuries become predisposed to form HTS in different regions of the body. The injuries need not to be severe, which makes me wonder that there might be some changes in the immune system that occurred due to the first severe injury, which are higher than the macrophages level, for examples, monocytes, bone marrow or even the DNA level. These changes can lead to abnormal behavior of cells in the wound region and result in HTS formation. It seems like there is a threshold that exists in the body. When a patient suffers from serious injury, severe enough to pass the threshold, then the immune system becomes hypersensitive. The bone marrow then produces sensitized blood borne cells such as monocytes, fibrocytes that infiltrate to the injured site and exert their hypersensitive functions compared to their normal functions in normal wound healing. Our lab has already found increased number of fibrocytes in burn patients compared to normal patients (14). A future potential research project may involve collection of samples of the bone marrow, blood, skin from burn patients before and after injury, and regular follow up for any patient who undergo another injury, hoping to find evidence that there is a hypersensitivity mechanism for HTS formation.

Recently, growing interests have focused on the therapeutic role of stem cells in HTS formation (15, 16). Among the many subsets of mesenchymal stem cells, adipose-derived stem cells are of particular interest because this is the primary type of stem cell found in the dermal cones and hypodermis and they are relatively easy to harvest. Thus, investigation of their role in HTS would be beneficial not only for developing new treatment strategies, but also for understanding the pathophysiology of scar development. Future studies could involve harvesting adipose-derived stem cells from the human skin tissue and injection of them back to the human skin graft region and see if the stem cells decrease scarring in our animal model.

In the *in vivo* study, an infiltration pattern of mouse mast cells from mouse skin to human skin grafts was observed. Questions related to this mast cell infiltration remain unanswered. For example, what is the roles of the mast cell subtypes (tryptase or chymase positive) in this infiltration? What signaling pathway is involved? What is the significance of the mast cell infiltration in the formation of HTS? A detailed literature study and future research are needed.

The monocyte fractions in the blood were investigated in the *in vivo* study. However, further investigations are needed. For instance, the subtypes of monocytes can be divided by the staining of the marker Ly6c. Then we can try to answer the question of which monocyte subtype differentiate into M1 macrophages and which monocyte subtype differentiates into M2 macrophages by labeling the monocyte subtypes prior to the grafting.

Taken together, the experiments conducted show an anti-fibrotic role of M1 macrophages and a pro-fibrotic role of M2 macrophages. The *in vivo* experiments

provide evidence for the pro-fibrotic role of M2 macrophages in HTS formation. Future experiments are needed to confirm that specific M2 macrophage depletion contributes to the development of HTS. We believe that our findings can be translated to future therapeutic strategies to reduce or prevent the HTS formation in patients. For example, in patients who suffer from injuries that could potentially develop HTS, we can either deplete M2 macrophages using the neutralizing antibody, stop the polarization from M1 to M2 macrophages, or disable the function of M2 macrophages by blocking the SDF-1/CXCR4 signaling pathway.

5.2 References

1. Desmouliere A, Chaponnier C, Gabbiani G. Tissue repair, contraction, and the myofibroblast. *Wound Repair Regen.* 2005;13:7-12.
2. van der Veer WM, Bloemen MC, Ulrich MM, Molema G, van Zuijlen PP, Middelkoop E, et al. Potential cellular and molecular causes of hypertrophic scar formation. *Burns.* 2009;35:15-29.
3. Gruber BL, Kew RR, Jelaska A, Marchese MJ, Garlick J, Ren SL, et al. Human mast cells activate fibroblasts - Tryptase is a fibrogenic factor stimulating collagen messenger ribonucleic acid synthesis and fibroblast chemotaxis. *Journal of Immunology.* 1997;158:2310-7.
4. Wynn TA. Fibrotic disease and the T(H)1/T(H)2 paradigm. *Nat Rev Immunol.* 2004;4:583-94.
5. Niessen FB, Schalkwijk J, Vos H, Timens W. Hypertrophic scar formation is associated with an increased number of epidermal Langerhans cells. *Journal of Pathology.* 2004;202:121-9.
6. Yang L, Scott PG, Dodd C, Medina A, Jiao H, Shankowsky HA, et al. Identification of fibrocytes in postburn hypertrophic scar. *Wound Repair Regen.* 2005;13:398-404.
7. Machesney M, Tidman N, Waseem A, Kirby L, Leigh I. Activated keratinocytes in the epidermis of hypertrophic scars. *Am J Pathol.* 1998;152:1133-41.
8. Baum CL, Arpey CJ. Normal cutaneous wound healing: clinical correlation with cellular and molecular events. *Dermatol Surg.* 2005;31:674-86; discussion 86.
9. Werner S, Grose R. Regulation of wound healing by growth factors and cytokines. *Physiol Rev.* 2003;83:835-70.
10. Song E, Ouyang N, Horbelt M, Antus B, Wang M, Exton MS. Influence of alternatively and classically activated macrophages on fibrogenic activities of human fibroblasts. *Cell Immunol.* 2000;204:19-28.

11. Lucas T, Waisman A, Ranjan R, Roes J, Krieg T, Muller W, et al. Differential roles of macrophages in diverse phases of skin repair. *J Immunol.* 2010;184:3964-77.
12. Ries CH, Cannarile MA, Hoves S, Benz J, Wartha K, Runza V, et al. Targeting tumor-associated macrophages with anti-CSF-1R antibody reveals a strategy for cancer therapy. *Cancer Cell.* 2014;25:846-59.
13. Sica A, Schioppa T, Mantovani A, Allavena P. Tumour-associated macrophages are a distinct M2 polarised population promoting tumour progression: potential targets of anti-cancer therapy. *Eur J Cancer.* 2006;42:717-27.
14. Yang L, Scott PG, Giuffre J, Shankowsky HA, Ghahary A, Tredget EE. Peripheral blood fibrocytes from burn patients: identification and quantification of fibrocytes in adherent cells cultured from peripheral blood mononuclear cells. *Lab Invest.* 2002;82:1183-92.
15. Wu Y, Huang S, Enhe J, Ma K, Yang S, Sun T, et al. Bone marrow-derived mesenchymal stem cell attenuates skin fibrosis development in mice. *Int Wound J.* 2014;11:701-10.
16. Zhang Q, Liu LN, Yong Q, Deng JC, Cao WG. Intralesional injection of adipose-derived stem cells reduces hypertrophic scarring in a rabbit ear model. *Stem Cell Res Ther.* 2015;6:145.

Bibliography

Agasse F, Nicoleau C, Petit J, Jaber M, Roger M, Benzakour O, et al. Evidence for a major role of endogenous fibroblast growth factor-2 in apoptotic cortex-induced subventricular zone cell proliferation. *Eur J Neurosci.* 2007;26:3036-42.

Aggarwal H, Saxena A, Lubana PS, Mathur RK, Jain DK. Treatment of keloids and hypertrophic scars using bleom. *J Cosmet Dermatol.* 2008;7:43-9. doi: 10.1111/j.473-2165.008.00360.x.

Aggarwal S, Das SN. Garcinol inhibits tumour cell proliferation, angiogenesis, cell cycle progression and induces apoptosis via NF-kappaB inhibition in oral cancer. *Tumour Biol.* 2015.

Ahn ST, Monafo WW, Mustoe TA. Topical silicone gel: a new treatment for hypertrophic scars. *Surgery.* 1989;106:781-6; discussion 6-7.

Akasaka Y, Ono I, Yamashita T, Jimbow K, Ishii T. Basic fibroblast growth factor promotes apoptosis and suppresses granulation tissue formation in acute incisional wounds. *J Pathol.* 2004;203:710-20.

Alexandrow MG, Moses HL. Transforming growth factor beta and cell cycle regulation. *Cancer Res.* 1995;55:1452-7.

Anzarut A, Olson J, Singh P, Rowe BH, Tredget EE. The effectiveness of pressure garment therapy for the prevention of abnormal scarring after burn injury: a meta-analysis. *J Plast Reconstr Aesthet Surg.* 2009;62:77-84.

Armour A, Scott PG, Tredget EE. Cellular and molecular pathology of HTS: basis for treatment. *Wound Repair Regen.* 2007;15 Suppl 1:S6-17.

Arno AI, Gauglitz GG, Barret JP, Jeschke MG. Up-to-date approach to manage keloids and hypertrophic scars: a useful guide. *Burns.* 2014;40:1255-66.

Atiyeh BS. Nonsurgical management of hypertrophic scars: evidence-based therapies,

standard practices, and emerging methods. *Aesthetic Plast Surg.* 2007;31:468-92; discussion 93-4.

Bain CC, Mowat AM. Macrophages in intestinal homeostasis and inflammation. *Immunol Rev.* 2014;260:102-17. doi: 10.1111/imr.12192.

Balkwill F. Cancer and the chemokine network. *Nat Rev Cancer.* 2004;4:540-50.

Barker TH. The role of ECM proteins and protein fragments in guiding cell behavior in regenerative medicine. *Biomaterials.* 2011;32:4211-4.

Bauer SM, Bauer RJ, Velazquez OC. Angiogenesis, vasculogenesis, and induction of healing in chronic wounds. *Vasc Endovascular Surg.* 2005;39:293-306.

Baum CL, Arpey CJ. Normal cutaneous wound healing: clinical correlation with cellular and molecular events. *Dermatol Surg.* 2005;31:674-86; discussion 86.

Beer HD, Longaker MT, Werner S. Reduced expression of PDGF and PDGF receptors during impaired wound healing. *J Invest Dermatol.* 1997;109:132-8.

Bleul CC, Fuhlbrigge RC, Casasnovas JM, Aiuti A, Springer TA. A highly efficacious lymphocyte chemoattractant, stromal cell-derived factor 1 (SDF-1). *J Exp Med.* 1996;184:1101-9.

Bock O, Yu H, Zitron S, Bayat A, Ferguson MW, Mrowietz U. Studies of transforming growth factors beta 1-3 and their receptors I and II in fibroblast of keloids and hypertrophic scars. *Acta Derm Venereol.* 2005;85:216-20.

Bock O, Yu HY, Zitron S, Bayat A, Ferguson MWJ, Mrowietz U. Studies of transforming growth factors beta 1-3 and their receptors I and II in fibroblast of keloids and hypertrophic scars. *Acta Dermato-Venereologica.* 2005;85:216-20.

Bombaro KM, Engrav LH, Carrougher GJ, Wiechman SA, Faucher L, Costa BA, et al. What is the prevalence of hypertrophic scarring following burns? *Burns.* 2003;29:299-302.

Bombaro KM, Engrav LH, Carrougher GJ, Wiechman SA, Faucher L, Costa BA, et al. What is the prevalence of hypertrophic scarring following burns? *Burns.* 2003;29:299-302.

Bonner JC. Regulation of PDGF and its receptors in fibrotic diseases. *Cytokine Growth Factor Rev.* 2004;15:255-73.

Braga TT, Correa-Costa M, Guise YF, Castoldi A, de Oliveira CD, Hyane MI, et al. MyD88 signaling pathway is involved in renal fibrosis by favoring a TH2 immune response and activating alternative M2 macrophages. *Mol Med.* 2012;18:1231-9.

Breslin WL, Strohacker K, Carpenter KC, Haviland DL, McFarlin BK. Mouse blood monocytes: standardizing their identification and analysis using CD115. *J Immunol Methods.* 2013;390:1-8. doi: 10.1016/j.jim.2011.03.005. Epub Apr 2.

Broekelmann TJ, Limper AH, Colby TV, McDonald JA. Transforming growth factor beta 1 is present at sites of extracellular matrix gene expression in human pulmonary fibrosis. *Proc Natl Acad Sci U S A.* 1991;88:6642-6.

Brown JJ, Bayat A. Genetic susceptibility to raised dermal scarring. *Br J Dermatol.* 2009;161:8-18.

Castagnoli C, Stella M, Berthod C, Magliacani G, Richiardi PM. TNF production and hypertrophic scarring. *Cell Immunol.* 1993;147:51-63.

Castagnoli C, Stella M, Magliacani G. Role of T-lymphocytes and cytokines in post-burn hypertrophic scars. *Wound Repair Regen.* 2002;10:107-8.

Chakraborti S, Mandal M, Das S, Mandal A, Chakraborti T. Regulation of matrix metalloproteinases: an overview. *Mol Cell Biochem.* 2003;253:269-85.

Chanprapaph K, Tanrattanakorn S, Wattanakrai P, Wongkitisophon P, Vachiramom V. Effectiveness of onion extract gel on surgical scars in asians. *Dermatol Res Pract.* 2012;2012:212945.:10.1155/2012/212945. Epub 2012 Aug 8.

Chanput W, Mes J, Vreeburg RA, Savelkoul HF, Wichers HJ. Transcription profiles of LPS-stimulated THP-1 monocytes and macrophages: a tool to study inflammation modulating effects of food-derived compounds. *Food Funct.* 2010;1:254-61.

Chanput W, Mes JJ, Savelkoul HF, Wichers HJ. Characterization of polarized THP-1 macrophages and polarizing ability of LPS and food compounds. *Food Funct.* 2013;4:266-76.

Chawla A, Nguyen KD, Goh YP. Macrophage-mediated inflammation in metabolic disease. *Nat Rev Immunol*. 2011;11:738-49.

Chen GJ, Forough R. Fibroblast growth factors, fibroblast growth factor receptors, diseases, and drugs. *Recent Pat Cardiovasc Drug Discov*. 2006;1:211-24.

Chen L, Liu S, Li SR, Cong L, Wu JL, Wang ZX. [Influence of substance P on the release of histamine in the human hypertrophic scar tissue]. *Zhonghua Shao Shang Za Zhi*. 2006;22:192-4.

Chen Y, Abraham DJ, Shi-Wen X, Pearson JD, Black CM, Lyons KM, et al. CCN2 (connective tissue growth factor) promotes fibroblast adhesion to fibronectin. *Mol Biol Cell*. 2004;15:5635-46.

Choi WT, An J. Biology and clinical relevance of chemokines and chemokine receptors CXCR4 and CCR5 in human diseases. *Exp Biol Med (Maywood)*. 2011;236:637-47.

Colwell AS, Phan TT, Kong W, Longaker MT, Lorenz PH. Hypertrophic scar fibroblasts have increased connective tissue growth factor expression after transforming growth factor-beta stimulation. *Plast Reconstr Surg*. 2005;116:1387-90; discussion 91-2.

Craig MJ, Loberg RD. CCL2 (Monocyte Chemoattractant Protein-1) in cancer bone metastases. *Cancer and Metastasis Reviews*. 2006;25:611-9.

Dagvadorj J, Naiki Y, Tumurkhuu G, Noman AS, Iftekar EKI, Koide N, et al. Interleukin (IL)-10 attenuates lipopolysaccharide-induced IL-6 production via inhibition of IkappaB-zeta activity by Bcl-3. *Innate Immun*. 2009;15:217-24.

Dang CM, Beanes SR, Lee H, Zhang XL, Soo C, Ting K. Scarless fetal wounds are associated with an increased matrix metalloproteinase-to-tissue-derived inhibitor of metalloproteinase ratio. *Plastic and Reconstructive Surgery*. 2003;111:2273-85.

Darby IA, Hewitson TD. Fibroblast differentiation in wound healing and fibrosis. *International Review of Cytology - a Survey of Cell Biology*, Vol 257. 2007;257:143-+.

Darzi MA, Chowdri NA, Kaul SK, Khan M. Evaluation of Various Methods of Treating Keloids and Hypertrophic Scars - a 10-Year Follow-up-Study. *British Journal of Plastic Surgery*. 1992;45:374-9.

Das S, Mandal M, Chakraborti T, Mandal A, Chakraborti S. Structure and evolutionary aspects of matrix metalloproteinases: a brief overview. *Mol Cell Biochem.* 2003;253:31-40.

Dasu MR, Hawkins HK, Barrow RE, Xue H, Herndon DN. Gene expression profiles from hypertrophic scar fibroblasts before and after IL-6 stimulation. *J Pathol.* 2004;202:476-85.

Davis PA, Corless DJ, Aspinall R, Wastell C. Effect of CD4(+) and CD8(+) cell depletion on wound healing. *Br J Surg.* 2001;88:298-304.

Desmouliere A, Chaponnier C, Gabbiani G. Tissue repair, contraction, and the myofibroblast. *Wound Repair Regen.* 2005;13:7-12.

Desmouliere A, Geinoz A, Gabbiani F, Gabbiani G. Transforming growth factor-beta 1 induces alpha-smooth muscle actin expression in granulation tissue myofibroblasts and in quiescent and growing cultured fibroblasts. *J Cell Biol.* 1993;122:103-11.

Ding J, Hori K, Zhang R, Marcoux Y, Honardoust D, Shankowsky HA, et al. Stromal cell-derived factor 1 (SDF-1) and its receptor CXCR4 in the formation of postburn hypertrophic scar (HTS). *Wound Repair and Regeneration.* 2011;19:568-78.

Ding J, Hori K, Zhang R, Marcoux Y, Honardoust D, Shankowsky HA, et al. Stromal cell-derived factor 1 (SDF-1) and its receptor CXCR4 in the formation of postburn hypertrophic scar (HTS). *Wound Repair Regen.* 2011;19:568-78. doi: 10.1111/j.524-475X.2011.00724.x.

Ding J, Ma Z, Liu H, Kwan P, Iwashina T, Shankowsky HA, et al. The therapeutic potential of a C-X-C chemokine receptor type 4 (CXCR-4) antagonist on hypertrophic scarring in vivo. *Wound Repair Regen.* 2014;22:622-30.

Ding J, Ma Z, Shankowsky HA, Medina A, Tredget EE. Deep dermal fibroblast profibrotic characteristics are enhanced by bone marrow-derived mesenchymal stem cells. *Wound Repair Regen.* 2013;21:448-55.

Doucet C, Brouty-Boye D, Pottin-Clemenceau C, Canonica GW, Jasmin C, Azzarone B. Interleukin (IL) 4 and IL-13 act on human lung fibroblasts. Implication in asthma. *J Clin Invest.* 1998;101:2129-39.

Draelos ZD. The ability of onion extract gel to improve the cosmetic appearance of postsurgical scars. *J Cosmet Dermatol.* 2008;7:101-4.

Duffield JS, Forbes SJ, Constandinou CM, Clay S, Partolina M, Vuthoori S, et al. Selective depletion of macrophages reveals distinct, opposing roles during liver injury and repair. *J Clin Invest*. 2005;115:56-65.

Duffield JS, Forbes SJ, Constandinou CM, Clay S, Partolina M, Vuthoori S, et al. Selective depletion of macrophages reveals distinct, opposing roles during liver injury and repair. *Journal of Clinical Investigation*. 2005;115:56-65.

Dunkin CS, Pleat JM, Gillespie PH, Tyler MP, Roberts AH, McGrouther DA. Scarring occurs at a critical depth of skin injury: precise measurement in a graduated dermal scratch in human volunteers. *Plast Reconstr Surg*. 2007;119:1722-32; discussion 33-4.

Egli A, Kumar D, Broscheit C, O'Shea D, Humar A. Comparison of the Effect of Standard and Novel Immunosuppressive Drugs on CMV-Specific T-Cell Cytokine Profiling. *Transplantation*. 2013;95:448-55.

Ehrlich HP, Desmouliere A, Diegelmann RF, Cohen IK, Compton CC, Garner WL, et al. Morphological and immunochemical differences between keloid and hypertrophic scar. *Am J Pathol*. 1994;145:105-13.

Eishi K, Bae SJ, Ogawa F, Hamasaki Y, Shimizu K, Katayama I. Silicone gel sheets relieve pain and pruritus with clinical improvement of keloid: possible target of mast cells. *J Dermatolog Treat*. 2003;14:248-52.

Elias JA, Gustilo K, Baeder W, Freundlich B. Synergistic stimulation of fibroblast prostaglandin production by recombinant interleukin 1 and tumor necrosis factor. *J Immunol*. 1987;138:3812-6.

Eming SA, Krieg T, Davidson JM. Inflammation in wound repair: molecular and cellular mechanisms. *J Invest Dermatol*. 2007;127:514-25.

Eming SA, Werner S, Bugnon P, Wickenhauser C, Siewe L, Utermohlen O, et al. Accelerated wound closure in mice deficient for interleukin-10. *Am J Pathol*. 2007;170:188-202.

Engrav LH, Garner WL, Tredget EE. Hypertrophic scar, wound contraction and hyperhypopigmentation. *J Burn Care Res*. 2007;28:593-7.

Eto H, Suga H, Aoi N, Kato H, Doi K, Kuno S, et al. Therapeutic potential of fibroblast

growth factor-2 for hypertrophic scars: upregulation of MMP-1 and HGF expression. *Lab Invest.* 2012;92:214-23.

Fernandez EJ, Lolis E. Structure, function, and inhibition of chemokines. *Annu Rev Pharmacol Toxicol.* 2002;42:469-99.

Ferrante CJ, Leibovich SJ. Regulation of Macrophage Polarization and Wound Healing. *Adv Wound Care (New Rochelle).* 2012;1:10-6.

Ferrara N, Heinsohn H, Walder CE, Bunting S, Thomas GR. The regulation of blood vessel growth by vascular endothelial growth factor. *Ann N Y Acad Sci.* 1995;752:246-56.

Ferreira AM, Takagawa S, Fresco R, Zhu X, Varga J, DiPietro LA. Diminished induction of skin fibrosis in mice with MCP-1 deficiency. *J Invest Dermatol.* 2006;126:1900-8.

Ferret PJ, Soum E, Negre O, Wollman EE, Fradelizi D. Protective effect of thioredoxin upon NO-mediated cell injury in THP1 monocytic human cells. *Biochemical Journal.* 2000;346:759-65.

Foley TT, Ehrlich HP. Through gap junction communications, co-cultured mast cells and fibroblasts generate fibroblast activities allied with hypertrophic scarring. *Plast Reconstr Surg.* 2013;131:1036-44. doi: 10.97/PRS.0b013e3182865c3f.

Fortunato SJ, Menon R, Swan KF, Lombardi SJ. Interleukin-10 inhibition of interleukin-6 in human amniochorionic membrane: transcriptional regulation. *Am J Obstet Gynecol.* 1996;175:1057-65.

Frazier K, Williams S, Kothapalli D, Klapper H, Grotendorst GR. Stimulation of fibroblast cell growth, matrix production, and granulation tissue formation by connective tissue growth factor. *J Invest Dermatol.* 1996;107:404-11.

Frieler RA, Nadimpalli S, Boland LK, Xie A, Kooistra LJ, Song J, et al. Depletion of macrophages in CD11b diphtheria toxin receptor mice induces brain inflammation and enhances inflammatory signaling during traumatic brain injury. *Brain Res.* 2015;1624:103-12.

Fritz JM, Tennis MA, Orlicky DJ, Lin H, Ju C, Redente EF, et al. Depletion of tumor-associated macrophages slows the growth of chemically induced mouse lung adenocarcinomas. *Front Immunol.* 2014;5:587.

Fujisaka S, Usui I, Bukhari A, Ikutani M, Oya T, Kanatani Y, et al. Regulatory mechanisms for adipose tissue M1 and M2 macrophages in diet-induced obese mice. *Diabetes*. 2009;58:2574-82.

Funayama E, Chodon T, Oyama A, Sugihara T. Keratinocytes promote proliferation and inhibit apoptosis of the underlying fibroblasts: an important role in the pathogenesis of keloid. *J Invest Dermatol*. 2003;121:1326-31.

Gallant CL, Olson ME, Hart DA. Molecular, histologic, and gross phenotype of skin wound healing in red Duroc pigs reveals an abnormal healing phenotype of hypercontracted, hyperpigmented scarring. *Wound Repair Regen*. 2004;12:305-19.

Garner WL. Epidermal regulation of dermal fibroblast activity. *Plast Reconstr Surg*. 1998;102:135-9.

Gassner HG, Brissett AE, Otley CC, Boahene DK, Boggust AJ, Weaver AL, et al. Botulinum toxin to improve facial wound healing: A prospective, blinded, placebo-controlled study. *Mayo Clin Proc*. 2006;81:1023-8.

Gauglitz GG, Korting HC, Pavicic T, Ruzicka T, Jeschke MG. Hypertrophic scarring and keloids: pathomechanisms and current and emerging treatment strategies. *Mol Med*. 2011;17:113-25.

Ghahary A, Marcoux Y, Karimi-Busheri F, Li YY, Tredget EE, Kilani RT, et al. Differentiated keratinocyte-releasable stratifin (14-3-3 sigma) stimulates MMP-1 expression in dermal fibroblasts. *Journal of Investigative Dermatology*. 2005;124:170-7.

Ghahary A, Shen YJ, Nedelec B, Scott PG, Tredget EE. Interferons gamma and alpha-2b differentially regulate the expression of collagenase and tissue inhibitor of metalloproteinase-1 messenger RNA in human hypertrophic and normal dermal fibroblasts. *Wound Repair Regen*. 1995;3:176-84.

Ghahary A, Shen YJ, Nedelec B, Wang R, Scott PG, Tredget EE. Collagenase production is lower in post-burn hypertrophic scar fibroblasts than in normal fibroblasts and is reduced by insulin-like growth factor-1. *J Invest Dermatol*. 1996;106:476-81.

Ghahary A, Shen YJ, Nedelec B, Wang R, Scott PG, Tredget EE. Collagenase production is lower in post-burn hypertrophic scar fibroblasts than in normal fibroblasts and is reduced by insulin-like growth factor-1. *J Invest Dermatol*. 1996;106:476-81.

Ghahary A, Shen YJ, Scott PG, Tredget EE. Immunolocalization of TGF-beta 1 in human hypertrophic scar and normal dermal tissues. *Cytokine*. 1995;7:184-90.

Gharaee-Kermani M, Denholm EM, Phan SH. Costimulation of fibroblast collagen and transforming growth factor beta 1 gene expression by monocyte chemoattractant protein-1 via specific receptors. *J Biol Chem*. 1996;271:17779-84.

Gharib SA, Johnston LK, Huizar I, Birkland TP, Hanson J, Wang Y, et al. MMP28 promotes macrophage polarization toward M2 cells and augments pulmonary fibrosis. *J Leukoc Biol*. 2014;95:9-18.

Gibbons MA, MacKinnon AC, Ramachandran P, Dhaliwal K, Duffin R, Phytian-Adams AT, et al. Ly6Chi monocytes direct alternatively activated profibrotic macrophage regulation of lung fibrosis. *Am J Respir Crit Care Med*. 2011;184:569-81.

Ginhoux F, Jung S. Monocytes and macrophages: developmental pathways and tissue homeostasis. *Nat Rev Immunol*. 2014;14:392-404.

Gold MH, Berman B, Clementoni MT, Gauglitz GG, Nahai F, Murcia C. Updated international clinical recommendations on scar management: part 1--evaluating the evidence. *Dermatol Surg*. 2014;40:817-24.

Gold MH, Foster TD, Adair MA, Burlison K, Lewis T. Prevention of hypertrophic scars and keloids by the prophylactic use of topical silicone gel sheets following a surgical procedure in an office setting. *Dermatologic Surgery*. 2001;27:641-4.

Gold MH, McGuire M, Mustoe TA, Pusic A, Sachdev M, Waibel J, et al. Updated international clinical recommendations on scar management: part 2--algorithms for scar prevention and treatment. *Dermatol Surg*. 2014;40:825-31.

Goldberg MT, Han YP, Yan C, Shaw MC, Garner WL. TNF-alpha suppresses alpha-smooth muscle actin expression in human dermal fibroblasts: an implication for abnormal wound healing. *J Invest Dermatol*. 2007;127:2645-55.

Gordon A, Kozin ED, Keswani SG, Vaikunth SS, Katz AB, Zoltick PW, et al. Permissive environment in postnatal wounds induced by adenoviral-mediated overexpression of the anti-inflammatory cytokine interleukin-10 prevents scar formation. *Wound Repair Regen*. 2008;16:70-9.

Gordon S. The macrophage: past, present and future. *Eur J Immunol.* 2007;37 Suppl 1:S9-17.

Gordon S, Hamann J, Lin HH, Stacey M. F4/80 and the related adhesion-GPCRs. *Eur J Immunol.* 2011;41:2472-6.

Gordon S, Martinez FO. Alternative activation of macrophages: mechanism and functions. *Immunity.* 2010;32:593-604.

Gordon S, Taylor PR. Monocyte and macrophage heterogeneity. *Nat Rev Immunol.* 2005;5:953-64.

Greenhalgh DG. The role of apoptosis in wound healing. *Int J Biochem Cell Biol.* 1998;30:1019-30.

Grinberg S, Hasko G, Wu D, Leibovich SJ. Suppression of PLCbeta2 by endotoxin plays a role in the adenosine A(2A) receptor-mediated switch of macrophages from an inflammatory to an angiogenic phenotype. *Am J Pathol.* 2009;175:2439-53.

Gruber BL, Kew RR, Jelaska A, Marchese MJ, Garlick J, Ren S, et al. Human mast cells activate fibroblasts: tryptase is a fibrogenic factor stimulating collagen messenger ribonucleic acid synthesis and fibroblast chemotaxis. *J Immunol.* 1997;158:2310-7.

Gruber BL, Kew RR, Jelaska A, Marchese MJ, Garlick J, Ren SL, et al. Human mast cells activate fibroblasts - Tryptase is a fibrogenic factor stimulating collagen messenger ribonucleic acid synthesis and fibroblast chemotaxis. *Journal of Immunology.* 1997;158:2310-7.

Halim AS, Emami A, Salahshourifar I, Kannan TP. Keloid scarring: understanding the genetic basis, advances, and prospects. *Arch Plast Surg.* 2012;39:184-9. doi: 10.5999/aps.2012.39.3.184. Epub May 10.

Hameedaldeen A, Liu J, Batres A, Graves GS, Graves DT. FOXO1, TGF-beta regulation and wound healing. *Int J Mol Sci.* 2014;15:16257-69.

Hammond MD, Taylor RA, Mullen MT, Ai YX, Aguila HL, Mack M, et al. CCR2(+)Ly6C(hi) Inflammatory Monocyte Recruitment Exacerbates Acute Disability Following Intracerebral Hemorrhage. *Journal of Neuroscience.* 2014;34:3901-9.

Hasegawa M, Sato S. The roles of chemokines in leukocyte recruitment and fibrosis in systemic sclerosis. *Frontiers in Bioscience*. 2008;13:3637-47.

Heckmann M, Adelman-Grill BC, Hein R, Krieg T. Biphasic effects of interleukin-1 alpha on dermal fibroblasts: enhancement of chemotactic responsiveness at low concentrations and of mRNA expression for collagenase at high concentrations. *J Invest Dermatol*. 1993;100:780-4.

Heldin CH, Eriksson U, Ostman A. New members of the platelet-derived growth factor family of mitogens. *Arch Biochem Biophys*. 2002;398:284-90.

Henderson J, Ferguson MW, Terenghi G. The reinnervation and revascularization of wounds is temporarily altered after treatment with interleukin 10. *Wound Repair Regen*. 2011;19:268-73. doi: 10.1111/j.524-475X.2011.00667.x.

Higashi K, Inagaki Y, Fujimori K, Nakao A, Kaneko H, Nakatsuka I. Interferon-gamma interferes with transforming growth factor-beta signaling through direct interaction of YB-1 with Smad3. *Journal of Biological Chemistry*. 2003;278:43470-9.

Holavanahalli RK, Helm PA, Kowalske KJ. Long-Term Outcomes in Patients Surviving Large Burns: The Musculoskeletal System. *J Burn Care Res*. 2015.

Honardoust D, Ding J, Varkey M, Shankowsky HA, Tredget EE. Deep dermal fibroblasts refractory to migration and decorin-induced apoptosis contribute to hypertrophic scarring. *J Burn Care Res*. 2012;33:668-77.

Honardoust D, Varkey M, Hori K, Ding J, Shankowsky HA, Tredget EE. Small leucine-rich proteoglycans, decorin and fibromodulin, are reduced in postburn hypertrophic scar. *Wound Repair Regen*. 2011;19:368-78.

Honardoust D, Varkey M, Marcoux Y, Shankowsky HA, Tredget EE. Reduced decorin, fibromodulin, and transforming growth factor-beta3 in deep dermis leads to hypertrophic scarring. *J Burn Care Res*. 2012;33:218-27.

Huang C, Murphy GF, Akaishi S, Ogawa R. Keloids and hypertrophic scars: update and future directions. *Plast Reconstr Surg Glob Open*. 2013;1:e25. doi: 10.1097/GOX.0b013e31829c4597. eCollection 2013 Jul.

Hume DA. The mononuclear phagocyte system. *Curr Opin Immunol*. 2006;18:49-53.

Ibrahim MM, Bond J, Bergeron A, Miller KJ, Ehanire T, Quiles C, et al. A novel immune competent murine hypertrophic scar contracture model: a tool to elucidate disease mechanism and develop new therapies. *Wound Repair Regen.* 2014;22:755-64.

Igarashi A, Nashiro K, Kikuchi K, Sato S, Ihn H, Fujimoto M, et al. Connective tissue growth factor gene expression in tissue sections from localized scleroderma, keloid, and other fibrotic skin disorders. *J Invest Dermatol.* 1996;106:729-33.

Italiani P, Boraschi D. From Monocytes to M1/M2 Macrophages: Phenotypical vs. Functional Differentiation. *Front Immunol.* 2014;5:514.

Ivkovic S, Yoon BS, Popoff SN, Safadi FF, Libuda DE, Stephenson RC, et al. Connective tissue growth factor coordinates chondrogenesis and angiogenesis during skeletal development. *Development.* 2003;130:2779-91.

Jablonski KA, Amici SA, Webb LM, Ruiz-Rosado Jde D, Popovich PG, Partida-Sanchez S, et al. Novel Markers to Delineate Murine M1 and M2 Macrophages. *PLoS One.* 2015;10:e0145342.

Jaguin M, Houlbert N, Fardel O, Lecureur V. Polarization profiles of human M-CSF-generated macrophages and comparison of M1-markers in classically activated macrophages from GM-CSF and M-CSF origin. *Cell Immunol.* 2013;281:51-61.

Jinnin M, Ihn H, Mimura Y, Asano Y, Yamane K, Tamaki K. Effects of hepatocyte growth factor on the expression of type I collagen and matrix metalloproteinase-1 in normal and scleroderma dermal fibroblasts. *J Invest Dermatol.* 2005;124:324-30.

Johnson DE, Williams LT. Structural and functional diversity in the FGF receptor multigene family. *Adv Cancer Res.* 1993;60:1-41.

Junker JP, Kratz C, Tollback A, Kratz G. Mechanical tension stimulates the transdifferentiation of fibroblasts into myofibroblasts in human burn scars. *Burns.* 2008;34:942-6.

Kawane K, Ohtani M, Miwa K, Kizawa T, Kanbara Y, Yoshioka Y, et al. Chronic polyarthritis caused by mammalian DNA that escapes from degradation in macrophages. *Nature.* 2006;443:998-1002.

Kibe Y, Takenaka H, Kishimoto S. Spatial and temporal expression of basic fibroblast

growth factor protein during wound healing of rat skin. *Br J Dermatol.* 2000;143:720-7.

Kilani RT, Delehanty M, Shankowsky HA, Ghahary A, Scott P, Tredget EE. Fluorescent-activated cell-sorting analysis of intracellular interferon-gamma and interleukin-4 in fresh and frozen human peripheral blood T-helper cells. *Wound Repair Regen.* 2005;13:441-9.

Kim JH, Lee D, Jung MH, Cho H, Jeon D, Chang S, et al. Macrophage Depletion Ameliorates Glycerol-Induced Acute Kidney Injury in Mice. *Nephron Exp Nephrol.* 2014;128:21-9.

Klass BR, Grobbelaar AO, Rolfe KJ. Transforming growth factor beta1 signalling, wound healing and repair: a multifunctional cytokine with clinical implications for wound repair, a delicate balance. *Postgrad Med J.* 2009;85:9-14.

Klingbeil CK, Cesar LB, Fiddes JC. Basic fibroblast growth factor accelerates tissue repair in models of impaired wound healing. *Prog Clin Biol Res.* 1991;365:443-58.

Kofford MW, Schwartz LB, Schechter NM, Yager DR, Diegelmann RF, Graham MF. Cleavage of type I procollagen by human mast cell chymase initiates collagen fibril formation and generates a unique carboxyl-terminal propeptide. *J Biol Chem.* 1997;272:7127-31.

Kolb M, Margetts PJ, Galt T, Sime PJ, Xing Z, Schmidt M, et al. Transient transgene expression of decorin in the lung reduces the fibrotic response to bleomycin. *Am J Respir Crit Care Med.* 2001;163:770-7.

Konig S, Nitzki F, Uhmann A, Dittmann K, Theiss-Suennemann J, Herrmann M, et al. Depletion of cutaneous macrophages and dendritic cells promotes growth of basal cell carcinoma in mice. *PLoS One.* 2014;9:e93555.

Kopp J, Preis E, Said H, Hafemann B, Wickert L, Gressner AM, et al. Abrogation of transforming growth factor-beta signaling by SMAD7 inhibits collagen gel contraction of human dermal fibroblasts. *J Biol Chem.* 2005;280:21570-6.

Kotch FW, Guzei IA, Raines RT. Stabilization of the collagen triple helix by O-methylation of hydroxyproline residues. *J Am Chem Soc.* 2008;130:2952-3.

Kupietzky A, Levi-Schaffer F. The role of mast cell-derived histamine in the closure of an in vitro wound. *Inflamm Res.* 1996;45:176-80.

Kushiya T, Oda T, Yamada M, Higashi K, Yamamoto K, Oshima N, et al. Effects of liposome-encapsulated clodronate on chlorhexidine gluconate-induced peritoneal fibrosis in rats. *Nephrol Dial Transplant*. 2011;26:3143-54.

Kwan P, Hori K, Ding J, Tredget EE. Scar and contracture: biological principles. *Hand Clin*. 2009;25:511-28.

Ladak A, Tredget EE. Pathophysiology and management of the burn scar. *Clin Plast Surg*. 2009;36:661-74.

Lam E, Kilani RT, Li YY, Tredget EE, Ghahary A. Stratifin-induced matrix metalloproteinase-1 in fibroblast is mediated by c-fos and p38 mitogen-activated protein kinase activation. *Journal of Investigative Dermatology*. 2005;125:230-8.

Lam E, Tredget EE, Marcoux Y, Li YY, Ghahary A. Insulin suppresses collagenase stimulatory effect of stratifin in dermal fibroblasts. *Molecular and Cellular Biochemistry*. 2004;266:167-74.

Lau K, Paus R, Tiede S, Day P, Bayat A. Exploring the role of stem cells in cutaneous wound healing. *Exp Dermatol*. 2009;18:921-33.

Ledon JA, Savas J, Franca K, Chacon A, Nouri K. Intralesional treatment for keloids and hypertrophic scars: a review. *Dermatol Surg*. 2013;39:1745-57.

Lee KK, Mehrany K, Swanson NA. Surgical revision. *Dermatologic Clinics*. 2005;23:141-+.

Lee KK, Mehrany K, Swanson NA. Surgical revision. *Dermatol Clin*. 2005;23:141-50, vii.

Lee YR, Kweon SH, Kwon KB, Park JW, Yoon TR, Park BH. Inhibition of IL-1beta-mediated inflammatory responses by the IkappaB alpha super-repressor in human fibroblast-like synoviocytes. *Biochem Biophys Res Commun*. 2009;378:90-4.

Li H, Nagai T, Hasui K, Matsuyama T. Depletion of folate receptor beta-expressing macrophages alleviates bleomycin-induced experimental skin fibrosis. *Mod Rheumatol*. 2014;24:816-22.

Liao WT, Yu HS, Arbiser JL, Hong CH, Govindarajan B, Chai CY, et al. Enhanced MCP-

1 release by keloid CD14+ cells augments fibroblast proliferation: role of MCP-1 and Akt pathway in keloids. *Exp Dermatol.* 2010;19:e142-50.

Lichtinghagen R, Michels D, Haberkorn CI, Arndt B, Bahr M, Flemming P, et al. Matrix metalloproteinase (MMP)-2, MMP-7, and tissue inhibitor of metalloproteinase-1 are closely related to the fibroproliferative process in the liver during chronic hepatitis C. *J Hepatol.* 2001;34:239-47.

Liechty KW, Adzick NS, Crombleholme TM. Diminished interleukin 6 (IL-6) production during scarless human fetal wound repair. *Cytokine.* 2000;12:671-6.

Liechty KW, Kim HB, Adzick NS, Crombleholme TM. Fetal wound repair results in scar formation in interleukin-10-deficient mice in a syngeneic murine model of scarless fetal wound repair. *J Pediatr Surg.* 2000;35:866-72; discussion 72-3.

Lin CH, Shih CH, Tseng CC, Yu CC, Tsai YJ, Bien MY, et al. CXCL12 induces connective tissue growth factor expression in human lung fibroblasts through the Rac1/ERK, JNK, and AP-1 pathways. *PLoS One.* 2014;9:e104746. doi: 10.1371/journal.pone.0104746. eCollection 2014.

Liu W, Chua C, Wu YL, Wang DR, Ying DM, Cui L, et al. Inhibiting scar formation in rat wounds by adenovirus-mediated overexpression of truncated TGF-beta receptor II. *Plastic and Reconstructive Surgery.* 2005;115:860-70.

London A, Itskovich E, Benhar I, Kalchenko V, Mack M, Jung S, et al. Neuroprotection and progenitor cell renewal in the injured adult murine retina requires healing monocyte-derived macrophages. *J Exp Med.* 2011;208:23-39.

Lu L, Saulis AS, Liu WR, Roy NK, Chao JD, Ledbetter S, et al. The temporal effects of anti-TGF-beta1, 2, and 3 monoclonal antibody on wound healing and hypertrophic scar formation. *J Am Coll Surg.* 2005;201:391-7.

Lucas T, Waisman A, Ranjan R, Roes J, Krieg T, Muller W, et al. Differential Roles of Macrophages in Diverse Phases of Skin Repair. *Journal of Immunology.* 2010;184:3964-77.

Lucas T, Waisman A, Ranjan R, Roes J, Krieg T, Muller W, et al. Differential roles of macrophages in diverse phases of skin repair. *J Immunol.* 2010;184:3964-77.

Machesney M, Tidman N, Waseem A, Kirby L, Leigh I. Activated keratinocytes in the epidermis of hypertrophic scars. *Am J Pathol.* 1998;152:1133-41.

Machida Y, Kitamoto K, Izumi Y, Shiota M, Uchida J, Kira Y, et al. Renal fibrosis in murine obstructive nephropathy is attenuated by depletion of monocyte lineage, not dendritic cells. *J Pharmacol Sci.* 2010;114:464-73.

Macintyre L, Baird M. Pressure garments for use in the treatment of hypertrophic scars - a review of the problems associated with their use. *Burns.* 2006;32:10-5.

Mahdavian Delavary B, van der Veer WM, van Egmond M, Niessen FB, Beelen RH. Macrophages in skin injury and repair. *Immunobiology.* 2011;216:753-62.

Mantovani A, Sica A, Sozzani S, Allavena P, Vecchi A, Locati M. The chemokine system in diverse forms of macrophage activation and polarization. *Trends Immunol.* 2004;25:677-86.

Manuel JA, Gawronska-Kozak B. Matrix metalloproteinase 9 (MMP-9) is upregulated during scarless wound healing in athymic nude mice. *Matrix Biology.* 2006;25:505-14.

Manuskiatti W, Fitzpatrick RE. Treatment response of keloidal and hypertrophic sternotomy scars: comparison among intralesional corticosteroid, 5-fluorouracil, and 585-nm flashlamp-pumped pulsed-dye laser treatments. *Arch Dermatol.* 2002;138:1149-55.

Martinez FO, Gordon S. The M1 and M2 paradigm of macrophage activation: time for reassessment. *F1000Prime Rep.* 2014;6:13.

Martinez FO, Gordon S, Locati M, Mantovani A. Transcriptional profiling of the human monocyte-to-macrophage differentiation and polarization: New molecules and patterns of gene expression. *Journal of Immunology.* 2006;177:7303-11.

Martinez FO, Helming L, Gordon S. Alternative activation of macrophages: an immunologic functional perspective. *Annu Rev Immunol.* 2009;27:451-83. doi:10.1146/annurev.immunol.021908.132532.

Martinez FO, Helming L, Gordon S. Alternative Activation of Macrophages: An Immunologic Functional Perspective. *Annual Review of Immunology.* 2009;27:451-83.

Martinez FO, Sica A, Mantovani A, Locati M. Macrophage activation and polarization. *Front Biosci.* 2008;13:453-61.

McDougall S, Dallon J, Sherratt J, Maini P. Fibroblast migration and collagen deposition during dermal wound healing: mathematical modelling and clinical implications. *Philos Trans A Math Phys Eng Sci.* 2006;364:1385-405.

McFarland-Mancini MM, Funk HM, Paluch AM, Zhou M, Giridhar PV, Mercer CA, et al. Differences in wound healing in mice with deficiency of IL-6 versus IL-6 receptor. *J Immunol.* 2010;184:7219-28.

McGee GS, Broadley KN, Buckley A, Aquino A, Woodward SC, Demetriou AA, et al. Recombinant transforming growth factor beta accelerates incisional wound healing. *Curr Surg.* 1989;46:103-6.

Mebius RE, Kraal G. Structure and function of the spleen. *Nat Rev Immunol.* 2005;5:606-16.

Midwood KS, Williams LV, Schwarzbauer JE. Tissue repair and the dynamics of the extracellular matrix. *Int J Biochem Cell Biol.* 2004;36:1031-7.

Miller MC, Nanchahal J. Advances in the modulation of cutaneous wound healing and scarring. *BioDrugs.* 2005;19:363-81.

Mills CD. Anatomy of a discovery: m1 and m2 macrophages. *Front Immunol.* 2015;6:212.

Mills CD, Kincaid K, Alt JM, Heilman MJ, Hill AM. M-1/M-2 macrophages and the Th1/Th2 paradigm. *J Immunol.* 2000;164:6166-73.

Mirshahi F, Pourtau J, Li H, Muraine M, Trochon V, Legrand E, et al. SDF-1 activity on microvascular endothelial cells: consequences on angiogenesis in in vitro and in vivo models. *Thromb Res.* 2000;99:587-94.

Misharin AV, Cuda CM, Saber R, Turner JD, Gierut AK, Haines GK, 3rd, et al. Nonclassical Ly6C(-) monocytes drive the development of inflammatory arthritis in mice. *Cell Rep.* 2014;9:591-604. doi: 10.1016/j.celrep.2014.09.032. Epub Oct 16.

Momeni M, Hafezi F, Rahbar H, Karimi H. Effects of silicone gel on burn scars. *Burns.*

2009;35:70-4.

Momtazi M, Kwan P, Ding J, Anderson CC, Honardoust D, Goekjian S, et al. A nude mouse model of hypertrophic scar shows morphologic and histologic characteristics of human hypertrophic scar. *Wound Repair Regen.* 2013;21:77-87. doi: 10.1111/j.524-475X.2012.00856.x. Epub 2012 Nov 5.

Monstrey S, Hoeksema H, Verbelen J, Pirayesh A, Blondeel P. Assessment of burn depth and burn wound healing potential. *Burns.* 2008;34:761-9.

Monteleone G, Pallone F, MacDonald TT. Smad7 in TGF-beta-mediated negative regulation of gut inflammation. *Trends Immunol.* 2004;25:513-7.

Moore KW, de Waal Malefyt R, Coffman RL, O'Garra A. Interleukin-10 and the interleukin-10 receptor. *Annu Rev Immunol.* 2001;19:683-765.

Mori R, Shaw TJ, Martin P. Molecular mechanisms linking wound inflammation and fibrosis: knockdown of osteopontin leads to rapid repair and reduced scarring. *J Exp Med.* 2008;205:43-51.

Mori T, Kawara S, Shinozaki M, Hayashi N, Kakinuma T, Igarashi A, et al. Role and interaction of connective tissue growth factor with transforming growth factor-beta in persistent fibrosis: A mouse fibrosis model. *J Cell Physiol.* 1999;181:153-9.

Mosmann TR, Coffman RL. TH1 and TH2 cells: different patterns of lymphokine secretion lead to different functional properties. *Annu Rev Immunol.* 1989;7:145-73.

Mosser DM, Edwards JP. Exploring the full spectrum of macrophage activation. *Nat Rev Immunol.* 2008;8:958-69.

Moulin V, Larochelle S, Langlois C, Thibault I, Lopez-Valle CA, Roy M. Normal skin wound and hypertrophic scar myofibroblasts have differential responses to apoptotic inductors. *J Cell Physiol.* 2004;198:350-8.

Moustakas A, Heldin CH. Non-Smad TGF-beta signals. *J Cell Sci.* 2005;118:3573-84.

Moyer KE, Siggers GC, Ehrlich HP. Mast cells promote fibroblast populated collagen lattice contraction through gap junction intercellular communication. *Wound Repair Regen.*

2004;12:269-75.

Murray JC. Keloids and hypertrophic scars. *Clin Dermatol*. 1994;12:27-37.

Murray PJ, Wynn TA. Protective and pathogenic functions of macrophage subsets. *Nat Rev Immunol*. 2011;11:723-37.

Mustoe TA, Cooter RD, Gold MH, Hobbs FD, Ramelet AA, Shakespeare PG, et al. International clinical recommendations on scar management. *Plast Reconstr Surg*. 2002;110:560-71.

Nagamoto T, Eguchi G, Beebe DC. Alpha-smooth muscle actin expression in cultured lens epithelial cells. *Invest Ophthalmol Vis Sci*. 2000;41:1122-9.

Nagaoka T, Kaburagi Y, Hamaguchi Y, Hasegawa M, Takehara K, Steeber DA, et al. Delayed wound healing in the absence of intercellular adhesion molecule-1 or L-selectin expression. *Am J Pathol*. 2000;157:237-47.

Nagasawa T. Role of chemokine SDF-1/PBSF and its receptor CXCR4 in blood vessel development. *Ann N Y Acad Sci*. 2001;947:112-5; discussion 5-6.

Nakamura T, Shinriki S, Jono H, Guo J, Ueda M, Hayashi M, et al. Intrinsic TGF-beta2-triggered SDF-1-CXCR4 signaling axis is crucial for drug resistance and a slow-cycling state in bone marrow-disseminated tumor cells. *Oncotarget*. 2014;25:25.

Nedelec B, Ghahary A, Scott PG, Tredget EE. Control of wound contraction. Basic and clinical features. *Hand Clin*. 2000;16:289-302.

Nedelec B, Shankowsky H, Scott PG, Ghahary A, Tredget EE. Myofibroblasts and apoptosis in human hypertrophic scars: the effect of interferon-alpha2b. *Surgery*. 2001;130:798-808.

Nedelec B, Shen YJ, Ghahary A, Scott PG, Tredget EE. The effect of interferon alpha 2b on the expression of cytoskeletal proteins in an in vitro model of wound contraction. *J Lab Clin Med*. 1995;126:474-84.

Niessen FB, Andriessen MP, Schalkwijk J, Visser L, Timens W. Keratinocyte-derived growth factors play a role in the formation of hypertrophic scars. *J Pathol*. 2001;194:207-

16.

Niessen FB, Schalkwijk J, Vos H, Timens W. Hypertrophic scar formation is associated with an increased number of epidermal Langerhans cells. *Journal of Pathology*. 2004;202:121-9.

Nishida M, Hamaoka K. Macrophage phenotype and renal fibrosis in obstructive nephropathy. *Nephron Exp Nephrol*. 2008;110:e31-6.

Nishida M, Hamaoka K. Macrophage phenotype and renal fibrosis in obstructive nephropathy. *Nephron Experimental Nephrology*. 2008;110:E31-E6.

Nissen NN, Polverini PJ, Gamelli RL, DiPietro LA. Basic fibroblast growth factor mediates angiogenic activity in early surgical wounds. *Surgery*. 1996;119:457-65.

O'Donoghue RJ, Knight DA, Richards CD, Prele CM, Lau HL, Jarnicki AG, et al. Genetic partitioning of interleukin-6 signalling in mice dissociates Stat3 from Smad3-mediated lung fibrosis. *EMBO Mol Med*. 2012;4:939-51.

O'Reilly S, Ciechomska M, Cant R, Hugle T, van Laar JM. Interleukin-6, its role in fibrosing conditions. *Cytokine Growth Factor Rev*. 2012;23:99-107.

O'Sullivan ST, Lederer JA, Horgan AF, Chin DH, Mannick JA, Rodrick ML. Major injury leads to predominance of the T helper-2 lymphocyte phenotype and diminished interleukin-12 production associated with decreased resistance to infection. *Ann Surg*. 1995;222:482-90; discussion 90-2.

Ono I, Akasaka Y, Kikuchi R, Sakemoto A, Kamiya T, Yamashita T, et al. Basic fibroblast growth factor reduces scar formation in acute incisional wounds. *Wound Repair Regen*. 2007;15:617-23.

Ornitz DM, Itoh N. Fibroblast growth factors. *Genome Biol*. 2001;2:REVIEWS3005.

Pan B, Liu G, Jiang Z, Zheng D. Regulation of renal fibrosis by macrophage polarization. *Cell Physiol Biochem*. 2015;35:1062-9.

Pannu J, Nakerakanti S, Smith E, ten Dijke P, Trojanowska M. Transforming growth factor-beta receptor type I-dependent fibrogenic gene program is mediated via activation of

Smad1 and ERK1/2 pathways. *Journal of Biological Chemistry*. 2007;282:10405-13.

Park EK, Jung HS, Yang HI, Yoo MC, Kim C, Kim KS. Optimized THP-1 differentiation is required for the detection of responses to weak stimuli. *Inflammation Research*. 2007;56:45-50.

Peranteau WH, Zhang L, Muvarak N, Badillo AT, Radu A, Zoltick PW, et al. IL-10 overexpression decreases inflammatory mediators and promotes regenerative healing in an adult model of scar formation. *J Invest Dermatol*. 2008;128:1852-60.

Pierce GF, Tarpley JE, Tseng J, Bready J, Chang D, Kenney WC, et al. Detection of platelet-derived growth factor (PDGF)-AA in actively healing human wounds treated with recombinant PDGF-BB and absence of PDGF in chronic nonhealing wounds. *J Clin Invest*. 1995;96:1336-50.

Ploeger DTA, Hoesper NA, Schipper M, Koerts JA, de Rond S, Bank RA. Cell plasticity in wound healing: paracrine factors of M1/M2 polarized macrophages influence the phenotypical state of dermal fibroblasts. *Cell Communication and Signaling*. 2013;11.

Prasse A, Pechkovsky DV, Toews GB, Jungraithmayr W, Kollert F, Goldmann T, et al. A vicious circle of alveolar macrophages and fibroblasts perpetuates pulmonary fibrosis via CCL18. *American Journal of Respiratory and Critical Care Medicine*. 2006;173:781-92.

Profyris C, Tziotzios C, Do Vale I. Cutaneous scarring: Pathophysiology, molecular mechanisms, and scar reduction therapeutics Part I. The molecular basis of scar formation. *J Am Acad Dermatol*. 2012;66:1-10; quiz 1-2.

Reinke JM, Sorg H. Wound repair and regeneration. *Eur Surg Res*. 2012;49:35-43.

Reynolds JJ. Collagenases and tissue inhibitors of metalloproteinases: a functional balance in tissue degradation. *Oral Dis*. 1996;2:70-6.

Ries CH, Cannarile MA, Hoves S, Benz J, Wartha K, Runza V, et al. Targeting tumor-associated macrophages with anti-CSF-1R antibody reveals a strategy for cancer therapy. *Cancer Cell*. 2014;25:846-59.

Robert R, Meyer W, Bishop S, Rosenberg L, Murphy L, Blakeney P. Disfiguring burn scars and adolescent self-esteem. *Burns*. 1999;25:581-5.

Roberts AB, Sporn MB, Assoian RK, Smith JM, Roche NS, Wakefield LM, et al. Transforming growth factor type beta: rapid induction of fibrosis and angiogenesis in vivo and stimulation of collagen formation in vitro. *Proc Natl Acad Sci U S A*. 1986;83:4167-71.

Robson MC, Steed DL, Franz MG. Wound healing: biologic features and approaches to maximize healing trajectories. *Curr Probl Surg*. 2001;38:72-140.

Rockey DC, Bell PD, Hill JA. Fibrosis--a common pathway to organ injury and failure. *N Engl J Med*. 2015;372:1138-49.

Saito S, Trovato MJ, You R, Lal BK, Fasehun F, Padberg FT, Jr., et al. Role of matrix metalloproteinases 1, 2, and 9 and tissue inhibitor of matrix metalloproteinase-1 in chronic venous insufficiency. *J Vasc Surg*. 2001;34:930-8.

Salgado RM, Alcantara L, Mendoza-Rodriguez CA, Cerbon M, Hidalgo-Gonzalez C, Mercadillo P, et al. Post-burn hypertrophic scars are characterized by high levels of IL-1beta mRNA and protein and TNF-alpha type I receptors. *Burns*. 2012;38:668-76.

Sarkhosh K, Tredget EE, Karami A, Uludag H, Iwashina T, Kilani RT, et al. Immune cell proliferation is suppressed by the interferon-gamma-induced indoleamine 2,3-dioxygenase expression of fibroblasts populated in collagen gel (FPCG). *Journal of Cellular Biochemistry*. 2003;90:206-17.

Sato Y, Ohshima T, Kondo T. Regulatory role of endogenous interleukin-10 in cutaneous inflammatory response of murine wound healing. *Biochem Biophys Res Commun*. 1999;265:194-9.

Saulis AS, Mogford JH, Mustoe TA. Effect of Mederma on hypertrophic scarring in the rabbit ear model. *Plast Reconstr Surg*. 2002;110:177-83; discussion 84-6.

Sawicki G, Marcoux Y, Sarkhosh K, Tredget E, Ghahary A. Interaction of keratinocytes and fibroblasts modulates the expression of matrix metalloproteinases-2 and-9 and their inhibitors. *Molecular and Cellular Biochemistry*. 2005;269:209-16.

Sayani K, Dodd CM, Nedelec B, Shen YJ, Ghahary A, Tredget EE, et al. Delayed appearance of decorin in healing burn scars. *Histopathology*. 2000;36:262-72.

Schneider JC, Harris NL, El Shami A, Sheridan RL, Schulz JT, 3rd, Bilodeau ML, et al. A

descriptive review of neuropathic-like pain after burn injury. *J Burn Care Res.* 2006;27:524-8.

Schonherr E, Hausser HJ. Extracellular matrix and cytokines: a functional unit. *Dev Immunol.* 2000;7:89-101.

Scott PG, Dodd CM, Tredget EE, Ghahary A, Rahemtulla F. Immunohistochemical localization of the proteoglycans decorin, biglycan and versican and transforming growth factor-beta in human post-burn hypertrophic and mature scars. *Histopathology.* 1995;26:423-31.

Scott PG, Ghahary A, Tredget EE. Molecular and cellular aspects of fibrosis following thermal injury. *Hand Clin.* 2000;16:271-87.

Shah M, Foreman DM, Ferguson MW. Neutralising antibody to TGF-beta 1,2 reduces cutaneous scarring in adult rodents. *J Cell Sci.* 1994;107 (Pt 5):1137-57.

Shah M, Foreman DM, Ferguson MW. Neutralisation of TGF-beta 1 and TGF-beta 2 or exogenous addition of TGF-beta 3 to cutaneous rat wounds reduces scarring. *J Cell Sci.* 1995;108 (Pt 3):985-1002.

Shen B, Liu XH, Fan Y, Qiu JX. Macrophages Regulate Renal Fibrosis Through Modulating TGF beta Superfamily Signaling. *Inflammation.* 2014;37:2076-84.

Shen H, Yao P, Lee E, Greenhalgh D, Soulika AM. Interferon-gamma inhibits healing post scald burn injury. *Wound Repair Regen.* 2012;20:580-91.

Shi-wen X, Stanton LA, Kennedy L, Pala D, Chen Y, Howat SL, et al. CCN2 is necessary for adhesive responses to transforming growth factor-beta1 in embryonic fibroblasts. *J Biol Chem.* 2006;281:10715-26. Epub 2006 Feb 16.

Sica A, Erreni M, Allavena P, Porta C. Macrophage polarization in pathology. *Cell Mol Life Sci.* 2015;72:4111-26.

Sica A, Mantovani A. Macrophage plasticity and polarization: in vivo veritas. *J Clin Invest.* 2012;122:787-95.

Sica A, Schioppa T, Mantovani A, Allavena P. Tumour-associated macrophages are a

distinct M2 polarised population promoting tumour progression: potential targets of anti-cancer therapy. *Eur J Cancer*. 2006;42:717-27.

Sidgwick GP, Bayat A. Extracellular matrix molecules implicated in hypertrophic and keloid scarring. *Journal of the European Academy of Dermatology and Venereology*. 2012;26:141-52.

Simon F, Bergeron D, Larochelle S, Lopez-Valle CA, Genest H, Armour A, et al. Enhanced secretion of TIMP-1 by human hypertrophic scar keratinocytes could contribute to fibrosis. *Burns*. 2012;38:421-7.

Sindrilaru A, Peters T, Wieschalka S, Baican C, Baican A, Peter H, et al. An unrestrained proinflammatory M1 macrophage population induced by iron impairs wound healing in humans and mice. *J Clin Invest*. 2011;121:985-97.

Sisco M, Kryger ZB, O'Shaughnessy KD, Kim PS, Schultz GS, Ding XZ, et al. Antisense inhibition of connective tissue growth factor (CTGF/CCN2) mRNA limits hypertrophic scarring without affecting wound healing in vivo. *Wound Repair Regen*. 2008;16:661-73. doi: 10.1111/j.524-475X.2008.00416.x.

Slemp AE, Kirschner RE. Keloids and scars: a review of keloids and scars, their pathogenesis, risk factors, and management. *Curr Opin Pediatr*. 2006;18:396-402.

Smith CJ, Smith JC, Finn MC. The possible role of mast cells (allergy) in the production of keloid and hypertrophic scarring. *J Burn Care Rehabil*. 1987;8:126-31.

Solinas G, Germano G, Mantovani A, Allavena P. Tumor-associated macrophages (TAM) as major players of the cancer-related inflammation. *Journal of Leukocyte Biology*. 2009;86:1065-73.

Song E, Ouyang N, Horbelt M, Antus B, Wang M, Exton MS. Influence of alternatively and classically activated macrophages on fibrogenic activities of human fibroblasts. *Cell Immunol*. 2000;204:19-28.

Stables MJ, Shah S, Camon EB, Lovering RC, Newson J, Bystrom J, et al. Transcriptomic analyses of murine resolution-phase macrophages. *Blood*. 2011;118:e192-208.

Stamenkovic I. Extracellular matrix remodelling: the role of matrix metalloproteinases. *J Pathol*. 2003;200:448-64.

Stawski L, Haines P, Fine A, Rudnicka L, Trojanowska M. MMP-12 deficiency attenuates angiotensin II-induced vascular injury, M2 macrophage accumulation, and skin and heart fibrosis. *PLoS One*. 2014;9:e109763.

Stein M, Keshav S, Harris N, Gordon S. Interleukin 4 potently enhances murine macrophage mannose receptor activity: a marker of alternative immunologic macrophage activation. *J Exp Med*. 1992;176:287-92.

Stewart DA, Yang Y, Makowski L, Troester MA. Basal-like breast cancer cells induce phenotypic and genomic changes in macrophages. *Mol Cancer Res*. 2012;10:727-38.

Stewart DA, Yang YM, Makowski L, Troester MA. Basal-like Breast Cancer Cells Induce Phenotypic and Genomic Changes in Macrophages. *Molecular Cancer Research*. 2012;10:727-38.

Stoddard FJ, Jr., Ryan CM, Schneider JC. Physical and psychiatric recovery from burns. *Surg Clin North Am*. 2014;94:863-78.

Stopa M, Anhuf D, Terstegen L, Gatsios P, Gressner AM, Dooley S. Participation of Smad2, Smad3, and Smad4 in transforming growth factor beta (TGF-beta)-induced activation of Smad7. THE TGF-beta response element of the promoter requires functional Smad binding element and E-box sequences for transcriptional regulation. *J Biol Chem*. 2000;275:29308-17.

Stout RD, Jiang C, Matta B, Tietzel I, Watkins SK, Suttles J. Macrophages sequentially change their functional phenotype in response to changes in microenvironmental influences. *J Immunol*. 2005;175:342-9.

Swirski FK, Nahrendorf M, Etzrodt M, Wildgruber M, Cortez-Retamozo V, Panizzi P, et al. Identification of splenic reservoir monocytes and their deployment to inflammatory sites. *Science*. 2009;325:612-6.

Tan EM, Qin H, Kennedy SH, Rouda S, Fox JWt, Moore JH, Jr. Platelet-derived growth factors-AA and -BB regulate collagen and collagenase gene expression differentially in human fibroblasts. *Biochem J*. 1995;310 (Pt 2):585-8.

Tanaka A, Hatoko M, Tada H, Iioka H, Niitsuma K, Miyagawa S. Expression of p53 family in scars. *J Dermatol Sci*. 2004;34:17-24.

Tanriverdi-Akhisaroglu S, Menderes A, Oktay G. Matrix metalloproteinase-2 and-9 activities in human keloids, hypertrophic and atrophic scars: a pilot study. *Cell Biochemistry and Function*. 2009;27:81-7.

Tiede S, Ernst N, Bayat A, Paus R, Tronnier V, Zechel C. Basic fibroblast growth factor: a potential new therapeutic tool for the treatment of hypertrophic and keloid scars. *Ann Anat*. 2009;191:33-44.

Tjiu JW, Chen JS, Shun CT, Lin SJ, Liao YH, Chu CY, et al. Tumor-associated macrophage-induced invasion and angiogenesis of human basal cell carcinoma cells by cyclooxygenase-2 induction. *J Invest Dermatol*. 2009;129:1016-25.

Tolboom TC, Pieterman E, van der Laan WH, Toes RE, Huidekoper AL, Nelissen RG, et al. Invasive properties of fibroblast-like synoviocytes: correlation with growth characteristics and expression of MMP-1, MMP-3, and MMP-10. *Ann Rheum Dis*. 2002;61:975-80.

Traore K, Trush MA, George M, Spannhake EW, Anderson W, Asseffa A. Signal transduction of phorbol 12-myristate 13-acetate (PMA)-induced growth inhibition of human monocytic leukemia THP-1 cells is reactive oxygen dependent. *Leukemia Research*. 2005;29:863-79.

Tredget EB, Demare J, Chandran G, Tredget EE, Yang L, Ghahary A. Transforming growth factor-beta and its effect on reepithelialization of partial-thickness ear wounds in transgenic mice. *Wound Repair Regen*. 2005;13:61-7.

Tredget EE, Iwashina T, Scott PG, Ghahary A. Determination of plasma Ntau-methylhistamine in vivo by isotope dilution using benchtop gas chromatography-mass spectrometry. *J Chromatogr B Biomed Sci Appl*. 1997;694:1-9.

Tredget EE, Iwashina T, Scott PG, Ghahary A. Determination of plasma Ntau-methylhistamine in vivo by isotope dilution using benchtop gas chromatography-mass spectrometry. *J Chromatogr B Biomed Sci Appl*. 1997;694:1-9.

Tredget EE, Nedelec B, Scott PG, Ghahary A. Hypertrophic scars, keloids, and contractures - The cellular and molecular basis for therapy. *Surgical Clinics of North America*. 1997;77:701-&.

Tredget EE, Nedelec B, Scott PG, Ghahary A. Hypertrophic scars, keloids, and contractures. The cellular and molecular basis for therapy. *Surg Clin North Am*. 1997;77:701-30.

Tredget EE, Shankowsky HA, Pannu R, Nedelec B, Iwashina T, Ghahary A, et al. Transforming growth factor-beta in thermally injured patients with hypertrophic scars: effects of interferon alpha-2b. *Plast Reconstr Surg*. 1998;102:1317-28; discussion 29-30.

Tredget EE, Wang R, Shen Q, Scott PG, Ghahary A. Transforming growth factor-beta mRNA and protein in hypertrophic scar tissues and fibroblasts: antagonism by IFN-alpha and IFN-gamma in vitro and in vivo. *J Interferon Cytokine Res*. 2000;20:143-51.

Tredget EE, Yang L, Delehanty M, Shankowsky H, Scott PG. Polarized Th2 cytokine production in patients with hypertrophic scar following thermal injury. *J Interferon Cytokine Res*. 2006;26:179-89.

Tritto M, Kanat IO. Management of keloids and hypertrophic scars. *J Am Podiatr Med Assoc*. 1991;81:601-5.

Tsou PS, Haak AJ, Khanna D, Neubig RR. Cellular mechanisms of tissue fibrosis. 8. Current and future drug targets in fibrosis: focus on Rho GTPase-regulated gene transcription. *Am J Physiol Cell Physiol*. 2014;307:C2-13.

Twigg HL, 3rd. Macrophages in innate and acquired immunity. *Semin Respir Crit Care Med*. 2004;25:21-31.

Ueda K, Furuya E, Yasuda Y, Oba S, Tajima S. Keloids have continuous high metabolic activity. *Plast Reconstr Surg*. 1999;104:694-8.

Ulrich D, Noah EM, von Heimburg D, Pallua N. TIMP-1, MMP-2, MMP-9, and PIIINP as serum markers for skin fibrosis in patients following severe burn trauma. *Plastic and Reconstructive Surgery*. 2003;111:1423-31.

Vaalamo M, Leivo T, Saarialho-Kere U. Differential expression of tissue inhibitors of metalloproteinases (TIMP-1,-2,-3, and-4) in normal and aberrant wound healing. *Human Pathology*. 1999;30:795-802.

van der Veer WM, Bloemen MC, Ulrich MM, Molema G, van Zuijlen PP, Middelkoop E, et al. Potential cellular and molecular causes of hypertrophic scar formation. *Burns*. 2009;35:15-29.

van Rooijen N, van Nieuwmegen R. Elimination of phagocytic cells in the spleen after intravenous injection of liposome-encapsulated dichloromethylene diphosphate. *An*

enzyme-histochemical study. *Cell Tissue Res.* 1984;238:355-8.

van Zuijlen PP, Ruurda JJ, van Veen HA, van Marle J, van Trier AJ, Groenevelt F, et al. Collagen morphology in human skin and scar tissue: no adaptations in response to mechanical loading at joints. *Burns.* 2003;29:423-31.

Varkey M, Ding J, Tredget EE. Fibrotic remodeling of tissue-engineered skin with deep dermal fibroblasts is reduced by keratinocytes. *Tissue Eng Part A.* 2014;20:716-27. doi: 10.1089/ten.TEA.2013.0434. Epub 2013 Nov 9.

Vogel DY, Heijnen PD, Breur M, de Vries HE, Tool AT, Amor S, et al. Macrophages migrate in an activation-dependent manner to chemokines involved in neuroinflammation. *J Neuroinflammation.* 2014;11:23.

Wang B, Hao J, Jones SC, Yee MS, Roth JC, Dixon IM. Decreased Smad 7 expression contributes to cardiac fibrosis in the infarcted rat heart. *Am J Physiol Heart Circ Physiol.* 2002;282:H1685-96.

Wang J, Chen H, Shankowsky HA, Scott PG, Tredget EE. Improved scar in postburn patients following interferon-alpha2b treatment is associated with decreased angiogenesis mediated by vascular endothelial cell growth factor. *J Interferon Cytokine Res.* 2008;28:423-34.

Wang J, Ding J, Jiao H, Honardoust D, Momtazi M, Shankowsky HA, et al. Human hypertrophic scar-like nude mouse model: characterization of the molecular and cellular biology of the scar process. *Wound Repair Regen.* 2011;19:274-85.

Wang J, Dodd C, Shankowsky HA, Scott PG, Tredget EE, Wound Healing Research G. Deep dermal fibroblasts contribute to hypertrophic scarring. *Lab Invest.* 2008;88:1278-90.

Wang J, Hori K, Ding J, Huang Y, Kwan P, Ladak A, et al. Toll-like receptors expressed by dermal fibroblasts contribute to hypertrophic scarring. *J Cell Physiol.* 2011;226:1265-73.

Wang J, Jiao H, Stewart TL, Shankowsky HA, Scott PG, Tredget EE. Increased TGF-beta-producing CD4+ T lymphocytes in postburn patients and their potential interaction with dermal fibroblasts in hypertrophic scarring. *Wound Repair Regen.* 2007;15:530-9.

Wang JF, Jiao H, Stewart TL, Shankowsky HA, Scott PG, Tredget EE. Fibrocytes from burn patients regulate the activities of fibroblasts. *Wound Repair Regen.* 2007;15:113-21.

Wang JF, Olson ME, Ma L, Brigstock DR, Hart DA. Connective tissue growth factor siRNA modulates mRNA levels for a subset of molecules in normal and TGF-beta 1-stimulated porcine skin fibroblasts. *Wound Repair Regen.* 2004;12:205-16.

Wang R, Ghahary A, Shen YJ, Scott PG, Tredget EE. Human dermal fibroblasts produce nitric oxide and express both constitutive and inducible nitric oxide synthase isoforms. *J Invest Dermatol.* 1996;106:419-27.

Weisser SB, McLarren KW, Voglmaier N, van Netten-Thomas CJ, Antov A, Flavell RA, et al. Alternative activation of macrophages by IL-4 requires SHIP degradation. *Eur J Immunol.* 2011;41:1742-53.

Weissig V, SpringerLink (Online service). *Liposomes Methods and Protocols, Volume 1: Pharmaceutical Nanocarriers. Methods in Molecular Biology, Methods and Protocols*,:XII, 546p. 304 illus., 152 illus. in color.

Werner S, Grose R. Regulation of wound healing by growth factors and cytokines. *Physiol Rev.* 2003;83:835-70.

Wilgus TA, Wulff BC. The Importance of Mast Cells in Dermal Scarring. *Adv Wound Care (New Rochelle).* 2014;3:356-65.

Wilson MS, Elnekave E, Mentink-Kane MM, Hodges MG, Pesce JT, Ramalingam TR, et al. IL-13 α 2 and IL-10 coordinately suppress airway inflammation, airway-hyperreactivity, and fibrosis in mice. *J Clin Invest.* 2007;117:2941-51.

Witte MB, Barbul A. General principles of wound healing. *Surg Clin North Am.* 1997;77:509-28.

Wu Y, Huang S, Enhe J, Ma K, Yang S, Sun T, et al. Bone marrow-derived mesenchymal stem cell attenuates skin fibrosis development in mice. *Int Wound J.* 2014;11:701-10.

Wynn TA. Fibrotic disease and the T(H)1/T(H)2 paradigm. *Nat Rev Immunol.* 2004;4:583-94.

Wynn TA. Cellular and molecular mechanisms of fibrosis. *J Pathol.* 2008;214:199-210.

Wynn TA. Integrating mechanisms of pulmonary fibrosis. *J Exp Med.* 2011;208:1339-50.

Wynn TA, Chawla A, Pollard JW. Macrophage biology in development, homeostasis and disease. *Nature*. 2013;496:445-55.

Xie JL, Bian HN, Qi SH, Chen HD, Li HD, Xu YB, et al. Basic fibroblast growth factor (bFGF) alleviates the scar of the rabbit ear model in wound healing. *Wound Repair Regen*. 2008;16:576-81.

Xu J, Mora A, Shim H, Stecenko A, Brigham KL, Rojas M. Role of the SDF-1/CXCR4 axis in the pathogenesis of lung injury and fibrosis. *Am J Respir Cell Mol Biol*. 2007;37:291-9. Epub 2007 Apr 26.

Xu LL, Warren MK, Rose WL, Gong W, Wang JM. Human recombinant monocyte chemotactic protein and other C-C chemokines bind and induce directional migration of dendritic cells in vitro. *J Leukoc Biol*. 1996;60:365-71.

Xue H, McCauley RL, Zhang W, Martini DK. Altered interleukin-6 expression in fibroblasts from hypertrophic burn scars. *J Burn Care Rehabil*. 2000;21:142-6.

Xue J, Schmidt SV, Sander J, Draffehn A, Krebs W, Quester I, et al. Transcriptome-based network analysis reveals a spectrum model of human macrophage activation. *Immunity*. 2014;40:274-88.

Yang DY, Li SR, Wu JL, Chen YQ, Li G, Bi S, et al. Establishment of a hypertrophic scar model by transplanting full-thickness human skin grafts onto the backs of nude mice. *Plast Reconstr Surg*. 2007;119:104-9; discussion 10-1.

Yang L, Scott PG, Dodd C, Medina A, Jiao H, Shankowsky HA, et al. Identification of fibrocytes in postburn hypertrophic scar. *Wound Repair Regen*. 2005;13:398-404.

Yang L, Scott PG, Giuffre J, Shankowsky HA, Ghahary A, Tredget EE. Peripheral blood fibrocytes from burn patients: identification and quantification of fibrocytes in adherent cells cultured from peripheral blood mononuclear cells. *Lab Invest*. 2002;82:1183-92.

Yona S, Gordon S. From the Reticuloendothelial to Mononuclear Phagocyte System - The Unaccounted Years. *Front Immunol*. 2015;6:328.

Younai S, Venters G, Vu S, Nichter L, Nimni ME, Tuan TL. Role of growth factors in scar contraction: an in vitro analysis. *Ann Plast Surg*. 1996;36:495-501.

Yuan W, Varga J. Transforming growth factor-beta repression of matrix metalloproteinase-1 in dermal fibroblasts involves Smad3. *J Biol Chem.* 2001;276:38502-10.

Zalkind SIA. Ilya Mechnikov, his life and work. Moscow: Foreign Languages Pub. House, 1959.

Zhang Q, Liu LN, Yong Q, Deng JC, Cao WG. Intralesional injection of adipose-derived stem cells reduces hypertrophic scarring in a rabbit ear model. *Stem Cell Res Ther.* 2015;6:145.

Zhang ZF, Zhang YG, Hu DH, Shi JH, Liu JQ, Zhao ZT, et al. Smad interacting protein 1 as a regulator of skin fibrosis in pathological scars. *Burns.* 2011;37:665-72.

Zhu Z, Ding J, Ma Z, Iwashina T, Tredget EE. The natural behavior of mononuclear phagocytes in HTS formation. *Wound Repair Regen.* 2015.

Zhu Z, Ding J, Shankowsky HA, Tredget EE. The molecular mechanism of hypertrophic scar. *J Cell Commun Signal.* 2013;7:239-52.

Zou YR, Kottmann AH, Kuroda M, Taniuchi I, Littman DR. Function of the chemokine receptor CXCR4 in haematopoiesis and in cerebellar development. *Nature.* 1998;393:595-9.